

12-11-2015 12:00 AM

The Mistastin Lake Impact Structure As A Terrestrial Analogue Site For Lunar Science And Exploration

Marianne M. Mader, *The University of Western Ontario*

Supervisor: Dr. Gordon Osinski, *The University of Western Ontario*

A thesis submitted in partial fulfillment of the requirements for the Doctor of Philosophy degree in Planetary Science

© Marianne M. Mader 2015

Follow this and additional works at: <https://ir.lib.uwo.ca/etd>



Part of the [Geology Commons](#)

Recommended Citation

Mader, Marianne M., "The Mistastin Lake Impact Structure As A Terrestrial Analogue Site For Lunar Science And Exploration" (2015). *Electronic Thesis and Dissertation Repository*. 3485.
<https://ir.lib.uwo.ca/etd/3485>

This Dissertation/Thesis is brought to you for free and open access by Scholarship@Western. It has been accepted for inclusion in Electronic Thesis and Dissertation Repository by an authorized administrator of Scholarship@Western. For more information, please contact wlsadmin@uwo.ca.

Abstract

The impact cratering record on the Moon is important for many reasons, from understanding early solar system chronology to probing the lunar interior. In order to maximize scientific return from future lunar missions, it is useful to: 1) study terrestrial impact craters to better understand impact processes and products, and 2) develop appropriate human and robotic exploration strategies aligned with geological goals.

This research shows that the intermediate-size Mistastin Lake impact structure, in northern Labrador, Canada, is an unparalleled lunar analogue site, which includes both an anorthositic target and an almost complete suite of impact lithologies, including proximal ejecta deposits. New remote sensing, field mapping, and microscopy data are used to develop new structural and geological models of the Mistastin Lake impact structure. The results of this study show that a multi-stage ejecta emplacement model is required to explain the observations. It is also shown that impact melt-bearing breccias or “suevites” at Mistastin were emplaced as flows, were never airborne, and were formed from the mixing of impact melt flows with underlying lithic materials.

In order to maximize scientific return from future lunar missions, this work also focused on developing appropriate human and robotic exploration strategies aligned with geological goals. We show that precursor reconnaissance missions provide surface geology visualization at resolutions and from viewpoints not achievable from orbit. Within such a mission concept, geological tasks are best divided between fixed-executional approaches, in which tasks are fairly repetitive and are carried out by an unskilled surface agent, and an adaptive-exploratory approach, where a skilled agent makes observations and interpretations and the field plan can adapt to these findings as the agent progresses. Operational considerations that help increase scientific return include: extensive pre-mission planning using remote sensing data; defining flexible plans and science priorities to respond to changing conditions; including mutually cross-trained scientists and engineers on the field team; and adapting traverses to accommodate field crew input and autonomy. A phased approach for human exploration proved

successful in incorporating astronaut feedback and allowed more autonomy for astronauts to determine optimal sampling localities and sites for detailed observations.

Keywords

Impact cratering, impact structure, impactite, impact ejecta, lunar exploration, analogue mission, comparative planetology, Moon, planetary science, Mistastin Lake impact structure.

Co-Authorship Statement

Chapter 1 was a compilation of the existing literature relevant to the topic of this study. Dr. G. R. Osinski contributed to the editing of the chapter.

Chapter 2 was published as a conference paper for the 63rd of the International Astronautical Congress conference in 2012. Co-authors include Dr. D. Eppler, Dr. G. R. Osinski, Dr. J. Brown, and Dr. N. Ghafoor. Dr. D. Eppler contributed to the writing and review of background material for the review of terrestrial field geology techniques. All co-authors contributed to the editing of the manuscript.

Chapter 3 was published as a conference paper for the 65th International Astronautical Congress conference in 2014. Co-authors include Dr. S. Love and Dr. G.R. Osinski. Dr. S. Love contributed to the writing of sections 3.2.1 and 3.2.5 and the editing of the entire document. Dr. G.R. Osinski contributed to the editing of the manuscript.

Chapter 4 was published as a conference paper for the 65th International Astronautical Congress conference in 2014. Co-authors include G.R. Osinski. Data used for analysis was generated as part of the Western University-led analogue mission campaign entitled Impacts: Lunar Sample Return (ILSR) funded by the Canadian Space Agency (CSA). Analogue missions are team endeavours, the entire team is listed in (Marion et al., 2012).

Data products generated by the team included traverse plans, transcribed notes from the Field and Mission control teams, geological data products as well as analogue mission reports to the CSA. The author was responsible for compiling all of the data products, analysing, and summarizing the results for this paper. G.R. Osinski contributed to writing and editing of this manuscript.

Chapter 5 was completed by M. Mader. Dr. L.L. Tornabene assisted with processing of data products using ENVI software program and provided training in how to use the program. Dr. G. R. Osinski was invaluable in helping to shape the outline of this paper, providing critical review of the discussion section, and editing of the entire chapter.

Chapter 6 was completed by M. Mader. C. Marion and A. Pickersgill assisted with sample collection and the author benefited from numerous discussions regarding the geology of the Mistastin Lake impact structure. M. Beauchamp assisted with collection of data using a JEOL JXA-8530F Field Emission Electron Probe Microanalyzer (FE-EPMA).

Chapter 7 provides a summary of the suitability of the Mistastin Lake impact structure as a lunar analogue site. Dr. G. Osinski contributed to writing and editing of this chapter.

Acknowledgments

It takes a village to create a thesis: by no means is the undertaking of a PhD dissertation a solitary experience. I have many people to thank for their contributions, support, and fellowship. A key person integral to the success of my research has been my supervisor, Dr. Gordon Osinski. He encouraged my interest in exploring a topic “outside of the box” of traditional field geology research projects, and has been a constant resource both academically and professionally. An environment of respect, academic integrity, and camaraderie is the backbone of our CPSX research group, which I attribute Dr. Osinski’s leadership. He believes in his students, and this has a lasting effect.

My research benefited from support of the impact cratering and analogue mission research communities. My field and lab work could not have been possible without the support of Cassandra Marion, Annemarie Pickersgill, and Marc Beauchamp. I’m grateful for the numerous academic discussions over the years with Dr. Dean Eppler (NASA), Dr. Livio Tornabene (UWO), Dr. Timothy Haltigin (CSA), Dr. Nadeem Ghafoor (MDA), and the entire Impacts Lunar Sample Return (ILSR) Analogue team. I’m also grateful for the support of Dr. Darlene Lim for my participation in the 2011 Pavilion Lake Research Project and Dr. Ralph Harvey for his support of my participation in the 2012-2013 Antarctic Search for Meteorites (ANSMET) campaign.

The bulk of my supportive village were helpful in the day-to-day trials and tribulations of the challenging, yet rewarding, research process. We are collaborators, confidants, and friends - the positive support of this group continues to propel us forward. Thank-you to Cassandra Marion, Annemarie Pickersill, Emily McCullough, Bhairavi Shankar, Haley Sapers, Melissa Battler, Alaura Singleton, Louisa Preston, Alexandra Pontefract, Marc Beauchamp, and Raymond Francis.

Finally, I’m confident that behind every successful scientist is a supportive family network. I’m thankful to Andy Forest, Julie Brown, my parents, sister, and brothers for always believing in me – you are my rock solid foundation from which I know anything is possible.

Table of Contents

Abstract.....	i
Co-Authorship Statement.....	ii
Acknowledgments.....	iv
List of Tables	x
List of Figures	xi
1 Introduction.....	1
1.1 Overview of lunar analogue activities	2
1.2 Hypervelocity impact events.....	5
1.2.1 Contact and compression stage.....	5
1.2.2 Excavation stage	6
1.2.3 Modification stage	7
1.2.4 Impactites.....	8
1.3 Mistastin Lake impact structure, Labrador	11
1.3.1 Significant prior research.....	13
1.4 Thesis outline	15
1.5 References.....	16
Chapter 2.....	23
2 Unifying science-driven and resource exploitation strategies for lunar missions: Applying lessons learned from terrestrial geological exploration and Canadian planetary analogue missions.	23
2.1 Review of terrestrial field geology techniques	25
2.1.1 Adaptive–exploratory geological mapping techniques.....	27
2.1.2 Fixed – executional geological mapping techniques	32
2.2 Review of the University of Western Ontario’s lunar analogue activities	36
2.2.1 Robotic precursor mission	38

2.2.2	Follow-on human with robotic assistant mission.....	38
2.2.3	Analogue mission findings	39
2.3	Adapting geological field work for lunar exploration	40
2.4	Lunar exploration strategies.....	43
2.5	Summary	45
2.6	References.....	47
Chapter 3.....		51
3	Geological Exploration of Other Planets: Insights from Terrestrial Desert, Sea, and Polar Analogue Mission Campaigns.....	51
3.1	Geological field approaches.....	52
3.2	Review of analogue programs	53
3.2.1	NASA Extreme Environment Mission Operations (NEEMO).....	53
3.2.2	Pavilion Lake Research Project (PLRP).....	57
3.2.3	NASA Desert Research and Technology Studies (Desert RATS).....	61
3.2.4	Impacts: Lunar Sample Return (ILSR).....	66
3.2.5	Antarctic Search for Meteorites (ANSMET).....	71
3.3	Comparison of analogue programs	77
3.3.1	Similarities	77
3.3.2	Differences.....	78
3.4	Lessons learned for exploring Moon and Mars	79
3.5	Current gaps and recommendations for future studies	80
3.6	References.....	81
Chapter 4.....		85
4	Optimizing Scientific Return for Robotic-Human Lunar Exploration: Case Study Impacts Lunar Sample Return (ILSR) Analogue Mission Program	85
4.1	Evaluation methods.....	86

4.2 Lunar analogue site	89
4.3 Case study: Impacts Lunar Sample Return Program	90
4.4 Results	95
4.4.1 Traverse planning and execution	97
4.4.2 Adaptability & phased approach.....	99
4.4.3 Geological data collection.....	101
4.4.4 Geological data interpretation.....	104
4.4.5 Geological data management.....	104
4.5 Discussion and lessons learned: Lunar exploration strategies	106
4.5.1 Utility of robotic precursor mission.....	106
4.5.2 New human exploration paradigm.....	107
4.5.3 Data management.....	108
4.6 Conclusions.....	110
4.7 References.....	111
Chapter 5	116
5 New insights into the structure of the Mistastin Lake impact structure, Labrador, Canada.....	116
5.1 Introduction.....	116
5.2 Geological setting of the Mistastin Lake impact structure	117
5.3 Methods.....	119
5.4 Results.....	120
5.4.1 Topography	120
5.4.2 Lineaments.....	125
5.4.3 Glacial fabrics and landforms	128
5.5 Interpretations and Discussion.....	129
5.5.1 Effect of pre-existing structures on crater modification	129

5.5.2	Tectonics of crater rim collapse at Mistastin	131
5.5.3	Post-impact modification of the Mistastin Lake impact structure	134
5.5.4	Size of the Mistastin Lake impact structure.....	134
5.6	Conclusions.....	136
5.7	References.....	137
Chapter 6		143
6	Impactites of the Mistastin Lake impact structure: Insights into impact ejecta emplacement	143
6.1	Introduction.....	143
6.2	Geological setting	144
6.3	Methods.....	148
6.4	Observations	150
6.4.1	Massive and fractured target rocks	151
6.4.2	Monomict impact breccia	155
6.4.3	Polymict lithic impact breccias (melt-free to -poor).....	158
6.4.4	Impact melt-bearing polymict lithic impact breccias.....	167
6.4.5	Melt Rocks.....	174
6.4.6	Summary of Mistastin Lake impactites	178
6.5	Discussion.....	178
6.5.1	Impactite stratigraphy	178
6.5.2	Impact ejecta	182
6.5.3	‘Suevite’ formation mechanism(s).....	186
6.5.4	Hydrothermal alteration	188
6.6	Summary: A new emplacement model for Mistastin Lake impactites	189
6.7	References.....	190
Chapter 7		198

7 Discussion of the suitability of the Mistastin Lake impact structure as a lunar analogue site.....	198
7.1 Choosing the Mistastin Lake impact structure as a lunar analogue site	199
7.2 Application of the Mistastin Lake lunar analogue site to lunar exploration.....	206
7.2.1 Comparative planetology	206
7.2.2 Lunar sample selection	207
7.3 Future work.....	209
7.3.1 Analogue mission evaluation.....	209
7.3.2 Mistastin Lake impact structure.....	210
7.4 References.....	211
Appendix A: Evaluation Plan for ILSR analogue program	214
Flight Director Daily Report Form	215
GIS Lead Daily Report Form.....	216
Planning Manager Daily Report Form.....	217
Science Interpretation Lead Daily Report Form	218
Science Manager Daily Report Form.....	219
Mission Control Science Documentarian	220
Mission Control Tactical Documentarian	221
List of Daily Meetings	222
Appendix B: Sun shaded relief images.....	224
Appendix C: Radial profiles	226
Appendix D: List of samples collected from Mistastin Lake impact structure	227
Curriculum Vitae	233

List of Tables

Table 1-1: Shock levels in quartzofeldspathic crystalline rocks based on data from French (1998) and Stöffler and Grieve (2007).....	10
Table 2-1: Prioritization of lunar science goals over time assuming that prospecting for lunar volatiles is the primary motivation (adapted from the Lunar Exploration Roadmap; Lunar Exploration Analysis Group, 2011a).....	26
Table 2-2: List of detailed geological goals over time needed to address Science Objective: “Characterize the environment and processes in lunar polar regions and in the lunar exosphere” (Lunar Exploration Analysis Group, 2011a).	44
Table 2-3: Potential lunar exploration strategy to characterize the environment and processes in a lunar South Pole crater (e.g., Shackleton crater). Description of mapping strategies over time needed to characterize cold traps and volatile deposits.	46
Table 4-1: General design of planetary analogue mission simulations.	88
Table 4-2: Evaluation plan using a Program logic model framework for the ILSR analogue mission simulation. Key observations made during planetary analogue mission simulation focused on geological studies linked to mission and objectives.	96
Table 4-3: List of remote imaging datasets for the Mistastin region and their respective resolutions.	98
Table 4-4: Traverse and data processing schedule for human exploration mission.	101
Table 4-5: Data collected during 4 day astronaut mission at Discovery Hill.	105
Table 6-1: Individual analysis of groundmass-forming clays from Mistastin polymict impact breccias from Côté Creek.....	160
Table 6-2: Average composition of zeolites from Mistastin Lake polymict impact breccias from Côté Creek.....	167

Table 6-3: Description of Mistastin Lake impactites units in stratigraphic order from bottom to top.	179
---	-----

Table 7-1: Requirements for selection of the Mistastin impact structure, Labrador as a lunar analogue site.	203
--	-----

List of Figures

Figure 1-1: Venn diagram illustrating relationship of three main aspects of analogue mission simulations: Science (comparative planetology), Technology Testing, and Operations.	4
---	---

Figure 1-2: Schematic of the formation process for a complex impact crater. Modified from (Osinski et al., 2011). (A) Excavation phase. Top: Transient cavity is characterized by an upper ‘excavated zone’ and a lower ‘displaced zone’. Bottom: Material in the upper zone is ejected ballistically out of the transient cavity forming an airborne “ejecta curtain”. (B) Modification stage. Top: Uplift of crater floor begins as excavation continues in rim region. Bottom: Uplift of crater floor can impart outward momentum to melt within transient cavity, and cause melt to flow onto collapsing crater rim, onto previously deposit ballistic ejecta.	7
---	---

Figure 1-3: Schematic cross-section of an impact target illustrates impact process. Shock pressures affecting the target decrease with distance from the point of impact. On the right side of the schematic diagram, those pressures decrease from >50 GPa to <1 GPa. As shock pressures decrease, their effect on the target decreases, which is shown on the left side of the diagram. Image credit: David A Kring, modified after French (2000) and Melosh (1989) from	
--	--

http://www.lpi.usra.edu/exploration/training/illustrations/shockMetamorphism/	9
---	---

Figure 1-4: Geological map of the Mistastin batholith. Modified from Emslie et al., (1980).	12
--	----

- Figure 1-5: Simplified geological map of the Mistastin Lake region. Target rocks were mapped by Currie, 1971; impact melt was mapped by Grieve, 1975; Marion and Sylvester, 2010. 14
- Figure 3-1: DeepWorker submersible with aquanaut during NEEMO XVI (photo credit: NASA/FIU). 54
- Figure 3-2: Reconnaissance flight paths of DeepWorker submersibles, Kelly Lake (Image credit: D. Lim, PLRP). 60
- Figure 3-3: Back-room Science Team watching live video feed from a DeepWorker submersible in the Mission Control Center. 61
- Figure 3-4: Two-person prototype rovers used in Desert RATS 2010 (Image credit: NASA). 62
- Figure 3-5: Field crew members performing shirt-sleeve 1-g "spacewalks" in Desert RATS (Image credit: NASA). 62
- Figure 3-6: A colourized shaded relief model of the Mistastin Lake impact structure. Black dashed lines represent interpreted faults defining a collapsed rim region are outlined in Tornabene et al., (2012). 66
- Figure 3-7: Radarsat-2 image of Mistastin Lake impact structure and surrounding area, showing (1) SOI - yellow dots, (2) Regions of Interest, based on groupings of SOI's – blue ellipses, and (3) Possible deployment landing sites - red markers (Shankar et al., 2011). Three separate regions around the Mistastin Lake were chosen for reconnaissance exploration by the rover. 68
- Figure 3-8: Searching for meteorites on blue ice using snowmobiles. 73
- Figure 3-9: Searching for meteorites within a moraine on foot. 74

- Figure 3-10: Sample collection during ANSMET. The entire team participates. Lower left: counter with designated number of meteorite. Lower right: sterile tongs lifting meteorite. 75
- Figure 3-11: Comparison of level of adaptability of traverses in real-time between analogue programs. 79
- Figure 4-1: Basic Logic Model (McDavid et al., 2013). 87
- Figure 4-2: A colourized shaded relief model of Mistastin. Red indicates higher elevations and blue indicates lowest elevations. Possible listric faults defining the collapsed rim region are outlined in black dashed lines (Tornabene et al., 2012). 90
- Figure 4-3: Radarsat-2 image of Mistastin Lake impact structure and surrounding area, showing (1) sites of interest - yellow dots, (2) Regions of Interest, based on groupings of sites of interest – blue ellipses, and (3) Possible deployment landing sites - red markers (Shankar et al., 2011). 92
- Figure 4-4: (A) 3D perspective of the Quick Bird panchromatic image compared with (B) 2010 ‘robotic’ precursor lidar scan, and (C) a ‘robotic’ precursor image of the southern slope of Discovery Hill. A light-toned outcrop (labelled “Fred” outcrop) appears to unconformably underlie the impact melt. The melt unit of Discovery Hill exhibits barely discernible columnar jointing in (A), which is better resolved by the ‘robotic’ precursor image (B and C) (Tornabene et al., 2012). Sub-outcrop scale SOI’s indicated by boxes in (D) were selected based on precursor data and science objectives. 93
- Figure 4-5: Reconnaissance EVA traverse comparing the planned (yellow dash line), relayed (green line), and actual GPS tracks (red line). 103
- Figure 5-1: Geological map of the Mistastin batholith. Modified from Emslie et al., (1980). Updated anorthosite boundary based on magnetic anomalies on residual total magnetic map (Dumont and Jones, 2012). 118
- Figure 5-2: A) Shadowed relief DEM showing topography of the Mistastin impact structure. Elevations are lowest near the shoreline, represented by purple and blue.

Highest elevations are red. The star marks the centre of the impact structure. Dashed lines mark ellipses defined by topographic highs. Labels B and C denote the locations of photos. B) Typical rock exposure and vegetation cover within the outer zone, NE quadrant. C) Typical rock exposure and vegetation cover within the inner zone, NW quadrant.

121

Figure 5-3: A) Tilted shaded relief DEM; vertical scale exaggerated. Red lines indicate location of representative profile lines for each quadrant. Letters correspond to Figures B–E). Representative profiles highlighting stepped topography in different quadrants surrounding Mistastin Lake.

123

Figure 5-4: Field images of target rocks in the rim region of the Mistastin Lake impact structure. Fractures are marked with dashed lines. (A) Massive granodiorite within the outer zone (see person in red jacket for scale). (B) Detail of coarse-grained granodiorite with primary igneous texture preserved. (C) Massive granodiorite and quartz monzonite along Mistastin River within the outer zone. (Photos is ~ 300 m across) Box outlines area shown in A. Inset: 14 structural data points for this region are plotted on an equal-angle stereonet as poles to fracture planes. (D) Two fracture sets observed within monomict impact breccias within the inner zone. Solid lines outline blocks of target rock. (See person in red jacket for scale). (E) Monomict breccia observed in ~5 m wide fault zone, interpreted as fault breccias that formed during the impact event, oriented parallel to the illustrated fracture set within the inner zone. (See person in blue jacket for scale).

124

Figure 5-5: Lineament map of the Mistastin Lake impact structure and surroundings. The basemap is a shaded relief image generated with a sun angle of 30° above the horizon, from an azimuth direction at 0°. Two groups of long lineaments outside of the crater are defined (purple dashed line): the NE-SW trending set and later W-SE trending curvilinear set are both interpreted as regional faults. The density of short lineaments < 10 km in length are concentrated within the outer zone and within 10 km from the apparent crater rim. A NE-SW glacial fabric is notably visible within the inner zone.

126

Figure 5-6: Rose diagrams depicting the frequency of lineaments for a given orientation associated with the Mistastin Lake impact structure. Note: dip data could not be collected

for lineaments using shaded relief images, therefore they are plotted bi-directionally (symmetrical) on the circular histogram. (A) Plot of all Mistastin lineaments as identified in Fig. 4. (B) Lineaments within the NW region. (C) Lineaments within the SE region.

127

Figure 5-7: (A) Discovery Hill feature, Mistastin Lake impact structure. Dark rocks are impact melt rocks. Maximum height of ramp is 120m above lake level. (B) Schematic of a crag and tail glacial feature.

128

Figure 5-8: Comparison of the lineament distribution of the Haughton impact structure (left) and the Mistastin Lake impact structure (right). Haughton exhibits a clear pattern of radial and curved concentric faults, whereas, Mistastin Lake exhibits shorter fractures and faults that are more randomly oriented in respect the crater centre or parallel to regional faults.

133

Figure 5-9: Schematic cross-section of the Mistastin Lake impact structure, idealized transect from southwest to northeast across the crater. Top section shows the hypothetical impact structure before erosion; D = diameter of final crater. The lower section shows the present-day surface after erosion and glaciation; D_a = diameter of apparent crater rim. Note: the original crater rim has been eroded and the apparent crater rim is larger in diameter in the SW-NE direction of glaciation. Curved, listric faults represented in cross-sections are not continuous laterally. Zones are bound by raised hills and short faults.

135

Figure 6-1: Geological map of the Mistastin batholith. Modified from Emslie et al., (1980). Anorthosite boundary based on magnetic anomalies on residual total magnetic map (Dumont and Jones, 2012). Box outlines area of maps in Figure 6-2.

146

Figure 6-2: (A) New geological map of the Mistastin Lake impact structure (adapted from Emslie et al., 1980 and Marion et al., Forthcoming) fused with Digital Elevation Model (Chapter 5). Boxes outline areas of interest in our study. Impactite stratigraphy indicated for each area. Insert: Basemap used by most previous studies of Mistastin Lake impact structure based on field mapping by Currie (1971). (B) Typical rock exposure and vegetation cover within the outer zone, NE quadrant; (C) Typical rock exposure and

vegetation cover within the inner zone, NW quadrant. (Figures B and C modified from Chapter 5). 147

Figure 6-3: Typical rock exposures in Mistastin Lake region. (A) Glacial deposits lying on top of monomict anorthosite breccias along South Creek. Photo shows typical example of vertical exposures along creek banks. (B) Example of flat exposures along the Mistastin Lake shoreline. Outcrop of quartz monzonite along the SW shoreline of Mistastin Lake. (C) Northeast rim region of the Mistastin impact structure, which is dominated by massive granodiorite. Boundaries of rim region outlined in black, dashed line. Box indicates area shown in Figure 6-5C. 151

Figure 6-4: Massive target rocks of the Mistastin Lake impact structure. (A) Coarse grained granodiorite. Primary igneous texture is preserved. (B) Thin section microphotograph of granodiorite (cross-polarized light). Primary igneous texture is preserved. Minor fracturing of feldspar crystals. (C) Knobby, weathered surface of quartz monzonite. Can be difficult to distinguish from monomict impact breccias of the same rock type. (D) Thin section microphotograph of massive quartz monzonite, SW shoreline, Mistastin Lake (plane-polarized light), dominated by feldspar and amphibole relatively little affected by impact event. (E) Coarse-grained (1-10 cm) fractured, massive anorthosite, Horseshoe Island. Inset: Fracturing along cleavage planes of feldspar. (F) Thin section microphotograph of massive anorthosite, Horseshoe Island (plane-polarized light) showing fractured nature of feldspar crystal. 153

Figure 6-5: Macroscopic fracturing in massive target rocks of the Mistastin Lake impact structure. (A) Massive quartz monzonite exposed along Côté Creek. Note: Perpendicular fracture sets. The more continuous set dips towards the crater centre. (B) Thin breccia-filled fracture parallel to cm-m spaced joint set within quartz monzonite target rock along SW shoreline. Fracture and joint set trend radially from crater centre. Inset: Detail of fragmental, breccia dyke. Note angular to sub-round, mm-cm fragments within fine (<0.5 mm), lithic matrix. 154

Figure 6-6: Textures of monomict breccias of Mistastin Lake impact structure. (A) Quartz monzonite monomict impact breccias from Côté Creek, ~6.5 km from crater

center. (B) Detail of Fig. 6A, showing fragmental nature of matrix and brecciated clasts that are larger than individual feldspar augen. (C) Monomict anorthosite impact breccia along South Creek, ~7.5 km from crater center. (D) Thin section microphotograph of monomict anorthosite impact breccia (cross polarized light) showing fragmental nature of crystals and supporting matrix. Fractures along cleavage planes in feldspar crystals form shards.

156

Figure 6-7: Monomict anorthosite breccias, South Creek, Mistastin Lake impact structure. (A) South Creek cliff face, ~15 m high reveals a cross-section of monomict impact breccias that overlies fractured anorthosite target rock. Metre-scale fracture set dipping ~ 40° to the northeast, with a strike line roughly radial from the crater centre is observed throughout these monomict anorthosite impact breccias. (B) Blocky habit of monomict anorthosite breccias defined by a perpendicular fracture set. Location of photo indicated by box in A. (C) Shattercone block within anorthosite monomict impact breccias along South Creek. Location indicated by box in B.

157

Figure 6-8: Melt-free to -poor, polymict impact breccias of the Mistastin Lake impact structure. (A) Poorly sorted nature of angular to subrounded rock fragments ranging up to m-scale in size. (B) Fragmental nature of fine-grained components of melt-poor, polymict impact breccias. Rare melt fragment indicated by red circle. Côté Creek. (C) Thin section microphotograph of melt-poor, polymict impact breccias (plane polarized light) showing fragments supported by a dark grey matrix. Sample from Côté Creek. (D) Back-scattered electron image showing same area as (C). Dark grey groundmass is likely amorphous clay. (E) Thin section microphotograph of melt-poor, polymict impact breccias (plane polarized light) showing predominantly black matrix that also includes irregular bodies of calcite (inside box). Sample from South Creek. (F) Back-scattered electron image of area outlined by box in Figure 6-8E, showing detailed image of irregular bodies of groundmass-forming calcite with embayed outlines.

159

Figure 6-9: Melt-free to -poor polymict impact breccias along Côté and Piccadilly Creeks. (A) Aerial view of Côté Creek showing distribution of impactites, looking east. Outcrops of impact melt rock outlined in red. Letter B indicate location of following

image. (B) Near mouth of Côté Creek, buff white cliffs, ~80 m long and ~20 m tall comprise melt-poor, polymict breccias dominated by anorthositic fragments (“An block”) (location marked as B in Fig. 6-9A). (C) 10 m high cliff face along Piccadilly Creek, ~6 km from crater centre showing melt overlying melt-poor polymict breccias. Inset: Detail of fragmental nature of unit. 162

Figure 6-10: South shore and South creek melt-poor, polymict lithic breccias. (A) Layer of polymict breccia overlying fractured anorthosite target rock, South Creek. (B) Detail of box outlined in A, showing anorthosite clast in breccia. (C) Flat outcrops of melt-poor polymict lithic breccias along the southern shoreline. (D) Detail of box outlined in C, showing cm size anorthosite fragments. 163

Figure 6-11: Discovery Hill (A) Aerial view of south side of Discovery Hill showing 80 m thick unit of impact melt rock with vertical cooling fractures. (B) Detailed view of box in A. (C) Detailed view of contact in B. Melt-poor, polymict lithic impact breccias underlying melt, Discovery Hill. Melt unit has cm-m spaced, vertical cooling fractures. (D) Detail of contact between impact melt rock overlying melt-poor polymict lithic impact breccia. 164

Figure 6-12: Thin section microphotographs showing range of metamorphic shock effects in polymict impact breccia fragments. (A) Planar deformation features observed in quartz from a melt-poor, polymict impact breccia, locality (plane-polarized light). (B) Toasted, ballen quartz observed in melt-poor, polymict impact breccias, South Creek (plane-polarized light). (C) Fragmental nature of melt-poor, polymict impact breccias, showing rare melt fragment and maskelynite, Côté Creek (plane-polarized light). (D) Same area as (C), cross-polarized light. Maskelynite and melt fragments are isotropic. (E) Maskelynite grain (clear) with patches of zeolite alteration and thin zeolite rim, South Creek (plane-polarized light). (F) Same area as (E), cross-polarized light. Maskelynite grain is isotropic (completely dark). 166

Figure 6-13: (A) Côté Creek site of U-shaped contact between impact melt rock and polymict breccia. Along the base of the U-shape contact, the amount of impact melt

fragments increases as proximity to the overlying melt rock contact increases, as indicated in (B) through (E). 169

Figure 6-14: Backscattered electron (BSE) images of impact melt fragments within transitional zone between polymict breccias and overlying impact melt rock along Coté Creek as seen in Figure 6-13. (A) Detail of impact melt fragment in polymict breccia with <2% impact melt rock fragment (Figure 6-13b). Note: sharp boundary that truncates internal flow fabric. (B) Irregular boundary of impact melt fragment in same unit as A. (C) Detail of lithic fragment mantled by impact melt in polymict breccia with over 10% melt rock fragments. (D) Glassy fragment containing small rock and mineral fragments that are aligned with elongated side. Same unit as C. (E) Crystallites within impactite unit composed of 50% impact melt and 50% lithic material, as seen in Figure 6-13d. 170

Figure 6-15: Steep Creek outcrop (A) Steeply dipping dyke (strike 100°, dip 80°) comprising polymict lithic breccia with 10-40% melt fragments. Exposed length ~18 m. (B) Detail of dyke looking up from bottom of exposure. (C) Chilled boundary of dyke is sharp and is characterized by a rusty, fine grained, 5-10 cm thick zone. (D) Randomly oriented, elongate, sinuous impact melt fragments. (E) Backscattered electron (BSE) image of irregular boundary of impact melt fragment. (F) BSE image of sharp edge of impact melt fragment (at top of image) that truncates internal fabric. (G) Elongated, sinuous impact melt fragment. Note sharp break in middle of melt fragment. (H) Feldspar fragment mantled by impact glass. 172

Figure 6-16: (A) Location of melt-bearing polymict impact breccias lens within 80 m thick Discovery Hill unit of impact melt. (B) Extent of 1 m x 6 m lens of rusty, polymict lithic impact breccia containing melt fragments. (C) Sharp to anastomosing contact between melt-bearing polymict impact breccia lens and impact melt. (D) Polished slab showing the sharp contact and crystallites within the impact melt unit up to 5 cm from boundary with polymict impact breccias lens. 173

Figure 6-17: Impact melt rocks. (A) Locally, a thin, veneer of melt rock, overlying massive, fractured anorthosite target rocks, along S shoreline of Mistastin lake. (B) Example of the numerous impact melt rock dykes found within massive anorthosite target

rock along S shoreline of Mistastin lake. (C) Piccadilly creek melt dyke, dipping 40° towards NNE (into the hill side). The surrounding rocks are quartz monzonite. 175

Figure 6-18: (A) Exceptional outcrop along steep bank of Côté Creek showing contact of melt-bearing polymict impact breccias underlying impact melt rocks. Note: Cooling cracks in overlying impact melt unit. Letters indicate locations of following photos. (B) Detail of clast-poor, impact melt rock. (C) Flow banding around a clast within basal portion of melt unit, indicates flow in westerly direction (away from the centre of the impact structure). (D) Melt-bearing polymict impact breccias. 177

Figure 6-19: Schematic cross-section of the Mistastin Lake impact structure, idealized transect from southwest to northeast across the crater. Present-day surface after erosion and glaciation; D_a = diameter of apparent crater rim. Curved, listric faults represented in cross-sections are not continuous laterally. Zones are bound by raised hills and short faults. 180

Figure 7-1: (A) Tycho crater, 86 km in diameter, 43.31°S 11.36°W . Image credit: Lunar Reconnaissance Orbiter, NASA. Black line indicates location of profile line used in B. (B) Profile showing stepped topography of Tycho crater rim region. (C) Melt ponds on terraced rim of Tycho Crater imaged by KAGUYA's Terrain Camera, JAXA. 207

Chapter 1

1 Introduction

Many space agencies across the globe consider human missions to the lunar surface as an essential step in preparation for human Mars missions (International Space Exploration Coordination Group (ISECG), 2013). These missions could allow critical demonstrations of planetary exploration capabilities and techniques, while pursuing the highest priority lunar science objectives to characterise the geology, topography, available resources, and conditions at destinations. Specific science concepts that relate to the study of hypervelocity impact structures, include (National Research Council, 2007):

- The bombardment history of the inner solar system is uniquely revealed on the Moon.
- The structure and composition of the lunar interior provide fundamental information on the evolution of a differentiated planetary body.
- Key planetary processes are manifested in the diversity of lunar crustal rocks.
- The Moon is an accessible laboratory for studying the impact process on planetary scales.

Key technology and operational objectives that support these lunar science objectives include (International Space Exploration Coordination Group (ISECG), 2013):

- Demonstrate the use of robots to explore autonomously and to supplement astronauts' exploration activities.
- Develop and validate tools, technologies, and systems that extract, process, and utilize resources to enable exploration missions.
- Learn how to best perform basic working tasks and develop protocols for operations.
- Develop and demonstrate technologies to support scientific investigation.

Conducting scientific studies, testing geological technologies, and implementing operational strategies at terrestrial impact structures allows refinement of system designs and mission concepts, helping prepare for lunar exploration.

1.1 Overview of lunar analogue activities

Many of the science, technical, and operational objectives that require further study in order to develop effective lunar exploration strategies require field testing and as such can be investigated using analogue studies. Analogue studies in the context of planetary exploration involve activities that take place at an analogue site. In the broadest sense this site need not even be a natural setting; it has been defined as "an environment on Earth, in nature or by simulation, for which there are, or could be, analogous characteristics on the planetary body in question, either at the present-day or sometime in the past" (Persaud, 2004; Osinski et al., 2006). For the purpose of this study, analogue sites will refer to natural terrestrial environments presenting, to some extent, similarities (e.g., climatological, geological, morphological, etc.) with the lunar surface.

Analogue activities have been an integral part of human space exploration since humans first achieved orbital flight; including varied activities such as practicing in reduced gravity environments (e.g., parabolic flights), training at geologically appropriate sites for the Apollo Moon landings, and more recently testing of instruments, landers, and rovers, which will assist surface planetary exploration. Analogue activities not only include preparation for future planetary missions, but also the fundamental study of planetary bodies by investigating comparative sites on Earth. L  veill   (2010) provides a concise overview of these activities.

The importance of using terrestrial analogue sites and activities for training, development and testing of technologies, developing surface operational strategies, and comparative sciences has been recognized by space agencies. The Canadian Space Agency (CSA) and National Aeronautic Space Administration (NASA) have both developed analogue programs that support field work at appropriate sites, including CSA's Canadian Analogue Research Network (CARN) and NASA's Planetary Science and Technology Through Analog Research (PSTAR) program (previously called Moon and Mars Analog Mission Activities (MAMMA) program. Space agencies aim to share lessons learned and plans for future analogue campaigns in order to gain maximum benefit from these activities (International Space Exploration Coordination Group (ISECG), 2013).

Analogue missions are essentially Earth-based expeditions with characteristics that are analogous to missions on the moon, Mars, or near Earth objects (NEO's) (Léveillé, 2010). An analogue mission can be broadly defined as an integrated set of space exploration activities, conducted by a team, at a site which offers multiple environmental conditions of a planetary target and results in an understanding of system level interactions (NASA, 2011). They can model an entire mission concept (e.g., short lunar sortie missions, long-duration missions) or focus on specific aspects of future planetary exploration missions (e.g., in-situ resource utilization, life support systems).

NASA describes the focus of their “Moon and Mars Analog Mission Activities” (MAMMA) program as providing high-fidelity scientific investigations, scientific input, and science operations constraints in the context of existing planetary field campaigns (NASA, 2011). Terrestrial analogue missions can play a key role in the preparations for lunar missions - in addition to their scientific value, these simulations can provide a means to safely prepare and test exploration strategies (Osinski et al., 2006).

Activities encompassed within analogue missions include three different categories: scientific, technological, and operational (Deems and Baroff, 2008; Mohanty and Nystrom, 2007; Snook and Mendell, 2004) (Figure 1-1). Deems and Baroff (2008) recommend, that precursor analogue missions, incorporating all three activities, should be conducted to best learn how to reduce risk. A key aspect of analogue missions is that they are learning experiences: they aim to understand performance and interactions among these systems and operations or procedures as well as their ability to achieve mission objectives. They record lessons learned that can be applied in the development of future planetary missions. In addition, analogue missions facilitate and can improve communication and cooperation between disciplines.

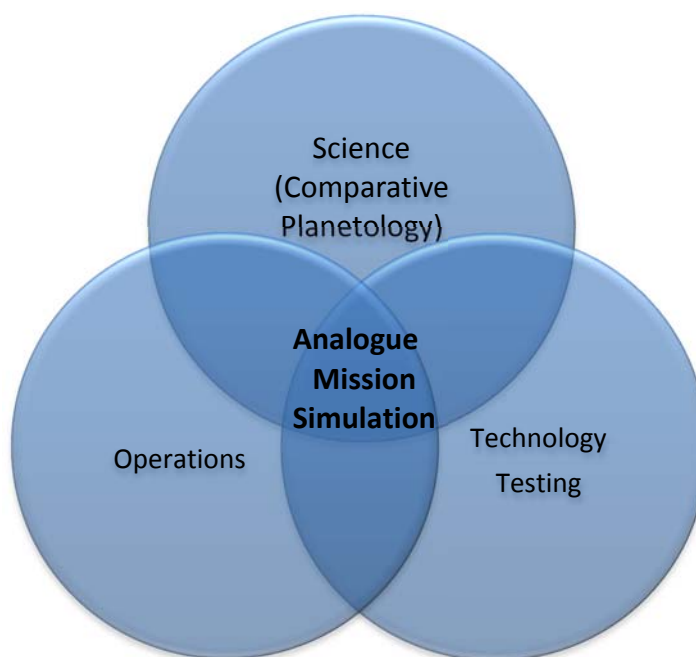


Figure 1-1: Venn diagram illustrating relationship of three main aspects of analogue mission simulations: Science (comparative planetology), Technology Testing, and Operations.

Analogue missions differ from Apollo full-scale simulations in which instruments and operational procedures were predefined and controlled. During Apollo training and simulations numerous individuals were available to check experimental deployment, to correct mistakes, and to help in difficult situations (Sullivan, 1994). This resulted in a difference in attitude between the training environment and the actual missions. When on the Moon, the astronauts were keenly aware of the fact that they had only one chance to complete their task, that their performance must be efficient, and that they were being intently observed by a large portion of the world population. In short, lunar EVA induced an attitude of great care in the execution of the allotted tasks (Sullivan, 1994).

Analogue missions aim to simulate a more realistic operational setting and through experiential learning, will help determine which instruments and technologies are most useful and will help define new field operational requirements for future lunar missions.

They allow a level of care and carefulness to be experienced. The selection of appropriate analogue sites is thus important to support this attitude of mindfulness.

1.2 Hypervelocity impact events

Within the past 50 years, impact cratering has been recognized as a dominant geological process that has affected the surface of all rocky planets within our solar system.

Preparation for the Apollo missions to the Moon, initiated detailed studies of hypervelocity impact structures based on lunar and terrestrial observations. Since then images of other rocky planetary bodies demonstrate the pervasive nature of this geological process in shaping and modifying planetary surfaces. Understanding the effect of impact cratering on various target lithologies is critical to help unravel the geological history of the Moon and to help guide future surface lunar exploration strategies.

Hypervelocity impact events, which by definition generate a shock wave upon impact of a target surface, are dynamic and complex events that occur in an extremely short period of time. Unlike other geological processes, rocks can change states, be metamorphosed and deformed within seconds of impact. In the minutes, hours, days and years following the impact event, rocks can continue to be affected by the event. A simple model dividing the impact event into three stages has helped bring order to this chaotic process, wherein an initial contact/compression stage is followed by an excavation stage and finally the modification stage (Gault et al., 1968; Melosh, 1989: Chapters 4, 5 and 8; Osinski and Pierazzo, 2013: Chapters 3, 4, and 5). In reality, these stages overlap and multiple impact ejecta products can be deposited during the excavation and modification stage (French, 1998; Kenkmann and Ivanov, 2000; Osinski et al., 2011; Turtle et al., 2005). The following sections describe these processes in relation to the formation of a complex impact crater, characterized by a structurally complicated rim, a down-faulted annular trough, and an uplifted central area.

1.2.1 Contact and compression stage

This initial stage starts the moment the impacting body contacts the surface of a planetary body. The projectile penetrates one to two times its diameter into the target rock (Kieffer

and Simonds, 1980; O'Keefe and Ahrens, 1982). The intense pressure at the point of contact is typically > 100 GPa (Shoemaker, 1960) and generates shock waves that travel faster than the speed of sound. These shock waves propagate into the target rock and back through the projectile. Upon reaching the rear surface of the projectile, the shock wave is reflected back into the projectile as a rarefaction wave. This tensional wave causes sudden unloading of shock pressures within the projectile resulting in complete vaporization or melting of the object (Ahrens and O'Keefe, 1972). The target rock close to the point of impact is vapourized, melted, or deformed through shock metamorphism – up to 50 GPa within quartzofeldspathic rocks (Ahrens and O'Keefe, 1972; Grieve et al., 1977; Stöffler and Grieve, 2007). The end of the contact and compression stage is marked by the complete passage of the refraction wave through the projectile. The entire stage lasts for a fraction of the entire crater forming process (Melosh, 1989).

1.2.2 Excavation stage

The initiation of the excavation stage briefly overlaps with the contact and compression stage. A roughly hemispherical shock wave propagates into the target rock and causes the target material to move downwards and outwards, although the shock wave loses strength the farther away it moves from the point of contact. Portions of the shock waves travel upwards and interact with the ground surface, where they are reflected back into the ground as rarefaction waves. An 'excavation flow' resulting from the combination of shock and rarefaction waves generates the transient cavity (Dence, 1968; Grieve and Cintala, 1981; Melosh, 1989). The transient cavity is characterized by an upper 'excavated zone' and a lower 'displaced zone' (Figure 1-2a).

Material in the upper zone is ejected ballistically out of the transient cavity forming an airborne "ejecta curtain" forming a sheet-like concentration of ejecta that moves outwards in a truncated cone geometry (Oberbeck, 1975). This ejected material contains material from a range of different shock levels. As ballistic material lands, secondary cratering, a process referred to as ballistic sedimentation (Oberbeck, 1975) occurs, and a continuous ejecta blanket forms.

1.2.3 Modification stage

The final stage of crater formation is the modification stage, which is controlled by the maximum size of the transient cavity and the properties of the target rock (Melosh and Ivanov, 1999). On Earth, simple bowl-shaped craters will form from slight modifications of transient cavities less than 2-4 km in diameter. Above this threshold, gravitational forces will cause the transient cavity floor to uplift and the rim walls to collapse, forming a complex crater characterized by a central uplift and collapsed rim defined by blocks and/or terraces.

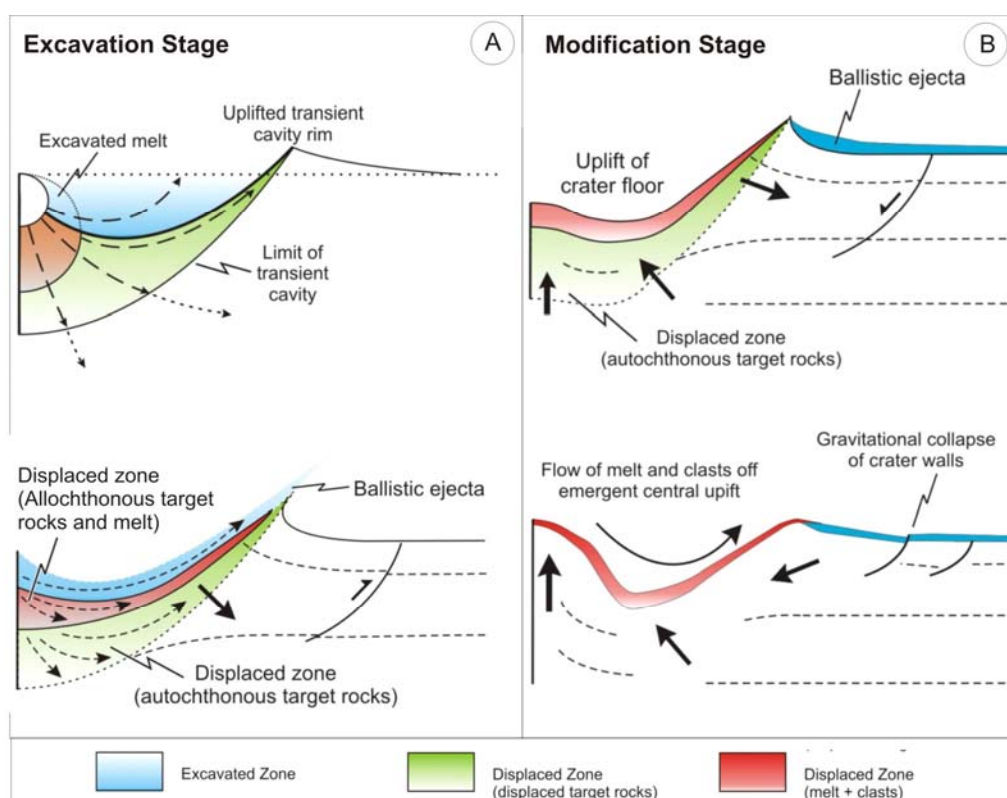


Figure 1-2: Schematic of the formation process for a complex impact crater. Modified from (Osinski et al., 2011). (A) Excavation phase. Top: Transient cavity is characterized by an upper ‘excavated zone’ and a lower ‘displaced zone’. Bottom: Material in the upper zone is ejected ballistically out of the transient cavity forming an airborne “ejecta curtain”. (B) Modification stage. Top: Uplift of crater floor begins as excavation continues in rim region. Bottom: Uplift of crater floor can impart outward momentum to melt within transient cavity, and cause melt to flow onto collapsing crater rim, onto previously deposit ballistic ejecta.

During outward crater growth of complex craters, rocks around the periphery of the bowl-shaped transient crater collapse downward and inward (Figure 1-2b) to form a series of blocks and/or terraces along the outer margin of the crater structure (French, 1998). Products of the ballistic ejecta blanket can therefore be expected within the modified, collapsed rim region of a complex crater where they were deposited prior to crater collapse, interior to the final crater rim (Dressler and Reimold, 2001; Osinski et al., 2011; Stöffler et al., 2002). In fact, in fresh craters, the ejecta blanket is thickest at the crater rim region, beyond which deposits are thin and patchy (Melosh, 1989; Osinski et al., 2011). Perhaps the most well-documented occurrence of an complex crater ejecta blanket deposit resulting from ballistic sedimentation on Earth, is the Bunte Breccia of the Ries impact structure (e.g., Hörz et al., 1983) a poorly sorted, massive, polymict lithic breccia unit of generally low shock level (Hörz, 1982).

Field observations of terrestrial craters and numerical models suggest that central uplifts partially collapse to varying degrees and may originally overshoot the original target surface and then collapse (Collins et al., 2002). This movement can impart an additional outward momentum to the melt within the transient cavity, resulting in flow toward and over the collapsing crater rim and onto the proximal ballistic ejecta blanket, forming a second thinner and potentially discontinuous layer of non-ballistic ejecta (Figure 1-2b, Osinski et al., 2011). Oblique impacts and local topography of the target region also influence the final resting place of melt deposits beyond the transient cavity. Later melt ejecta phases, deposited as ‘melt ponds’, have been observed on top of ballistic ejecta blanket deposits in lunar images (Hawke and Head, 1977; Howard and Wilshire, 1975). Recent studies using images from the Lunar Reconnaissance Orbiter Camera (LROC) have revealed flow features within terrace rim melt deposits (Ashley et al., 2012; Öhman and Kring, 2012).

1.2.4 Impactites

The term impactite refers to rocks produced or affected by the hypervelocity impact event. The target rock becomes shock metamorphosed as the shock wave passes through it in a hemispherical fashion, ranging in intensity from the highest shock level at the point

of impact to lower shock levels within concentric zones further away from the site of impact (Figure 1-3, Table 1-1).

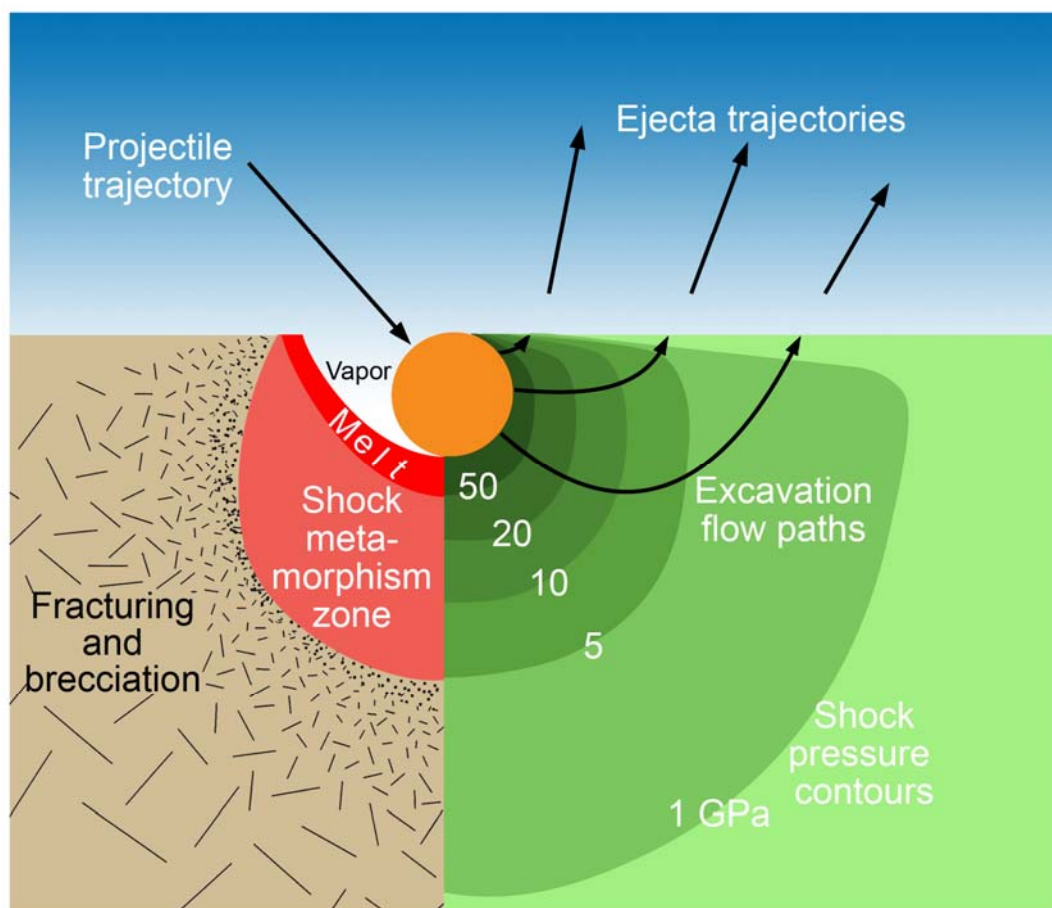


Figure 1-3: Schematic cross-section of an impact target illustrates impact process.

Shock pressures affecting the target decrease with distance from the point of impact. On the right side of the schematic diagram, those pressures decrease from >50 GPa to <1 GPa. As shock pressures decrease, their effect on the target decreases, which is shown on the left side of the diagram. Image credit: David A

Kring, modified after French (2000) and Melosh (1989) from

<http://www.lpi.usra.edu/exploration/training/illustrations/shockMetamorphism/>

Table 1-1: Shock levels in quartzofeldspathic crystalline rocks based on data from French (1998) and Stöffler and Grieve (2007)

Shock Stage	Pressure Range (GPa)	Major microscopic evidence in quartz	Major bulk rock effects
0	<5	Fracturing	Rock fracturing; brecciation; shatter cones
	5-7	Planar fractures; mosaicism	Shatter cones
	10-25	Planar deformation features; toasted quartz	
Ia	12-15	Stishovite	
	20	Reduced refractive indices; lowered birefringence	
	25-30	Toasted quartz; planar deformation features	
Ib	<30	Coesite; planar deformation features; ballen quartz	Loss of shatter cones
	35	Diaplectic glass	
II	35-45	Diaplectic glass; coesite; loss of planar deformation features	Partial melting
	45	Diaplectic glass (Maskelynite)	
III	45-55	Loss of diaplectic glass; flow textures	
IV		Lechatelierite (Si glass)	
V	60-80	Bulk melting of all components	
	80-100	Bulk glasses form	
VI	>100	Complete vapourization	

Impactites are grouped according to the extent to which they have been moved from their original pre-impact location by the impact. They are subdivided into three categories: 1) autochthonous (formed in place), 2) parautochthonous (moved but appear to be in place), and 3) allochthonous (formed elsewhere and clearly moved to their current location; Grieve and Therriault, 2013). Many terrestrial impact structures have been eroded to such a degree that only the underlying autochthonous target rocks are preserved or the crater structure has been infilled by later sedimentary units and thus impactites can only be accessed through drilling. In both cases, it is difficult to have a clear understanding of the spatial occurrence of impactites with respect to the crater structure.

Overall, a general impact structure stratigraphy observed within the rim region of a complex impact crater, from bottom to top, as observed at the Manicouagan, Haughton, and Ries impact structures, includes (Currie, 1972; Hörz, 1982; Murtaugh, 1976; Osinski et al., 2005):

- A) Unshocked target rocks;
- B) Autochthonous/paraautochthonous shocked and fractured target rocks;
- C) Paraautochthonous monomict lithic breccias;
- D) Allochthonous polymict lithic breccias (melt-poor and melt-bearing);
- E) Allochthonous impact melt rocks (grading from clast-rich to clast-poor from bottom to top);

1.3 Mistastin Lake impact structure, Labrador

The Mistastin Lake impact structure (55°53'N; 63°18'W) formed within the Mesoproterozoic (~1.4 Ga; Emslie et al., 1980) Mistastin batholith, which is part of the Nain plutonic suite of Labrador. The N-S oriented, elliptical-shaped batholith covers ~5000 km² (Emslie et al., 1980). Mistastin Lake is located in the upper NE quadrant of the batholith (Figure 1-4). The glacial history of Labrador is complex, having experienced numerous glacial events throughout the Pleistocene epoch. The most recent glacial event experienced by the Mistastin Lake region flowed from the Labrador Trough and northeastwards across the Mistastin Lake region (Klassen and Thompson, 1990).

The original impact crater has been differentially eroded; however, a subdued rim and distinct central uplift are still observed (Grieve, 1975). The inner portion of the structure is covered by the Mistastin Lake and the surrounding area is locally covered by soil/glacial deposits and vegetation. The crystalline target rocks of the Mistastin Lake region are dominated by anorthosite, granodiorite, and pyroxene-quartz monzonite. Locally, allochthonous impactite units, including impact melt rocks and various types of breccias, are unevenly distributed around the lake and on Horseshoe Island (interpreted as the remains of a central uplift structure). Apart from a large butte called Discovery Hill, impactite units are best exposed along the lake shoreline and steep banks of creeks. The vertical sections along creek banks allow for local unit thicknesses and contact relationships to be observed.

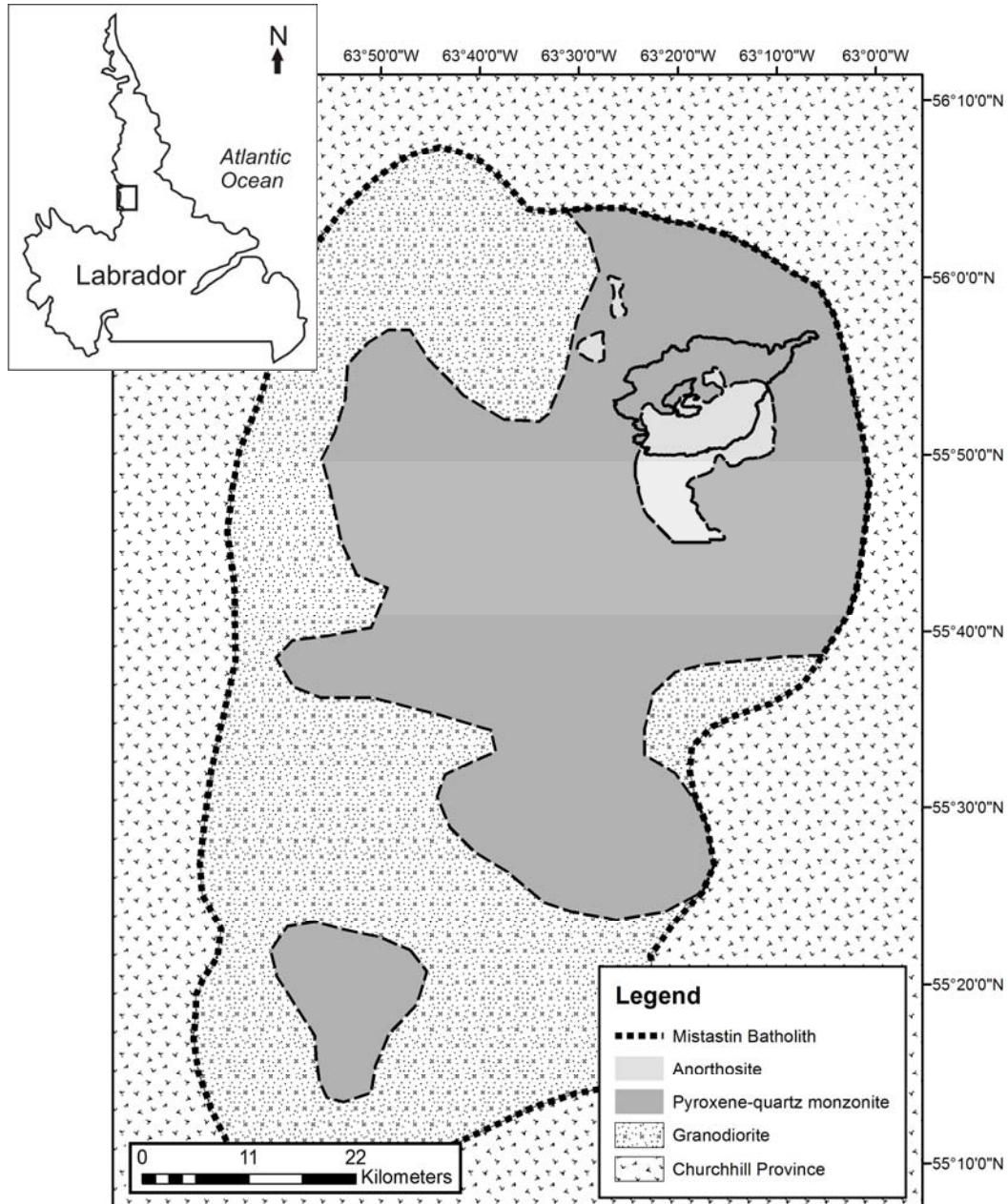


Figure 1-4: Geological map of the Mistastin batholith. Modified from Emslie et al., (1980).

Some impactites on Earth, such as breccias, are easily eroded due to their fractured and altered nature; the preservation of an almost complete suite of impact lithologies at Mistastin Lake facilitates the construction of a near intact section through an

intermediate, complex crater. In addition, the central uplift is dominated by anorthosite, a rock type similar to the lunar highlands.

1.3.1 Significant prior research

The earliest geological studies of the Mistastin Lake area were conducted as part of a reconnaissance mapping initiative by the Geological Survey of Canada (Currie, 1971a; Taylor and Dence, 1969). Taylor and Dence (1969) subsequently attributed the structure's origin to a comet or asteroid impact based on field and microscopic evidence including shattercones, planar deformation features (PDFs) in quartz and feldspar, and diaplectic quartz and feldspar glasses. Currie (1971) produced a map of the area, though he interpreted the roughly circular structure as being of volcanic origin. This interpretation has been refuted in all subsequent studies of the crater, which attribute its structure to an impact origin.

In the following decades, relatively little field mapping and geochronological work was conducted. The long accepted age of 36 ± 4 Ma, is based on $^{40}\text{Ar}/^{39}\text{Ar}$ from over 30 years ago (Mak et al., 1976). Recent work by Young et al. (2014) used *in situ* laser ablation $^{40}\text{Ar}/^{39}\text{Ar}$ geochronology to date the impact event at 36.6 ± 2.0 Ma (2σ) on impact melt samples. Their study suggested that the Mistastin impact was not part of the larger impact event that produced the Popigai 35.7 ± 0.2 Ma (Bottomley et al., 1997) and Chesapeake impact structures ~ 35 Ma (Deutsch and Koeberl, 2006), nor that it was the source of tektites collected from North America that have been dated at 35.3 ± 0.2 Ma (Deutsch and Koeberl, 2006).

The regional map of the Mistastin Lake area by (Currie, 1971a) remains the most detailed map published (1:50,000) to date, however, it includes inferred geological boundaries for melt rocks based on a volcanic origin interpretation. In addition, Currie's map show elongated belts of anorthosite and quartz monzonite trending northwest to southeast across a large granodiorite unit (Currie, 1971a) (Figure 1-5). Emslie et al. (1980) reinterpreted the distribution of Mistastin batholith components as amoeboid bodies, most notably expanding the boundaries of the anorthosite unit to include double the area previously mapped by Currie. Currie's (1971) map has been used as a basemap for all

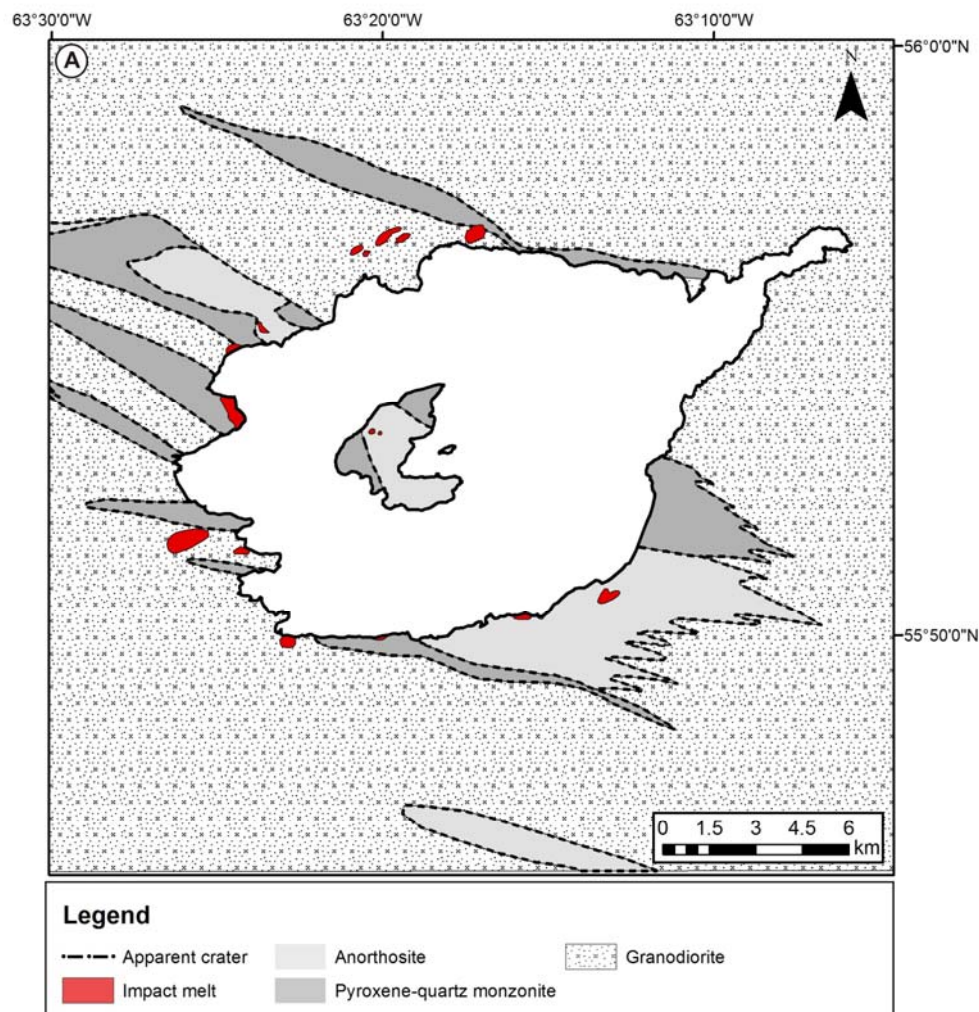


Figure 1-5: Simplified geological map of the Mistastin Lake region. Target rocks were mapped by Currie, 1971; impact melt was mapped by Grieve, 1975; Marion and Sylvester, 2010.

subsequent studies (e.g., Grieve, 1975; Marion and Sylvester, 2010; McCormick et al., 1989), which highlighted the distribution of melt rock exposures within the impact structure.

Most of the studies of the Mistastin impact structure have been geochemical in nature and have focused on characterizing the impact melt rocks (Grieve, 1975; Marchand and Crocket, 1977; Marion and Sylvester, 2010; McCormick et al., 1989). Little to no structural mapping of the Mistastin impact structure has previously been conducted. This

study presents new geological mapping results of the Mistastin Lake impact structure, highlighting structural features, distribution and field relationships of impactites and target rocks.

1.4 Thesis outline

The international community is motivated to continue lunar exploration to advance scientific knowledge of the Moon, and to learn how to live and work on the lunar surface. These endeavours benefit from analogue mission and comparative planetology studies to help inform future exploration strategies. Analogue simulations provide testing grounds on Earth and provide a means to safely prepare and advance lunar scientific instruments, enabling technologies, exploration strategies, system designs, and mission concepts. Currently, terrestrial impact craters provide the only means with which to ground truth such observations, particularly with respect to the third dimension, i.e., subsurface characteristics and contacts between units, which are not evident in lunar images or sampling. Overall, this thesis presents results of using the Mistastin Lake impact structure as a lunar analogue site for science and exploration goals.

Chapter 2 assesses (1) Potential hybrid geological field approaches for lunar exploration where objectives from both science-discovery and ISRU frameworks will be used during the same mission (either robotic precursor or human–robotic missions), and; (2) The possible evolution of a hybrid approach over the lifespan of lunar exploration from early (robotic precursor), middle (robotic and/or human short duration stays – possible establishment of an outpost), to late (long duration stays at an established outpost).

Chapter 3 reviews 5 key human exploration planetary analogue programs, including the NASA Extreme Environment Mission Operations (NEEMO), NASA Desert Research and Technology Studies (Desert RATS), NASA and Canadian Space Agency (CSA)-funded Pavilion Lake Research Project (PLRP), CSA-funded Impacts: Lunar Sample Return (ILSR), and the NASA and NSF-funded Antarctic Search for Meteorites (ANSMET). This study compares the mission operations and geological approaches of each campaign; identifies key operational commonalities and lessons learned; and highlights existing gaps that could be addressed in future analogue studies.

Chapter 4 presents results and conclusions from the Impacts: Lunar Sample Return (ILSR) campaign, that included two analogue missions conducted at the Mistastin Lake impact structure, Canada. The overarching goal for this study was to understand how to conduct human lunar exploration and to assess the utility of a robotic field reconnaissance mission as a precursor to a human sortie sample return mission. By implementing a rigorous evaluation plan, lessons learned related to developing new exploration strategies for robotic precursor and human lunar exploration, as well as guidelines for data management could be supported from multiple perspectives.

Chapter 5 provides the first detailed structural geology study of the Mistastin Lake impact structure based on structural mapping of remote sensing images and in the field. This study provides insights into crater formation and modification in crystalline target rocks, specifically the fault history, preservation state, crater form, and ultimately insights into the morphometrics of mid-size terrestrial complex structures (e.g., ~20–40 km).

Chapter 6 presents new geological mapping results of the Mistastin Lake impact structure highlighting textural features, distribution, and field relationships of impactites and target rocks within the collapsed rim region. It also includes petrographic results that place the impactite units in relation to the crater form based on field mapping, with particular focus on their origin and timing of formation.

Chapter 7 provides a discussion on the suitability of the Mistastin Lake impact structure as a lunar analogue site. It described the process for choosing this impact structure as a lunar analogue site, application to lunar exploration, and future work.

1.5 References

Ahrens, T.J., O’Keefe, J.D., 1972. Shock melting and vaporization of Lunar rocks and minerals. *Moon* 4, 214–249.

Ashley, J.W., Robinson, M.S., Hawke, B.R., Van Der Bogert, C.H., Hiesinger, H., Sato, H., Speyerer, E.J., Enns, a. C., Wagner, R. V., Young, K.E., Burns, K.N., 2012. Geology of the King crater region: New insights into impact melt dynamics on the Moon. *J. Geophys. Res. E Planets* 117, 1–13. doi:10.1029/2011JE003990

- Bottomley, R., Grieve, R., York, D., Masaitis, V., 1997. The age of the popigai impact event and its relation to events at the Eocene/Oligocene boundary. *Nature* 388, 365–368.
- Collins, G.S., Melosh, H.J., Morgan, J. V, Warner, M.R., 2002. Hydrocode Simulations of Chicxulub Crater Collapse and Peak-Ring Formation. *Icarus* 157, 24–33.
doi:10.1006/icar.2002.6822
- Currie, K.L., 1971. Geology of the resurgent cryptoexplosion crater at Mistastin Lake, Labrador: Geological Survey of Canada, Bulletin 207. Dept. of Energy, Mines and Resources, Ottawa, Canada.
- Currie, K.L., 1972. Geology and petrology of the Manicouagan resurgent caldera, Quebec, *Geol. Surv. Can. Bull.*
- Deems, E., Baroff, L., 2008. A systems engineering process for the development of analog missions for the Vision for Space Exploration, in: *Proceedings of the AIAA Space 2008 Conference*. San Diego, California.
- Dence, M.R., 1968. Shock zoning at Canadian craters: petrography and structural implications, in: French, B.M., Short, N.M. (Eds.), *Shock Metamorphism of Natural Materials*. Mono Book Corp, Baltimore, MD, pp. 169–184.
- Dence, M.R., 1972. The nature and significance of terrestrial impact structures, in: *24th International Geological Congress Section*. pp. 77–89.
- Deutsch, A., Koeberl, C., 2006. Establishing the link between the Chesapeake Bay impact structure and the North American tektite strewn field: The Sr-Nd isotopic evidence. *Meteorit. Planet. Sci.* 41, 689–703. doi:10.1111/j.1945-5100.2006.tb00985.x
- Dressler, B.O., Reimold, W.U., 2001. Terrestrial impact melt rocks and glasses. *Earth-Science Rev.* 56, 205–284. doi:10.1016/S0012-8252(01)00064-2
- Emslie, R.F., Cousens, B., Hamblin, C., Bielecki, J., 1980. The Mistastin Batholith, Labrador-quebec : An Elsonian Composite Rapakivi Suite. doi:10.4095/124073

French, B.M., 1998. Traces of Catastrophe: A handbook of shock-metamorphic effects in terrestrial meteorite impact structures, LPI Contribution No. 954. Lunar and Planetary Institute, Houston.

Gault, D.E., Quaide, W.L., Oberbeck, V.R., 1968. Impact cratering mechanics and structures, in: French, B.M., Short, N.M. (Eds.), *Shock Metamorphism of Natural Materials*. Mono Book Corp, Baltimore, MD, pp. 87–99.

Grieve, R.A.F., 1975. Petrology and chemistry of the impact melt at Mistastin Lake crater, Labrador. *Geol. Soc. Am. Bull.* 86, 1617–1629.

Grieve, R.A.F., Cintala, M.J., 1981. A method for estimating the initial impact conditions of terrestrial cratering events, exemplified by its application to Brent crater, Ontario, in: *Proceedings of the Lunar and Planetary Science Conference*. pp. 1607–1621.

Grieve, R.A.F., Dence, M.R., Robertson, P.B., 1977. Cratering processes: as interpreted from the occurrences of impact melts, in: Roddy, D.J., Pepin, R.O., Merrill, R.B. (Eds.), *Impact and Explosion Cratering*. Pergamon Press, New York, pp. 791–814.

Grieve, R.A.F., Therriault, A.M., 2013. Impactites: their characteristics and spatial distribution, in: Osinski, G.R., Pierazzo, E. (Eds.), *Impact Cratering: Processes and Products*. Wiley-Blackwell, Hoboken, NJ, pp. 90–105.

Hawke, B.R., Head, J.W., 1977. Impact melt on lunar crater rims, in: Roddy, D.J., Pepin, R.O., Merrill, R.B. (Eds.), *Impact and Explosion Cratering*. Pergamon Press, New York, pp. 815–841.

Hörz, F., 1982. Ejecta of the Ries Crater, Germany, in: Silver, L.T., Schultz, P.H. (Eds.), *Geological Implications of Impacts of Larger Asteroids and Comets on the Earth*. Geological Society of America, Boulder, pp. 39–55.

Hörz, F., Ostertag, R., Rainey, D.A., 1983. Bunte Breccia of the Ries - Continuous deposits of large impact craters. *Rev. Geophys. Sp. Phys.* 21, 1667–1725.

Howard, K.A., Wilshire, H.G., 1975. Flows of impact melt at lunar craters. *J. Res. U.S. Geol. Surv.* 237–251.

International Space Exploration Coordination Group (ISECG), 2013. The Global Exploration Roadmap.

Kenkmann, T., Ivanov, B.A., 2000. Low-angle faulting in the basement of complex impact craters; numerical modelling and field observations in the Rochechouart Structure, France, in: Gilmour, I., Koeberl, C. (Eds.), *Impacts and the Early Earth*. Springer, Berlin, pp. 279–308.

Kieffer, S.W., Simonds, C.H., 1980. The role of volatiles and lithology in the impact cratering process. *Rev. Geophys. Sp. Phys.* 18, 143–181.

Klassen, R.A., Thompson, F.J., 1990. Open File 2170: Glacial history, drift composition, and till geochemistry, Labrador.

Léveillé, R., 2010. A half-century of terrestrial analog studies: From craters on the Moon to searching for life on Mars. *Planet. Space Sci.* 58, 631–638.
doi:10.1016/j.pss.2009.04.001

Mak, E.K., York, D., Grieve, R.A.F., Dence, M.R., 1976. The age of the Mistastin Lake crater, Labrador, Canada. *Earth Planet. Sci. Lett.* 31, 345–357.

Marchand, M., Crocket, J.H., 1977. Sr isotopes and trace element geochemistry of the impact melt and target rocks at the Mistastin Lake crater, Labrador. *Geochim. Cosmochim. Acta* 41, 1487–1495.

Marion, C.L., Osinski, G.R., Abou-Aly, S., Antonenko, I., Barfoot, T., Barry, N., Bassi, A., Battler, M., Beauchamp, M., Bondy, M., Blain, S., Capitan, R.D., Cloutis, E.A., Cupelli, L., Chanou, A., Clayton, J., Daly, M., Dong, H., Ferrière, L., Flemming, R., Flynn, L., Francis, R., Furgale, P., Gammel, J., Garbino, A., Ghafoor, N., Grieve, R.A.F., Hodges, K., Hussein, M., Jasiobedzki, P., Jolliff, B.L., Kerrigan, M.C., Lambert, A., Leung, K., Mader, M., McCullough, E., McManus, C., Moores, J., Ng, H.K., Otto, C., Ozaruk, A., Pickersgill, A. E. Pontefract, A., Preston, L.J., Redman, D., Sapers, H.,

Shankar, B., Shaver, C., Singleton, A., Souders, K., Stenning, B., Stooke, P., Sylvester, P., Tripp, J., Tornabene, L.L., Unrau, T., Veillette, D., Young, K., Zanetti, M., 2012. A Series of robotic and human analogue missions in support of lunar sample return, abstract #2333, in: 43rd Lunar and Planetary Science Conference. The Woodlands, Texas.

Marion, C.L., Sylvester, P.J., 2010. Composition and heterogeneity of anorthositic impact melt at Mistastin Lake crater, Labrador. *Planet. Space Sci.* 58, 552–573.

doi:10.1016/j.pss.2009.09.018

McCormick, K.A., Taylor, G.J., Keil, K., Spudis, P.D., Grieve, R.A.F., Ryder, G., 1989. Sources of clasts in terrestrial impact melts: Clues to the origin of LKFM, in: *Proceedings of the 19th Lunar and Planetary Science Conference*. Lunar and Planetary Institute, pp. 691–696.

Melosh, H.J., 1989. *Impact cratering: A geologic process*. Oxford University Press, New York.

Melosh, H.J., Ivanov, B.A., 1999. Impact crater collapse. *Annu. Rev. Earth Planet. Sci.* 27, 385–415.

Mohanty, S., Nystrom, M., 2007. Fidelity Evaluation Framework for Planetary Mission Simulator: Part III: Applying the Framework, in: *IAC-07-E5.4.02, 58th International Astronautical Congress*. Hyderabad, India.

Murtaugh, J.G., 1976. Manicouagan impact structure. Pen-File Report DPV-432.

NASA, 2011. *NASA's Analog Missions: Paving the Way for Space Exploration*. NASA Langley Research Center, Hampton, VA.

National Research Council, 2007. *The Scientific Context for Exploration of the Moon: Final Report*. The National Academies Press, Washington, DC.

O'Keefe, J.D., Ahrens, T.J., 1982. Cometary and meteorite swarm impact on planetary surfaces. *J. Geophys. Res.* 103, 28607.

- Oberbeck, V.R., 1975. The role of ballistic erosion and sedimentation in lunar stratigraphy. *Rev. Geophys. Sp. Phys.* 13, 337–362.
- Öhman, T., Kring, D. a., 2012. Photogeologic analysis of impact melt-rich lithologies in Kepler crater that could be sampled by future missions. *J. Geophys. Res. E Planets* 117, 1–21. doi:10.1029/2011JE003918
- Osinski, G.R., L  veill  , R., Berinstain, A., Lebeuf, M., Bamsey, M., 2006. Terrestrial analogues to Mars and the moon: Canada’s role. *Geosci. Canada* 33, 175–188.
- Osinski, G.R., Pierazzo, E., 2013. *Impact cratering: processes and products*. Wiley-Blackwell, Hoboken, NJ.
- Osinski, G.R., Spray, J.G., Lee, P., 2005. Impactites of the Haughton impact structure, Devon Island, Canadian High Arctic. *Meteorit. Planet. Sci.* 40, 1789–1812.
- Osinski, G.R., Tornabene, L.L., Grieve, R. a. F., 2011. Impact ejecta emplacement on terrestrial planets. *Earth Planet. Sci. Lett.* 310, 167–181. doi:10.1016/j.epsl.2011.08.012
- Persaud, R., 2004. A systematic approach to investigations at Mars analog research stations, in: Cockell, C. (Ed.), *Martian Expedition Planning*. American Astronautical Society: Science and Technology Series.
- Shoemaker, E.M., 1960. Penetration mechanics of high velocity meteorites, illustrated by Meteor Crater, Arizona, in: 21st International Geological Congress. Int. Union of Geol. Sci., Trondheim, Norway, pp. 418 – 434.
- Snook, K.J., Mendell, W.W., 2004. The need for analogue missions in scientific human and robotic planetary missions, in: XXXV Lunar and Planetary Science Conference, Abstract #2130. League City, Texas.
- St  ffler, D., Artemieva, N.A., Pierazzo, E., 2002. Modeling the Ries-Steinheim impact event and the formation of the moldavite strewn field. *Meteorit. Planet. Sci.* 37, 1893–1907. doi:10.1111/j.1945-5100.2002.tb01171.x

Stöffler, D., Grieve, R.A.F., 2007. 11. Impactites. Recommendations by the IUGS Subcommission on the Systematics of Metamorphic Rocks, in: Fettes, E., Desmons, J. (Eds.), *Metamorphic Rocks : A Classification and Glossary of Terms : Recommendations of the International Union of Geological Sciences Subcommission on the Systematics of Metamorphic Rocks*. Cambridge University Press, pp. 82–92.

Sullivan, T.A., 1994. *Catalog of Apollo Experiment Operations: NASA Reference Publication 1317*, NASA Reference Publication 1317. NASA, Houston, TX.

Taylor, F.C., Dence, M.R., 1969. A probable meteorite origin for Mistastin Lake, Labrador. *Can. J. Earth Sci.* 6, 39–45.

Turtle, E.P., Pierazzo, E., Collins, G.S., Osinski, G.R., Melosh, H.J., Morgan, J.V., Reimold, W.U., 2005. Impact structures: What does crater diameter mean?, in: Kenkmann, T., Hörz, F., Deutsch, A. (Eds.), *Large Meteorite Impacts III*, Geological Society of America Special Paper 384. Geological Society of America, Boulder, CO, pp. 1–24. doi:10.1130/2005.2388 (06).

Young, K.E., Mercer, C.M., Soest, M.C. Van, Hodges, K. V, Wartho, J.-A., Biren, M.B., 2014. An examination of noble gas geochronology and thermochronology in the context of dating impact events, in: *45th Lunar and Planetary Science Conference, Abstract #2670*. Woodlands, TX, pp. 4–5. doi:10.1002/jgre.20118.

Chapter 2

2 Unifying science-driven and resource exploitation strategies for lunar missions: Applying lessons learned from terrestrial geological exploration and Canadian planetary analogue missions.

Future lunar missions will be based on a very different framework than what was used for the Apollo program. A “Moon First” scenario as envisioned in the Global Exploration Roadmap (International Space Exploration Coordination Group, 2011) specifically leverages lunar exploration as a means to develop capabilities that will enable further human exploration to near Earth asteroids (NEA) and Mars. Within this context, there is a need to develop lunar resources as a paradigm for extended human exploration of both the Moon and other planetary destinations. In parallel, the scientific community aims to advance our knowledge of the Moon’s geologic history and evolution in order to address fundamental questions about the solar system, the universe, and our place in them (CSEW6 Steering Committee, 2009; Lunar Exploration Analysis Group, 2011a; National Research Council, 2007). Attaining these goals will require conducting geological investigations on the lunar surface.

The objectives of this study were two-fold:

- 1) Review terrestrial geological field approaches and field strategies tested in Canadian lunar analogue missions and compare them to current lunar exploration goals related to geological field work;
- 2) Devise potential hybrid geological field approaches for lunar exploration that address objectives of science-discovery and *in situ* resource utilization (ISRU) frameworks, and map their evolution over time.

In conducting this study, findings and recommendations were used from the current version of the Lunar Roadmap (Lunar Exploration Analysis Group, 2011a), the June 16-17, 2011 LEAG Lunar Exploration Roadmap Workshop focussed on development of a robotic implementation strategy (Lunar Exploration Analysis Group, 2011b), and the

workshop on Strategic Knowledge Gaps for the “Moon First” Human Exploration Scenario conducted by LEAG and the GAP-Specific Action Team (Shearer and Neal, 2012). All of these documents are available on the LEAG website (see <http://www.lpi.usra.edu/leag>). This study assumes the same stages for lunar exploration as defined by these reports:

- Early: Robotic precursors and up to the second human landing in this new (post-Apollo) exploration series (≤ 14 Earth days);
- Middle: Initial outpost build-up to including stays of ~ 30 Earth days and including part of the lunar night, as well as robotic missions;
- Late: Outpost established, stays of > 30 days, including robotic missions.

A pivotal outcome of the LEAG reports (Lunar Exploration Analysis Group, 2011a, 2011b; Shearer and Neal, 2012) is that surface prospecting will be a primary geological driver for early missions. Surface prospecting involves searching for materials on the lunar surface that can be used to help sustain a human presence on the Moon and that will help to reduce payloads launched from Earth required for Solar System exploration. Key geological resources of interest are volatiles, notably hydroxyl (OH-) and frozen water (H₂O). Recent remote sensing studies suggest that the formation and retention of hydroxyl and water are on-going surficial processes (Pieters et al., 2009) and that water ice may make up as much as, 5-22% (up to 30%) of the surface material in cold traps such as permanently shadowed craters (Thomson et al., 2012; Zuber et al., 2012). The lunar regolith is a primary candidate source for these volatiles.

Lunar prospecting will involve (Lunar Exploration Analysis Group, 2011b):

- Identifying resource-rich sites for targeting future missions;
- Establishing accuracy of remote sensing measurements;
- Defining the composition, form, and extent of the resource (both laterally and vertically over a km scale);

- Characterizing the environment in which the resources are found;
- Defining the accessibility/extractability of the resources;
- Quantifying the geotechnical properties of the lunar regolith in the areas where resources are found.


Although prospecting for volatiles may be a primary geological goal of early missions, many of the science goals as outlined in the “Scientific context for the exploration of the Moon” report (National Research Council, 2007) and in the “Lunar Roadmap” (Lunar Exploration Analysis Group, 2011a) can be addressed by the above mentioned tasks (see Table 2-1). To gain a better understanding of what is required for lunar prospecting and geological field mapping, the following study outlines terrestrial field mapping practices, reviews findings from geological lunar analogue missions led by the University of Western Ontario, Canada, discusses adapting geological field approaches for lunar environment, and ultimately links these field techniques and lessons learned to develop a geological exploration strategy by highlighting mapping methods needed to address a specific lunar science goal.

2.1 Review of terrestrial field geology techniques

On Earth, there is no one universal technique for geological fieldwork and strategies for geological exploration are highly dependent on science objectives, which in turn influence what type of data will be collected and what instruments will be used. The same is true for lunar exploration.

Terrestrial geological exploration involves many sub-disciplines, including, but not limited to, field mapping, geophysical surveying, geochemical sampling, and supporting laboratory practices. Often these disciplines complement one another. However, they are typically not conducted simultaneously and often not even during the same field season. They involve varying amounts of time to complete, and they use different approaches (e.g., the exploratory approach of field mapping versus the execution approach of geophysical surveys).

Table 2-1: Prioritization of lunar science goals over time assuming that prospecting for lunar volatiles is the primary motivation (adapted from the Lunar Exploration Roadmap; Lunar Exploration Analysis Group, 2011a).

Priority	ROBOTIC MISSIONS ONLY (including Precursors)	ROBOTIC and SHORT HUMAN SORTIES (within 1 lunar day)	ROBOTIC and MEDIUM HUMAN SORTIES (Including part of the lunar night)	OUTPOST and ROBOTIC MISSIONS
High 	Objective Sci-A-3: Characterize the environment and processes in lunar polar regions and in the lunar exosphere.	Objective Sci-A-2: Development and implementation of sample return technologies and protocols.	Objective Sci-A-2: Development and implementation of sample return technologies and protocols.	Objective Sci-A-2: Development and implementation of sample return technologies and protocols.
	Objective Sci-A-2: Development and implementation of sample return technologies and protocols.	Investigation-Sci-A-3A: Map and characterize polar cold traps.	Investigation-Sci-A-3C: Determine bedrock geology of polar regions.	Investigation-Sci-A-3C: Determine bedrock geology of polar regions.
	Investigation-Sci-A-3A: Map and characterize polar cold traps.	Investigation-Sci-A-3B: Map and characterize quasi-permanently illuminated areas.	Investigation-Sci-A-3D: Understand volatile sources and mechanisms of transport and deposition.	Investigation-Sci-A-3D: Understand volatile sources and mechanisms of transport and deposition.
	Investigation-Sci-A-3B: Map and characterize quasi-permanently illuminated areas.	Objective Sci-A-4: Understand the dynamical evolution and space weathering of the regolith.	Objective Sci-A-4: Understand the dynamical evolution and space weathering of the regolith.	Objective Sci-A-4: Understand the dynamical evolution and space weathering of the regolith.
	Objective Sci-A-4: Understand the dynamical evolution and space weathering of the regolith.	Objective Sci-B-1: Understand the impact history of the inner Solar System as recorded on the Moon.	Objective Sci-B-1: Understand the impact history of the inner Solar System as recorded on the Moon.	Objective Sci-B-1: Understand the impact history of the inner Solar System as recorded on the Moon.
	Objective Sci-B-1: Understand the impact history of the inner Solar System as recorded on the Moon.	Objective Sci-B-2: Regolith as a recorder of extra-lunar processes.	Objective Sci-B-2: Regolith as a recorder of extra-lunar processes.	Objective Sci-B-2: Regolith as a recorder of extra-lunar processes.
	Objective Sci-B-2: Regolith as a recorder of extra-lunar processes.	Objective Sci-D-9: Investigate the production of oxygen from lunar regolith in lunar gravity.		

A generalized geological exploration approach for an unknown area may involve starting from a large scale and then progressively focusing the geographic area of study. This could include first reviewing remote sensing images (e.g., satellite images), followed by reconnaissance geophysical surveys (typically airborne), reconnaissance field mapping, then ground geophysical surveys and perhaps statistical sampling. The aforementioned may lead to the identification of zones of interest which are then mapped in detail by a field geologist who can identify sites for drilling, trenching, and detailed sampling. Following field work, detailed petrological and chemical studies can be conducted on collected samples in laboratory facilities. This allows for a much better definition of the different geologic units within a given field area, their relationship to each other, and it assists in deciphering the geological history of the area.

Geological field methods can broadly be divided into two types herein termed adaptive-exploratory and fixed-executional styles. Each requires a field plan (e.g., traverse routes, sampling style) to be made beforehand. The primary differences between the two approaches is the necessity to adapt the field plan, or not, during the traverse and the geological expertise of the agent conducting the field work. An adaptive-exploratory style requires a skilled-agent able to observe and interpret geological features as they progress along the traverse. The agent's expertise allows them to adapt the traverse plan to best address the mission objectives. In contrast, the fixed-execution style requires that a given set of instructions is followed - the traverse route does not change based on the data collected during the survey. A skilled agent in geological field mapping is not necessarily required to conduct this fixed approach.

2.1.1 Adaptive–exploratory geological mapping techniques

Geologic mapping involves gathering information in the field on rock type, mineralogy, and structure at as many bedrock exposures ("outcrops") as possible. The data is in turn used to interpret the geology of a particular area, including geological processes and climatic histories which affected/formed the rocks. Geological data is plotted on a geographic base – usually either a topographic map or an aerial photograph – and then contact lines between the various geologic units are drawn.

In general, the accuracy of the geological contacts is dependent on the accessibility of exposed bedrock and the number of observations that are taken in an area. A geological contact can be drawn using different types of lines that represent the geologist's confidence in the location of the contact; including, inferred (least confident), approximately located, and defined, and thus reflects the accuracy of the map.

Traditionally, mapping in the field has been done 'manually' using pen and paper. It is now becoming increasingly popular to use digital mapping practices which utilize GIS software and handheld or tablet computers. The use of remotely sensed images layered in a GIS has also greatly enhanced the process of geological field mapping as they can provide more geological information for the base map while in the field.

2.1.1.1 Reconnaissance mapping

'Classical' field mapping is often referred to as reconnaissance mapping and is achieved through the study of bedrock exposed at the surface in outcrops. This method interprets the distribution of geological units and the extent of the resultant map depends on the area covered, level of detail desired and the time available for the mapping project. Mapping scales can vary (e.g., 1:10,000 to 1:250,000), and tend to use air photos or topographic maps as a base for mapping onto.

Each discrete locality of interest is treated as a 'station'. Its location is marked on a base map and geological data including a description, GPS coordinates, sketches, photographs, structural measurements, and samples are collected (see "Data acquisition at a specific site" section below). The final products are typically a map dividing the area into representative rock units (based on a combination of defined, approximate, and inferred lines of contact) and a suite of samples representing each unit, including intra-unit variations.

Reconnaissance mapping utilizes both a variety of terrain features to maximize the access to exposed bedrock (e.g., looking at stream channels to find exposures) and pre-conceived ideas about the geology of a particular area in order to plan field operations, typically in the form of traverses. Traverse planning is based on the objective of the

mapping and access to the relevant terrain and exposed bedrock. Reconnaissance mapping can be used for a range of scales; the level of detail is dependent on the objective of the study and on the map base. Reconnaissance mapping can incorporate specific mapping techniques and data acquisition techniques as listed below, and/or lead to follow-on detailed studies which utilize these techniques.

2.1.1.2 Contact mapping

Contact mapping is used in areas that are well exposed; a geologist is able to follow the line of contact between two adjacent rock units across the area of interest. The route of travel is thus dependant on the information gathered at each progressive field site and an ‘on-the-fly’, adaptable approach to setting traverses is required. The contact between different rock units can provide information on a multitude of critical aspects of geology, including the type of geological processes the unit has undergone (e.g., deformation, metamorphic), method of formation (e.g., depositional, igneous emplacement) and the relationship between different rock units.

The geologist follows the line of contact and marks the boundary on the base map as the traverse progresses. In order to conduct a complete investigation, traverse lines perpendicular to contacts are necessary to understand the variability within a particular unit. As the mapping proceeds, the map becomes progressively filled in with the underlying bedrock geology. The final products are typically a map dividing the area into representative rock units (based largely on defined contacts) and samples of rock units from the vicinity of contacts.

2.1.1.3 Pace-and-compass mapping

This style of mapping is typically used in areas where the underlying bedrock is obscured and long distance viewing is difficult. Pace-and-compass mapping involves a set course that is predetermined by analysing the topography and estimating the likely location of bedrock outcrops, and a geologist follows a particular azimuth in the hope of encountering an outcrop. Historically, geologists have used a compass and length of their walking stride to measure the set traverses and to stay on course. Today, a hand-held global positioning system (GPS) device is typically used and has greatly increased the

accuracy of this type of mapping. This type of mapping is usually complemented by remote data gathering such as aeromagnetic surveys or ground-based gravimetric surveys to help fill in the gaps of geological information and to provide more information on a regional scale.

The products include a map which shows where the outcrops are, a geological map based on the interpretation of the outcrop map (mostly approximate contacts), and representative samples from each outcrop. The geological map will not likely represent the complexity of the area due to the limited exposure, which can lead to misinterpretations of rock units. Pace-and-compass mapping is one of the least efficient forms of mapping as the geologist must follow specific lines of traverses (e.g., a grid), which may or may not have outcrops along them. However, in many parts of the world, it is the only way to do a preliminary assessment of the geology of a particular area.

Data acquisition at a specific site

For adaptive-exploratory methods, specific tasks are performed at each site of interest, including:

- A description (typically written) is completed of the site (e.g., outcrop of rocks), regional context, as well as of any samples collected (e.g., describe mineralogy, texture, colour, etc.).
- The location is noted on a base map and GPS coordinates are recorded.
- Typically an overview photograph and/or sketch are taken which provides the regional context of the outcrop; it is important to note the direction in which the photograph is taken. A scale is used in all photographs and sketches. Detailed photographs and sketches are taken of critical features. Sketches remain important even today as it is only in this way that important observations (e.g., presence of a fault, different rock unit) are noted – this can be replaced by digitally annotated photographs. Sketches are interpretative, and are often more illustrative of the geology than a photograph, particularly in areas where significant surface cover

obscures large scale relationships. However, both photographs and sketches are critical field data.

- Geological measurements such as the attitudes of any structural features are measured and recorded (e.g., planar features such as beds, foliations, cross-cutting features such as dykes; linear features such as fold axes, mineral lineations). Other geological measurements could include measuring stratigraphic sections, which are representations of the vertical variation in rock units at a site.
- Representative samples of exposed rock types or overburden (e.g., float, soil) are collected. Samples are collected in conjunction with mapping (from localities marked on the base map). It is critical to have an understanding of the regional context from which the sample was collected in order to interpret how rock units relate to each other.

Samples are typically analysed in a laboratory after they have been returned from the field. Micro-scale features are observed using various microscopic techniques and the chemical composition of the rock is measured. Data collected from the sample are often extrapolated and considered representative of the sampled rock unit. This information is used to interpret the crystallization history, deformation history, deposition history and environment, geochemical evolution, isotopic composition, radiometric age and mode(s) of origin of the rock unit.

Techniques and tools used to collect samples include:

- Rock hammer: Allows samples to be collected from outcrops and can break large samples into smaller pieces. Although lacking the precision of a drill, a hammer is simple, and often more adaptable to field environments.
- Drill: Allows collection of core samples and remaining boreholes can be useful in providing three-dimensional geological information, particularly in areas that lack topography and rock exposures. Drilling is, by definition, expensive, and drill holes are only sited after a good understanding of the geology is in hand.

- Trenching tools: A trench can be dug by hand or by heavy machinery (bulldozer, excavator, or back-hoe), which are commonly used in mineral exploration campaigns. Ideally, trenches should be at least 1 m in width and the excavator should be able to penetrate at least 1 m into recognizable bedrock (Marjoribanks, 2010). A trench will allow detailed description and sampling of a particular location, with more lateral detail available than can be seen in a single deep drill core.
- Shovel: Can be used to collect unconsolidated samples from the surface and can be used to create trenches, which allow for mapping vertical variations exposed along trench walls. In unconsolidated rocks, such as glacial deposits and some volcanic rocks, holes are dug with a simple field shovel and are often used to characterize geologic relationships at the cm-scale that are otherwise not exposed.

2.1.2 Fixed – executional geological mapping techniques

Several geological mapping techniques involve collecting data along a set course and interpreting the data after the survey is completed. The survey route does not change while the data is being collected – it is fixed. In many cases, an untrained geologist can conduct the survey, although interpretation of the data requires geological expertise.

2.1.2.1 Float/soil mapping

Float/soil mapping is used in areas in which there is no access to and/or exposure of bedrock. The distribution of a particular rock type is determined based on “float” or distinctive soil characteristics developed through weathering of the parent unit. “Float” is a geologic term that refers to pieces of rock that have become detached from an outcrop and which may have also been moved by erosion to a new location (e.g., at the base of a steep slope).

Float/soil mapping is particularly useful in filling in the gaps when constructing a large-scale reconnaissance map. This style of mapping results in a suite of samples that are subsequently used to compare with samples from outcrops within the area of interest. Contacts on geological maps are inferred based on the relative abundance of float

samples from different rock units, suggestive second-order data such as topography, and on interpretations that might be inferred from any outcrops within the field area. It is rare to produce an entire geologic map strictly on the basis of float and it is generally considered the least effective geological approach to developing a map.

2.1.2.2 Geostatistical sampling

Geostatistical sampling is used in areas in which there is little or no bedrock exposure. It involves the systematic collection of data, either through collection of surface soil samples or by drilling boreholes. Geostatistical sampling is meant to be predictive, and is based on the assumption that the properties of the overburden (e.g., geochemistry of soil) are dependent on geological principals (e.g., pattern of deposition or emplacement of underlying bedrock).

Samples are typically collected along some form of defined grid, which is designed to be dense enough to allow for statistically meaningful predictions for a given area. This method is often used for mineral exploration. Samples collected along a grid are assayed and the element of interest can be plotted on a geographic base (e.g., topographic map) using statistical analysis. Contour lines can be plotted which indicate higher and lower zones of concentration. This is a standard procedure that can be performed using GIS software. Often, the primary map can define areas that deserve more detailed sampling and mapping.

Geostatistical sampling can also be used in an attempt to sample all the geological units of a particular area. At each site, samples of a given size are collected and categorized based on rock type. The abundance of different rock types collected at different sites is assumed to represent the relative abundance of surrounding rock units. The products include a statistically significant number of samples and a geographic map showing sample locations. Various derivatives of this map can be created using statistical analysis (e.g., creation of a contour map showing element concentrations).

2.1.2.3 Field geophysical techniques

Geophysical techniques gather information of the subsurface remotely. Typically, for investigations on land, aerial surveys are initially conducted to assist geological mapping and to help identify target areas for more detailed surveys. Ground techniques are subsequently used to test targets discovered by the reconnaissance surveys.

Geophysical data are plotted on graphs and/or can be represented on a geographic base using GIS software. Geophysical methods do not typically give unique, unambiguous solutions. The confidence of the interpretation increases with better understanding of the surface geology and topography. Remotely gathered geophysical data can be very useful in helping to fill in blank spots of a geological map by providing a better sense of either regional structure and fabric, or regional variations in the overall distribution of rock units. All geophysical data require extensive, post-collection data reduction and modelling to generate a useful product.

Gravity survey

Gravity surveying for geological studies is a passive technique that measures the variations in the gravitational pull of the Earth. Subtle changes in gravity result from variations in the density of materials within the subsurface. These variations can be due to local changes in rock types; for example, clastic sedimentary rocks are less dense than granite, which is in turn less dense than basalt. An understanding of the geology of a particular area by way of an accurate geologic map is necessary to extrapolate surficial geology to presumed subsurface rocks

Gravimetric surveys involve taking repeated measurements of the magnitude of gravitational acceleration throughout the area in question, with periodic reacquisition of base stations to re-calibrate the gravimeter. The effects of tidal and instrument drift that would otherwise mask any subtle anomalies are overcome by repeat readings at a fixed base station throughout the survey. Accurate topographic levelling is carried out at each station in order to correct for the effects of terrain.

Magnetics survey

Magnetic profiling is a passive technique that involves measurement of the total amplitude of the Earth's magnetic field. Magnetometer surveys map local disturbances in the earth's magnetic field that are caused by magnetic minerals in the upper regions of the earth's crust.

If the object of the survey is to make a rapid reconnaissance of an area, a magnetic-intensity profile is made only over the target area. If the object of the survey is to delineate already discovered structures, the geophysicist sets up a grid over the area and makes measurements at each station on the grid. The corrected data that is recorded is then entered on a scale drawing of the grid, and contour lines are drawn between points of equal intensity to give a magnetic map of the target area that may clearly indicate the size and extent of the anomalous body to the trained eye of the interpreting geophysicist.

Electrical and electromagnetic surveys

Electrical and electromagnetic methods are both used to map variations in the electrical properties of the subsurface and essentially measures electrical conductivity (i.e., how easily an electrical current can pass through a material). Electrical surveys pass an electrical current directly into the ground using electrodes and measure the resulting potential difference within the subsurface using detectors which are placed along a surveyed line. In comparison, electromagnetic methods induce currents in the ground by the passage of electromagnetic waves. The indirect nature of electromagnetic methods makes it possible to take measurements from the ground and also from specially adapted aircraft, whilst electrical methods are restricted to ground based measurements.

Subsurface materials exhibit a very large range of electrical conductivity values, which is primarily governed by the amount of water filling the gaps between the mineral grains and the amount of salt dissolved in this water. Areas of high interstitial water content have lower resistance to an electrical current than do dry areas. Rock units of differing composition will have variable natural electrical conductivity. Metallic minerals

containing are very good conductors in their native metal state and are easily detected using electrical and electromagnetic methods (e.g., iron, copper, nickel, silver, gold).

Seismic surveys

Seismic surveys essentially generate a ‘picture’ of the subsurface geology. A controlled seismic source of energy is provided by a source ('shot') located on the surface. Energy radiates out from the shot point and travels laterally and/or vertically before returning to the surface. Reflected and refracted signals are recorded by an array of receivers called geophones. Sound waves travel through the subsurface and change speed when passing through rocks of different densities, and reflect (bounce back) at the contact between these rock types. By noting the time it takes for a reflected or refracted wave to arrive at a receiver, the depth of the feature that generated the reflection is estimated. In order to estimate this depth, the subsurface geology is assumed based on previous (surface) field work.

The detail and depth investigated by seismic surveys is based on input energy magnitude, input energy frequency, and number and spacing of the geophone lines. The quality of the final seismic survey is only as good as the input parameters to the model. Complex geology can go undetected if the modelling does not bring it out of the seismic signals. The depth of investigation can range from near surface to, in extreme cases, the radius of a particular planet, making it very useful for conducting investigations at multiple scales.

2.2 Review of the University of Western Ontario’s lunar analogue activities

Lunar analogue (i.e., simulated) missions on Earth at scientifically relevant sites, can help test and advance lunar scientific instruments, enabling technologies, exploration strategies, system designs, and mission concepts. NASA and other space agencies have acknowledged the usefulness of analogue activities for decades to prepare for space missions (Deems and Baroff, 2008; NASA, 2011) and the international community has identified analogue activities as a strategic mechanism for collaboration (Ehrenfreund et al., 2012; International Space Exploration Coordination Group (ISECG), 2013).

In order to prepare and test protocols for future lunar sample return missions, The University of Western Ontario-led team carried out two geology-focussed analogue missions at the Mistastin Lake impact structure lunar analogue site, funded by the Canadian Space Agency (CSA) (Marion et al., 2012). The field approach for each mission was driven by the overarching science objectives: to further our understanding of impact chronology, shock processes, impact ejecta and potential resources. Our scientific approach mirrored exploration strategies for traditional geological exploration and field campaigns conducted on Earth, by 1) Using orbital and aerial data sets to assess geologic diversity, landing site selection, and accessibility/traverse planning; 2) Conducting reconnaissance surface mapping to get an overview of the site from the ground; 3) Follow-up detailed traverses, to study sites of interest in detail.

The first mission was a robotic precursor mission in advance of a follow-on human mission that would then use the existing robotic agent as a field assistant. For each deployment a Mission Control team was based at the University of Western Ontario located in London, Ontario, over 1900 km away; communication was via satellite terminal in the field, with total daily data budgets of ~100 MB at a variable rate between 85-400 kb/s. Neither the Mission Control team nor the ‘astronauts’ had visited the site and only had access to remote sending precursor data, consistent with present-day lunar data sets, prior to the mission.

It is important to note that, analogue missions conducted on Earth can only ever simulate some aspects of actual planetary missions, and it is necessary to state these limitations for each test mission. For example, the University of Western Ontario-led analogue mission campaign was science-driven and was, thus, conducted at a suitable geological lunar analogue site (i.e., an impact crater with anorthositic target rock). The rocks types were similar to a crater in the lunar highlands, however, the exposure sizes, vegetation cover, lighting conditions, atmosphere, temperature, gravity, were all different than the lunar surface. In addition, numerous technical and operational mission aspects were not simulated. For example, no mechanical robot was used for the robotic precursor mission; instead, a field team of five people, including the first author, acted collectively as the robot. For the second analogue mission of the campaign, the ‘astronauts’ conducted

geology in a shirt-sleeve environment (i.e., they did not wear simulated space suits), and off-the-shelf instruments and rover platforms were used, instead of flight ready hardware.

2.2.1 Robotic precursor mission

The first mission took place over three weeks in August and September 2010 and involved robotic reconnaissance mapping of sites selected using remote sensing satellite data and aerial images. A field team of five people simulated the rover data collection – they made traverses with science instruments, collected data as requested by Mission Control, and sent the data to the remote Mission Control team using satellite communication (Mader et al., 2012; Mader et al., 2011).

For each site of interest (SOI), the Mission Control science team conducted a general site survey (Shankar et al., 2011) using panoramic image data collected by the ‘rover’ in order to 1) identify the prime direction for rover traverse, 2) identify and prioritize several outcrop scale sites of interest from surface data, and 3) select a primary target for detailed analysis. Once data from a primary target was acquired, site surveying followed the same trend of identifying and prioritizing sub-outcrop scale SOI’s to capture higher resolution images and geochemical data based on scientific interest. At sub-outcrop scales, locations for X-Ray Fluorescence (XRF) analyses were selected using high resolution digital photos. Care was taken to avoid strongly weathered and lichen-covered surfaces. Lidar data were used to interpret rover position and orientation. Ground penetrating radar (GPR) profiles were collected along rover paths to examine and help interpret the geology beneath the surface (i.e., stratigraphy and structural geology). All rover instructions to the ‘rover’ and interpretations were conducted by the Mission Control team; the ‘rover’ did not make autonomous decisions regarding data collection and interpretation.

2.2.2 Follow-on human with robotic assistant mission

The reconnaissance robotic mission was followed by a second, one-week mission, at the same location in 2011, which included an actual mechanical rover and simulated astronaut surface operations. Two PhD students acted as astronauts – one a geology graduate student with prior geological mapping field experience and specializing in

impact cratering products (i.e., impactites), and the other, a pilot with an engineering background and some geologic training (similar to many Apollo astronauts).

A ROC6-type six-wheeled rover was used as a robotic field assistant to the astronauts. The rover was equipped with a vision-based autonomous navigation system (Furgale and Barfoot, 2010) and the same instruments as in the precursor rover scenario. The vision system allowed the rover to be commanded to return to any point it had previously occupied; these capabilities greatly reduced the amount of detailed mobility planning required in Mission Control compared to what would have been required in the absence of the navigation system (Francis et al., 2012).

The greater mobility, judgment, and visibility of the astronauts was used to augment the navigation system by having the engineer astronaut direct the rover to sites of interest, thus building up a network of safe paths. Once taught a path by the astronaut, the rover's autonomous-return capability allowed it to return along that path to the site of the lander, or to revisit the same or another site, as desired.

To make use of this capability, EVAs were scheduled to begin with a period of robotic operations, in which the engineer astronaut would direct the rover to a new site of interest, while the geologist astronaut would conduct geological tasks at a nearby site. Once the rover's destination was reached, both astronauts would move away to work at a separate site, with the rover left to collect data from the outcrop of interest with its suite of instruments, under the direction of Mission Control.

2.2.3 Analogue mission findings

Exploratory, robotic reconnaissance controlled by a Mission Control has the potential to significantly improve scientific return from lunar surface exploration. In particular, data from robotic precursor missions can be used to narrow scientific focus (i.e., develop specific research questions and hypotheses to test), improve traverse planning, reduce operational risk, and increase crew productivity (Mader et al., 2011).

The main scientific value of an exploratory reconnaissance mission is providing surface geology visualization at resolutions and from viewpoints not achievable from orbit,

including high resolution surface imagery of surrounding areas on the scale of 10's of meters up to several km in extent. The most used data sets included large scale panoramic images that allowed a full contextual view of the surrounding area including exposure of rocks and traversability of the area and lidar scans that provided range and scale information (Mader et al., 2012).

The most useful data products for Mission Control scientists were panoramic images and lidar scans taken from 'safe' vantage points looking at 1) steep topography (which allows a cross-sectional view of stratigraphy within rocks) taken from below the rock exposure; and 2) overview of landscape taken from a topographic high.

This precursor rover could be used as an assistant for a later human mission. We found that a robotic assistant contributes in off-loading particular tasks from the astronauts (Francis et al., 2012). Tedious or precise instrument work, such as GPR surveys, XRF analyses, drilling, is better assigned to the robot, leaving the astronauts to spend the EVA time on other activities best suited to humans. There is a safety implication as well – instruments whose operation might be hazardous to an astronaut – perhaps x-ray sources or drills – can be operated when the astronauts are safely away from the rover. As well, the rover's navigation system, with its ability to return to the lander precisely and on command, presents the possibility of a safe route home for a disoriented astronaut.

Finally, the astronaut operator provides benefits to the rover beyond better terrain judgment and swifter operation (Francis et al., 2012). The astronaut can not only judge terrain more quickly than the remote operators, but can also modify it, removing small obstacles to open up new areas to the rover. This was done on several occasions in the scenario, enabling the rover to move into areas it otherwise could not have reached.

2.3 Adapting geological field work for lunar exploration

Contemporary geological maps are modeled after the first published geological map of England and Wales, made by William Smith in 1815 (Smith, 1820). The same basic requirements for geological field work have been used for the past 200 years, including (Eppler, 2008):

1. Access to the locations of interest;
2. Position knowledge;
3. Tools that allow collection of a variety of samples;
4. Ability to discriminate between different surface units and to take detailed observations of outcrops and rocks;
5. Image capture of locality of interest and surrounding area;
6. Recording data (e.g., sample documentation, position, marking location on map).

These tasks will also be necessary for lunar geological work; however, the nature of the Moon creates complications for field mapping. The impact-generated regolith covers most planar surfaces and exposed bedrock is restricted to topographic features such as impact crater central peaks, terrace rim walls, and walls of volcanic channels (i.e., rilles). As a result, more problematic field mapping techniques (e.g., “pace-and-compass” mapping, float mapping and statistical sampling) may provide the most appropriate starting points for developing techniques for surface lunar mapping.

The J-class Apollo missions did not use mapping techniques on the lunar surface. Pre-mission planners used orbital images to develop, in effect, geomorphic maps from which sampling localities were chosen that would help satisfy the mission science objectives. These localities were then “woven” into a traverse plan, using not only the science objectives but the operational practices and both the strengths and limitations of the surface hardware (e.g., rover range, suit walk-back constraints, etc.).

Sampled materials at designated sites along the set Apollo traverse routes, included: large (>10 cm) rocks collected from either ejecta blocks around impact craters or along topographical promontories (e.g., the edge of Hadley Rille), smaller clasts in the regolith, and bulk regolith. The collected materials were used to characterize the extent of rock types on the lunar surface. This approach was used because of a lack of exposed rock and accounted for accessibility from the various landing sites, and the tight time frames of these missions, which prevented lengthy surface excursions. None of the samples

collected from the Moon were from in-place outcroppings of rocks, although the Apollo 17 crew were able to sample boulders that had rolled down from bedrock outcrops much higher on the slopes of the North and South Massifs. The key in gleaned as much valuable information from the collected samples as possible was to record where these samples were collected and describe in detail the surrounding area, both to establish the local and regional geologic context, and to establish sample provenance.

Early in the analysis of Apollo samples, it was recognized that the lunar regolith consisted of a variety of clasts, most of which were locally derived, but with a small but significant population that was introduced ballistically from distant (kms to hundreds of kms range) impacts. In order to systematically collect cm-sized clasts from landing site regolith, a rake tool was used to collect a statistically-significant number of these smaller samples. The results were used to document the variation in lunar rock types that were either not exposed or were not visited during a particular mission. The combination of these techniques allowed for later interpretations on a much larger scale and helped form the basis for new theories related to the geological history of the Moon.

A limitation for mapping methods on the lunar surface is the difficulty in differentiating between different units due to lighting conditions and general lack in colour variation (i.e., blacks and whites and a limited range of greys) of the lunar surface (Eppler, 1991). The Apollo 17 crew noted that contacts between different regolith units that were obvious from orbit were in fact transitional over tens of meters and were difficult to pin point on the ground surface (Eppler, 1991). Other ground-based imaging techniques, such as lidar, could help in this task. A 3D model of the ground surface can be produced using lidar range measurements and intensity measurements (energy reflected by the investigated surface) may help differentiate geological units, and is a topic of current research (Osinski et al., 2010).

Future lunar missions may visit sites that have access to exposed bedrock (e.g., walls of impact craters) in which case a more traditional approach to field mapping using principles of reconnaissance mapping could be incorporated. Future lunar missions could also make use of the “pace-and-compass mapping” technique. Schmitt (pers. comm.)

suggested that a “Rover and Compass” variant be used which would make use of human-driven rovers to access field sites of interest, including outcrops and regolith boundaries. Rovers would need to be able to operate in the rough terrain areas (e.g., crater walls, rille slopes, massif slopes) in which exposed bedrock is expected to be found.

2.4 Lunar exploration strategies

The Lunar Exploration Roadmap identifies and prioritises scientific goals for future lunar missions. It provides an overview of geological investigations; however, it does not delve into the detailed field methods used to conduct these studies. This study specifically considers the Objective Sci-A-3 from the Lunar Roadmap (Lunar Exploration Analysis Group, 2011a): “Characterize the environment and processes in lunar polar regions and in the lunar exosphere”, that includes both prospecting and geological mapping tasks. Table 2-2 outlines these detailed geological goals over time.

Critical factors to consider when planning lunar exploration strategies are the specific physical conditions of the site (e.g., topography, temperature, lighting conditions, radiation conditions), which would dictate if a human or robot agent is more suitable, and if traverse adaptability and geological expertise is needed to conduct the field task (e.g., adaptive-exploratory methods). In terms of lunar exploration, a skilled agent required for adaptive-exploratory approaches would preferably be a trained geologist astronaut. A rover operated with the input of a science team of geologists back on Earth (e.g., Mars Exploration Rover analogy) could also be used; however, much longer timelines would be needed to gather a comparable amount of data. An “unskilled” agent used for fixed-executional approaches could be a rover carrying out a set of instructions (typically fairly repetitive tasks), either autonomously or telerobotically without needing to adapt the route based on results during the traverse.

Table 2-2: List of detailed geological goals over time needed to address Science Objective: “Characterize the environment and processes in lunar polar regions and in the lunar exosphere” (Lunar Exploration Analysis Group, 2011a).

Time Phases for Science Objective: Characterize the environment and processes in lunar polar regions and in the lunar exosphere.			
ROBOTIC MISSIONS ONLY (including Precursors)	ROBOTIC and SHORT HUMAN SORTIES	ROBOTIC and MEDIUM HUMAN SORTIES	OUTPOST and ROBOTIC MISSIONS
Orbital mapping and characterization of cold traps, sunlight, polar deposits. <ul style="list-style-type: none"> • Determine the extent, settings, physical properties and locations of permanently dark cold traps near the lunar poles. • Understand the thermal environment of these areas, including the effects of this thermal regime on lunar regolith and geotechnical properties. • Understand the temporal history of lunar cold traps. 	Surface characterization from lander. <ul style="list-style-type: none"> • Map and characterize polar cold traps and quasi-permanently illuminated areas – ground truth remote sensing observations. 	Determine bedrock geology of polar regions <ul style="list-style-type: none"> • Understand the geological setting of both polar areas, including their relation to local and distant impact craters and basins and regional compositional provinces. • Map and determine the structure of local geological features and their relation to polar volatile deposits and micro-environments. Understand volatile sources and mechanisms of transport and deposition <ul style="list-style-type: none"> • Characterize the volatile phase in the permanently shadowed regions near the lunar poles, and determine their concentrations, chemistry, mineralogy, phase relations, temperatures, and geotechnical properties. 	Continuation of bedrock geology characterization of polar regions. <ul style="list-style-type: none"> Active volatile release experiment and network. • Characterize the volatile phase in the permanently shadowed regions near the lunar poles, and determine their concentrations, chemistry, mineralogy, phase relations, temperatures, and geotechnical properties.

Executional tasks, such as geostatistical sampling and grid-style geophysical surveys, are well suited for autonomous or teleoperated robotic operations. Exploratory approaches, such as reconnaissance and contact mapping, require an understanding of regional geological context and are best carried out by an astronaut with ‘boots on the ground’. To outline a potential lunar exploration strategy to address Science Objective A-3, the Shackleton crater (21 km diameter) is used as an assumed field site. This crater is located near the lunar South Pole and thus has unique lighting conditions. Areas along its rim receive almost continual sunlight, whereas the interior of the crater receives almost no direct sunlight. Recent studies (Thomson et al., 2012; Zuber et al., 2012) have highlighted the potential presence of volatiles within the crater floor and walls.

Based on the review of terrestrial geological mapping techniques and lessons learned from analogue missions, Table 2-3 outlines a mapping strategies that could be used to characterize cold traps and polar deposits in the Shackleton crater.

2.5 Summary

Future surface lunar missions will address numerous science objectives. To ensure maximum science return the strengths of different surface agents (humans or robotic) in relation to specific geological mapping methods requires consideration. Humans are uniquely well-suited to conduct adaptive-exploratory geological field methods, however, only if they are trained as geologists. Geology is an accumulative science, in that greater exposure to different rock types and geological environments, allows a better understanding of what observations are most important in the field and how they link to broader scientific goals and interpretations.

Rovers are useful to conduct fixed-executional geological methods, which typically include repetitive tasks along a fixed route, and the collected data is not used to make decisions as the traverse progresses. Teleoperated rovers (e.g., MER) style can be used in areas where humans cannot safely operate (e.g., perhaps permanently shadowed regions).

Table 2-3: Potential lunar exploration strategy to characterize the environment and processes in a lunar South Pole crater (e.g., Shackleton crater). Description of mapping strategies over time needed to characterize cold traps and volatile deposits.

South Pole impact crater exploration strategy:	
Mapping strategies to characterize cold traps and polar deposits.	
<p>Robotic Missions Only</p> <p>(including precursors)</p>	<p>Recent orbital studies indicate that cold traps in impact craters may host H₂O ice deposits (e.g., Shackleton crater near the lunar south pole, 21 km diameter).</p> <p>Conduct robotic reconnaissance precursor mission to map cold traps:</p> <ul style="list-style-type: none"> - collect remote sensing images from vantage points that allow line of site to crater floor, walls, and terraces (e.g. crater floor) as decided by Mission Control. - plan geophysical surveys along crater floor using results from remote sensing surface data. - conduct GPR and electrical and/or electromagnetic surveys (e.g., within 4 km blocks along crater floor). - Ground truth volatile-rich zones in regolith by using geostatistical sampling of regolith along a grid survey (km-scale). At each sample site, the regolith would be sampled along vertical intervals up to 2-5 m maximum depth and the volatile content could be analysed [e.g., by X-Ray Diffraction (XRD)]. The samples would not be stored on the rover. The most appropriate samples could be returned to Earth for more detailed analysis.
<p>Robotic and Short</p> <p>Human Sorties</p> <p>(<14 Earth days)</p>	<p>It is uncertain if human missions could operate within permanently shadowed regions due to very cold temperatures and difficulty of lighting conditions.</p> <p>Astronauts along the rim of Shackleton crater could work in quasi-permanent sunlight conditions. Even in a short duration mission (< 14 Earth days), geologist astronauts could potentially cover as much ground as the MER rovers have in 8 years (~25 km) on foot, and even more with the use of a vehicle. They could conduct reconnaissance and bedrock mapping where rocks are exposed along the crater rim, and “rover-and-compass” style mapping in areas covered in regolith.</p> <p>The astronaut could scout areas for a robotic assistant to complete surveys independent of the astronaut for repetitive tasks (e.g., geophysical survey, XRF analyses).</p>

Robotic & Medium	Over longer missions, astronauts could expand upon bedrock mapping, using the same techniques as described for Short missions.
Human Sortie (~ 30 Earth days)	Regional scale reconnaissance mapping (over 100s km) would allow investigations of the relationship of local and distant impact craters and basins and regional compositional provinces. Tele-operated rovers can continue to explore the permanently shadowed crater floor. In defined areas, surveys could be set to characterize the volatile phase by measuring their concentrations, chemistry, mineralogy, phase relations, temperatures, and geotechnical properties.
Outpost & Robotic Missions (> 30 Earth days)	With a permanent lunar outpost outfitted with a laboratory detailed analysis of volatile samples could be conducted. The concentrations of volatile species from the solar wind, the regolith, volcanic deposits, present-day degassing of the lunar interior, and exogenic sources such as comets could be determined.

2.6 References

- CSEW6 Steering Committee, 2009. Canadian Scientific Priorities for the Global Exploration Strategy, in: 6th Canadian Space Exploration Workshop Dec 1–3 2008. St. Hubert, Qc.
- Deems, E., Baroff, L., 2008. A systems engineering process for the development of analog missions for the Vision for Space Exploration, in: Proceedings of the AIAA Space 2008 Conference. San Diego, California.
- Ehrenfreund, P., McKay, C., Rummel, J.D., Foing, B.H., Neal, C.R., Masson-Zwaan, T., Ansdell, M., Peter, N., Zarnecki, J., MacKwell, S., Perino, M.A., Billings, L., Mankins, J., Race, M., 2012. Toward a global space exploration program: A stepping stone approach. *Adv. Sp. Res.* 49, 2–48. doi:10.1016/j.asr.2011.09.014
- Eppler, D., 1991. Lighting Constraints to Lunar Surface Operations: NASA TM-4271. Houston, TX.
- Eppler, D., 2008. Lunar Field Geology Operations Model.

Francis, R., Osinski, G.R., Moores, J., Barfoot, T., ILSR Team, 2012. Co-operative Human-Robotic Exploration of Lunar Analogue Sites, Abstract #1996, in: 43rd Lunar and Planetary Science Conference. Woodlands, TX.

Furgale, P., Barfoot, T.D., 2010. Visual Teach and Repeat for Long-Range Rover Autonomy. J. F. Robot. Spec. issue “Visual Mapp. Navig. outdoors” 27, 534–560. doi:10.1002/rob

International Space Exploration Coordination Group, 2011. The Global Exploration Roadmap The Global Exploration Roadmap.

International Space Exploration Coordination Group (ISECG), 2013. The Global Exploration Roadmap.

Lunar Exploration Analysis Group, 2011a. The Lunar Exploration Roadmap: Exploring the Moon in the 21st Century: Themes, Goals, Objectives, Investigations, and Priorities, Version 1.1.

Lunar Exploration Analysis Group, 2011b. Development of a robotic implementation strategy, in: LEAG Lunar Exploration Roadmap Workshop. Houston, TX.

Mader, M.M., Osinski, G.R., Antonenko, I., Barfoot, T., Battler, M., Beauchamp, M., Chanou, A., Cloutis, E., Daly, M., Ghafoor, N., Grieve, R.A.F., Hodges, K., Jolliff, B.L., Kerrigan, M., McCullough, E., Moores, J., Otto, C., Pickersgill, A., Preston, L., Redman, D., Sapers, H., Shankar, B., Singleton, A., Sylvester, P., Tornabene, L.L., Unrau, T., Young, K., Zanetti, M., 2011. Use of robotic precursor mission for follow-on human exploration: Case study lunar analogue mission at the Mistastin Lake impact structure, abstract #2033, in: Annual Meeting of the Lunar Exploration Analysis Group. Houston, TX, pp. 2010–2011.

Mader, M.M., Osinski, G.R., Shankar, B., Tornabene, L.L., Pickersgill, A.E., Marion, C.L., Barfoot, T., Beauchamp, M., Francis, R., Ghafoor, N., McCullough, E., Moores, J., Preston, L.J., Team, I., 2012. Baseline scientific requirements for a lunar robotic precursor mission: Lessons learned from analogue missions at the Mistastin

(Kamestastin) Lake impact structure, Canada, IAC-12-A5.3-B3.6.3, in: 63rd International Astronautical Congress. International Astronautical Federation, Naples, Italy.

Marion, C.L., Osinski, G.R., Abou-Aly, S., Antonenko, I., Barfoot, T., Barry, N., Bassi, A., Battler, M., Beauchamp, M., Bondy, M., Blain, S., Capitan, R.D., Cloutis, E.A., Cupelli, L., Chanou, A., Clayton, J., Daly, M., Dong, H., Ferrière, L., Flemming, R., Flynn, L., Francis, R., Furgale, P., Gammel, J., Garbino, A., Ghafoor, N., Grieve, R.A.F., Hodges, K., Hussein, M., Jasiobedzki, P., Jolliff, B.L., Kerrigan, M.C., Lambert, A., Leung, K., Mader, M., McCullough, E., McManus, C., Moores, J., Ng, H.K., Otto, C., Ozaruk, A., Pickersgill, A. E. Pontefract, A., Preston, L.J., Redman, D., Sapers, H., Shankar, B., Shaver, C., Singleton, A., Souders, K., Stenning, B., Stooke, P., Sylvester, P., Tripp, J., Tornabene, L.L., Unrau, T., Veillette, D., Young, K., Zanetti, M., 2012. A Series of robotic and human analogue missions in support of lunar sample return, abstract #2333, in: 43rd Lunar and Planetary Science Conference. The Woodlands, Texas.

Marjoribanks, R., 2010. Geological Methods in Mineral Exploration and Mining.

NASA, 2011. NASA's Analog Missions: Paving the Way for Space Exploration. NASA Langley Research Center, Hampton, VA.

National Research Council, 2007. The Scientific Context for Exploration of the Moon: Final Report. The National Academies Press, Washington, DC.

Osinski, G.R., Barfoot, T.D., Ghafoor, N., Izawa, M., Banerjee, N., Jasiobedzki, P., Tripp, J., Richards, R., Auclair, S., Sapers, H., Thomson, L., Flemming, R., 2010. Lidar and the mobile Scene Modeler (mSM) as scientific tools for planetary exploration. *Planet. Space Sci.* 58, 691–700. doi:10.1016/j.pss.2009.08.004

Pieters, C.M., Goswami, J.N., Clark, R.N., Annadurai, M., Boardman, J., B, B., Combe, J.-P., Dyar, M.D., Green, R., Head, J.W., Hibbitts, C., Hicks, M., Isaacson, P., Klima, R., Kramer, G., Kumar, S., Livo, E., Lundeen, S., Malaret, E., McCord, T., Mustard, J., Nettles, J., Petro, N., Runyon, C., Staid, M., Sunshine, J., Taylor, L.A., Tompkins, S., Varanasi, P., 2009. Character and Spatial Distribution of OH/H₂O on the Surface of the Moon Seen by M3 on Chandrayaan-1. *Science* (80). 326, 568–573.

Shankar, B., Antonenko, I., Osinski, G.R., Mader, M.M., Preston, L., Battler, M., Beauchamp, M., Chanou, A., Cupelli, L., Francis, R., Marion, C., McCullough, E., Pickersgill, A., Unrau, T., Veillette, D., 2011. Lunar analogue mission: Overview of the site selection process at Mistastin Lake impact Structure, Labrador, Canada, abstract #2594, in: 42nd Lunar and Planetary Science Conference. The Woodlands, Texas.

Shearer, C.K., Neal, C., 2012. Strategic Knowledge Gaps for the “Moon First” Human Exploration Scenario: Analysis and Findings of Lunar Exploration Analysis Group (LEAG) GAP-Specific Action Team (SAT).

Smith, W., 1820. A New Geological Map of England and Wales, with the Inland Navigations; Exhibiting the Districts of Coal and other Sites of Mineral Tonnage.

Thomson, B.J., Bussey, D.B.J., Neish, C.D., Cahill, J.T.S., Heggy, E., Kirk, R.L., Patterson, G.W., Raney, R.K., Spudis, P.D., Thompson, T.W., Ustinov, E. a., 2012. An upper limit for ice in Shackleton crater as revealed by LRO Mini-RF orbital radar. *Geophys. Res. Lett.* 39. doi:10.1029/2012GL052119

Zuber, M.T., Head, J.W., Smith, D.E., Neumann, G.A., Mazarico, E., Torrence, M.H., Aharonson, O., Tye, A.R., Fassett, C.I., Rosenburg, M.A., Melosh, H.J., 2012. Constraints on the volatile distribution within Shackleton crater at the lunar South Pole. *Nature* 486, 378–381.

Chapter 3

3 Geological Exploration of Other Planets: Insights from Terrestrial Desert, Sea, and Polar Analogue Mission Campaigns

The international scientific community is striving to answer fundamental questions concerning planetary evolution by exploring other planets. Presently, no human planetary missions are being conducted; however, analogue mission simulations conducted in challenging environments on Earth are testing technologies and exploration strategies that will help in the development of future missions focused on the study of planetary surfaces.

Analogue missions typically include fully staffed control centers and realistic mission timelines lasting one to two weeks. NASA has simulated planetary exploration missions in analogue activities at remote field sites on Earth [e.g., NASA analogue missions (Reagan et al., 2012)], including NASA Extreme Environment Mission Operations (NEEMO) (Chappell et al., 2013, 2011) Desert Research And Technology Studies (Desert RATS) (Abercromby et al., 2013; Abercromby, 2012) and the Pavilion Lake Research Project (PLRP or simply Pavilion Lake) (Lim et al., 2011). The last of these was also funded by the Canadian Space Agency (CSA). Independently, the CSA has funded a series of multi-deployment analogue missions including the Impacts: Lunar Sample Return (ILSR) deployment to the Mistastin Lake impact structure in Labrador, Canada, which investigated how best to combine human and robotic capabilities for sample return selection. The Antarctic Search for Meteorites (ANSMET) is an annual expedition to the south polar plateau to collect meteorites. Although its intent is not to simulate a space mission, the handful of astronauts who have participated in ANSMET agree that it is very similar to a long-duration space flight (Love and Harvey, 2014).

These analogue programs facilitate novel research combining scientific discovery, geologist-astronaut learning and training, technology innovations, challenges to planetary mission design, and general policy applied to planetary missions. Our study reviews their contribution to the development of geological exploration strategies of planetary surfaces.

3.1 Geological field approaches

Planetary geological exploration focuses on deciphering the geological history of an area and, increasingly, conducting resource exploration and extraction. On Earth, there is no one universal technique for geological field work and strategies for geological exploration are highly dependent on science objectives, which in turn influence what type of data will be collected and what instruments will be used. The same is true for planetary exploration.

Terrestrial geological exploration involves many sub-disciplines, including field mapping, geophysical surveying, geochemical sampling, and supporting laboratory procedures. Often these disciplines complement one another. However, they are typically not conducted simultaneously, often not even during the same field season. They involve varying amounts of time to complete, and they use different approaches (e.g., the exploratory approach of field mapping versus the execution approach of geophysical surveys).

A generalized geological exploration approach for an unknown area may involve starting from a large scale and then progressively focusing the geographic area of study. This could include first reviewing remote sensing images (e.g., satellite images), followed by reconnaissance geophysical surveys (typically airborne), reconnaissance field mapping, then ground geophysical surveys and perhaps statistical sampling; the aforementioned may lead to the identification of zones of interest which are then mapped in detail by a field geologist who can identify sites for drilling, trenching, and detailed sampling. Following field work, detailed petrological and chemical studies can be conducted on collected samples in laboratory facilities. This allows for a much better definition of the different geologic units within a given field area and their relationship to each other. It also assists in deciphering the geological history of the area.

Geological field methods can be broadly divided into two types, termed adaptive-exploratory and fixed-executional styles (Mader et al., 2012). Each requires a field plan (e.g., traverse routes, sampling style) to be made beforehand. The primary differences between the two approaches are the necessity to adapt the field plan (or not) during the

traverse, and the geological expertise of the agent conducting the field work. An adaptive-exploratory style requires a skilled agent able to observe and interpret geological features as they progress along the traverse. The agent's expertise allows them to adapt the traverse plan to best address the mission objectives. In contrast, the fixed-execution style requires that a given set of instructions is followed - the traverse route does not change based on the data collected during the survey. A skilled agent in geological field mapping is not necessarily required to conduct this fixed approach.

3.2 Review of analogue programs

The following sections review each analogue mission from a field research perspective. They focus on geological approaches and activities and do not review technology testing and mission control operations in detail.

3.2.1 NASA Extreme Environment Mission Operations (NEEMO)

3.2.1.1 NEEMO overview

In NASA Extreme Environment Mission Operations (NEEMO) expeditions (Chappell et al., 2013), six-person crews, including four astronauts, live for about 10 days in the Aquarius undersea habitat, located off Key Largo, Florida, at a depth of about 15 m. During the mission, the crew tests operational techniques and engineering prototypes that may be used in the future human exploration of deep space. Science dives also contribute important observations in order to monitor the health of the Florida Keys coral reef, a complex and dynamic biogeological system.

Aquarius is an isolated, confined space with an outside environment that does not support human life. It is also a saturation-dive facility, so a return to the surface is not possible without a decompression protocol that takes nearly 24 hours to complete. NEEMO crews don diving gear to conduct "spacewalks" outside the habitat, taking advantage of the water's buoyancy to simulate reduced or zero gravity. A topside control center acts as Mission Control, assisting and monitoring the "aquanauts" via voice, data, and video communication links. Over the last decade and a half, NASA has carried out almost 20 NEEMO missions, with variation in their durations and priorities.

The following discussion is based on NEEMO XVI, which was conducted in June 2012. Unusually for NEEMO, NEEMO XVI augmented its operational and engineering goals with scientific research: night-time traverses in single-pilot DeepWorker submersibles. Co-author S. Love participated in NEEMO XVI as a Capcom and as a DeepWorker pilot for one of the science dives (Figure 3-1).

3.2.1.2 NEEMO field team composition

A typical crew complement includes four astronauts, at least one of whom is an experienced space flyer who serves as the crew commander, and two habitat technicians, whose primary responsibility is the safe operation of the facility.

The field team for the science dives in NEEMO XVI included the submersible pilots (variously marine biologists, planetary scientists, and astronauts with and without scientific backgrounds); a science team composed of planetary scientists, astrobiologists, and marine biologists stationed on the support ship that launched and retrieved the submersibles; the crew of the support ship; and the submersible support team. The last group maintained the subs and their systems between missions. During missions, they tracked the subs, transmitted verbal navigation cues for the pilots, and provided direction for the pilots in managing the life-support system and other onboard equipment.



Figure 3-1: DeepWorker submersible with aquanaut during NEEMO XVI (photo credit: NASA/FIU).

3.2.1.3 NEEMO field site

NEEMO XVI's science traverses took place on a section of Conch Reef, the coral reef that surrounds the Aquarius habitat. The sea bottom in the research area was carbonate reef at depths of 15-25 m. The research problem that drove the science dives was to understand major ongoing changes in the Florida Keys coral reef system. Decades ago, the reef was composed primarily of hard corals, while today it is dominated by sponges. The reason for this shift is not well understood.

Because the typical flight profile for a DeepWorker involves settling to the sea floor just after launch and just before recovery, and because "landing" a submersible on a living reef is likely to damage organisms, the science traverses were planned to begin and end at points near the reef with a soft sand substrate. Appropriate points for the beginning and end of the traverse were chosen using sonar imagery.

3.2.1.4 Prior knowledge of NEEMO field site

Submersible pilots for the science dives in NEEMO XVI had a wide range of prior knowledge of the science traverse sites. At least one pilot had never before visited the field site, while another had studied it in detail for years. All submersible pilots, regardless of their level of familiarity with the site, followed pre-planned traverse routes that had been developed by scientists who knew the area very well. All pilots had the opportunity to study sonar maps of the area for basic orientation.

In practice, the maps proved too coarse and too difficult to relate to the actual terrain visible in the limited range of the submersible's lights to be of much use to the pilots, who had to rely on verbal direction from topside to fly their planned routes.

3.2.1.5 NEEMO field work approach and activities

The approach of NEEMO XVI's science dives was to plan representative transects across the reef based on sonar remote sensing data, and to navigate along those paths recording the state of the reef and its marine life, and in particular the number, size, morphology, and health of young coral colonies and mature barrel sponges, organisms likely to

dominate the future reef ecosystem. (This goal spanned the fields of biology and geology.)

Two submersibles were deployed simultaneously, tracing complementary paths across the study area. Pilots collected data using onboard video recorders, temperature-depth-conductivity sensors, and their own verbal observations, which were transmitted by means of an ultrasonic through-water-communication system to the science team on the support ship. One of the two submersibles was physically connected to the surface ship via a fiber-optic tether which allowed the science team to view real-time video from that sub. Although the traverses were planned in advance, pilots were authorized to make small deviations in flight path and heading to investigate unexpected features of interest. The science team collected the recorded videos at the end of each dive. The researchers used the images and the pilots' recorded commentary to create a census of reef-forming organisms.

3.2.1.6 NEEMO communications plan

One of the chief goals of NEEMO XVI was to investigate the effect of the significant speed-of-light communication delays that future space crews will face when they explore targets beyond the Moon. NEEMO XVI simulated a mission to a near-Earth asteroid at a distance of 0.1 Astronomical Unit from the Earth, which corresponds to a 50-s one-way delay for radio transmissions. This communication delay was maintained during the night-time science dives as well as during the daytime engineering activities. This required both pilots and Capcoms to anticipate communication needs ahead of time and allow sufficient time for questions, answers, and recommendations to travel back and forth. For example, when the pilot was almost finished observing an interesting feature, he or she would have to ask the science team if they wished any further observations about two minutes before the pilot was ready to leave the area, to avoid wasting time returning to the site (which might be difficult to find in the dark) to satisfy a request for images after the sub had already left. Scientific and technical communication shared the same voice channel, requiring coordination between the science team, the sub support team, and the pilot to keep calls from interfering with one another.

3.2.2 Pavilion Lake Research Project (PLRP)

3.2.2.1 PLRP overview

The Pavilion Lake Research Project (PLRP) (Lim et al., 2011) is a scientific investigation that also serves as a space flight analogue. It studies microbialites, unusual microbial structures, in mountain lakes in British Columbia (BC), Canada. PLRP was established in 2005. Starting in 2008 DeepWorkers, single-person submersibles, were used in addition to SCUBA and autonomous underwater vehicles (AUV) to explore the lake bottom. As in NEEMO, the underwater environment poses real challenges and risks, and the submersibles are excellent stand-ins for spacecraft. The need to constantly monitor life support systems while performing other science duties such as sampling, photographing, etc. and at the same time piloting the submersible provides a high fidelity analogue to conducting science operations in hostile environments. The submersible pilots make science dives typically lasting three to six hours, in close communication with scientists in the boats that tracked the subs.

In 2011, an international and interdisciplinary team of researchers came together to investigate the biology and chemistry of Kelly Lake, BC with questions and hypotheses based on observations made at Pavilion Lake during previous seasons. Scientific priorities included:

1. Map the distribution and characterize the morphology of the microbialites at Kelly Lake;
2. Measure the growth rates of the microbialites at Kelly Lake;
3. Characterize the microbial community (bacteria, viruses, algae) that live on/in the microbialites;
4. Identify processes that contribute to the formation of microbialites.

During this season different operational modes of a DeepWorker submersible were tested including real-time communication between the pilot and a science back-room team, and delayed communication, testing a 50 sec delay as simulation for an asteroid mission.

Different communications protocols were compared to maximize scientific return in a real science and exploration setting. Unlike NEEMO and Desert RATS, the space mission simulation was limited to the dive and did not continue during surface time or off-duty hours.

The following discussion is based on PLRP project that took place in Kelly Lake, BC, which was conducted in July 2011. Co-author M. Mader participated as a member of the science back-room team and as an observer of the operational science success metrics process.

3.2.2.2 PLRP field team composition

The field team for the science dives in PLRP 2011 included the submersible pilots (variously marine biologists and astronauts with and without scientific backgrounds). A science team composed of geologists and marine biologists were stationed in support ships and in a mission control trailer located in the town of Clinton, 15 km away from Kelly Lake. A submersible support team maintained the subs and their systems between missions.

3.2.2.3 PLRP 2011 field site

Kelly Lake is located near Clinton, BC, Canada at a latitude $51^{\circ} 0'17''$ N and longitude $121^{\circ}46'47''$ W. Meter-scale microbialites were noted in Kelly Lake during SCUBA exploration in the early years of the PLRP. The lake is 1283 m in length and 374 m in width, with an average depth of ~38 m.

3.2.2.4 Prior knowledge of PLRP 2011 field site

There were limited photographs of the floor of Kelly Lake prior to the 2011 field season, however, a microbialite facies distribution map was created using 3-D sonar mapping using AUVs (Gutsche and Trembanis, 2010; Trembanis et al., 2010). The resulting high-resolution (<1 m/pixel) maps of bathymetry, slope, rugosity (roughness), and backscatter, were used as the basemap for mission planning.

3.2.2.5 PLRP 2011 field work approach and activities

Flight paths for two DeepWorker submersibles were planned based on sonar data base maps. Three phases of field work were planned over the course of 7 days including, Phase 1: exploration and mapping (Figure 3-2), Phase 2: processing day and exploration of extra points of interest, and Phase 3: Detailed investigations and sampling. Data collected during each phase would influence the flight paths and detailed investigations of the subsequent phases.

During the exploration and mapping phase, the submersibles followed a contour path along the outside edge of the lake and a transect grid that covered the rest of the lake bottom (Figure 3-2). The goal was to obtain photographic and video coverage of the entire lake floor and thus the flights did not deviate much from their set paths. Data from these early flights helped determine exact locations and paths for detailed investigations and sampling. As pilots explored features of interest, they had more leeway in the flight plan to observe a specific area for extended periods of time or deviate from the flight path to observe an interesting feature in greater detail.

Each DeepWorker submersible was equipped with a video camera that recorded the dives. Pilots would vocalize observations while flying the submersible. Notable features were recorded by scientist observers listening to the commentary in a track boat following the submersible topside and the science back-room team situated in a mission control room 15 km from the lake. The science back-room team was able to see live video feed from one submersible (Figure 3-3) and could also record their own observations of the video feed in a specialized web-based software system termed xGDS (Deans et al., 2012). This system included applications that linked recorded notes by mission control observers to specific locations on a Google Earth map showing the traverse path and current location of the DeepWorker.



**Figure 3-2: Reconnaissance flight paths of DeepWorker submersibles, Kelly Lake
(Image credit: D. Lim, PLRP).**

3.2.2.6 PLRP2011 communication plan

During the 2011 PLRP season two DeepWorker submersibles were used, one of which was connected to the surface control vessel with a fiber optic cable, and real-time voice and video data could be broadcast wirelessly to the science back-room team 15 km away. Similar to NEEMO XVI, this capability allowed different operational modes to be tested including real-time communication between submersible pilots and the science back-room team, and delayed communication, testing a 50 sec delay as simulation for an asteroid mission.



Figure 3-3: Back-room Science Team watching live video feed from a DeepWorker submersible in the Mission Control Center.

3.2.3 NASA Desert Research and Technology Studies (Desert RATS)

3.2.3.1 DRATS overview

Desert RATS was a series of space mission simulations at geologically interesting field sites near Flagstaff, Arizona, conducted over a span of nearly two decades. This discussion is based on Desert RATS 2010, one of the most ambitious tests of the series (see *Acta Astronautica* Special Issue Vol. 90 dedicated to this field season). In this simulation, two 2-person crews drove prototype rovers (Figure 3-4) on one-week missions that simulated scientific exploration traverses on the Moon or Mars. Wearing instrumented backpacks, crew members performed two or three shirt-sleeve 1-g "spacewalks" each day to evaluate tools and techniques for planetary geological research (Figure 3-5). They ate and slept in the rovers, gathering human factors data for designers of future vehicle cockpits and habitation spaces. As in NEEMO, a distant control center participated in the operation.

Desert RATS 2010 tested contrasting modes of communication and rover operations. Communication modes included 6 days of "continuous communication" where the crews were in continuous contact with Mission Control and the tactical science teams, and 6 days of absolutely no communications except once in the morning and once in the

evening (2X for short). Co-author S. Love contributed to Desert RATS 2010 as one of the rover operators.



Figure 3-4: Two-person prototype rovers used in Desert RATS 2010 (Image credit: NASA).

3.2.3.2 Desert RATS 2010 field team composition

Desert RATS 2010 employed two electric rovers. Each rover crew consisted of one astronaut or aerospace engineer whose primary duty was to operate the vehicle, and one professional planetary geologist, whose main task was to make observations and to collect, describe, and analyze geological samples.



Figure 3-5: Field crew members performing shirt-sleeve 1-g "spacewalks" in Desert RATS (Image credit: NASA).

Each rover was followed by a chase team in a four-wheel-drive pickup truck. The chase team was responsible for keeping the rovers working, correcting malfunctions (all too

common in prototype equipment) and keeping the batteries charged. The chase teams typically kept a respectful distance during daily operations, in order not to interfere with the quality of the test as a space mission simulation.

The science back-room staffers were all professional geologists. Most of them had some expertise in planetary science or planetary geology. As mentioned above, the science back-room and the rover crews were evaluated by a supervisory science team, whose task was to judge how well the combined team was able to synthesize a geological history of the area from the observations and samples collected during the mission. One or two members of the supervisory team directly observed the rover crews on their "spacewalks."

3.2.3.3 Desert RATS 2010 field site

Desert RATS 2010 took place at Black Point Lava Flow, a volcanic field north of Flagstaff, at elevations near 2,000 m above sea level. The site was chosen for its accessibility and for its similarity to some lunar volcanic terrains. Black Point Lava Flow is part of the privately-owned Parker Ranch, whose owners graciously permit NASA to conduct operations there. The area includes a wide variety of volcanic landforms, including a large recent cinder cone (SP Mountain), a 300-m-deep maar (Colton Crater), and numerous smaller vents and flows. At lower elevations, sandstones, mudstones, and limestones are exposed in between the lava flow fronts. Higher up, juniper trees grow thickly enough to make route-finding challenging. Many of the older lava flows have been smoothed by erosion and colonized by grasses, so that they could be safely traversed by the twelve-wheeled all-terrain electric rovers used in the 2010 test. Some of the new flows, in particular the fresh SP Mountain flow, are too rugged for any wheeled vehicle. Graded but unpaved roads allow easy access to much of the region.

Temperatures during the 2010 test, which took place in early September, ranged from 20 °C at night to 35 °C during the day. The afternoon peak temperatures posed challenges for the rovers' electric motors and internal air conditioners, occasionally forcing pauses in the simulation to allow the machinery to recover. The weather for the 2010 test was dry.

3.2.3.4 Prior knowledge of Desert RATS 2010 field site

The 2010 Desert RATS test built upon extensive exploration of the field site during previous expeditions. The supervising science team made use of prior seasons' discoveries, as well as comprehensive, detailed remote sensing data in a wide range of wavelengths, to plan the fixed traverse routes the rovers would follow.

The rover crews, and some of the science back-room team, who followed the mission via radio and transmitted images from a hotel conference room in Flagstaff, were deliberately kept uninformed of the details of the field site. The better-informed supervising science team could therefore assess the cooperative performance of the rover crews and the science back-room staffers in their ability to gain a correct understanding of the geology of the region, as if they were actually exploring unknown territory on the Moon or Mars.

3.2.3.5 Desert RATS 2010 field work approach and activities

Desert RATS 2010 provided its rover crews with a pre-planned traverse route, remote sensing maps of the area, a suite of geological sampling tools, instrumented "spacewalking" backpacks with GPS receivers and still and motion cameras, and panoramic imaging cameras on each rover. Each day, the crews would awaken early, conduct a short briefing with the science back-room, and begin the day's operations. The field crews followed a strict timeline and traverse paths, with only minor leeway for deviations.

Typically, the rover would drive to a site of geological interest (a lava flow margin, vent, tumulus, or outcrop). There, the geologist would describe the site using the rover's cameras and windows, while the astronaut prepared the backpacks for a "spacewalk." Both crewmembers would exit the vehicle, don their packs, and proceed on foot to points of interest, such as the top of an outcrop that the rover could not reach. They would collect, photograph, and describe a few samples of rock and soil, then return to the rover, document and stow the samples, and ingress the vehicle. Two or three field sites could be visited in a typical work day. On one day, the rover crews made an extended "spacewalk" to explore the ~2 km diameter, ~300 m deep maar called Colton Crater. One of the two rover teams hiked halfway around the rim, while the other descended to the crater floor.

3.2.3.6 Desert RATS 2010 communication

Desert RATS 2010 formally tested the operational pros and cons of two different communication schemes. In the first, communication between the two rovers, and between the rovers and the science back-room, was available continuously. In the other, simulating a mission on the Moon or Mars with close horizons and no communication satellites, a link between the rovers was available only when they were within line-of-sight of one another, and interaction with the science back-room was allowed only twice a day, during limited windows in the morning and late afternoon.

In practice, continuous communication was unreliable because of the difficulty of creating and maintaining a mobile radio-frequency network in mountainous terrain. Frequently, rover crews had to fall back on their own judgment after trying and failing to contact the control center. Communication was also hampered by some of the science personnel's lack of familiarity with standard aviation radio jargon, including the international phonetic alphabet.

With twice-a-day communication, the rover crews were spared the time and effort needed to keep the science back-room constantly informed of their activities. Crews generally felt that the lack of communication did not affect their productivity (Bleacher et al., 2013). But the science back-room team members found their work greatly hampered by the lack of context to go with the images and audio recordings they received at the end of each day.

During both communication protocols, the two rovers shared a single radio channel while driving, but the two crews switched to separate loops for "spacewalks" so that a pair working together could communicate with one another without interfering with the other team.

3.2.4 Impacts: Lunar Sample Return (ILSR)

3.2.4.1 Overview

The Impacts Lunar Sample Return (ILSR) program, funded by the Canadian Space Agency (CSA) and led by the Centre for Planetary Science and Exploration (CPSX) at the University of Western Ontario, included two contingent lunar exploration analogue missions undertaken at the Mistastin Lake impact structure, Labrador, Canada (Figure 3-6) – a robotic precursor mission followed by human-led sample return mission (Marion et al., 2012).

The scientific context of the study was to further the understanding of impact chronology, shock processes, impact ejecta and potential mineral resources. The following sections describe the 1-week human-led mission.

Co-author G. Osinski was the PI of this analogue mission and M. Mader was the Mission Program Evaluation Lead.

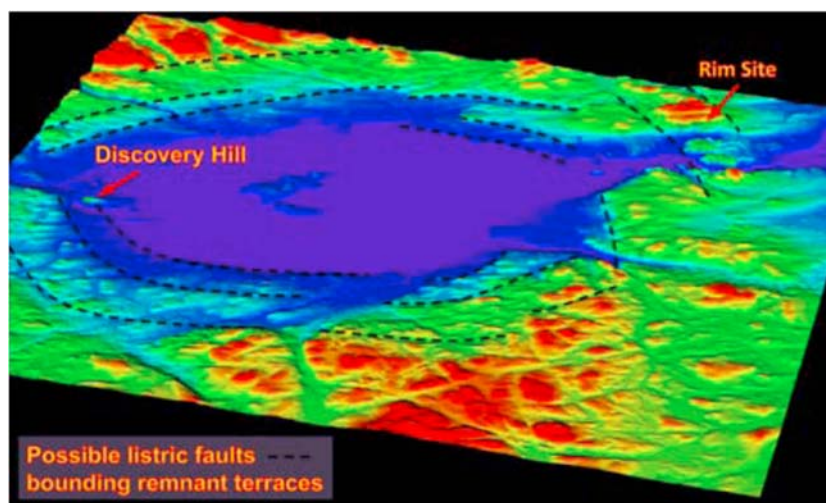


Figure 3-6: A colourized shaded relief model of the Mistastin Lake impact structure. Black dashed lines represent interpreted faults defining a collapsed rim region are outlined in Tornabene et al., (2012).

3.2.4.2 ILSR field team composition

Two PhD students acted as astronauts and explored the sites of interest – one a geology graduate student with prior geological mapping field experience and specializing in impact cratering products (i.e., impactites), and the other a pilot with an engineering background and some geologic training. A Mission control team including Science, Tactical, and Communications groups was largely staffed by planetary scientists and engineers.

3.2.4.3 ILSR field site

The Mistastin Lake impact structure (Figure 3-6), in northern Labrador, Canada (55°53'N; 63°18'W), was chosen because it represents an exceptional analogue for a lunar highland crater (Mader et al., 2012). This site includes both an anorthositic target and preserved ejecta deposits (including melt and breccias) (Mader and Osinski, 2011). The intermediate-size crater formed by a meteorite impact ~36 million years ago. The original crater has been differentially eroded; however, a subdued rim (diameter ~ 28 km) and distinct central uplift are still observed. The inner portion of the Mistastin Lake impact structure is covered by the Mistastin Lake and the surrounding area is locally covered by soil/glacial deposits and vegetation. The topography directly surrounding the lake is slightly elevated in blocky steps extending up to 5 km away from the shoreline, that were interpreted as the remains of the collapsed rim region.

3.2.4.4 Prior knowledge of ILSR field site

A site selection workshop was conducted prior to the deployments (results detailed in Shankar et al., 2011). Sites were selected first at a regional level (selecting regions of interest – ROI's, landing sites), moving onto more localized sites (SOI's), and ultimately zooming in on a prime site of geologic interest (Figure 3-7). This was accomplished using available georeferenced satellite data, air photos, and geophysical datasets. At the impact structure-wide scale, landing sites, regions, and localized SOI were selected keeping crater material sampling in mind (Figure 3-7). Sites were prioritized based on location within the impact structure (identification of crater-scale features like crater rim, impact melt, ejecta materials) and logistical accessibility. Landing sites were selected

based on close proximity to SOI's, exploration prospects, and accessibility, such as landing site opportunities, topography, lakes, etc.

Following the robotic precursor mission, the data collected from the sites were reviewed by Mission Control. Two sites, each characterized by rugged terrain, and steep topographic relief, were chosen for further detailed work by human exploration.

Prior to the follow-on human mission, neither the Mission Control team nor the 'astronauts' had visited the site and only had access to data from the robotic precursor mission and satellite remotely sensed data, consistent with resolutions of present-day lunar data sets.

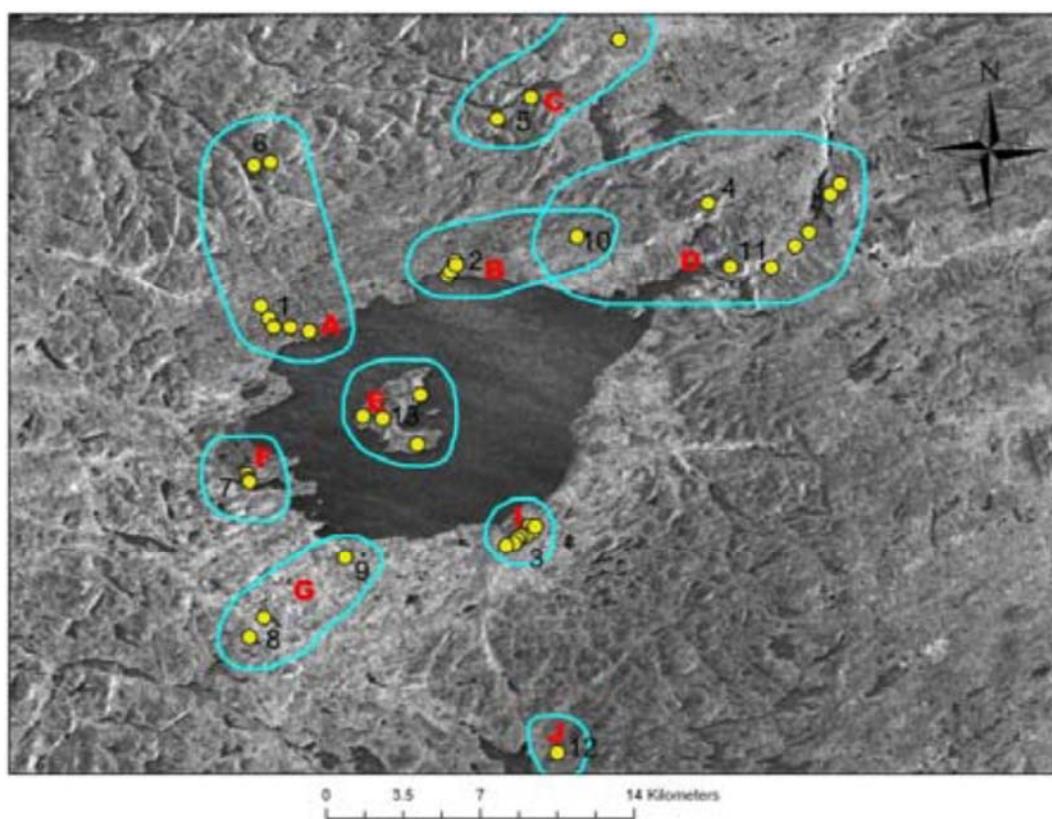


Figure 3-7: Radarsat-2 image of Mistastin Lake impact structure and surrounding area, showing (1) SOI - yellow dots, (2) Regions of Interest, based on groupings of SOI's – blue ellipses, and (3) Possible deployment landing sites - red markers (Shankar et al., 2011). Three separate regions around the Mistastin Lake were chosen for reconnaissance exploration by the rover.

3.2.4.5 ILSR field work approach and activities

The ILSR scientific approach mirrored exploration strategies for traditional geological exploration and field campaigns conducted on Earth, by 1) Using orbital and aerial datasets to assess geologic diversity, landing site selection, and accessibility/traverse planning; 2) Conducting reconnaissance surface mapping to get an overview of the site from the ground; 3) Follow-up detailed traverses, to study sites of interest in detail.

Through the review of remote sensing and Robotic Precursor Mission data, the science goals were focussed to test two hypotheses. Traverse paths were designed keeping in mind SOIs and ROIs of high science priority that could test the hypotheses, and, more importantly, routes that met traversability thresholds defined from the use of hazard maps derived from remote sensing data (e.g., slope, vegetation, water coverage, radar roughness, etc.).

With only five days to explore the main site of interest, a focused traverse strategy was developed for the human exploration that allowed for flexibility and adaptability to allow input from the astronauts. Initially, Mission Control suggested the best and most effective way of sending astronauts to each of these sites within the allotted time for extra-vehicular activity (EVA) and ultimately achieving all of the scientific objectives of the traverse. Mission Control recognized that, due to their better situational awareness, the exact paths travelled by the astronauts would differ from the planned traverse paths. Mission Control provided the first EVA path, which could then be modified as necessary based on astronaut input to allow for maximum scientific return.

Standard science data products collected by the astronauts in the field and then sent to mission control included: 2D visual images (digital photos), 3D visual models generated from stereo images, 3D laser surface models generated from lidar point cloud data, ground penetrating radar (GPR) profiles, X-ray Fluorescence (XRF) spectra, Raman spectra, astronaut geological notes and descriptions (Pickersgill et al., 2012).

The human analogue mission simulation generated a total of >15 GB for a 10 day human mission. A daily limit of 100 MB of data was sent from the field to mission control. The remainder of the data was transferred after the mission.

At each SOI, astronauts completed the following mapping checklist:

1. Upon arrival, mark the point on handheld computer (PDA).
2. Decide on a name for the site if one does not already exist (Mission Control has a list of possibilities).
3. Take ~10 minutes to familiarize themselves with the outcrop.
4. Take a context photo of the outcrop (large scale) for later annotation, including a scale bar or other object to indicate scale. Begin a basic, outcrop-scale characterization (visual observations only) of the rock.
5. Measure any relevant structural measurements (e.g., strike and dip of contacts, layering, etc.).
6. Take close up photos of the specific outcrops being described, including a scale card. The arrow on scale card can point to specific features. The scale card should be as close to a straight-on view as possible.
7. Take Raman, XRF, or Mobile Scene Modeller (stereo image) measurements as required. Both astronauts must work together to operate these instruments.
8. Record a discussion and interpretation of the "big picture." Where does this outcrop fit within the crater?
9. If a sample is taken, photograph the sample site before and after sampling. Use the scale card.

While travelling from one SOI to the next on planned traverse route, periodically, the astronaut team was instructed to:

1. Correlate the route provided by Mission Control with the route they actually take.
2. Mark any known deviations from the suggested route on the digital maps.
3. Look around for potentially interesting outcrops (outcrops are more important than boulders).
4. Determine whether newly discovered sites might address science objectives better than SOIs indicated on the traverse plan.
5. Watch for bears, caribou, and porcupines.

3.2.4.6 ILSR communication plan

During the human-led analogue mission a Mission Control team was based at the University of Western Ontario located in London, Ontario, over 1900 km away; communication was via satellite terminal in the field, with total daily data budgets of ~100 MB at a variable rate between 85-400 kb/s. Instructions were relayed to the field team once a day. The Mission Control team had not visited the site and only had access to remote sensing precursor data, consistent with present-day lunar data sets, prior to the mission. The astronauts discussed scientific data and discoveries with the Mission Control team during a debrief meeting at the end of the day, after the traverse was completed.

3.2.5 Antarctic Search for Meteorites (ANSMET)

3.2.5.1 ANSMET overview

The Antarctic Search for Meteorites (ANSMET) is an annual expedition to Antarctica to collect meteorites for scientific study (Love, 2014). Funding for ANSMET has been provided by the National Science Foundation (NSF) with supplemental funds from NASA in some years. ANSMET teams have journeyed to Antarctica every year but one since 1976. They have collected over 20,000 meteorites, including rare and scientifically important specimens from the Moon and Mars. Field seasons typically last six weeks. All authors have participated in ANSMET field seasons as meteorite hunters.

Co-author S. Love and M. Mader participated in the 2012-2013 ANSMET campaign and co-author G. Osinski participated in the 2003-2004 and 2004-2005 campaigns.

3.2.5.2 ANSMET field team composition

The ANSMET PI selects team members from a pool of interested people (mostly planetary scientists), based on his knowledge of their character and capabilities. About half of the members of each team are veterans of past ANSMET expeditions. Veterans are especially valuable as they require less training in the field, and can help to train the rookies. They also self-select as participants who liked their Antarctic experience well enough to seek another.

3.2.5.3 ANSMET field site

Although meteorites fall no more commonly on Antarctica than anywhere else, Antarctica is the best place to find them. The cold dry climate preserves meteorites, the scarcity of Earth rocks makes meteorites easier to spot, and the flow and erosion of the ice concentrates meteorites. Meteorites are typically found on the surface of solid blue ice patches on the south polar plateau alongside the Transantarctic Mountains.

The sun is above the horizon 24 hours a day. Typical temperatures are near -20°C , with wind chill factors reaching -40°C . High wind, snowfall, drifting snow, or thick overcast and flat light that make travel dangerous can prevent searching on a quarter or more of the days the team spends in the field.

3.2.5.4 Prior knowledge of ANSMET field site

A mobile reconnaissance team of four people explores areas of blue ice, where Antarctic meteorites are most commonly found, that are identified from remote sensing. Separately, an eight-person systematic search team goes to a place previously confirmed by the reconnaissance team to be rich in meteorites, and collects as many as possible.

3.2.5.5 ANSMET field work approach and activities

ANSMET teams search for meteorites on snowmobiles or on foot. Ski-Doos are used for large stretches of blue ice. To search on ice that is rich in meteorites, the team lines up their Ski-Doos four to eight abreast, 10-30 m apart and facing parallel or anti-parallel to the wind direction (Figure 3-8). On a hand signal from the leader, they drive forward at 5-8 km/h, scanning the ice by eye and trying to maintain spacing between their teammates to the left and right. The Ski-Doos usually create a "U" formation, with the leader on one flank. A designated team member, who accepts the responsibility of maintaining the other end of the formation at the expense of not being able to devote as much attention to meteorite searching, takes the other flank.



Figure 3-8: Searching for meteorites on blue ice using snowmobiles.

In areas of blue ice that are being explored for the first time, or that are expected to have few meteorites, or that have already been searched but may possibly have meteorites that were missed the first time, Ski-Doo searchers may adopt a "loose" formation with a separation of 30-100 m between machines. No attempt is made to maintain precise spacing or ordering, and riders may S-turn left and right of course to scan for rocks. Loose sweeps are conducted at higher speed, 15-25 km/h.

In glacial moraines, where the rocks are too large for Ski-Doos to safely traverse and too plentiful for a human searcher to evaluate at any speed above a very slow walk, ANSMET teams park their Ski-Doos and search on foot (Figure 3-9). As with motorized searches, foot searches are a team effort. The participants line up facing upwind or

downwind, moving slowly forward and trying to keep a constant spacing of 3-5 m between searchers. Their walking speed is about 0.5 km/h. The people on the left and right wings of the formation place flags or build rock cairns to mark which areas have been searched. They tear down the cairns or remove the flags when no longer needed.

Some moraines are poor in meteorites, or in need of only a cursory reconnaissance, or have already been searched but are worth a quick second look. In these cases the team may assume a "loose" foot formation with greater spacing, faster walking speed, and less rigid control of course and lateral order.



Figure 3-9: Searching for meteorites within a moraine on foot.

The ANSMET team leader has full authority to make decisions that affect the scientific return of the mission. In particular, the ANSMET team leader constantly adjusts science tasks and priorities in real time, using an adaptive exploratory approach (Mader et al., 2012), efficiently responding to unforeseen changes in schedule, weather, terrain, equipment readiness, and other factors (Love and Harvey, 2014).

Collecting Antarctic meteorites follows an established protocol that balances the challenges of working in the harsh environment against scientific priorities such as protecting the samples, recording location data, and mapping searched areas.

When an ANSMET participant spots a meteorite, he or she may take a moment to make sure it's not a "meteor-wrong:" a terrestrial rock that resembles a meteorite. Diagnostic

features of meteorites include rounded corners; regmaglypts (depressions that look like thumbprints); and the ability to attract a small magnet held nearby. The best diagnostic for meteorites is fusion crust, a thin layer of black material coating the outside of the rock. Fusion crust is an artifact of a meteorite's high-temperature passage through the Earth's atmosphere. Meteorite diagnostics can be mimicked by terrestrial processes, so identification is not always positive.

Upon discovery, the location of the meteorite is marked using a differential GPS mounted on a snowmobile. The entire team participates in sample collection (Figure 3-10). The minder of the collection kit brings the backpack over, opens it, and pulls out the sterile tongs, the hand-held counter, a roll of white freezer tape, and a pair of scissors. The designated photographer lies prone on the ice, facing the meteorite with the sun at his or her back, and readies the camera. The collection kit minder pulls out a metal tag with a unique sample number on it and announces it to the party. The leader records the number in a field notebook.



Figure 3-10: Sample collection during ANSMET. The entire team participates. Lower left: counter with designated number of meteorite. Lower right: sterile tongs lifting meteorite.

Another party member clicks the counter's thumbwheels to display the sample number, and then uses the centimetre scale on the counter to estimate the size of the meteorite in three orthogonal axes. The same person then holds the counter near the meteorite for the photograph. A team member prepares a marker flag, writing the sample number on the flag pole with a permanent pen. Yet another party member pulls from the collection kit a clean Teflon bag to contain the meteorite. The bags are available in a variety of sizes to handle larger and smaller samples, but they are infamously difficult to open with gloved fingers. Often someone must expose a bare hand to the cold and wind to open the bag. Most people can tolerate bare hands for only a few seconds.

When the photo is complete, a party member (often the discoverer) takes the tongs, picks up the sample, looks at it from all directions, announces what percentage of its surface is covered by fusion crust, determines whether it is a chondrite or an achondrite, and places it in the bag. Using the tongs is also a bare-hand task. Achondrites and especially fragile meteorites may be wrapped in aluminum foil before being bagged. When the sample is in the bag, the holder folds the bag around it, slips the metal tag into the fold so that it does not directly contact the sample, and holds the bag up for a teammate to tape it closed. Peeling the end of the tape from the roll, and using the scissors to cut the tape after the bag is sealed, are also bare-hand tasks. When the sample is safely bagged, another team member moves in with an ice chipper or ice auger to drill a hole for the marker flag. The bagged meteorite goes into the collection kit along with the various collecting tools. The collection kit itself is then returned to its minder's Ski-Doo. An experienced team can accomplish all of this in little longer than the one minute it takes the leader's GPS unit to establish a position fix.

3.2.5.6 ANSMET communication plan

ANSMET field camps are autonomous except for satellite telephone communication and aircraft resupply flights. There is no 24-hour "Mission Control" dedicated to the expedition, as in a space mission. Instead, there are experts who support many projects on the continent and who may be reachable by satellite phone during business hours. Resupply flights to the field camp might occur only twice during the season. They deliver critical spares and remove trash and unwanted equipment. Medical evacuation of an

ANSMET team member by aircraft has occurred a handful of times in the project's history.

3.3 Comparison of analogue programs

3.3.1 Similarities

There are numerous similarities between the human planetary analogue missions reviewed in this study. All of the analogue missions took place at natural field sites that had some elements similar to a planetary surface environment. Priorities for each site were a reflection of the overarching goals of the project. For example, NEEMO's focus was on testing operational techniques and engineering prototypes that may be used in the future human exploration of deep space; thus a reduced gravity environment and one that posed real hazards was needed. In contrast, ANSMET is a purely scientific program and the field sites are chosen based on the presence of meteorites. Using natural sites during the analogue campaigns ensured that lessons learned from science operations were meaningful in the context of planetary exploration.

Common capabilities across all analogue missions that enabled geological investigations included:

1. Crewmember access to the locations of interest;
2. Position knowledge;
3. Tools that allowed collection of a variety of samples;
4. Ability to discriminate between different surface units and to take detailed observations of outcrops and rocks;
5. Image capture of locality of interest and surrounding area;
6. Recording data (e.g., sample documentation, position, marking location on map);
7. Communications for geological feedback and/or safety protocols (between geologists in the field and with a base camp).

All of the analogue missions employed a mixed field team of scientists and engineers, and included cross-training prior to their mission. The advantage of having scientists built into the field crews from the outset is to use their skill and experience to recognize and take advantage of serendipitous events that lead to significant discoveries (Hoffman and Voels, 2012).

3.3.2 Differences

All of the analogue missions planned for an adaptive exploratory approach for geological exploration; however, their level of adaptability during traverses varied (Figure 3-11). An adaptive exploratory approach allows changes to the original field plan as a traverse progresses based on data collected during the traverse. The variation in level of adaptability was influenced by differences in style of geological field work and traverse planning.

Adherence to a set plan for a given traverse was most emphasized during the Desert RATS 2010 and NEEMO XVI missions. There was only minor leeway for deviations and the rovers and submersibles were constantly tracked. Each traverse was a ‘stand-alone’ plan, as the field workers did not revisit sites explored during earlier traverses. Their continuous communication experiments were most similar to the J-class Apollo missions where deviations from the plan required approval by a Mission Control team back on Earth. During Desert RATS 2010, the greatest flexibility within traverses was during a two times a day communication schedule with Mission Control. In this situation, the geologist in the rover ahead would scout for the best sites for the rovers in preparation for EVAs and acquisition of images (Bleacher et al., 2013). This style of field geology: reconnaissance explorations followed by a detailed investigations was characteristic of the other analogue missions that had greater adaptability of the field plan.

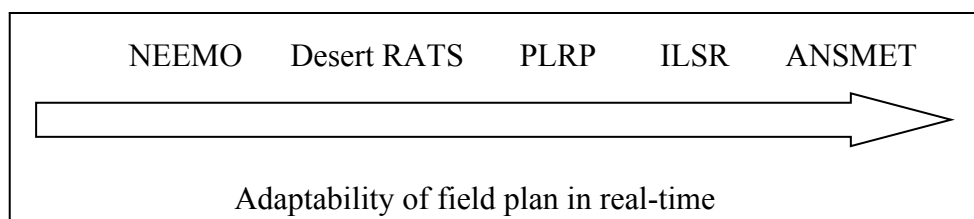


Figure 3-11: Comparison of level of adaptability of traverses in real-time between analogue programs.

PLRP, ILSR, and ANSMET all included reconnaissance field work followed by detailed traverses of specific sites previously visited on separate days. During PLRP and ILSR, the field team followed a set traverse path during reconnaissance exploration, but during follow-on detailed traverses, the field team was allowed more autonomy in terms of defining how long to stay at each site and where to focus their attention. Field workers on the ground have better situational awareness of the geological environment than experts back in Mission Control on Earth. Deciphering the geological history of an area is inherently a three dimensional problem, and timely decision making is expedited by having someone on the ground make geological observations and relate them to the regional context obtained during reconnaissance exploration.

Field worker autonomy was best utilized when field plans included geological hypotheses to test and the field crews helped plan the traverses. Both in the ILSR and Desert RATS missions, early traverses focused more on sample collection objectives. The crews preferred to be working on a testable geologic hypothesis (Bleacher et al., 2013; Tornabene et al., 2012) that would drive sample requirements and notable observations.

3.4 Lessons learned for exploring Moon and Mars

Human exploration of the Moon and Mars will involve longer duration missions than experienced during the Apollo era, and in the case of Mars the communication with the ground control center will be delayed and diminished. The field crews will assume greater autonomy during traverses of the surface. The analogue missions reviewed in this study support several lessons learned that would help increase scientific return:

- Collect detailed remote sensing data during precursor missions at resolutions that allow sub-meter scale features to be observed. This data is critical for landing site selection and traverse planning.
- Plan reconnaissance traverse routes followed by detailed traverses that can revisit sites of interest in greater detail.
- Include mutually cross-trained scientists and engineers on the field team.
- Ensure that astronauts have a degree of autonomy during field work and contribute to traverse planning, especially during detailed traverses following reconnaissance exploration, as they have superior situational awareness of field site.
- As field work evolves from reconnaissance exploration of a new site, ensure that traverse planning is driven by testable scientific hypothesis, which will help astronauts take advantage of serendipitous events that lead to significant discoveries.

3.5 Current gaps and recommendations for future studies

The Global Exploration Roadmap (International Space Exploration Coordination Group, 2013) suggests that space agencies anticipate continued use of analogue missions as part of a stepwise approach for implementing new capabilities needed for missions beyond low-Earth orbit. This report encourages human-robotic partnerships by using robotic precursor missions to prepare for human missions by acquiring strategic knowledge about future destinations and using robots to assist and complement crew activities.

All of the analogue missions reviewed in this study used precursor data to aid in mission planning and used a form of mechanical mobility, be it snowmobile, rover, ATV, or submersible, for the field crew to access sites of interest. However, a gap in knowledge that could be addressed in future analogue missions is how separate robots working in tandem with astronauts can enhance productivity during a planetary surface mission.

For example, autonomous or telerobotically operated rovers could conduct fixed-executional style geological surveys (Mader et al., 2012) in which a given set of instructions is followed - the traverse route does not change based on the data collected during the survey. Executional tasks, such as geostatistical sampling and grid-style geophysical surveys, are well suited for this type of work. Additionally, teleoperated rovers (e.g., MER) can be used in areas where humans cannot safely operate (e.g., permanently shadowed regions).

3.6 References

- Abercromby, A.F., Chappell, S.P., Litaker, H., Reagan, M., Gernhardt, M.L., 2013. NASA Research and Technology Studies (RATS) 2012: Virtual Simulation and Evaluation of Human and Robotic Systems for Exploration of Near-Earth Asteroids, in: 43rd International Conference on Environmental Systems, International Conference on Environmental Systems (ICES). American Institute of Aeronautics and Astronautics, Vail, CO. doi:doi:10.2514/6.2013-3506
- Abercromby, A.F.J., 2012. Desert RATS 2011: Human Exploration of Near-Earth Asteroids, in: GLEX-2012,06,1,3,x12571.
- Bleacher, J.E., Hurtado, J.M., Young, K.E., Rice, J.W., Garry, W.B., 2013. The effect of different operations modes on science capabilities during the 2010 Desert RATS test: Insights from the geologist crewmembers. *Acta Astronaut.* 90, 356–366. doi:10.1016/j.actaastro.2011.10.018
- Chappell, S.P., Abercromby, A.F., Reagan, M., Gernhardt, M.L., Todd, W., 2013. NEEMO 16: Evaluation of Systems for Human Exploration of Near-Earth Asteroids, in: 43rd International Conference on Environmental Systems, International Conference on Environmental Systems (ICES). American Institute of Aeronautics and Astronautics. doi:doi:10.2514/6.2013-3508
- Chappell, S.P., Abercromby, A.F., Todd, W.L., Gernhardt, M.L., 2011. Final Report of NEEMO 14 : Evaluation of a Space Exploration Vehicle, Cargo Lander , and Crew

Lander during Simulated Partial-gravity Exploration and Construction Tasks, NASA/TP-2011-216152. Houston,.

Deans, M.C., Lees, D.S., Smith, T., Cohen, T.E., Morse, T.F., Fong, T.W., 2012. Field Testing Next-Generation Ground Data Systems for Future Missions, abstract 2518, in: 43rd Lunar and Planetary Science Conference. The Woodlands, Texas.

Gutsche, J., Trembanis, A.C., 2010. Geoacoustic investigations of microbialite patterns and distribution in Pavilion Lake, British Columbia, Paper No. 50-7, in: Geological Society of America Abstracts with Programs, v. 42.

Hoffman, S.J., Voels, S.A., 2012. Antarctic exploration parallels for future human planetary exploration: The role and utility of long range, long duration traverses, NASA CP-2012-217355. Houston, TX.

International Space Exploration Coordination Group (ISECG), 2013. The Global Exploration Roadmap.

Lim, D.S.S., Brady, A.L., Abercromby, A.F., Andersen, D.T., Andersen, M., Arnold, R.R., Bird, J.S., Bohm, H.R., Booth, L., Cady, S.L., Cardman, Z., Chan, A.M., Chan, O., Chénard, C., Cowie, B.R., Davila, A., Deans, M.C., Dearing, W., Delaney, M., Downs, M., Fong, T., Forrest, A., Gernhardt, M.L., Gutsche, J.R., Hadfield, C., Hamilton, A., Hansen, J., Hawes, I., Heaton, J., Imam, Y., Laval, B.L., Lees, D., Leoni, L., Looper, C., Love, S., Marinova, M.M., McCombs, D., McKay, C.P., Mireau, B., Mullins, G., Nebel, S.H., Nuytten, P., Pendery, R., Pike, W., Pointing, S.B., Pollack, J., Raineault, N., Reay, M., Reid, D., Sallstedt, T., Schulze-Makuch, D., Seibert, M., Shepard, R., Slater, G.F., Stonehouse, J., Sumner, D.Y., Suttle, C.A., Trembanis, A., Turse, C., Wilhelm, M., Wilkinson, N., Williams, D., Winget, D.M., Winter, C., 2011. A historical overview of the Pavilion Lake Research Project—Analog science and exploration in an underwater environment. *Geol. Soc. Am. Spec. Pap.* 483, 85–115. doi:10.1130/2011.2483(07)

Love, S.G., 2014. The Antarctic Search for Meteorites : A model for deep space exploration, NASA/TM-2014-217388. Houston, TX.

Love, S.G., Harvey, R.P., 2014. Crew autonomy for deep space exploration: Lessons from the Antarctic Search for Meteorites. *Acta Astronaut.* 94, 83–92.
doi:10.1016/j.actaastro.2013.08.001

Mader, M.M., Eppler, D., Osinski, G.R., Brown, J., Ghafoor, N., 2012. Unifying science-driven and resource exploitation strategies for lunar missions: applying lessons learned from terrestrial geological exploration and Canadian planetary, IAC-12,A3,2C,5,x15499 analogue missions, in: 63rd International Astronautical Congress. Naples, Italy.

Mader, M.M., Osinski, G.R., 2011. Insight into lunar impact cratering processes based on field mapping of the Mistastin Lake Impact Structure, Labrador, abstract #P43C-1698, in: American Geophysical Union, Fall Meeting 2011. San Francisco.

Mader, M.M., Osinski, G.R., Marion C.L., Sylvester, P., 2010. Mistastin Lake Crater, Labrador as a lunar analogue site. GeoCanada conference, Calgary, AB, Canada.

Marion, C.L., Osinski, G.R., Abou-Aly, S., Antonenko, I., Barfoot, T., Barry, N., Bassi, A., Battler, M., Beauchamp, M., Bondy, M., Blain, S., Capitan, R.D., Cloutis, E.A., Cupelli, L., Chanou, A., Clayton, J., Daly, M., Dong, H., Ferrière, L., Flemming, R., Flynn, L., Francis, R., Furgale, P., Gammel, J., Garbino, A., Ghafoor, N., Grieve, R.A.F., Hodges, K., Hussein, M., Jasiobedzki, P., Jolliff, B.L., Kerrigan, M.C., Lambert, A., Leung, K., Mader, M., McCullough, E., McManus, C., Moores, J., Ng, H.K., Otto, C., Ozaruk, A., Pickersgill, A. E. Pontefract, A., Preston, L.J., Redman, D., Sapers, H., Shankar, B., Shaver, C., Singleton, A., Souders, K., Stenning, B., Stooke, P., Sylvester, P., Tripp, J., Tornabene, L.L., Unrau, T., Veillette, D., Young, K., Zanetti, M., 2012. A Series of robotic and human analogue missions in support of lunar sample return, abstract #2333, in: 43rd Lunar and Planetary Science Conference. The Woodlands, Texas.

Pickersgill, A.E., Osinski, G.R., Beauchamp, M., Marion, C., Mader, M.M., Francis, R., McCullough, E., Shankar, B., Barfoot, T., Bondy, M., Chanou, A., Daly, M., Dong, H., Furgale, P., Gammell, J., Ghafoor, N., Hussein, M., Jasiobedzki, P., Lambert, A., Leung, K., McManus, C., Ng, H.K., Pontefract, A., Stenning, B., Tornabene, L.L., Tripp, J., Science, K., Teams, O., 2012. Scientific Instrumentation for a Lunar Sample Return

Analogue, abstract #2657, in: 43rd Lunar and Planetary Science Conference. The Woodlands, Texas.

Reagan, M., Janoiko, B., Johnson, J., Steven Chappell, P.D., Abercromby, A., 2012. NASA's Analog Missions: Driving Exploration Through Innovative Testing, in: AIAA SPACE 2012 Conference & Exposition, SPACE Conferences & Exposition. American Institute of Aeronautics and Astronautics. doi:doi:10.2514/6.2012-5238

Shankar, B., Antonenko, I., Osinski, G.R., Mader, M.M., Preston, L., Battler, M., Beauchamp, M., Chanou, A., Cupelli, L., Francis, R., Marion, C., McCullough, E., Pickersgill, A., Unrau, T., Veillette, D., 2011. Lunar analogue mission: Overview of the site selection process at Mistastin Lake impact Structure, Labrador, Canada, abstract #2594, in: 42nd Lunar and Planetary Science Conference. The Woodlands, Texas.

Tornabene, L.L., Osinski, G.R., Mader, M.M., Chanou, A., Francis, R., Joliff, B.L., Marion, C., McCullough, E., Pickersgill, A., Sapers, H., Souders, K., Sylvester, P., Young, K., Zanetti, M., Operations, K., Team, S., 2012. Utility of Remote Sensing, Robotic Precursor Data and a Focused Science Hypothesis for a Follow-On Human Exploration Lunar Analogue Mission at the Mistastin Lake (Kamestastin) Impact Structure, abstract # 2390, in: 43rd Lunar and Planetary Science Conference. The Woodlands, Texas.

Trembanis, A.C., Gutsche, J., Nebel, S., 2010. Precursor exploration missions in Kelly Lake, British Columbia—MARSLIFE project, abstract P13B-1399, in: American Geophysical Union, Fall 2010 Meeting. San Francisco.

Chapter 4

4 Optimizing Scientific Return for Robotic-Human Lunar Exploration: Case Study Impacts Lunar Sample Return (ILSR) Analogue Mission Program

Sample return from the Moon and Mars is a high priority for scientific communities interested in testing theories about planetary formation and surface processes. Building off of the success of Ranger, Surveyor, and Lunar Orbiter missions that preceded the Apollo Moon landings, robotic missions followed by human exploration missions have been proposed as an effective strategy for surface exploration (Fong et al., 2010; International Space Exploration Coordination Group (ISECG), 2013).

In order to understand how to maximize scientific return and how to plan for sample return missions, the Canadian Space Agency (CSA) and other space agencies use terrestrial analogue (i.e., simulated) activities (NASA, 2011). The international community has identified analogue activities as a strategic mechanism for collaboration (Ehrenfreund et al., 2012; International Space Exploration Coordination Group (ISECG), 2013).

An analogue mission simulation is an activity designed to represent specific scientific, technical, and operational aspects of a future space mission using actual or functionally representative systems and operations under analogous environmental conditions (Deems and Baroff, 2008; NASA, 2011). The purpose of these activities is to understand performance and interactions among these systems and operations as well as their ability to achieve mission objectives. Analogue mission simulations can model an entire mission concept (e.g., short lunar sortie missions, long-duration missions) or focus on specific aspects of future planetary exploration missions (e.g., in-situ resource utilization, life support systems).

A key aspect of analogue missions is that they are learning experiences: they aim to facilitate communication and cooperation between disciplines, and record lessons learned that can be applied in the development of future planetary missions. Defining an

appropriate, systematic evaluation scheme to capture and understand lessons learned is essential.

To prepare and test protocols for future lunar sample return missions, our team carried out two contingent analogue missions at the Mistastin Lake impact structure, Canada, as part of a campaign entitled Impacts: Lunar Sample Return (ILSR) funded by the Canadian Space Agency. This was the first multi-year Canadian lunar analogue program of its kind.

4.1 Evaluation methods

Analogue missions that integrate scientific, technological, and operational activities are still in their infancy, with missions across the globe all happening within the past 5-10 years. Some operations and robotic groups have used quantitative metrics to measure field operations in order to maximize Science Return. They measured EVA time, samples collected, and distance covered (Fong et al., 2010; Schreckenghost et al., 2010; Weisbin et al., 2007). However, as noted by Fong et al. (2010), “a quantitative comparison of the executed crew traverses themselves is difficult, given the number of uncontrolled and highly variable factors”.

Others have aimed to incorporate geological considerations of a given site into a metrics approach in the hopes of maximizing scientific significance of potential field excursions (Bleacher et al., 2008; Clark et al., 2009). Lim et al. (2011) emphasized that one of the critical elements to maximize the scientific return of an exploration campaign is the development of mission evaluation tools that measure not just the engineering but also the exploration success of a mixed human-robotic campaign.

In regards to evaluation design, when metrics and anecdotal feedback methods are employed, their development process and data analysis are not described in the literature. This makes it difficult to test the validity and reliability of these methods. For example, without this transparency (e.g., who collected data, when was data collected, who analysed data and how was it analysed) it is uncertain if the data collection process itself is affecting the quality of data collected.

To address these concerns, our study used a comprehensive framework based on Program Theory - the application of program logic models that focus (at a minimum) on program inputs, outputs, outcomes and impacts (Figure 4-1).

A program logic model is a visual representation (flowchart or table) that shows how a program is intended to work by categorizing program activities and outlining the intended flow of activities from outputs to outcomes (McDavid et al., 2013).

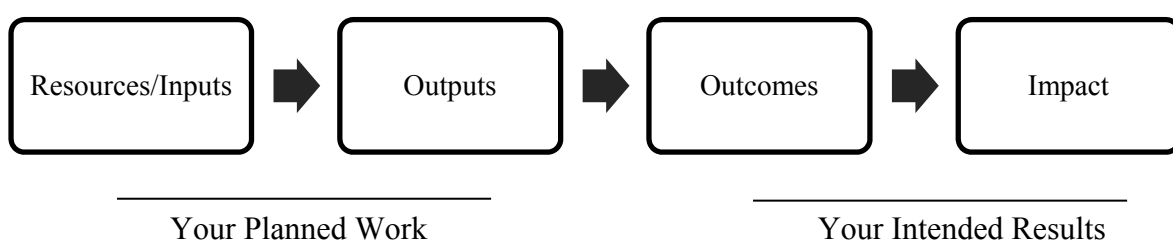


Figure 4-1: Basic Logic Model (McDavid et al., 2013).

It is a useful tool for clarifying objectives, improving the relationship between activities and those objectives, and developing and integrating evaluation plans and strategic plans (Wholey et al., 2010). For example, using a Program Theory framework, Table 4-1 defines the multiple disciplines and activities of an analogue mission simulation using a logic model table, which allows the complexity of such an undertaking to be easily visualized.

Table 4-1: General design of planetary analogue mission simulations.

Inputs (Disciplines)	Activities/Output	Outcomes (Results)	Impact (Long Term Outcomes)
Science Engineering Operations Evaluation Administration/ Logistics	<ul style="list-style-type: none"> • Select reference mission (Moon, Mars, architecture) • Develop Goal & Objectives – what do you want to learn from analogue mission? 	Analogue mission conducted at appropriate analogue site, with one or more geological conditions similar to reference mission destination and enables stated goals and objectives.	Technical, operational, and science requirements linked to needs of scientific investigations.
	Site Selection		
	Develop Operational Plan, considerations: Resources (equipment, people) <ul style="list-style-type: none"> • Field plan • Mission control plan • Communication plan • Data management plan 	Baseline plan from which to start from. Can be modified/adapted during analogue mission as lessons are learned.	Increase capacity, cross-disciplinary knowledge, and collaboration between various disciplines.
	<ul style="list-style-type: none"> • Develop Evaluation Plan • Link activities to expected results and indicates what data to collect to inform future actions (lessons learned) 	Data collected to address objectives of study.	Systematic approach that records methods and results. Can more easily compare results with other analogue mission studies.
	<ul style="list-style-type: none"> • Dry-Run(s) of various components (different disciplines practice together) • Test equipment • Test procedures 	<ul style="list-style-type: none"> • Lessons learned to be carried forward to analogue mission. • Modify operational and evaluation plans as needed. 	Increased communication and cross-disciplinary understanding between participants.
	Conduct Analogue Mission	Observations/data collected during mission, as outlined in Evaluation Plan.	Systematic approach that allows results to be compared with other analogue mission studies.
	Post-Mission Analysis Science evaluation	Lessons learned and recommendations that address technical, science, operational objectives and unexpected outcomes.	Suggest requirements and recommendations for design of future planetary missions.

4.2 Lunar analogue site

The Mistastin Lake impact structure, in northern Labrador, Canada (55°53'N; 63°18'W), was chosen because it represents an exceptional analogue for a lunar highland crater (Mader et al., 2010). This site includes both an anorthositic target and preserved ejecta deposits (including melt and breccias) (Mader and Osinski, 2011). The intermediate-size crater formed by a meteorite impact ~36 million years ago. The original crater has been differentially eroded; however, a subdued rim (diameter ~ 28 km) and distinct central uplift are still observed (Grieve, 1975). The inner portion of the Mistastin Lake impact structure is covered by the Mistastin Lake and the surrounding area is locally covered by soil/glacial deposits and vegetation. The topography directly surrounding the lake is slightly elevated in blocks extending up to 5 km away from the shoreline, that are interpreted as the remains of the collapsed crater rim.

Two main sites were identified for robotic precursor and human exploration during the ILSR mission, including a site within the rim region of the crater structure and a distinct topographic high near the southeast shoreline of Mistastin Lake, called Discovery Hill (Figure 4-2). Each of these regions is characterized by rugged terrain and steep topographic relief.

The second week of the human analogue mission, which is described in detail in this study, took place at Discovery Hill. This ramped-shape hill dips towards the lake. The high end of Discovery Hill is situated ~ 2 km radially inland (west) from the Mistastin shore at an elevation of 120 m above lake level. The top part of the ramp is primarily covered by unconsolidated material and some vegetation; however, the north, west, and south sides reveal exceptional exposures of impact melt rock. The exposed melt unit is wedge-shaped and is thickest on the west end. The basal contact of the melt package is mostly obscured as the lower portion of the cliff faces is covered by unconsolidated talus slopes or vegetation. The contact between the melt and underlying unit was a focus for the human analogue mission. Prior to the analogue mission, the mission control and astronauts did not know the geological nature of Discovery Hill.

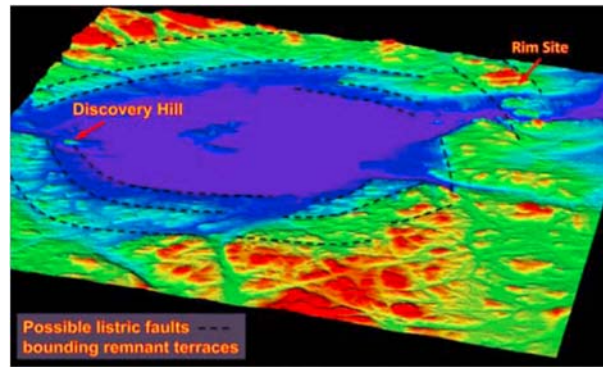


Figure 4-2: A colourized shaded relief model of Mistastin. Red indicates higher elevations and blue indicates lowest elevations. Possible listric faults defining the collapsed rim region are outlined in black dashed lines (Tornabene et al., 2012).

4.3 Case study: Impacts Lunar Sample Return Program

The Impacts Lunar Sample Return (ILSR) program, funded by the Canadian Space Agency (CSA) and led by the Centre for Planetary Science and Exploration (CPSX) at Western University, included two contingent lunar exploration analogue mission simulations undertaken at the Mistastin Lake impact structure, Labrador, Canada (Marion et al., 2012), in 2011 and 2012. This analogue mission program was driven by the paradigm that the operational and technical objectives are conducted while conducting new science and addressing real overarching scientific objectives. The scientific context of the study was to further our understanding of the Mistastin impact structure, in Labrador, Canada. By combining these goals in an analogue mission campaign the following specific objectives were examined in the context of increasing scientific return:

1. Assess the utility of a robotic field reconnaissance mission as a precursor to a human sortie sample return mission;
2. Develop field mapping protocols for human lunar exploration;
3. Develop data processing protocols and data management procedures for mission control.

The first mission was a robotic precursor mission in advance of a follow-on human mission. No mechanical robot was used on this deployment; instead, a field team of up to five people acted collectively as the robot – they made traverses with the instruments, collected data as requested by mission control, and sent the data to the remote mission control team using satellite communication (Mader et al., 2011).

During the follow-on, sample return human mission, two PhD students acted as astronauts (herein termed astronauts) – one a geology graduate student with prior geological mapping field experience and specializing in impact cratering products (i.e., impactites), and the other a pilot with an engineering background and some geologic training (similar to many lunar astronauts). A mission control team included Science, Tactical, and Communications teams, largely staffed by planetary scientists and engineers.

For each deployment the Mission Control team was based at the University of Western Ontario located in London, Ontario, over 1900 km away; communication was via satellite terminal in the field, with total daily data budgets of ~100 MB at a variable rate between 85-400 kb/s. Neither the Mission Control team nor the astronauts had visited the site and only had access to remote sending precursor data, consistent with present-day lunar data sets, prior to the mission. Anyone with more detailed knowledge of the site was asked to not contribute to the scientific decision-making process.

A site selection workshop was conducted prior to the deployments (results detailed in Shankar et al., 2011). Sites were selected first at a regional level (selecting regions of interest and landing sites), moving onto more localized sites of interest, and ultimately zooming in on a prime site of geologic interest (Figure 4-3). This was accomplished using available georeferenced satellite data, air photos, and geophysical datasets. At the impact structure-wide scale, landing sites, regions and localized sites of interest were selected keeping crater material sampling in mind (Figure 4-3). Sites were prioritized based on overall science objectives, location within the impact structure (identification of crater-scale features like crater rim, impact melt, ejecta materials) and logistical accessibility. Landing sites were selected based on close proximity to sites of interest,

exploration prospects, and accessibility, such as landing site opportunities, topography, lakes, etc.

This study focuses on the Discovery Hill portion of the analogue mission. Specific sites of interest within this region were identified based on the robotic precursor images. For example, remote sensing images (Tornabene et al., 2012) images show that Discovery hill is capped by massive, almost vertical outcrop of a dark toned material that appears to exhibit multiple vertical fractures or joints (Figure 4-4). A closer examination of these materials in the highest-resolution robotic precursor images indicated that these features are consistent with columnar joints (e.g., Milazzo et al., 2009). Given the geologic context, Mission Control interpreted the “cap” unit to be an impact melt deposit. Because impact melts could address the overall science mission objective, an investigation by the acting astronauts of this outcrop was given the highest priority.

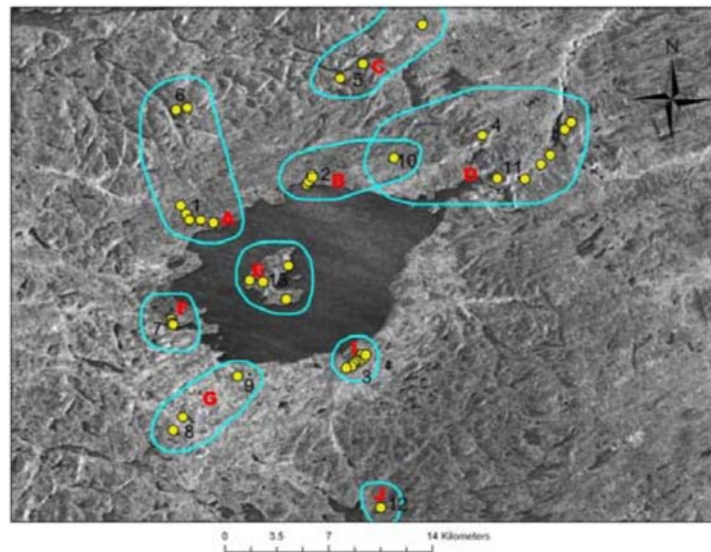


Figure 4-3: Radarsat-2 image of Mistastin Lake impact structure and surrounding area, showing (1) sites of interest - yellow dots, (2) Regions of Interest, based on groupings of sites of interest – blue ellipses, and (3) Possible deployment landing sites - red markers (Shankar et al., 2011).

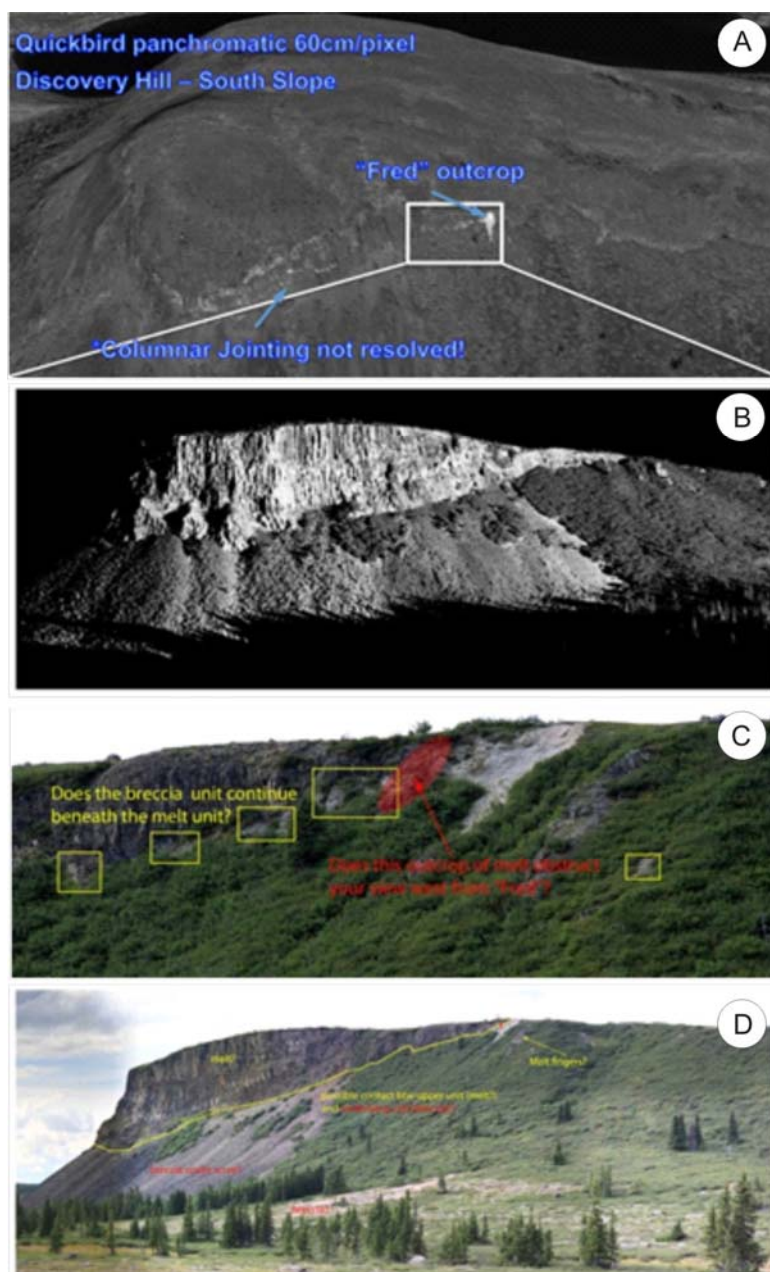


Figure 4-4: (A) 3D perspective of the Quick Bird panchromatic image compared with (B) 2010 ‘robotic’ precursor lidar scan, and (C) a ‘robotic’ precursor image of the southern slope of Discovery Hill. A light-toned outcrop (labelled “Fred” outcrop) appears to unconformably underlie the impact melt. The melt unit of Discovery Hill exhibits barely discernible columnar jointing in (A), which is better resolved by the ‘robotic’ precursor image (B and C) (Tornabene et al., 2012). Sub-outcrop scale SOI’s indicated by boxes in (D) were selected based on precursor data and science objectives.

A specific hypothesis was developed to test the interpretation that Discovery Hill cap unit is an impact melt-bearing rock unit and specifically if it is a portion of the coherent melt sheet of the crater-fill deposits, or a remnant of a terrace melt pond similar to those commonly observed in and around lunar craters (Bray et al., 2010; Osinski et al., 2011).

In order to test the origin and provenance hypothesis, attributes drawn from field observations of impact melt deposits from crater interiors and exterior (note that we include impact melt in the collapsed crater rim region as exterior, as our frame of reference is the transient cavity “rim”), were summarized and given to the astronauts for detailed field examinations. The hope was to find consistent observations from the remote sensing images and field observations that would be generally consistent with one origin over the other.

A set of flight rules governing astronaut EVAs were created, using both experience from past fieldwork and reference to Apollo limitations. Astronaut travel range and time limitations, together with assumptions about the speed of travel on foot and by all terrain vehicles (ATVs) and the time required for expected tasks, set a framework for planning out daily schedules. Prior to each traverse, mission control sent the astronauts maps and instructions of planned traverses for each day.

This analogue mission was carried out under the assumption that human explorers on the Moon or Mars would not be aided by a global positioning system (GPS) network similar to that available on Earth. The astronauts used visual and radar satellite images in conjunction with digital elevation models to position themselves using digital mapping tools in the form of ruggedized, handheld computers. They then relayed their positions (in UTM coordinates) to mission control where their locations were displayed on a map using ArcGIS and/or Google Earth.

The astronauts were equipped with ultra-high frequency (UHF) radios networked and relayed by voice over internet protocol (VOIP) with a satellite connection using an Inmarsat Broadband Global Area Network terminal. The plan was that while the astronauts followed the traverse plans, an open line of communication would allow for discussion and flexibility during EVAs based on the ground-truth information relayed by

the astronauts. Unfortunately, conditions in the field at Mistastin did not permit effective two-way communications when the astronauts were located outside of their base camp. At best, the astronauts were able to relay their interpreted UTM positions to the mission control every hour.

4.4 Results

In the context of planetary missions focusing on geological studies, scientific return is a key deliverable by which mission success is measured, and generally refers to the understanding of the geology of a given planet. There is no standardized metric for measuring scientific return for planetary analogue missions. It is a difficult concept to quantify, as there is a subjective element in terms of what is considered significant or exceptional. In addition, discoveries can continue to be made long after the mission and thus measuring the potential scientific return at any given moment is problematic. For example, in the case of Apollo, many significant discoveries were made soon after missions were completed; however, discoveries have continued over the subsequent decades using the samples and data collected.

Numerous factors influence scientific return: geological investigations are dependent on quality of field site in terms of rock exposures and accessibility, quality of the data collected, quality of data analysis during and after the mission, the expertise of the geologist making interpretations, and the interaction and communication between astronauts and the scientists on the ground during the mission. Each of these factors comprise innumerable variables that are difficult to control and thus baseline criteria for comparison cannot be established.

This study focuses on several activities that are expected to affect scientific return of a human lunar mission, based on best practices for how geological fieldwork is conducted on Earth, including:

- Traverse planning and execution;
- Geological data collection and interpretation; and

- Data management.

An evaluation plan was developed for this study using a program logic model, which links these activities with necessary qualitative observations to be made, that would address specific analogue mission objectives (Table 4-2; Appendix A). By implementing a rigorous evaluation plan, lessons learned could be supported from multiple perspectives.

Table 4-2: Evaluation plan using a Program logic model framework for the ILSR analogue mission simulation. Key observations made during planetary analogue mission simulation focused on geological studies linked to mission and objectives.

Activities for Human Mission	Outputs (Data Products)	Outcomes (Results)	Impact (Objectives addressed in Discussion)
Traverse Planning	Written instructions Traverse Plan Map Feedback from debrief meetings and Mission Control Lead reports	What data products from precursor mission were used to make traverse plan? Was plan adaptable? If so, - How was adaptability accounted for in traverse plan? - What aspects of plan were adaptable?	Assess the utility of a robotic field reconnaissance mission as a precursor to a human sortie sample return mission. Determine if the operational concepts/scenarios considered in the space mission can be performed accurately/quickly without the dependence on satellite-based global positioning.
Traverse Execution	Map - Plot planned path and actual path Documentarian Notes: - Record any issues (e.g., reason for deviations from plan).	Was plan followed? What aspects of plan were adapted? - Reason for any deviations. - Was level of autonomy for astronauts appropriate?	
Geological data collection (by field team)	Geological Observations by astronauts (oral recordings and transcriptions) Digital photographs	Develop mapping protocols that increase scientific return: - Where were field instruments used? (e.g., in the field or in habitat).	Understand the decision-making process during site selection and detailed outcrop mapping and sampling. Develop appropriate

	Measurements (data): - Chemistry - Mineralogy - Structural geology - Location Samples collected	- Recommendations for how to maximize observation time in the field (and thus increase scientific return).	operational concepts for geological-based exploration instruments.
Geological interpretation and data management	Processed geological data products: - Digital images - Map with labelled sites of interest - Chemical (XRF) and mineralogical (Raman) plots Geological interpretations by astronauts and mission control Feedback from daily debriefs and Mission Control Lead reports	# of each data product How were data products modified? How was data managed, categorized, and stored?	Input into traverse planning & sample collection protocols. Develop data processing protocols and data management procedures for mission control. Recommendations for planning software and mapping tools and software. Increased knowledge of site. (Science objectives).

4.4.1 Traverse planning and execution

Precursor Mission Data Products

Prior to the human field deployment, a series of EVA traverse planning workshops were held in the mission control facility at the University of Western Ontario. The following data sets were used to create traverse plans for each of the four days during the human mission:

- Precursor data (digital photos, lidar scans) obtained during the robotic scenario of the 2010 field deployment;
- Remote-sensing data covering the field site and surrounding area (see Table 4-3);
- GIS map data including topography, water body layouts, and other geographical information.

The most used data sets by mission control to plan the follow-on human mission included large scale panoramic images (e.g., 25 x 4 Mp), which allowed a full contextual view of the surrounding area including exposure of rocks and traversability of the area, and lidar scans that provided range and scale information at a meter scale and up to 1 km away. These images aided in identifying outcrops of variable colour and textures suggesting different target lithologies, alteration, or surface coatings, which helped in interpreting the geologic history of the area.

The remote sensing and precursor data were particularly useful towards addressing the focused science hypotheses: a key outcrop, labelled “Fred” in Figure 4-4, would not have been easily discovered in the field without the aid of remote sensing and precursor images. Due to the small areal occurrence (only on the south slope) and steep slopes the astronauts would have completely missed this outcrop without the aid of the science team back in Mission Control.

Table 4-3: List of remote imaging datasets for the Mistastin region and their respective resolutions.

Data Set	Maximum Resolution
Landsat 5	30 – 120 m
Landsat7 (ETM+)	15 - 120 m
RadarSat1 (HH polarization)	8 – 100 m
RadarSat2 (HH, VV polarization)	
Topographic (Contour) Map	1:50,000
Panchromatic Airphotos	1:4000 ; 1:7000
DEM Model	100 m spacing
Lakes and Streams	<100 m
Gravity data	2000m
Magnetic data	200m
Geologic map	1:50,000
Google Earth	15 – 30 m
Aster data	15 - 90 m
Quickbird Imagery	60 7- cm (panchro) 2.4 - 2.8 m (multispec)

4.4.2 Adaptability & phased approach

Traverse paths for the human mission were designed considering sites and regions of interest of high science priority that could test the hypotheses, and, more importantly, routes that met traversability thresholds defined from the use of hazard maps derived from remote sensing data from satellite images and images collected from the robotic precursor mission (e.g. slope, vegetation, water coverage, radar roughness, etc.). Mission control suggested the best and most effective way of sending astronauts to each of these sites within the allotted time for extra-vehicular activity (EVA) and ultimately achieving all of the scientific objectives of the traverse.

Traverse planning for human exploration was designed to account for key factors:

1. Astronauts have better situational awareness than Mission Control (Antonenko et al., 2013);
2. Best practices from terrestrial exploratory geological field methods can be applied to planetary exploration by conducting reconnaissance traverses first followed by detailed mapping (Mader et al., 2012). This allows the scientific return from the reconnaissance traverse to influence the planning and execution of the following traverse;
3. Apollo lessons learned included the recognition that there is a need to design in maximum flexibility, in order to be able to respond to short-term changes in landing sites, traverses, sampling strategies, equipment manifests, etc. (LEAG Science Scenarios for Human Exploration Specific Action Team, 2009).

Over a four-day mission at the Discovery Hill site, the first two days included two separate reconnaissance traverses that allowed the geologists to gain an overview of different regions of the site and select key outcrops to visit during a subsequent traverses. These initial traverse paths were planned by mission control using data from the robotic precursor mission. Astronauts were advised to prioritize completing the entire traverse and getting a ‘lay of the land’ rather than spending more time at specific sites. The latter two days were spent focussing on specific outcrops that the mission control team and

astronauts agreed were of scientific value. Astronauts were allowed more discretion to spend time making observations and collecting samples during these detailed traverses. Each EVA was a maximum of 5 hours in duration.

The mission control team was able to analyse data collected during the mission and review it with the astronauts by using a phased approach, wherein data collected during a given reconnaissance traverse was processed the next day and used to plan a traverse for detailed work two days after the original reconnaissance traverse (see Table 4-4 outlining phased approach). This approach allowed the astronaut crew to work together with ground support (i.e., mission control) and to be involved in making decisions regarding traverse planning, one of the key recommendations based on feedback from Apollo astronauts (LEAG Science Scenarios for Human Exploration Specific Action Team, 2009).

Pre-EVA and post-EVA debriefs between the mission control and astronauts were essential. Due to communication difficulties, astronauts did not relay scientific observations in real-time. The traverse plan and scientific priorities were reviewed during the pre-EVA debrief each morning. The traverse plan included a general description of the traverse and priorities, science questions to be addressed, reason for the priority of sites, and detailed instructions on activities to be completed. Annotated photos of key outcrops were also included, which highlighted key questions to be addressed. The post-EVA debrief allowed the astronauts to share their observations and provide input into traverse planning for the subsequent days. The astronauts also sent a report that included a brief description of the completed traverse and descriptions for each photo taken. Their input was essential in deciding what sites to prioritize for detailed exploration.

Table 4-4: Traverse and data processing schedule for human exploration mission.

Date	Astronaut Traverse	Data Processing Mission Control
Prior to start of mission		Plan reconnaissance 1&2 traverse based on robotic precursor data.
Day 1	Traverse 1: Reconnaissance loop	Review traverse with astronauts during debrief.
Day 2	Traverse 2: Reconnaissance loop	Process traverse 1 data during day. Review traverse 2 with astronauts during post-EVA debrief meeting.
Day 3	Traverse 3: Detailed outcrops from traverse 1	Process traverse 2 data during day. Review traverse 3 with astronauts during post-EVA debrief.
Day 4	Traverse 4: Detailed outcrops from traverse 2	Traverse 3: Detailed outcrop data. Review traverse 4 with astronauts during post-EVA debrief.

4.4.3 Geological data collection

Standard science data products collected by the astronauts in the field during the four-day mission at Discovery Hill included 2D visual images (digital photos), X-ray Fluorescence (XRF) spectra, Raman spectra, interpreted UTM coordinates, and geological notes and descriptions (Kerrigan et al., 2012).

During the four-day mission at Discovery Hill, the astronauts completed the following mapping and data collection checklist at each site of interest:

1. Upon arrival, mark the point on handheld ruggedized computer (Trimble YUMA).
2. Decide on a name for the site if one does not already exist.
3. Take ~10 minutes to familiarize themselves with the outcrop.
4. Take a context photo of the outcrop (large scale) for later annotation, including a scale bar or other object to indicate scale. Begin a basic, outcrop-scale characterization (visual observations only) of the rock.
5. Measure any relevant structural measurements (e.g., strike and dip of contacts, layering, etc.).

6. Take close up photos of the specific outcrops being described, including a scale card. The arrow on scale card can point to specific features. The scale card should be as close to a straight-on view as possible.
7. Record a discussion and interpretation of the "big picture." How does this outcrop help address scientific goals and hypotheses?"
8. If a sample was taken, photograph the sample site before and after sampling. Use the scale card.

While travelling from one site of interest to the next on planned traverse route, periodically, the astronaut team was instructed to:

1. Correlate the route provided by mission control with the route they actually took.
2. Mark any known deviations from the suggested route on the digital maps.
3. Look around for potentially interesting outcrops (outcrops are more important than boulders).
4. Determine whether newly discovered sites might address science objectives better than sites of interest indicated on the traverse plan.
5. Watch for bears, caribou, and porcupines (all observed in the area by previous field workers).

Geological observations were recorded by a stenographer in the field in lieu of having real-time communications with mission control. Raman and XRF measurements were taken on collected samples at the base camp after the completion of traverses in order to decrease the amount of equipment astronauts had to carry, maximize the time astronauts had in the field to take observations, and to have more stable environmental conditions (e.g., lighting, clean surface) for taking measurements. For future missions, samples should be ground into powder to obtain a more accurate XRF and Raman measurements.

The astronauts were accompanied in the field by a support team who were equipped with a GPS receiver. The location data recorded with the receiver were used to measure the accuracy of the astronaut-relayed coordinates after the completion of the missions (Kerrigan et al., 2012). Figure 4-5 is a map of a reconnaissance EVA traverse at Discovery Hill. It shows the original traverse plan provided by mission control, the traverse as tracked by mission control with astronaut-relayed coordinates, and the traverse as recorded by the GPS receiver.

The reason for the differences between the traverses is two-fold; the astronauts had multi-layer maps with aerial and satellite imagery available to them on their handheld ruggedized computer; however, due to the amount of time it took for these layers to render, the astronauts often used only the basic topographic map to position themselves. This led to the misidentification of features and scale due to the low resolution of the topographic map. As a result, general spatial orientation allowed the approximate shape of the traverse to be correctly mapped, but enlarged to an incorrect scale.

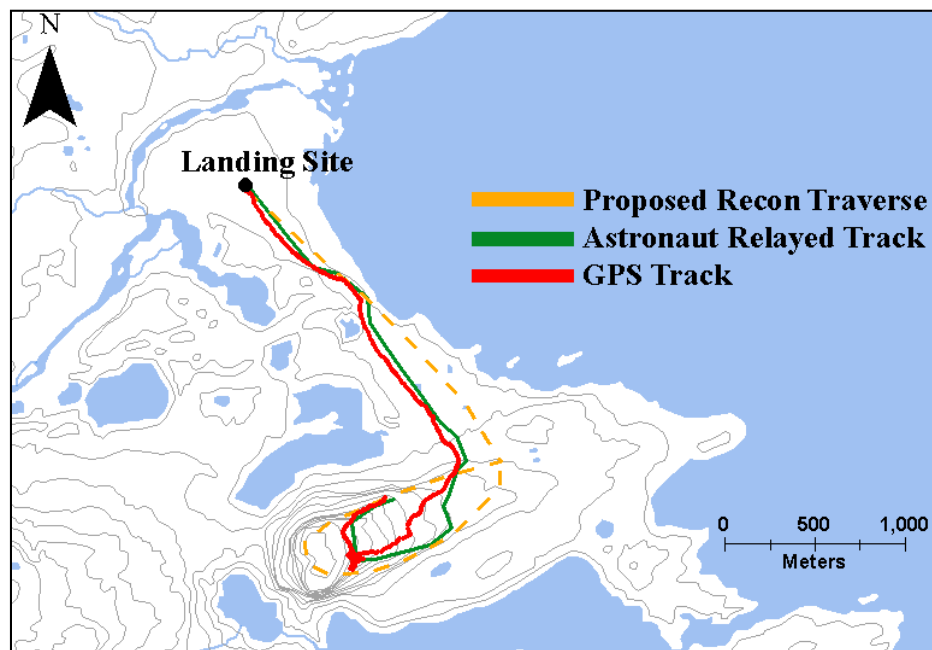


Figure 4-5: Reconnaissance EVA traverse comparing the planned (yellow dash line), relayed (green line), and actual GPS tracks (red line).

4.4.4 Geological data interpretation

Processing of geological data was completed in mission control by a team of scientists. For geological field mapping, the primary scientific data used by mission control were field photographs (McCullough et al., 2012). In particular, mosaic images were of great value for gaining increased field of view. Digital images were typically modified using Adobe Photoshop by science team members in a number of ways: 1) geological features (e.g., contacts) were drawn on the image; 2) image processing: contrast-stretch was optimized for highlighting features in the image; 3) image name was added; 4) images were cropped to highlight key areas; and 5) 3D red-blue anaglyphs were made of selected stereo pairs (see Figure 4-4c,d as an example of modified images).

Mission control also used ArcGIS software to view available aerial and satellite data. All the data during each phase of the analogue mission were compiled together in one ArcMap and referred to multiple times during the analogue mission. In addition to viewing data, ArcGIS has the unique ability to create and store new features. During the mission, the mission control teams created new layers (shape files) that stored details of scientific value (e.g., storing locations of regions of interest, sites of interest, landing sites, crater rim, and astronaut locations). Hazard maps (highlighting areas to avoid due to various factors such as water coverage, steep slopes, inaccessibility, etc.) were generated using ArcGIS and greatly assisted mission control when selecting sites. ArcMap was used to update the astronaut tracking paths (i.e., recording the current position based on astronaut's relayed coordinates) and assist members when necessary with the available satellite datasets.

4.4.5 Geological data management

Due to the daily limit of 100 MB for how much data could be sent to mission control from the field, the astronauts were required to down select their images. Approximately a quarter of the images were sent back during the mission operations (see Table 4-5). Additionally, some data products logically needed to be studied before others, therefore, as the analogue mission evolved, mission control started to prioritize requests for data in

order to streamline the data interpretation process. The field team would try to send back-prioritized data first.

Table 4-5: Data collected during 4 day astronaut mission at Discovery Hill.

Data Product	Number of individual data product collected in the field
Photos	~350 (only ~100 sent to mission control during mission)
Samples	17 (returned after 4 day mission)
XRF	16 measurements
Astronaut notes recorded by stenographer	~3000 words per astronaut

A typical flow of science data between Mission Control and the field team was:

1. Data from the field was requested by Mission Control.
2. Data was uploaded from the field using a remote satellite terminal by a field team member to an FTP site. Folders were organized by date and included subfolders for each science instrument.
3. A designated Mission Control member transferred the files from the FTP site to a UWO server. Two copies were saved – one in an Archived folder for storage of unmodified data, and another in a Working Data folder, for storage of modified data products.
4. The Science Team in Mission Control viewed all of the data and renamed each file, adding the place name (either designated by astronauts or previously assigned by Mission Control) and data description to the end of the filename.
5. A separate folder of “Browsable Products” in the Working Data folder was designated for key images that the science team needed to share with each other

(e.g., labeled photographs, plotted geochemical data) and that were useful as a quick reference. Hierarchical folder structures and browsable image file names included the locality name and brief description of the image modification (e.g., stitched, stretched).

6. Astronaut notes were manually transcribed (from handwritten notes to typed, digital format). Notes and photos were manually linked to a map produced using GIS software (ArcMap) (Kerrigan et al., 2012).
7. New data products (e.g., labeled images) were used in instructions sent to field members.

Choosing an effective file naming system that eased searchability in a fast-paced environment was difficult. Finding particular data products was often a bottleneck in mission control. In addition, long filenames and even changing original file names, was problematic for some software applications.

Manually transcribing astronaut field descriptions, and linking these notes and corresponding photos into a GIS platform, was time consuming (Kerrigan et al., 2012). During this time lag, new data products were generated by modifying initial data (e.g., annotating images) and thus could not be incorporated into the map in real-time.

Overall, it proved to be extremely beneficial to have an active record of what data was requested by mission control, what data was returned, and what data was either returned corrupted (due to incomplete file transfer) or did not arrive at all. A low-tech solution was to keep an ongoing log posted on paper in a highly visible location in mission control.

4.5 Discussion and lessons learned: Lunar exploration strategies

4.5.1 Utility of robotic precursor mission

Exploratory, robotic reconnaissance controlled by a mission control has the potential to significantly improve scientific return from lunar surface exploration. In particular, data from robotic precursor missions can be used to narrow scientific focus (i.e., develop

specific research questions and hypotheses to test), improve traverse planning, reduce operational risk, and increase crew productivity.

We found that the primary scientific value of an exploratory reconnaissance mission is providing surface geology visualization at resolutions and from viewpoints not achievable from orbit. High-resolution surface imagery of surrounding areas on the scale of 10's of meters up to several km in extent was most useful. The most used data sets included large scale panoramic images that allowed a full contextual view of the surrounding area including exposure of rocks and traversability of the area and lidar scans that provided range and scale information.

From this experience, it is suggested that the reconnaissance mobility can be more reduced than the mobility needed later for crew transport (i.e., crew rover). A 'small' rover with the ability to collect panoramic photography and lidar scans would meet baseline needs. This type of rover would be required to access low lying areas (e.g., floor of impact crater) to view side of steep topography and reach high points to get panoramic views of the region.

4.5.2 New human exploration paradigm

During the Apollo EVAs, planned timelines were carefully followed by teams of mission controllers and science support personnel in the back rooms on Earth. Rarely were the crews "allowed" to get far behind this timeline (Eppler et al., 2013). New geological operation strategies for the Moon should be more flexible and allow the ability to change EVA schedules in real time, whether the final authority in making changes lie with the lunar crew or Mission Control.

On Earth, time spent at a specific locality can range from brief noting of position and the geology, to a multi-hour session involving considerable sampling, note-taking, and observation. A more flexible exploration approach can take advantage of the level of crewmember capabilities and adapt to the complexity of the geology observed at a particular site (Mader et al., 2012). In addition, future lunar missions will have an advantage over Apollo missions in that higher resolution images from orbital spacecraft

will be available and the astronauts will have access to these images in the field using display units. This will allow field crews to have access to the same background information as the ground support back on Earth, which would further enhance their ability to make decisions in the field.

In addition to better data sets and viewing capabilities in the field, future lunar missions will likely involve real-time data return. Other analogue missions that have tested real-time data return have had difficulty in analyzing data in a time to affect the next day's traverse plan (Eppler et al., 2013; Yingst et al., 2014). The ILSR phased-approach accounts for limited timelines of EVA's by maximizing the time spent making observations and ensuring that expertise of mission control scientists can help inform the planning of subsequent traverses. The focus of the reconnaissance traverse is to get a regional understanding of the geology and choose specific sites to study in detail during the follow-on detailed traverses.

By focusing on specific hypotheses to test, the astronauts and mission control were better able to prioritize geological tasks in a short four-day mission. However, a real challenge of planetary missions is answering a complex set of related and disparate problems with limited resources. In future work it would be useful to test the ILSR phased approach while addressing multiple hypotheses addressing different geological questions.

4.5.3 Data management

Simulating planetary missions on Earth can help test data management procedures, in order to help identify where current needs in data management architectures exist. Future surface lunar missions will operate on much faster time scales than the Mars Exploration Rover missions or other deep space missions. In addition, more data will be generated during a human mission than a rover mission over the same time scale. Operators and scientists will be required to maintain real-time situational awareness, quickly assimilate data from a rover or astronaut crew, and be able to plan or re-plan activities in response to incoming information (Deans et al., 2012).

The process of documentation and the roles of humans, machines, and automation in the process, will have a large impact on science return and the optimization of surface activities. Crew time required for traverse planning, data analysis, and other pre/post EVA activities will vary with mission duration and level of crew autonomy. Keeping track of incoming data products and their modification during a fast-paced exploration campaign is not trivial.

The UWO analogue mission program did not construct or use a specific software program for managing science data (e.g., NASA xGDS; Deans et al., 2012). Much of our data management was done manually. A customized system could automate many key processes, such as file naming and storage, aid in recording data history, and enable effective searching of raw and modified data. Key recommendations for designing and/or adding to existing systems include:

- Allow multiple ways of searching data, for example use “Tags” that would allow data to be queried by: instrument, date and time, site (e.g., site name, station number), location (e.g., enter coordinates or draw a point or area on map), who modified it, type of modifications, and if data (e.g. image) was used in instructions to the field team;
- Link raw and modified versions of the same data;
- Develop an indicator signal that informs mission control that data has arrived from the field;
- Automate file naming, archiving, and sorting of data into appropriate file structure;
- Create conventions addressing which software programs will be used to modify data (e.g., Photoshop, Adobe Illustrator) and ensure that file formats being used are compatible across applications.

4.6 Conclusions

The ILSR analogue mission was designed to focus on identifying, outlining, and organizing our understanding of how a precursor robotic field reconnaissance mission as a precursor to a human sortie sample return mission can affect science return; namely by examining field mapping protocols and guidelines for data collection, processing, and management. The results are based on qualitative observations from multiple perspectives. No one person can be witness to all aspects of an analogue mission and thus documentation of field and mission control processes was essential. By linking these recorded observations with mission objectives using a Program Theory table, a greater understanding of relationships between tasks and data products generated, and how they relate to the geological mapping process was gained.

Our study revealed the value of precursor reconnaissance missions in providing surface geology visualization at resolutions and from viewpoints not achievable from orbit, including high-resolution surface imagery on the scale of 10s of metres to kilometres. The datasets most used by mission control were:

1. 3D images of up to 360° extent generated from LiDAR cloud point data that provided range and scale information up to 1 kilometre away;
2. Large panoramic digital camera images allowing full context regional views including rock outcroppings and traversability of the area and side views of steep topography.

These data sets were used to construct reconnaissance traverses for a follow-on human mission. A phased approach for human exploration, was used, wherein, a given reconnaissance traverse was processed the next day by mission control and used to plan a traverse for detailed work two days after the original reconnaissance traverse. The detailed traverse plans incorporated astronaut feedback and allowed more autonomy for astronauts to determine optimal sampling localities and sites for detailed observations.

The fast-paced nature of processing and interpreting returned geological data by the mission control team requires streamlined data management. An automated system that

tracks data history, names files, and enables effective searching of raw and modified data would help improve the process and increase scientific return of the mission.

4.7 References

Antonenko, I., Osinski, G.R., Battler, M., Beauchamp, M., Cupelli, L., Chanou, A., Francis, R., Mader, M.M., Marion, C., McCullough, E., Pickersgill, A.E., Preston, L.J., Shankar, B., Unrau, T., Veillette, D., 2013. Issues of geologically-focused situational awareness in robotic planetary missions: Lessons from an analogue mission at Mistastin Lake impact structure, Labrador, Canada. *Adv. Sp. Res.* 52, 272–284.
doi:10.1016/j.asr.2012.11.024

Bleacher, J.E., Helper, M., Neal, C.R., Osinski, G.R., Robinson, M.S., Shearer, C.K., Snoke, A.W., Spudis, P.D., 2008. Lunar Field Geology and EVA Planning Based on Science Rationale, in: NLSI Lunar Science Conference. pp. 1–2.

Bray, V.J., Tornabene, L.L., Keszthelyi, L.P., McEwen, A.S., Hawke, B.R., Giguere, T.A., Kattenhorn, S.A., Garry, W.B., Rizk, B., Caudill, C.M., Gaddis, L.R., Van Der Bogert, C.H., 2010. New insight into lunar impact melt mobility from the LRO camera. *Geophys. Res. Lett.* 37. doi:10.1029/2010GL044666

Clark, P.E., Bleacher, J., Mest, S., Petro, N., Leshin, L., 2009. Lunar field exploration scenarios for a South Pole outpost, in: 40th Lunar and Planetary Science Conference, Abstract 1135. pp. 5–6.

Deans, M.C., Lees, D.S., Smith, T., Cohen, T.E., Morse, T.F., Fong, T.W., 2012. Field Testing Next-Generation Ground Data Systems for Future Missions, abstract 2518, in: 43rd Lunar and Planetary Science Conference. The Woodlands, Texas.

Deems, E., Baroff, L., 2008. A systems engineering process for the development of analog missions for the Vision for Space Exploration, in: Proceedings of the AIAA Space 2008 Conference. San Diego, California.

Ehrenfreund, P., McKay, C., Rummel, J.D., Foing, B.H., Neal, C.R., Masson-Zwaan, T., Ansdell, M., Peter, N., Zarnecki, J., MacKwell, S., Perino, M.A., Billings, L., Mankins,

J., Race, M., 2012. Toward a global space exploration program: A stepping stone approach. *Adv. Sp. Res.* 49, 2–48. doi:10.1016/j.asr.2011.09.014

Eppler, D., Adams, B., Archer, D., Baiden, G., Brown, A., Carey, W., Cohen, B., Condit, C., Evans, C., Fortezzo, C., Garry, B., Graff, T., Gruener, J., Heldmann, J., Hodges, K., Hörz, F., Hurtado, J., Hynek, B., Isaacson, P., Juranek, C., Klaus, K., Kring, D., Lanza, N., Lederer, S., Lofgren, G., Marinova, M., May, L., Meyer, J., Ming, D., Monteleone, B., Morisset, C., Noble, S., Rampe, E., Rice, J., Schutt, J., Skinner, J., Tewksbury-Christle, C.M., Tewksbury, B.J., Vaughan, A., Yingst, A., Young, K., 2013. Desert Research and Technology Studies (DRATS) 2010 science operations: Operational approaches and lessons learned for managing science during human planetary surface missions. *Acta Astronaut.* 90, 224–241. doi:10.1016/j.actaastro.2012.03.009

Fong, T., Abercromby, A., Bualat, M.G., Deans, M.C., Hodges, K. V, Hurtado, J.M., Landis, R., Lee, P., Schreckenghost, D., 2010. Assessment of robotic recon for human exploration of the Moon. *Acta Astronaut.* 67, 1176–1188.
doi:10.1016/j.actaastro.2010.06.029

Grieve, R.A.F., 1975. Petrology and chemistry of the impact melt at Mistastin Lake crater, Labrador. *Geol. Soc. Am. Bull.* 86, 1617–1629.

International Space Exploration Coordination Group (ISECG), 2013. The Global Exploration Roadmap.

Kerrigan, M.C., Shankar, B., Marion, C.L., Francis, R., Pickersgill, A.E., Capitan, R.D., Osinski, G.R., Team, I., 2012. Real-Time Mission Control Tracking of Astronaut Positions During Analogue Missions, abstract 2756, in: 43rd Lunar and Planetary Science Conference. The Woodlands, Texas.

LEAG Science Scenarios for Human Exploration Specific Action Team, 2009. Meeting report Phase I Final.

Lim, D., Abercromby, A., Gernhardt, M., Shepard, R., Brady, A., Forrest, A., Laval, B., Marinova, M., Slater, G., Reid, D., Love, S., McKay, D., 2011. A report on the

development and application of Pavilion Lake Research Project (PLRP) science and data acquisition success (SDAS) metrics: Canadian Space Agency White Paper.

Mader, M.M., Eppler, D., Osinski, G.R., Brown, J., Ghafoor, N., 2012. Unifying science-driven and resource exploitation strategies for lunar missions: applying lessons learned from terrestrial geological exploration and Canadian planetary, IAC-12,A3,2C,5,x15499 analogue missions, in: 63rd International Astronautical Congress. Naples, Italy.

Mader, M.M., Osinski, G.R., 2011. Insight into lunar impact cratering processes based on field mapping of the Mistastin Lake Impact Structure, Labrador, abstract #P43C-1698, in: American Geophysical Union, Fall Meeting 2011. San Francisco.

Mader, M.M., Osinski, G.R., Antonenko, I., Barfoot, T., Battler, M., Beauchamp, M., Chanou, A., Cloutis, E., Daly, M., Ghafoor, N., Grieve, R.A.F., Hodges, K., Jolliff, B.L., Kerrigan, M., McCullough, E., Moores, J., Otto, C., Pickersgill, A., Preston, L., Redman, D., Sapers, H., Shankar, B., Singleton, A., Sylvester, P., Tornabene, L.L., Unrau, T., Young, K., Zanetti, M., 2011. Use of robotic precursor mission for follow-on human exploration: Case study lunar analogue mission at the Mistastin Lake impact structure, abstract #2033, in: Annual Meeting of the Lunar Exploration Analysis Group. Houston, TX, pp. 2010–2011.

Marion, C.L., Osinski, G.R., Abou-Aly, S., Antonenko, I., Barfoot, T., Barry, N., Bassi, A., Battler, M., Beauchamp, M., Bondy, M., Blain, S., Capitan, R.D., Cloutis, E.A., Cupelli, L., Chanou, A., Clayton, J., Daly, M., Dong, H., Ferrière, L., Flemming, R., Flynn, L., Francis, R., Furgale, P., Gammel, J., Garbino, A., Ghafoor, N., Grieve, R.A.F., Hodges, K., Hussein, M., Jasiobedzki, P., Jolliff, B.L., Kerrigan, M.C., Lambert, A., Leung, K., Mader, M., McCullough, E., McManus, C., Moores, J., Ng, H.K., Otto, C., Ozaruk, A., Pickersgill, A. E. Pontefract, A., Preston, L.J., Redman, D., Sapers, H., Shankar, B., Shaver, C., Singleton, A., Souders, K., Stenning, B., Stooke, P., Sylvester, P., Tripp, J., Tornabene, L.L., Unrau, T., Veillette, D., Young, K., Zanetti, M., 2012. A Series of robotic and human analogue missions in support of lunar sample return, abstract #2333, in: 43rd Lunar and Planetary Science Conference. The Woodlands, Texas.

McCullough, E., Pickersgill, A.E., Francis, R., Bassi, A., Shankar, B., Mader, M.M., Beauchamp, M., Osinski, G.R., KRASH Operations and Science Team, 2012. Scientific Application of Visual Systems Instrumentation used during Lunar Sample Return Analogue Missions, abstract #2687, in: 43rd Lunar and Planetary Science Conference. The Woodlands, Texas.

McDavid, J.C., Huse, I., Hawthorn, L.R.L., 2013. Program evaluation & performance measurement: an introduction to practice, 2nd ed. SAGE Publications, Thousand Oaks, Calif.

Milazzo, M.P., Keszthelyi, L.P., Jaeger, W.L., Rosiek, M., Mattson, S., Verba, C., Beyer, R.A., Geissler, P.E., McEwen, A.S., Team, H., Team, the H., 2009. Discovery of columnar jointing on Mars. *Geology* 37, 171–174. doi:10.1130/G25187A.1

NASA, 2011. NASA's Analog Missions: Paving the Way for Space Exploration. NASA Langley Research Center, Hampton, VA.

Osinski, G.R., Tornabene, L.L., Grieve, R. a. F., 2011. Impact ejecta emplacement on terrestrial planets. *Earth Planet. Sci. Lett.* 310, 167–181. doi:10.1016/j.epsl.2011.08.012

Schreckenghost, D., Milam, T., Fong, T., 2010. Measuring Performance in Real Time during Remote Human-Robot Operations with Adjustable Autonomy. *IEEE Intell. Syst.* 25, 36–45. doi:10.1109/MIS.2010.126

Shankar, B., Antonenko, I., Osinski, G.R., Mader, M.M., Preston, L., Battler, M., Beauchamp, M., Chanou, A., Cupelli, L., Francis, R., Marion, C., McCullough, E., Pickersgill, A., Unrau, T., Veillette, D., 2011. Lunar analogue mission: Overview of the site selection process at Mistastin Lake impact Structure, Labrador, Canada, abstract #2594, in: 42nd Lunar and Planetary Science Conference. The Woodlands, Texas.

Tornabene, L.L., Osinski, G.R., Mader, M.M., Chanou, A., Francis, R., Joliff, B.L., Marion, C., McCullough, E., Pickersgill, A., Sapers, H., Souders, K., Sylvester, P., Young, K., Zanetti, M., Operations, K., Team, S., 2012. Utility of Remote Sensing, Robotic Precursor Data and a Focused Science Hypothesis for a Follow-On Human

Exploration Lunar Analogue Mission at the Mistastin Lake (Kamestastin) Impact Structure, abstract # 2390, in: 43rd Lunar and Planetary Science Conference. The Woodlands, Texas.

Weisbin, C., Elfes, A., Lincoln, W., Smith, J.H., Hua, H., Mrozinski, J., Shelton, K., 2007. Collaborative Human-Robot Science Exploration on the Lunar Surface, in: LEAG Annual Meeting. Houston, TX.

Wholey, J.S., Hatry, H.P., Newcomer, K.E., 2010. Handbook of practical program evaluation, 3rd ed. Jossey-Bass, San Francisco.

Yingst, R. a., Cohen, B. a., Hynek, B., Schmidt, M.E., Schrader, C., Rodriguez, a., 2014. Testing Mars Exploration Rover-inspired operational strategies for semi-autonomous rovers on the moon II: The GeoHeuristic operational Strategies Test in Alaska. *Acta Astronaut.* 99, 24–36. doi:10.1016/j.actaastro.2014.01.019

Chapter 5

5 New insights into the structure of the Mistastin Lake impact structure, Labrador, Canada

5.1 Introduction

Our understanding of the impact cratering process continues to advance with new investigations of hypervelocity impact craters on rocky planetary surfaces using topographic, geophysical, and high-resolution image data sets produced by ongoing orbital missions and from field studies at terrestrial craters. Studies of planetary and terrestrial craters are complimentary: while planetary crater forms are often preserved in a pristine state, we can only very rarely investigate their geological units *in situ* (e.g., the Mars Exploration Rover Opportunity's investigations of craters on Mars: Squyres et al., 2009; Apollo 16 investigations of North Ray crater ejecta: Heiken et al., 1991). In contrast, active geological processes on Earth have eroded and modified impact craters, though we can more easily reach them to study in the field. For these reasons, it is important to compare complimentary data sets in order to correlate impactite units to specific features (e.g., rim, floor, central uplift) of the particular impact crater being studied.

The systematic study of mid-size complex impact structures was recommended as a priority at the first Bridging the Gap conference in 2003 (Herrick and Pierazzo, 2003) and provided the motivation for this study. This study forms part of a multi-year investigation of a series of impact craters in the 20 to 40 km size range, in different target rocks (Osinski et al., 2008). Very few complex impact craters have been mapped in detail; most of the ones that have, are located in sedimentary targets including: the ~5 km diameter Upheaval Dome (Kriens and Shoemaker, 1999), ~6 km diameter Decaturville (Offield and Pohn, 1979), ~12 km diameter Wells Creek (Wilson and Stearns, 1968), ~13 km diameter Sierra Madera (Wilshire et al., 1972), ~23 km diameter Houghton (Osinski and Spray, 2005), and the ~24 km diameter Gosses Bluff (Milton et al., 1996a, 1996b) impact structures.

The Mistastin Lake impact structure provides a unique opportunity to study a moderately eroded complex impact structure in crystalline rocks where the structural features, such as the collapsed crater rim and central uplift, are still intact, with some modification. Almost no previous structural mapping has been conducted at this site. Here, we present the results of geological, structural, and morphological analyses of the Mistastin Lake impact structure based on field work and lineament mapping of remote sensing images. This includes new interpretations about the fault history, preservation state, crater form, and ultimately, the morphometrics of mid-size terrestrial complex structures (e.g., ~20–40 km). Our field and remote sensing observations provide new insights into crater formation and modification in crystalline target rocks.

5.2 Geological setting of the Mistastin Lake impact structure

The Mistastin Lake impact structure (55°53'N; 63°18'W) formed within the Mesoproterozoic Mistastin batholith (~1420 Ma; Emslie, 1993; Emslie et al., 1980), which itself is part a suite of Elsonian intrusive rocks (~1230 Ma to 1460 Ma; Gower and Krogh, 2002) in central Labrador. The batholith was emplaced after the Hudsonian (~2 to 1.8 Ga) but prior to Grenvillian (~1.2 to 1.0 Ga) orogenesis, and is considered to be anorogenic (Emslie et al., 1980). The north-south elliptical batholith covers an area of ~5000 km², and has undergone minimal metamorphism, preserving pristine igneous textures within the target rocks surrounding Mistastin Lake (Emslie et al., 1980) (Figure 5-1).

The glacial history of Labrador is complex, having experienced numerous glacial events throughout the Pleistocene epoch. The last glacial advance to affect the study area proceeded from the Labrador Trough northeastwards across the Mistastin Lake region (Klassen and Thompson, 1990). Early studies provide broad estimates of erosion in the study area (~100 m) (Grieve and Cintala, 1992; Phinney and Simonds, 1977), based on the assumption of an initial single coherent melt sheet that was at least 200 m thick with a pre-erosional impact melt volume of 20 km³. More recent work (Marion et al., Forthcoming) examined the vesicularity and crystallization temperatures of melt rocks and suggested that the melt sheet was more variable in thickness. This study attributed

the present-day differences in melt rock thicknesses at different locations to topographical effects that affected melt emplacement as well as differential erosion Marion et al. (Forthcoming).

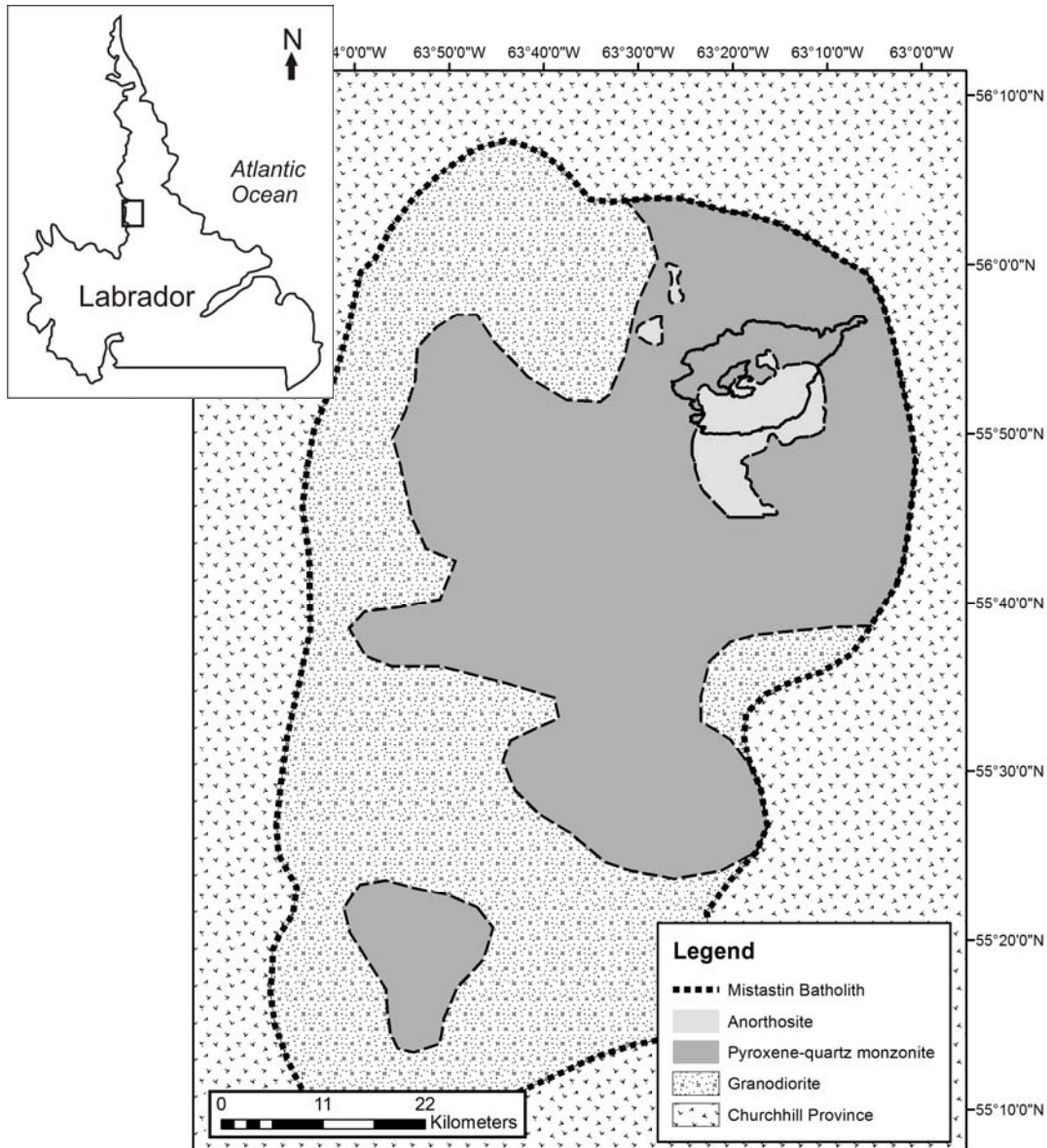


Figure 5-1: Geological map of the Mistastin batholith. Modified from Emslie et al., (1980). Updated anorthosite boundary based on magnetic anomalies on residual total magnetic map (Dumont and Jones, 2012).

The earliest geological studies of the Mistastin Lake area were conducted as part of a reconnaissance mapping initiative by the Geological Survey of Canada (Currie, 1971; Taylor and Dence, 1969). Taylor and Dence (1969) proposed an asteroid impact origin for the structure based on field and microscopic evidence that identified shattercones, planar deformation features (PDFs) in quartz, and diaplectic quartz and feldspar glasses. Currie (1971) produced a geological map of the area, where he interpreted the roughly circular structure as being volcanic in origin. This interpretation has since been refuted and all subsequent studies have attributed the origin of the crater structure to an asteroid impact.

Relatively little field work has been conducted since the early 1970s. Studies of the Mistastin Lake impact structure have predominantly focused on geochemistry and on characterizing the impact melt rocks (Grieve, 1975; Marchand and Crocket, 1977; Marion and Sylvester, 2010; McCormick et al., 1989). Little to no structural mapping of the Mistastin impact structure has previously been conducted. This study presents the results of new geological mapping of the Mistastin Lake impact structure, highlighting structural features, preservation state, and crater morphology.

5.3 Methods

A digital elevation model (DEM) mosaic of the Mistastin Lake region was generated using standard processing and mosaic techniques for DEMs with the Environment for Visualizing Images (ENVI) version 4.8 software package. The DEM data was sourced from the Geobase website (<http://www.geobase.ca/>) and was generated by the Government of Canada, Natural Resources Canada, and the Centre for Topographic Information (CTI), Sherbrooke, Quebec. Canadian Digital Elevation Data (CDED) was sourced from a variety of datasets including: 1) hypsographic and hydrographic elements of the National Topographic Data Base (NTDB) at scales of 1:50 000 and 1:250 000, 2) the Geospatial Data Base (GDB), 3) various scaled positional data acquired by the provinces and territories, or 4) remotely sensed imagery. For more information on CDED data, see <http://www.geobase.ca/geobase/en/data/cded/description.html>.

Shaded relief images from different sun angles were generated using the ENVI software program (see Appendix B), and lineaments were traced on raster images using version 10 of the ArcGIS software. Eight different shaded relief images were generated with a sun angle of 30° above the horizon, each from a different azimuth direction at 45° intervals starting at north (see Appendix B). The low sun angle was useful in highlighting lineaments at high angles to the azimuth direction of the sun. Lineaments equal to or greater than ~ 1 km in length were plotted. A schematic map of lineaments within and around the Mistastin Lake impact structure extending to a distance of approximately two crater radii was compiled. Twenty radial profiles across the impact structure were created in ENVI using the mosaic DEM as the reference image (Appendix C). The profile lines were spaced 22.5° apart, starting from the lakeshore across the greatest topographical high, extending outward to a distance of ~ 42 km from the impact structure centre. Topographic highs were recorded along these profiles.

Field mapping was conducted over three field seasons, in the late summers of 2009, 2010, and 2011. Most field mapping was conducted along the shoreline and in creek beds, within a 3 km radial distance from the lakeshore. The primary focus for geological exploration was at sites that offered three dimensional exposures of stratigraphy, such as vertical cliffs. Outcrops were accessed by zodiac boat and on foot. Key outcrops within this zone, which included contacts between various impactites, were studied in detail. Fractures, faults, and dyke orientations were measured *in situ* and digitized onto a basemap using ArcGIS 10.2 and the NAD83 UTM Zone 20 geodetic datum.

5.4 Results

5.4.1 Topography

Points of topographic highs recorded along profile lines across the DEM generated for this study define two discontinuous ellipsoids (Figure 5-2). The major and minor axes of the outer ellipse are 30 km and 26 km, respectively, and the axes of the inner ellipse are 23 km and 19 km, respectively. The maximum height of the outer ellipse ranges from 145 m to 300 m above lake level and is highest in the northwest quadrant of the study area

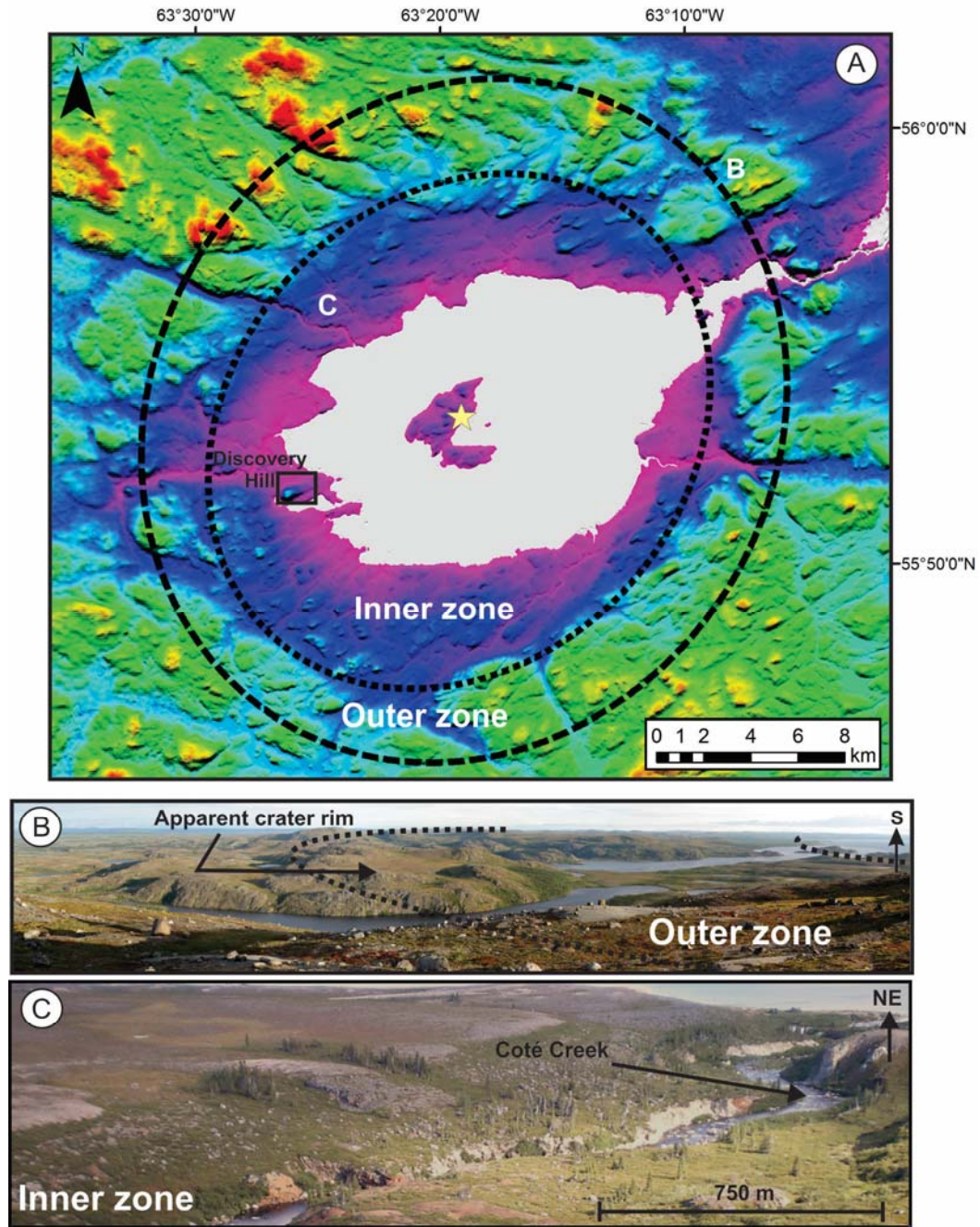


Figure 5-2: A) Shadowed relief DEM showing topography of the Mistastin impact structure. Elevations are lowest near the shoreline, represented by purple and blue.

Highest elevations are red. The star marks the centre of the impact structure. Dashed lines mark ellipses defined by topographic highs. Labels B and C denote the locations of photos. B) Typical rock exposure and vegetation cover within the outer zone, NE quadrant. C) Typical rock exposure and vegetation cover within the inner zone, NW quadrant.

(Figure 5-3b). The outer ellipse is lower in the southwest quadrant where maximum height ranges from 145 m to 210 m (Figure 5-3d).

The discontinuous rings of hills divide the region between the lakeshore and the outer ellipse into two zones, herein termed the inner and outer zones (Figures 5-2, 5-3). The inner zone surrounds the lake and extends up to 5 km radially from the lakeshore. It is notably lower in elevation, has a gradual slope, fewer rock exposures, and more vegetation cover than the outer zone (Figures 5-2c, 5-3). The inner zone is also characterized by radial streams controlled by the inward facing slope of the zone, similar to stream patterns observed in other terrestrial impact structures (McHone et al., 2002). The outer zone is defined by a variable slope, abundant bedrock exposure, and is most pronounced in the northwest quadrant surrounding the lake (Figure 5-2b, 5-3b).

A unique ramp-shaped hill of predominantly impact melt rock is found within the inner zone (Figures 5-2a, 5-3d). Locally known as Discovery Hill, this is the largest and thickest (~80 m) outcrop of impact melt in the Mistastin Lake impact structure and has been described in detail by Grieve (1975) and Marion et al. (Forthcoming).

The inner and outer zones of the Mistastin Lake structure are dominated by quartz monzonite and granodiorite. Within the outer zone these rocks have retained their original coarse-grained igneous textures and characteristic massive appearance (Figures 5-4a,b,c). The inner zone is dominated by more fractured target rock and monomict impact breccias (Figures 5-4d and e).

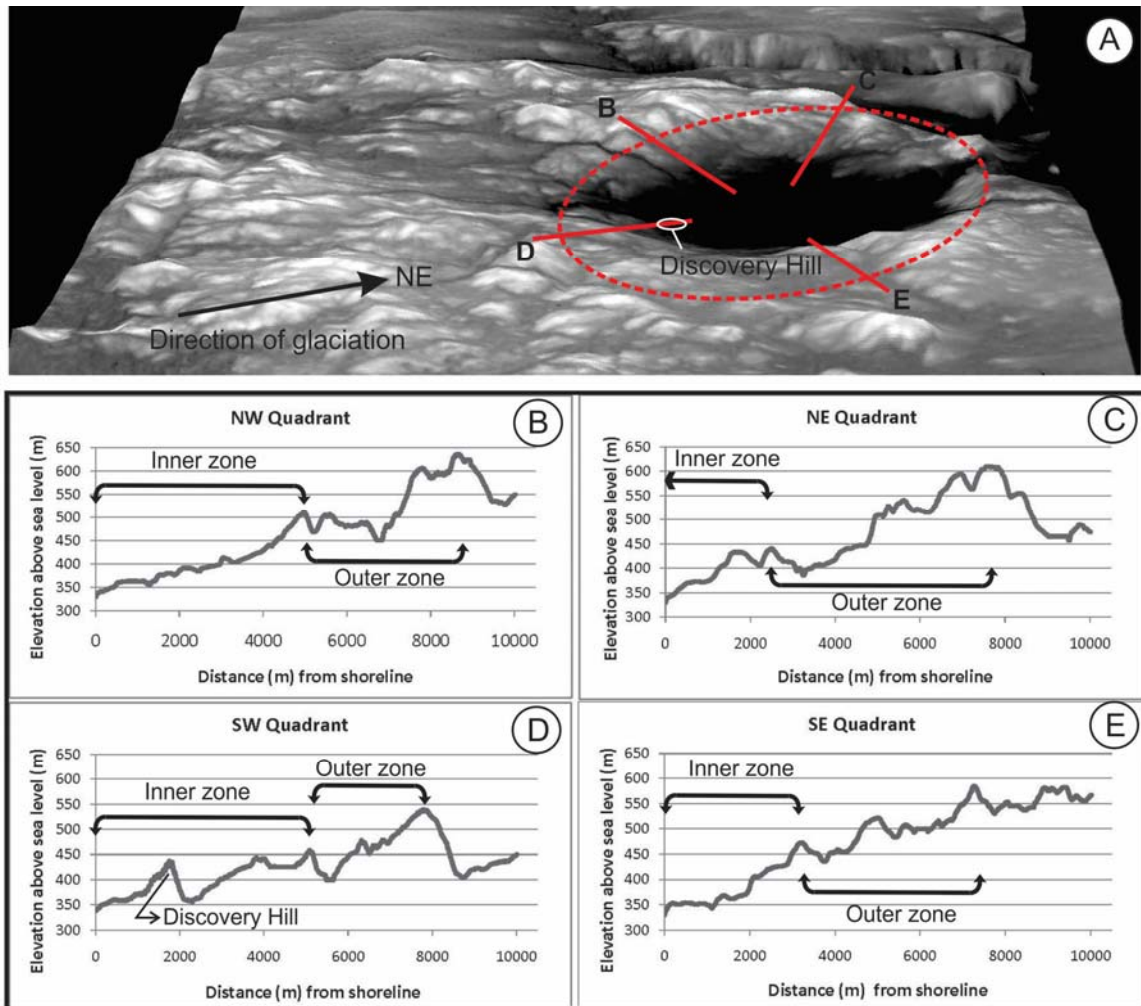


Figure 5-3: A) Tilted shaded relief DEM; vertical scale exaggerated. Red lines indicate location of representative profile lines for each quadrant. Letters correspond to Figures B–E). Representative profiles highlighting stepped topography in different quadrants surrounding Mistastin Lake.

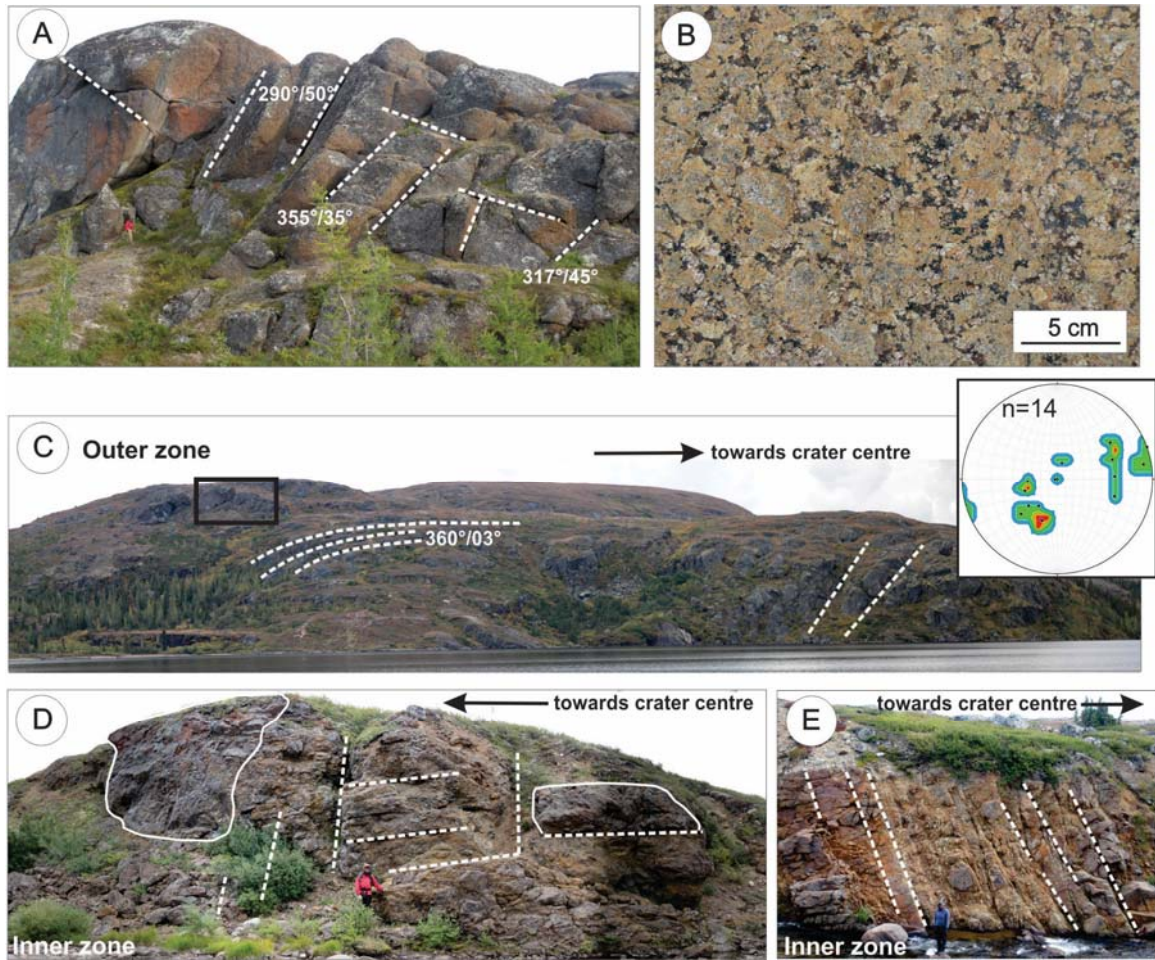


Figure 5-4: Field images of target rocks in the rim region of the Mistastin Lake impact structure. Fractures are marked with dashed lines. (A) Massive granodiorite within the outer zone (see person in red jacket for scale). (B) Detail of coarse-grained granodiorite with primary igneous texture preserved. (C) Massive granodiorite and quartz monzonite along Mistastin River within the outer zone. (Photos is ~ 300 m across) Box outlines area shown in A. Inset: 14 structural data points for this region are plotted on an equal-angle stereonet as poles to fracture planes. (D) Two fracture sets observed within monomict impact breccias within the inner zone. Solid lines outline blocks of target rock. (See person in red jacket for scale). (E) Monomict breccia observed in ~5 m wide fault zone, interpreted as fault breccias that formed during the impact event, oriented parallel to the illustrated fracture set within the inner zone. (See person in blue jacket for scale).

5.4.2 Lineaments

Regional-scale lineaments outside of the crater structure to the southwest are tens of kms in length and have a spacing of 4 to 5 km. There are two main groups: one set oriented ENE–WSW (azimuth $\sim 050\text{--}060^\circ$), and a second set of parallel, curvilinear NE–SW regional faults (azimuth $\sim 135^\circ$) that offset the first set and are concave towards the southwest (Figure 5-5). There are several E–W trending regional lineaments to the north of the impact structure.

The density of shorter (<10 km, average ~ 2.5 km) linear depressions increases closer to the crater structure and are concentrated within a region located 10–23 km radially from the crater centre (Figure 5-5). They define a zone of lineaments inside and beyond the outermost raised ring of hills that is best defined in the southeast and northwest regions. Overall, 184 lineaments were mapped, 73 inside the raised ring of hills and 111 beyond this ring (Figure 5-6).

The southeast region surrounding Mistastin Lake is dominated by lineaments parallel to ENE–WSW trending regional faults. In contrast, the northwest region, is dominated by two lineament sets oriented at roughly 90° to one other, and are not parallel to regional faults (Figures 5-6b, c). Overall, approximately 25% of these short linear features are roughly parallel to regional lineaments (Figure 5-6a).

Irregular fractures and m-scale fracture sets are observed throughout the inner and outer zone of the impact structure within fractured target rocks and monomict breccias.

Typically, two fracture sets at right angles to each other are observed with strike orientations perpendicular to the crater centre direction with dips ranging from 5° to 85° , though most are close to 45° (e.g., Figures 5-4a, d, and c stereonet inset). Within the inner zone, some of the steeply dipping fracture sets, oriented radially to the centre of the impact structure, are marked by the presence of breccias (Figure 5-4e). The breccias units are 1 to 10 m in width and both the clast population and the matrix are the same composition as are the adjacent wall rocks. The matrix consists of lithic fragments that are less than 0.5 mm in diameter. Angular to subrounded clasts make up 50–60% of

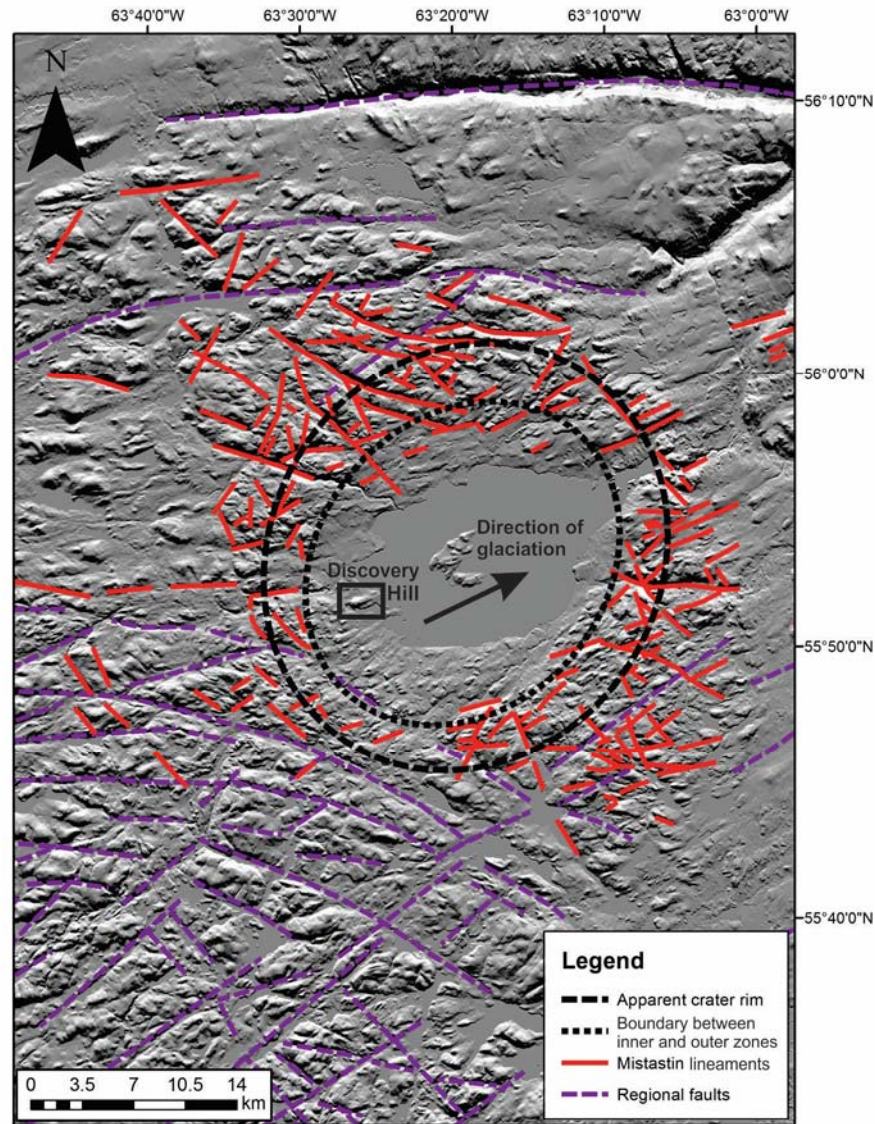


Figure 5-5: Lineament map of the Mistastin Lake impact structure and surroundings. The basemap is a shaded relief image generated with a sun angle of 30° above the horizon, from an azimuth direction at 0°. Two groups of long lineaments outside of the crater are defined (purple dashed line): the NE-SW trending set and later W-SE trending curvilinear set are both interpreted as regional faults. The density of short lineaments < 10 km in length are concentrated within the outer zone and within 10 km from the apparent crater rim. A NE-SW glacial fabric is notably visible within the inner zone.

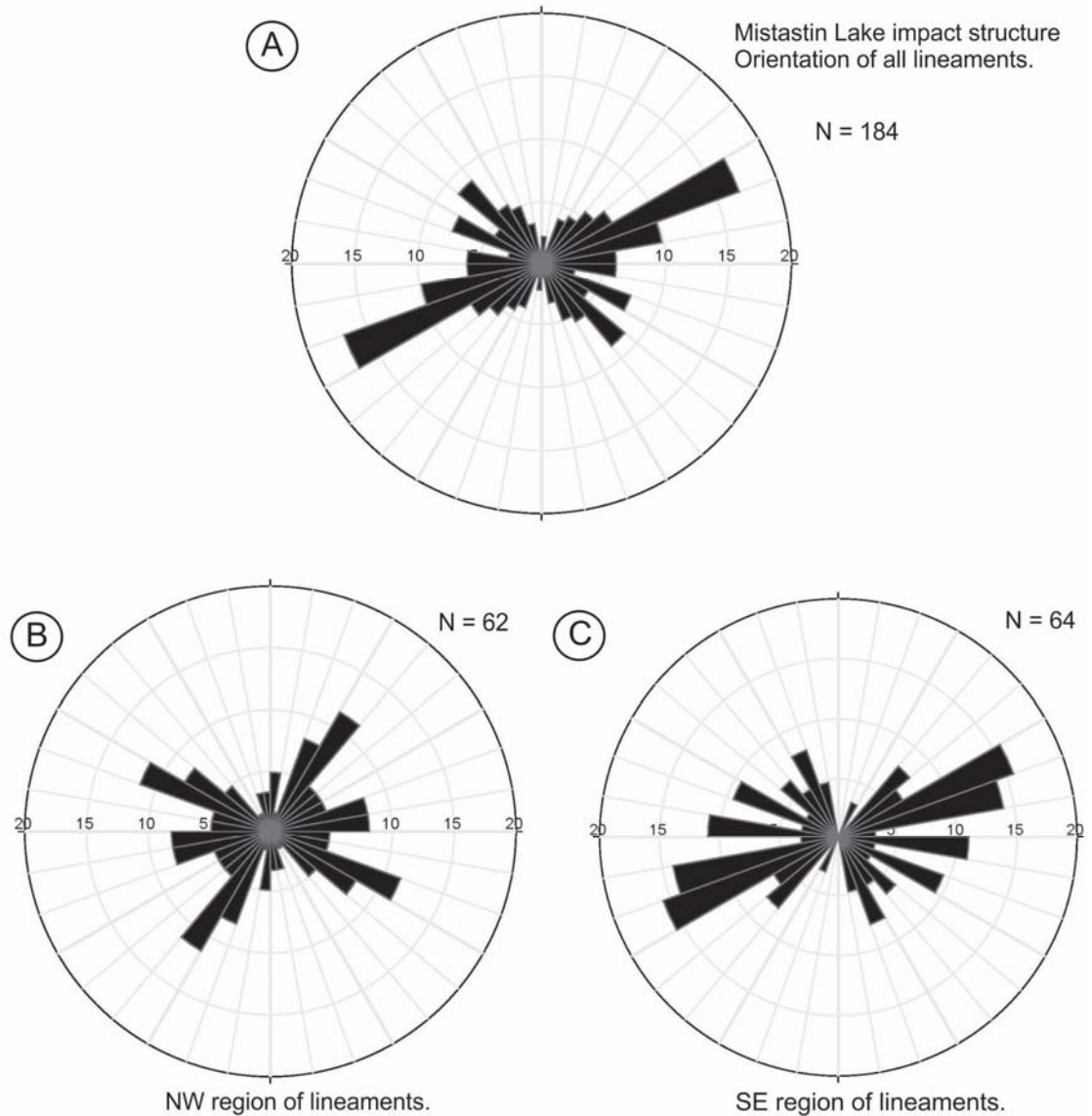


Figure 5-6: Rose diagrams depicting the frequency of lineaments for a given orientation associated with the Mistastin Lake impact structure. Note: dip data could not be collected for lineaments using shaded relief images, therefore they are plotted bi-directionally (symmetrical) on the circular histogram. (A) Plot of all Mistastin lineaments as identified in Fig. 4. (B) Lineaments within the NW region. (C) Lineaments within the SE region.

breccia units and range in size from mm to cm in breccia units that are less than 1 m in width, up to m-scale fragments occur in the large units (e.g., see Figure 5-4e).

5.4.3 Glacial fabrics and landforms

A regional northeast-southwest glaciation fabric defined by fluted drift ridges (Currie, 1971) is prominent in non-rocky areas such as the southwestern quadrant of the inner zone (Figure 5-5). Scattered glacial crag and tail structures, both inside and outside of the outer ring of hills, are oriented in a southwest to northeast direction. They are characterized by elongate, streamlined hills consisting of resistant rock at the high end, and a tapering tail extending down ice (Benn and Evans, 1998). Within the Mistastin Lake impact structure Discovery Hill defines a classic crag and tail shape, with a ramp dipping towards the lake in a north-easterly direction (Figure 5-7).

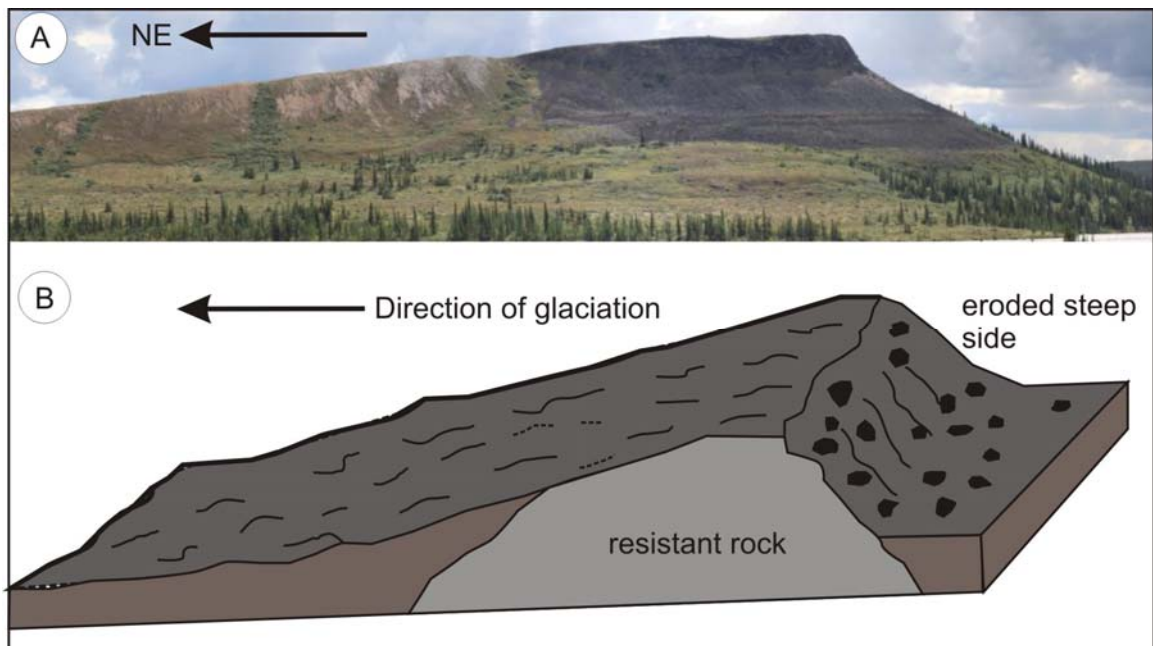


Figure 5-7: (A) Discovery Hill feature, Mistastin Lake impact structure. Dark rocks are impact melt rocks. Maximum height of ramp is 120m above lake level. (B) Schematic of a crag and tail glacial feature.

5.5 Interpretations and Discussion

On Earth, erosion and tectonics have modified the surface morphology of all impact craters to a greater or lesser extent. As such, the original morphologic and morphometric characteristics have been enhanced, modified, or removed. New geological field mapping of the collapsed rim region synthesized with remote sensing datasets allows us to make the first structural interpretations of the Mistastin Lake impact structure. Field mapping for this study did not focus on the central uplift region, which was targeted by complementary studies by Singleton et al. (2014, 2012, 2011).

5.5.1 Effect of pre-existing structures on crater modification

Pre-existing structures can influence the impact cratering process and result in atypical crater forms. The presence of pre-existing faults can also influence fault development during the impact event, as some of the strain can be accommodated along pre-existing planes of weakness. However, as noted by Melosh (1989), it is unlikely that the number of pre-impact fractures sets would have been sufficient to accommodate the strain imposed by impact crater excavation or collapse, thus new fractures at different orientations must develop. Lineament mapping of the Mistastin region clearly show the presence of long, km-scale, lineaments trending ENE–WSW (azimuth $\sim 050\text{--}060^\circ$) and NE–SW regional lineaments (azimuth $\sim 135^\circ$) (Figure 5-5). There are several E–W trending long lineaments to the north of the impact structure. The absolute age of the development of these lineaments is unknown, though we interpret these as pre-impact regional faults likely related to Grenvillian tectonics (Rivers and Corrigan, 2000 and references therein) and post-date the emplacement of the 1420 Ma Mistastin batholiths (Emslie, 1993; Emslie et al., 1980). The Grenville Orogen developed along the southeastern margin of Laurentia between ca. 1200 and 1000 Ma (Rivers and Corrigan, 2000 and references therein), as a continental thrusting event. The northeast-southwest trending Grenville front was located ~ 250 km southwest of the Mistastin Lake batholith. The Mistastin Lake curvilinear regional faults (Figure 5-5) that locally offset the northeast-southwest faults at high angles, may also be related to this regional thrusting event.

We mapped a complex network of lineaments within the collapsed crater rim region and beyond the outermost raised ring of hills of the Mistastin Lake impact structure. Locally, breccias were observed within steeply dipping fracture sets, oriented radially to the centre of the impact structure, within the inner zone (Figure 5-4e). The breccia clast populations and matrices are composed of the same rock type as the adjacent wall rocks. Based on breccia unit location and trend, as well as clast morphology and composition, we interpret them as chaotic fault breccias based on the classification scheme of Woodcock and Mort (2008). Overall, the network of lineaments within the Mistastin Lake region is interpreted here as a fracture and fault system that formed as a result of the impact event.

A rose diagram of lineament orientations shows that, overall, approximately a quarter of the fractures and faults associated with the Mistastin lake structure are parallel to the two main regional fault systems (Figure 5-6a). It is significant that more of the lineaments are parallel to regional faults in the southeast quadrant than in the northwest quadrant (Figures 5-6b, c). The northwest region is dominated by lineaments oriented radially and concentrically with respect to the centre of the crater. Though the reason for this remains unclear, one possible explanation is that there was a non-uniform distribution of pre-existing faults, wherein there were fewer regional faults in the northwest quadrant. Alternatively, this may simply be the result of the impact cratering process where the collapse of the crater rim was non-symmetrical, which has been shown to be the case at other similar-sized impact craters (Osinski and Spray, 2005).

The El'gygytgyn impact structure, which formed in felsic volcanic rocks, also has a complex system of short faults within and beyond the 18 km apparent crater rim (Gurov et al., 2007). The density of these faults is highest at the inner slopes of the crater rim and gradually decreases outwards, a trend also determined for the Deep Bay impact structure, Canada (Innes, 1964), and for 29 lunar impact structures (Baldwin, 1978). In comparison, the density of fractures and faults within the southeast quadrant of the Mistastin Lake impact structure increases beyond the outermost raised ring of hills, whereas, the density of fractures and faults within the northwest region decreases beyond the outermost raised ring of hills. This discrepancy is attributed to the distribution of pre-existing, regional faults. Reactivated regional faults beyond the raised ring of hills in the southeast quadrant

are thought to have caused a higher density of small fractures and faults generated during impact. In comparison, the lower density of short lineaments beyond the raised ring of hills in the northwest quadrant is attributed to a lesser number of regional faults in this region.

The effect of pre-existing faults can also cause asymmetries in the crater form and result in polygonal crater shapes (Eppler et al., 1983; Öhman et al., 2010). The rectangular shape of Meteor Crater in Arizona is one of the best terrestrial examples of this process. Shoemaker (1960) observed two mutually perpendicular sets of pre-impact vertical joints of uniform strike (NE-SW and NW-SE) that are interpreted to have influenced the final shape of the 1.2 km crater (Kumar and Kring, 2008). Similarly, the pre-existing, regional faults within the Mistastin batholiths may have influenced the final shape of the Mistastin Lake impact structure and may have contributed to its present-day elongated shape.

5.5.2 Tectonics of crater rim collapse at Mistastin

We have defined inner and outer zones at Mistastin that are apparent on a hill shaded, colourized DEM and in the field (Figure 5-2). The boundary of the inner and outer zones is marked by an ellipse defined by topographic high points, variation in slope within each zone, changes in lineament patterns, and differences in nature and extent of rock exposure (Figures 5-2, 5-3). The lower zone is covered in glacial till and is characterized by radial streams controlled by the slope of the zone, similar to stream patterns observed in other terrestrial impact structures (e.g., Zhamanshin impact structure, Kazakhstan and Connolly Basin impact structure, Australia; McHone et al., 2002). Discovery Hill, a large outcropping of impact melt rock, located within the inner zone, is not thought to be continuous with the impact melt sheet within the original transient cavity, contrary to previous interpretations (Grieve, 2006, 1975). Instead, we suggest that it may be analogous to melt ponds observed within terraces (i.e., collapsed rim region) of lunar craters, emplaced during the crater modification stage (Hawk and Head, 1977; Howard and Wilshire, 1975). Overall, the stepped topography of the Mistastin Lake rim region is interpreted as the collapsed rim region formed during the modification stage of crater formation.

The style of faulting in the rim region at Mistastin is in stark contrast to craters developed in layered sedimentary targets that have pre-existing planes of weaknesses between boundaries of rock units. This is particularly evident when comparing the Mistastin Lake impact structure to the similarly sized 23 km diameter Haughton impact structure, which developed within a gently dipping, 1.9 km thick sequence of sedimentary rocks.

Haughton exhibits a very clear pattern of faulting in the rim region with sub-vertical radial faults, sub-horizontal bedding parallel detachment faults, and long, multi-km scale curved concentric listric normal faults (Osinski and Spray, 2005) (Figure 5-8).

Continuous, clearly defined, curvilinear faults bounding plateaus are not evident in the field or in remote sensing datasets for the Mistastin Lake impact structure. Instead, the outer zone is characterized by many 1–5 of km² blocks (Figure 5-8).

It is well known that target properties such as rheology and stratigraphic layering can influence the geometry and distribution of faults produced from an impact event. Based largely on studies of craters in sedimentary targets, it has been proposed that strain associated with transient cavity collapse of impact craters on Earth is typically concentrated into rheologically soft beds, and that low-angle faults or detachments develop along stratigraphic boundaries (Kenkmann et al., 2013). A simple explanation for the different style of faulting at Mistastin is attributed to the competent, homogenous nature of the crystalline target rocks. Instead of forming the long, curved listric slump blocks along pre-existing bedding planes, at Mistastin the deformation is characterized by blocky angular fault blocks. This is evident in radial transects taken across the topography in each quadrant (Appendix C). The range of fracture set orientations may reflect the displacement of large blocks on the scale of 100s of metres to kilometres, although, without any internal crystalline layering, it is difficult to know if the target rocks have been displaced or not.

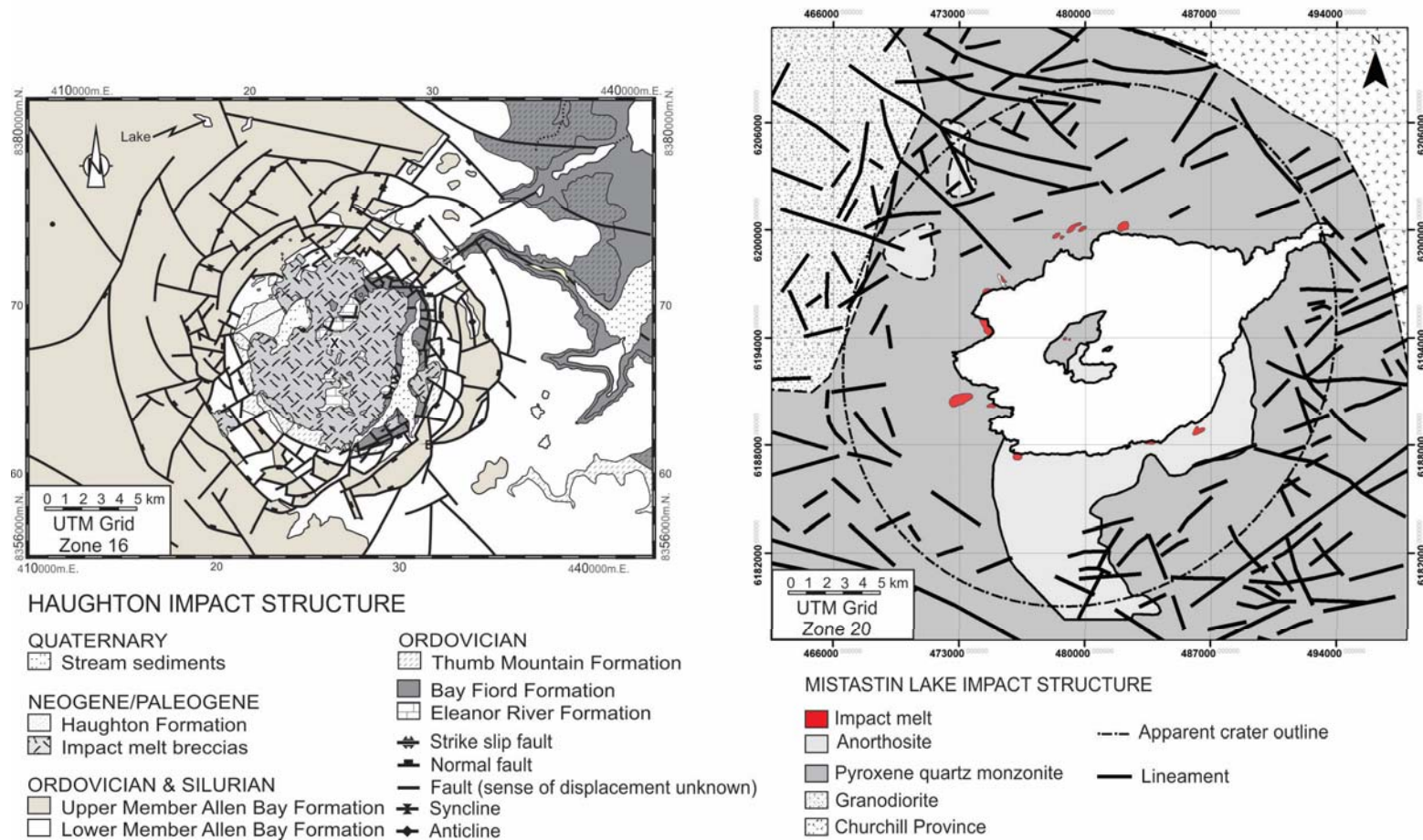


Figure 5-8: Comparison of the lineament distribution of the Haughton impact structure (left) and the Mistastin Lake impact structure (right). Haughton exhibits a clear pattern of radial and curved concentric faults, whereas, Mistastin Lake exhibits shorter fractures and faults that are more randomly oriented in respect the crater centre or parallel to regional faults.

5.5.3 Post-impact modification of the Mistastin Lake impact structure

The elongated nature of the Mistastin Lake, the elliptical shape of the inner and outer rings of hills, as well as crag and tail structures and glacial striations on Horseshoe Island (Currie, 1971) are attributed to the latest glacial event that flowed from southwest to northeast (Klassen and Thompson, 1990). Early studies of the Mistastin Lake impact structure, made broad estimates of ~100 m of erosion (Grieve and Cintala, 1992; Phinney and Simonds, 1977). These estimates could account for the lower elevation of the apparent crater rim in the southwestern region (Figure 5-3d), which may have experienced the brunt of glacial advancement within a comparatively flat regional terrain. The preservation of Discovery Hill outcrop of impact melt, may be due to the strength of the impact melt unit. It may have been more resistant than surrounding fractured target rocks.

Higher rim elevations in other quadrants surrounding the lake could be an effect of differential erosion. Glacial advance from the southwest may have been impeded by the southwest portion of the original crater rim and been deflected around the crater form. This effect could also explain the much lower erosion estimates reported by Marion et al. (Forthcoming) along the southern shoreline within the lower zone. Their study estimated a minimum erosion level of 10–20 m locally based on vesicularity of melt rock exposures. Figure 5-9 provides a schematic representation of the original and present-day Mistastin lake structure.

5.5.4 Size of the Mistastin Lake impact structure

When mapping terrestrial craters an important distinction is made between final crater diameter and the apparent crater diameter because most craters are eroded such that the original crater rim – represented as a topographic high – is no longer preserved (Turtle et al., 2005). In such cases, the diameter of the outermost ring of semi-continuous concentric normal faults, measured with respect to the pre-impact surface (i.e., accounting for the amount of erosion that has occurred) is typically used to define the apparent crater diameter (Osinski and Spray, 2005; Turtle et al., 2005). For the Mistastin

Lake impact structure, laterally continuous, curvilinear fault scarps bounding the outermost topographic raised ring of hills are not observed and displacement along faults is difficult to determine due to the homogenous nature of the target rocks, therefore different criteria are needed to define the apparent crater rim.

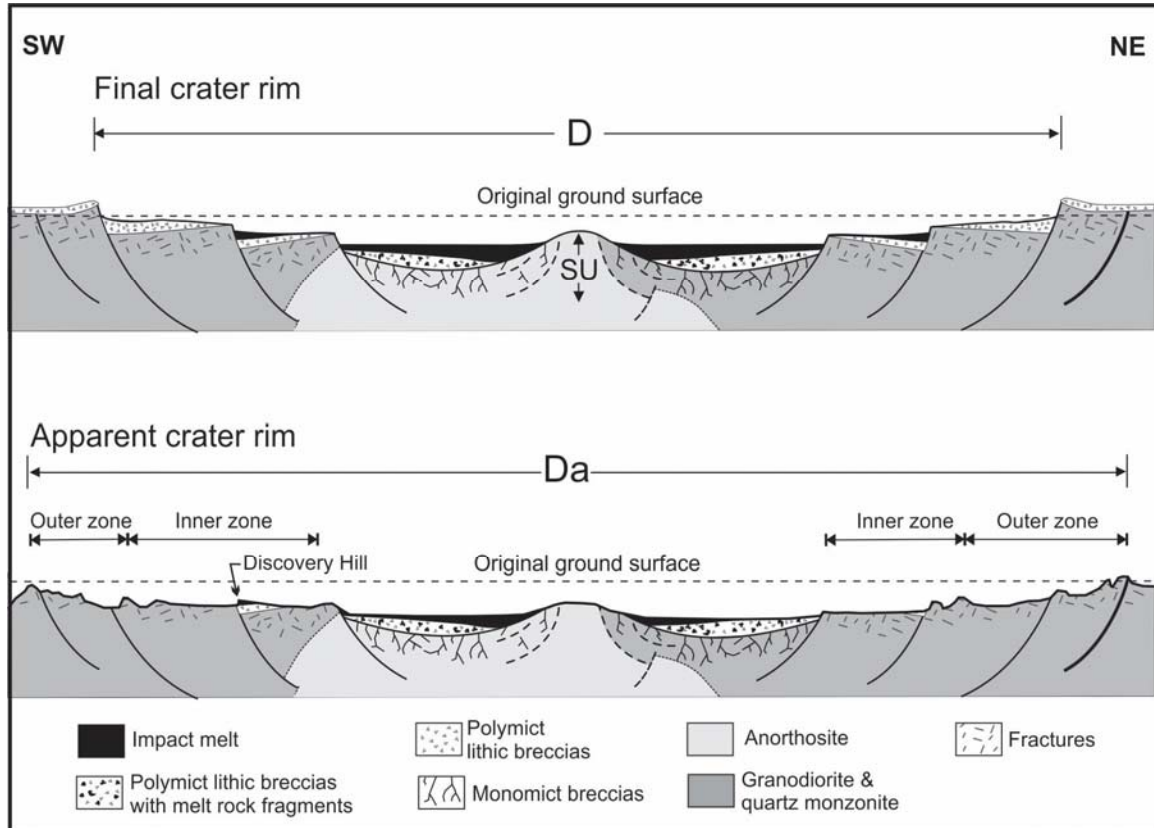


Figure 5-9: Schematic cross-section of the Mistastin Lake impact structure, idealized transect from southwest to northeast across the crater. Top section shows the hypothetical impact structure before erosion; D = diameter of final crater. The lower section shows the present-day surface after erosion and glaciation; D_a = diameter of apparent crater rim. Note: the original crater rim has been eroded and the apparent crater rim is larger in diameter in the SW-NE direction of glaciation. Curved, listric faults represented in cross-sections are not continuous laterally.

Zones are bound by raised hills and short faults.

The Mistastin Lake impact structure has been differentially eroded; however, a 30 x 26 km raised ring of hills (Figure 5-3) and regions of fractures, best developed in the northwest and southeast quadrants, are apparent (Figure 5-5). We propose that these two structural and morphometric features can be used to define the apparent crater diameter. The density of fractures associated with impact structures in crystalline target rocks tends to be highest at the inner slopes of the crater rim and gradually decreases outwards from there, as observed in preserved lunar craters (Baldwin, 1978). This relationship is observed in the northwest region of the Mistastin Lake impact structure, where there are few pre-existing regional faults. Thus the oval-shaped, raised ring of hills surrounding the Mistastin Lake is interpreted as the apparent crater diameter at 30 x 26 km.

The elongated nature of the raised ring of hills could be attributed to:

- 1) Pre-existing regional faults;
- 2) Differential erosion during glaciation event(s).

Considering the present day elevation difference of 100 m within the outer ring of hills, with the lowest elevations along the SW section, which would have experienced the brunt of glacial advancement, the latter explanation is preferred. We conclude that the apparent crater diameter was preserved in the NW-SE direction (i.e., the minor axes of present day ring of hills) and was modified in the SW-NE direction. Thus, the apparent crater diameter for the Mistastin Lake impact structure is interpreted to be 26 km, smaller than previous estimates of 28 km (e.g., Grieve, 2006).

5.6 Conclusions

Little structural mapping has previously been conducted at the Mistastin Lake impact structure. New structural mapping reveals a moderately eroded complex impact structure with two unique zones that define a collapsed rim region and the preserved remains of a central uplift. These zones are bound by raised rings of hills and short, discontinuous faults. Regions of fractures within the outer zone and beyond, best defined in the southwest and northeast quadrants, are similar to other impact structures in igneous targets (e.g., El'gygytgyn impact structure; Gurov et al., 2007). The highest, outermost

ring of hills is used to define the apparent crater rim for the Mistastin Lake impact structure. It defines a 30 x 26 km ellipse, whose long axis is roughly parallel to southwest to northeast directed glaciation. A range of erosion levels from <10 m up to 100 m is attributed to differential erosion during glaciation. Locally, lower amounts of erosion account for impact melt observed within the inner zone, and likely the partial preservation of the melt sheet that may be underlying Mistastin Lake. Overall, this new structural mapping provides a basis from which geological mapping of impactite units can be compared and correlated.

5.7 References

- Baldwin, R.B., 1978. An overview of impact cratering. *Meteoritics* 13, 364–379.
- Benn, D.I., Evans, D.J.A., 1998. *Glaciers & glaciation*. Arnold, New York; London.
- Currie, K.L., 1971. Geology of the resurgent cryptoexplosion crater at Mistastin Lake, Labrador: Geological Survey of Canada, Bulletin 207. Dept. of Energy, Mines and Resources, Ottawa, Canada.
- Dumont, R., Jones, A., 2012. Aeromagnetic Survey Mistastin Batholith, NTS 13M/14, Quebec and Newfoundland and Labrador, Geological Survey of Canada, Open File 7159, scale 1:50 000.
- Emslie, R.F., Cousens, B., Hamblin, C., Bielecki, J., 1980. The Mistastin Batholith, Labrador-quebec : An Elsonian Composite Rapakivi Suite. doi:10.4095/124073
- Emslie, R.F., Stirling, J.A.R., 1993. Rapakivi and related granitoids of the Nain Plutonic Suite: Geochemistry, mineral assemblages and fluid equilibria. *Can. Mineral.* 31, 821–847.
- Eppler, D.T., Ehrlich, R., Nummedal, D., Schultz, P.H., 1983. Sources of shape variation in lunar impact craters. Fourier shape analysis. *Geol. Soc. Am. Bull.* 94, 274 – 291.
- Gower, C.F., Krogh, T.E., 2002. A U-Pb geochronological review of the Proterozoic history of the eastern Grenville Province. *Can. J. Earth Sci.* 39, 795. doi:10.1139/e01-090

- Grieve, R.A.F., 1975. Petrology and chemistry of the impact melt at Mistastin Lake crater, Labrador. *Geol. Soc. Am. Bull.* 86, 1617–1629.
- Grieve, R.A.F., 2006. Mistastin, in: *Impact Structures in Canada*. Geological Association of Canada, pp. 115–120.
- Grieve, R.A.F., Cintala, M.J., 1992. An analysis of differential impact melt-crater scaling and implications for the terrestrial impact record. *Meteoritics* 27, 526–538.
- Grieve, R.A.F., Rupert, J., Smith, J., Therriault, A., 1995. The record of terrestrial impact cratering. *GSA Today* 5.
- Gurov, E.P., Koeberl, C., Yamnichenko, A., 2007. El'gygytgyn impact crater, Russia: Structure, tectonics, and morphology. *Meteorit. Planet. Sci.* 42, 307–319.
doi:10.1111/j.1945-5100.2007.tb00235.x
- Heiken, G.H., Vaniman, D., French, B.M., (Eds.) 1991. *The Lunar sourcebook: A user's guide to the Moon*. Cambridge University Press, Cambridge.
- Herrick, R.R., Pierazzo, E., 2003. Results of the Workshop on Impact Cratering: Bridging the Gap Between Modeling and Observations, LPI Contribution No. 1162. Houston, TX.
- Innes, M.J.S., 1964. Recent advances in meteorite crater research at the Dominion Observatory, Ottawa, Canada. *Meteoritics* 2, 219– 242.
- Kenkmann, T., Collins, G.S., Wunnemann, K., 2013. The modification stage of crater formation, in: Osinski, G.R., Pierazzo, E. (Eds.), *Impact Cratering: Processes and Products*. Wiley-Blackwell, Hoboken, NJ, pp. 60–75.
- Klassen, R.A., Thompson, F.J., 1990. Open File 2170: Glacial history, drift composition, and till geochemistry, Labrador.
- Kriens, B.J., Shoemaker, E.M., 1999. Geology of the Upheaval Dome impact structure, southeast Utah. *J. Geophys. Res.* 104, 18,867 – 18,887.

- Kumar, P.S., Kring, D. a., 2008. Impact fracturing and structural modification of sedimentary rocks at Meteor Crater, Arizona. *J. Geophys. Res. E Planets* 113, 1–17. doi:10.1029/2008JE003115
- Marchand, M., Crocket, J.H., 1977. Sr isotopes and trace element geochemistry of the impact melt and target rocks at the Mistastin Lake crater, Labrador. *Geochim. Cosmochim. Acta* 41, 1487–1495.
- Marion, C.L., Sylvester, P.J., 2010. Composition and heterogeneity of anorthositic impact melt at Mistastin Lake crater, Labrador. *Planet. Space Sci.* 58, 552–573. doi:10.1016/j.pss.2009.09.018
- Marion, C.L., Sylvester, P.J., Leitch, A.M., Forthcoming. Vesicularity and distribution of impact melt at Mistastin Lake crater, Labrador, Canada. *Meteorit. Planet. Sci.*
- McCormick, K.A., Taylor, G.J., Keil, K., Spudis, P.D., Grieve, R.A.F., Ryder, G., 1989. Sources of clasts in terrestrial impact melts: Clues to the origin of LKFM, in: *Proceedings of the 19th Lunar and Planetary Science Conference*. Lunar and Planetary Institute, pp. 691–696.
- McHone, J.F., Greeley, R., Williams, K.K., Blumberg, D.G., Kuzmin, R.O., 2002. Space shuttle observations of terrestrial impact structures using SIR-C and X-SAR radars. *Meteorit. Planet. Sci.* 37, 407–420. doi:10.1111/j.1945-5100.2002.tb00824.x
- Milton, D.J., Barlow, B.C., Brown, A.R., Moss, F.J., Manwaring, E.A., Sedmik, E.C.E., Young, G.A., Van Son, J., 1996a. Gosses Bluff—A latest Jurassic impact structure, central Australia. Part 2: Seismic, magnetic, and gravity studies. *J. Aust. Geol. Geophys.* 16, 487–527.
- Milton, D.J., Glikson, A.Y., Brett, R., 1996b. Gosses Bluff—A latest Jurassic impact structure, central Australia. Part 1: geological structure, stratigraphy, and origin. *J. Aust. Geol. Geophys.* 453–486.
- Offield, T.W., Pohn, H.A., 1979. *Geology of the Decaturville impact structure, Missouri*. United States Geological Survey Professional Paper #1042. Washington, D. C.

Öhman, T., Aittola, M., Kortenien, J., Al, E., 2010. Polygonal impact craters in the Solar System: observations and implications, in: Gibson, R.L., Reimold, W.U. (Eds.), *Large Meteorite Impacts and Planetary Evolution IV*; Geological Society of America Special Paper 465. Geological Society of America, Boulder, Boulder, CO, pp. 51–65.

Osinski, G.R., Grieve, R.A.F., Collins, G.S., Marion, C., Sylvester, P., 2008. The effect of target lithology on the products of impact melting. *Meteorit. Planet. Sci.* 43, 1939–1954.

Osinski, G.R., Spray, J.G., 2005. Tectonics of complex crater formation as revealed by the Haughton impact structure, Devon Island, Canadian High Arctic. *Meteorit. Planet. Sci.* 40, 1813–1834.

Phinney, W.C., Simonds, C.H., 1977. Dynamical implications of the petrology and distribution of impact melt rocks, in: Roddy, D.J., Pepin, R.O., Merrill, R.B. (Eds.), *Impact and Explosion Cratering*. Pergamon Press, New York, pp. 771–790.

Pilkington, M., Grieve, R.A.F., 1992. The geophysical signature of terrestrial impact craters. *Rev. Geophys.* 30, 161–181. doi:10.1029/92RG00192

Pilkington, M., Hildebrand, A.R., 2000. Three-dimensional magnetic imaging of the Chicxulub Crater. *J. Geophys. Res.* 105, 23479–23491. doi:10.1029/2000JB900222

Pilkington, M., Hildebrand, A.R., 2003. Transient and disruption cavity dimensions of complex terrestrial impact structures derived from magnetic data. *Geophys. Res. Lett.* 30, 2087. doi:10.1029/2003GL018294

Rivers, T., Corrigan, D., 2000. Convergent margin on southeastern Laurentia during the Mesoproterozoic: tectonic implications. *Can. J. Earth Sci.* 37, 359–383. doi:10.1139/e99-067

Shoemaker, E.M., 1960. Penetration mechanics of high velocity meteorites, illustrated by Meteor Crater, Arizona, in: 21st International Geological Congress. Int. Union of Geol. Sci., Trondheim, Norway, pp. 418 – 434.

Singleton, A.C., Osinski, G.R., Grieve, R.A.F., Shaver, C., 2011. Characterization of impact melt-bearing impactite dykes from the central uplift of the Mistastin Lake impact structure, Labrador. Abstract 2250, in: 42nd Lunar and Planetary Science Conference. The Woodlands, Texas.

Singleton, A.C., Osinski, G.R., Grieve, R.A.F., Shaver, C., 2012. Characterization of glasses in impact breccia dykes at the Mistastin Lake impact structure, Labrador, in: 43rd Lunar and Planetary Science Conference. The Woodlands, Texas.

Singleton, A.C., Ward, M.J., Woll, A.R., Osinski, G.R., 2014. Characterization of impact glass clasts from the Mistastin impact structure using synchrotron radiation spectroscopy. Abstract 5404, in: 77th Annual Meteoritical Society Meeting. Casablanca, Morocco, p. 5404.

Squyres, S.W., Knoll, a H., Arvidson, R.E., Ashley, J.W., Bell, J.F., Calvin, W.M., Christensen, P.R., Clark, B.C., Cohen, B. a, de Souza, P. a, Edgar, L., Farrand, W.H., Fleischer, I., Gellert, R., Golombek, M.P., Grant, J., Grotzinger, J., Hayes, a, Herkenhoff, K.E., Johnson, J.R., Jolliff, B., Klingelhöfer, G., Knudson, a, Li, R., McCoy, T.J., McLennan, S.M., Ming, D.W., Mittlefehldt, D.W., Morris, R. V, Rice, J.W., Schröder, C., Sullivan, R.J., Yen, a, Yingst, R. a, 2009. Exploration of Victoria crater by the Mars rover Opportunity. *Science* 324, 1058–1061. doi:10.1126/science.1170355

Taylor, F.C., Dence, M.R., 1969. A probable meteorite origin for Mistastin Lake, Labrador. *Can. J. Earth Sci.* 6, 39–45.

Turtle, E.P., Pierazzo, E., Collins, G.S., Osinski, G.R., Melosh, H.J., Morgan, J.V., Reimold, W.U., 2005. Impact structures: What does crater diameter mean?, in: Kenkmann, T., Hörz, F., Deutsch, A. (Eds.), *Large Meteorite Impacts III*, Geological Society of America Special Paper 384. Geological Society of America, Boulder, CO, pp. 1–24. doi:10.1130/2005.2388(06).

Wilshire, H.G., Offield, T.W., Howard, K.A., Cummings, D., 1972. *Geology of the Sierra Madera Cryptoexplosion Structure, Pecos County, Texas*. USGS Professional Paper #599-H. Washington, D. C.

Wilson, C.W., Stearns, R.G., 1968. Geology of the Wells Creek Structure, Tennessee. State of Tennessee Department of Conservation Division of Geology Bulletin #68. Nashville, Tennessee.

Woodcock, N.H., Mort, K., 2008. Classification of fault breccias and related fault rocks. *Geol. Mag.* 145, 435–440.

Chapter 6

6 Impactites of the Mistastin Lake impact structure: Insights into impact ejecta emplacement

6.1 Introduction

Impact craters are the dominant geological landform on rocky planetary surfaces. Despite their ubiquitous occurrence, several important processes relating to their formation remain poorly constrained. The term impactite refers to “rocks produced or affected by a hypervelocity impact event” (Grieve and Therriault, 2013). A complete suite of preserved impactites typically includes shocked basement rocks, autochthonous and parautochthonous monomict impact breccias, allochthonous impact breccias and/or impact melt rock (Grieve and Therriault, 2013). Impact breccias and melt dykes may intrude any of these units.

It is difficult to discern both the extent of and contact relationships between these units from orbital planetary data sets when studying other rocky bodies in our solar system. Field observations at impact structures on Earth provide the necessary ground-truth. An advantage of terrestrial investigations is that subsurface characteristics can sometimes be investigated directly at cross-cut rock exposures. Conversely, two factors that inhibit impact crater studies on Earth including: 1) erosion due to their fractured and altered nature, such that original form and impactite units are no longer preserved, and/or 2) burial by post-impact sediments almost immediately after formation (e.g., Chicxulub, Mexico; Montagnais, Canada). In the latter case, the preservation of the crater form may be pristine, but samples can only be obtained by drilling.

Determining the context of impactites in terms of location within the crater structure and formation mechanism can be difficult. The study of impact ejecta in particular has been controversial, in particular with respect to emplacement mechanisms. Impact ejecta is defined here as any target material, regardless of its physical state, that is transported beyond the rim of the transient cavity (Osinski et al., 2011), including impact melt or impact breccias. Ejecta can be transported through the air forming an ejecta blanket upon landing through the ballistic sedimentation process (Oberbeck, 1975); alternatively, it can

form ground-hugging flows that were never airborne (Osinski, 2004; Osinski et al., 2011). These two types of mechanisms tend to occur sequentially, which is supported by studies of lunar images that show melt ponds overlying ejecta blanket deposits within rim terraces of complex craters (Hawke and Head, 1977; Howard and Wilshire, 1975; Neish et al., 2014; Osinski et al., 2011).

The Mistastin Lake impact structure offers a unique opportunity to study an almost complete suite of impact lithologies, including previously unrecognized impact ejecta deposits. The exposure at Mistastin allows the investigation of a near intact section through an intermediate, complex crater in crystalline target rock. This is a rare occurrence as only ~25% of impact craters identified on Earth formed within purely crystalline target rocks. Furthermore, the Mistastin Lake structure is one of only two impact structures with anorthosite as the major target rock, providing a unique opportunity for comparison with lunar craters.

Most previous studies of the Mistastin impact structure are geochemical in nature, focusing on characterizing the impact melt rocks (Grieve, 1975; Marchand and Crocket, 1977; Marion and Sylvester, 2010; Marion et al., Forthcoming; McCormick et al., 1989). New structural mapping reveals a moderately eroded complex impact structure with two unique zones that define a collapsed rim region; a central uplift region is also partially preserved (Chapter 5). The zones are bound by raised rings of hills and short, discontinuous faults. This study presents new geological mapping results highlighting textural features, distribution, and field relationships of impactites and target rocks within the collapsed rim region. We also present petrographic results that place the impactite units in relation to the crater form based on field mapping, with a particular focus on impactite origin and timing of formation.

6.2 Geological setting

The Mistastin Lake impact structure (55°53'N; 63°18'W) formed within the Mesoproterozoic (~1.4 Ga; Emslie et al., 1980) Mistastin batholith, which is part of the Nain plutonic suite. The north-south oriented, elliptical-shaped batholith covers ~5000

km² (Emslie et al., 1980). Mistastin Lake is located in the upper northeast quadrant of the batholith (Figure 6-1).

The earliest geological studies of the Mistastin Lake area were conducted as part of a reconnaissance mapping initiative by the Geological Survey of Canada (Currie, 1971a; Taylor and Dence, 1969). Taylor and Dence (1969) subsequently attributed the structure's origin to a comet or asteroid impact based on field and microscopic evidence from shattercones, planar deformation features (PDFs) in quartz, and diaplectic quartz and feldspar glasses. Currie (1971) produced a map of the area, though he interpreted the roughly circular structure as being of volcanic origin. This interpretation has been refuted in all subsequent studies of the crater, which attribute its structure to an impact origin.

In the decades that followed further mineral and rock analyses were conducted, though relatively little fieldwork. Recent work by Young et al. (2014) used *in situ* laser ablation ⁴⁰Ar/³⁹Ar geochronology to date the impact event at 36.6 ± 2.0 Ma (2σ) on impact melt samples. This age is in agreement with the previous accepted age of 36 ± 4 Ma, which is based on ⁴⁰Ar/³⁹Ar obtained over 30 years ago by Mak et al. (1976). A magnetic study of the Mistastin impact structure by (Hervé et al., 2015) suggests that the basement rocks less than 1 metre from impact melt were thermally overprinted, while rocks more than a metre away retained their original magnetization. Pickersgill et al., (2015) studied the shock effects in andesine and labradorite in target rocks, impact breccias, and impact melt rocks.

The regional map of the Mistastin Lake area by Currie (1971) remains the most detailed map published (1:50,000) to date, however, it includes inferred geological boundaries for melt rocks based on a volcanic origin interpretation. In addition, Currie's map show elongated belts of anorthosite and quartz monzonite (referred to as mangerite) trending northwest to southeast across a large granodiorite unit Currie (1971) (Figure 6-2 inset). Emslie et al. (1980) reinterpreted the distribution of Mistastin batholith components as amoeboid bodies of predominantly granite and quartz monzonite, and redefined the boundaries of the anorthosite unit to span an area which doubles the region previously mapped by Currie (1971).

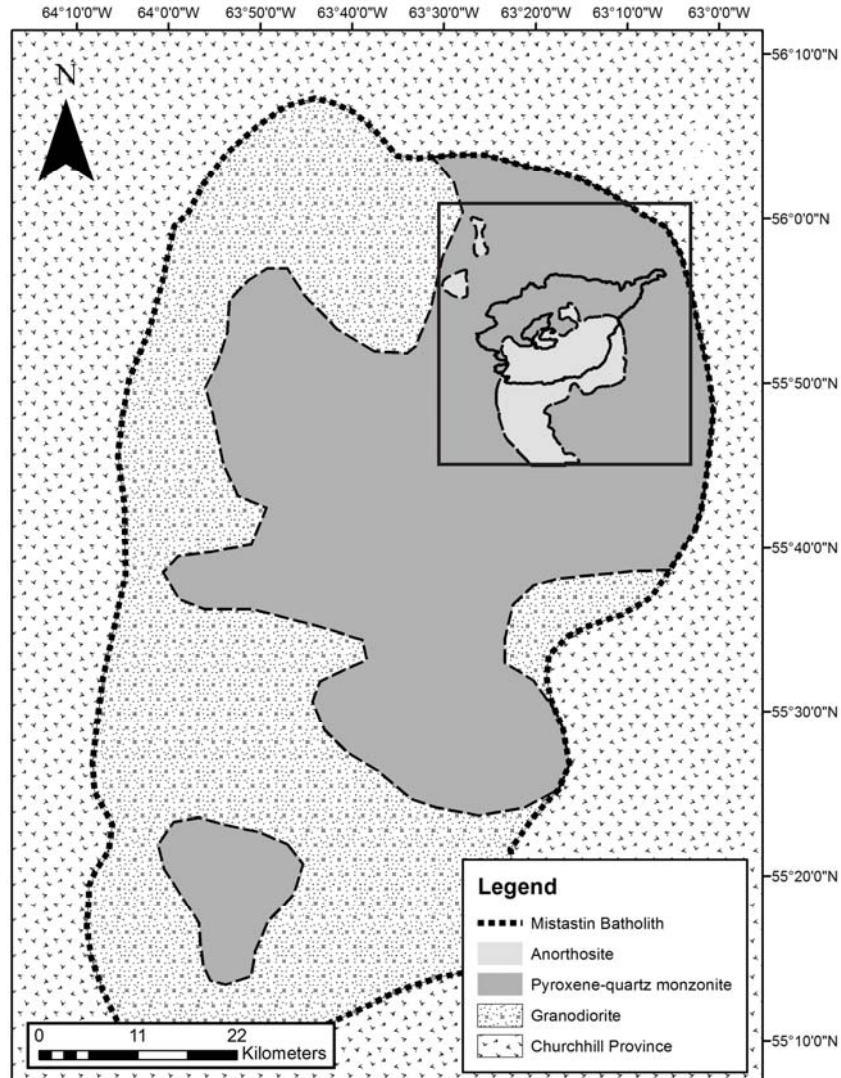


Figure 6-1: Geological map of the Mistastin batholith. Modified from Emslie et al., (1980). Anorthosite boundary based on magnetic anomalies on residual total magnetic map (Dumont and Jones, 2012). Box outlines area of maps in Figure 6-2.

Currie's 1971 map has been used as a basemap for all subsequent studies (e.g., Grieve, 1975; Hervé et al., 2015; Marion and Sylvester, 2010; Marion et al., Forthcoming; McCormick et al., 1989; Pickersgill et al., 2015), which highlight the distribution of melt rock exposures within the impact structure. Our study uses the boundaries for the anorthosite unit as defined by Emslie et al. (1980) (Figure 6-2).

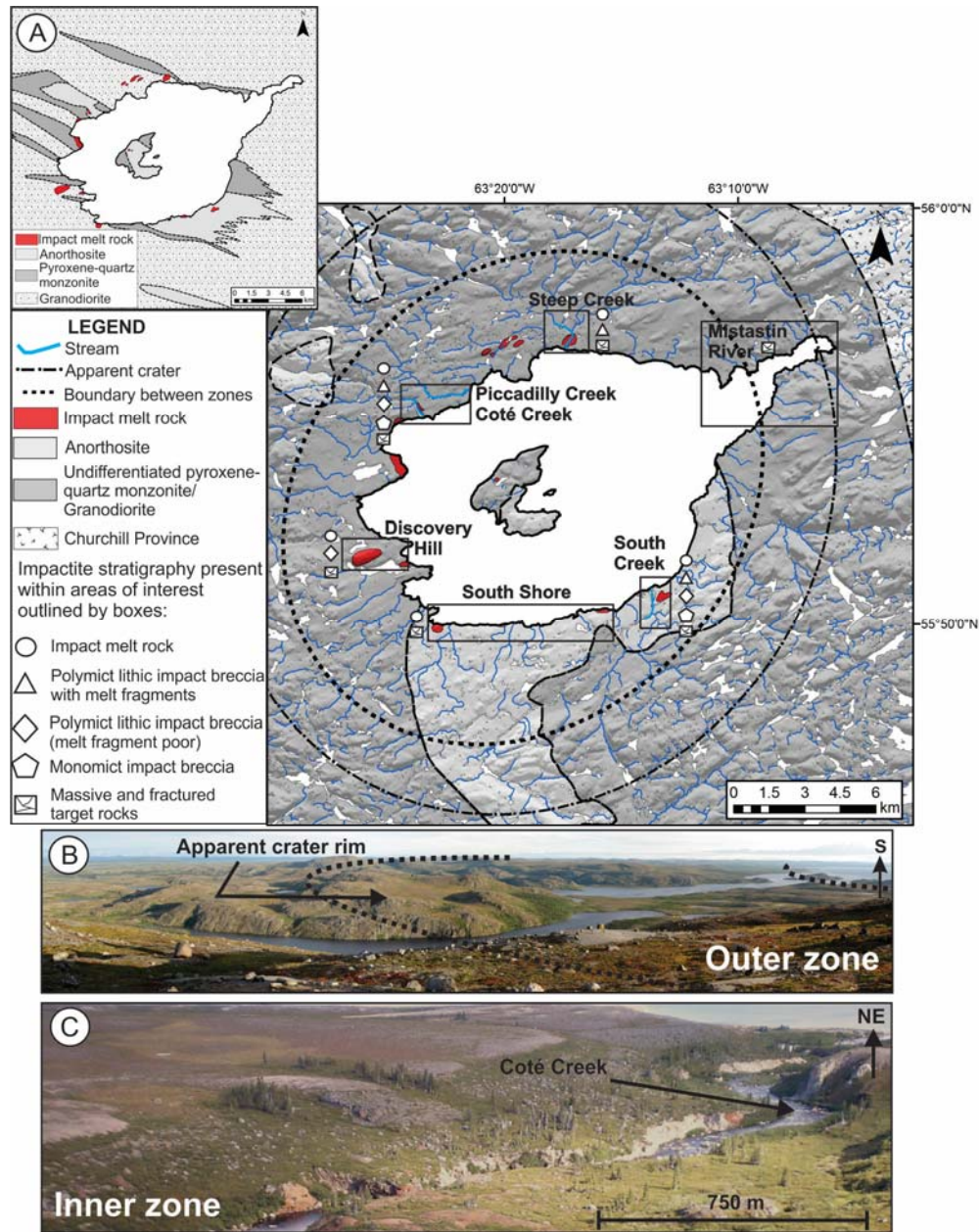


Figure 6-2: (A) New geological map of the Mistastin Lake impact structure (adapted from Emslie et al., 1980 and Marion et al., Forthcoming) fused with Digital Elevation Model (Chapter 5). Boxes outline areas of interest in our study. Impactite stratigraphy indicated for each area. Insert: Basemap used by most previous studies of Mistastin Lake impact structure based on field mapping by Currie (1971). (B) Typical rock exposure and vegetation cover within the outer zone, NE quadrant; (C) Typical rock exposure and vegetation cover within the inner zone, NW quadrant. (Figures B and C modified from Chapter 5).

Blocky, stepped topography extends from the edge of Mistastin Lake to a topographically raised ring of hills (Figure 6-2). The highest and furthest part of the hills, is interpreted as the apparent crater rim with a diameter of 30 x 26 km, which is consistent with previous work (see Chapter 5; Grieve, 2006; Marion et al., Forthcoming). Two distinct zones are defined between the lakeshore and apparent crater rim. These zones are marked by steep changes in elevation, fracture and fault patterns, extent of rock exposure, and changes in drainage patterns (see Chapter 5). The two islands, Horseshoe and Bullseye Islands, located roughly within the centre of the lake, are interpreted as the remains of the central uplift, characteristic of complex impact structures.

The glacial history of Labrador is complex, having experienced numerous glacial events throughout the Pleistocene epoch. The Mistastin Lake region is largely covered by vegetation and glacial deposits that are 0.5 – 5 m in depth. The last glacial advance to affect the study area proceeded from the Labrador Trough northeastwards across the Mistastin Lake region (Klassen and Thompson, 1990). In glaciated areas, impact craters can experience substantial erosion removing crater rims and central uplifts [e.g., Manicouagan impact structure only ~600 km away (Currie, 1972; Murtaugh, 1976)]. Early studies of the Mistastin Lake impact structure estimated ~100 m of erosion (Grieve and Cintala, 1992; Phinney and Simonds, 1977). These estimates could account for the lower elevation of the apparent crater rim in the southwestern region, which may have experienced the brunt of glacial advancement within comparatively flat regional terrain. Higher rim elevations in other quadrants surrounding the lake could reflect differential erosion. Glacier advancement from the southwest may have been impeded by the southwest portion of the original crater rim and been deflected around the crater form. This effect could also explain the much lower erosion estimates as reported by Marion et al. (Forthcoming) along the southern shoreline within the lower zone. Their study estimated a minimum erosion level of 10-20 m, locally, based on vesicularity of local melt rock exposures.

6.3 Methods

Field mapping was conducted over three field seasons, in the late summers of 2009, 2010, and 2011. Most field mapping was conducted along the shoreline and creeks,

within 3 km of the lakeshore. Field work focused on sites that offered three-dimensional exposures of stratigraphy, such as vertical cliffs. Key outcrops within this zone included exposures where the contacts between various impactites were studied in detail and we documented unit thickness, sketched field relationships, and otherwise described observations of the outcrop. Access to outcrops was by zodiac boat and on foot. All available remote sensing images, air photos, previous geological maps (Currie, 1971; Emslie et al., 1980; Marion et al., Forthcoming) and field mapping data collected during this study were compiled using ArcGIS version 10.2 using the NAD83 UTM Zone 20 geodetic datum. We used this information to produce a new geological map for the study area.

Samples of different impactite lithologies were collected from various locations within the collapsed rim region of the Mistastin Lake impact structure (Figure 6-2, Appendix D) with the intent of obtaining a complete suite of preserved impactites. Ninety polished thin sections were examined for microscopic shock metamorphic effects, using a Nikon Eclipse LV100POL compound petrographic microscope. Further detailed study of microtextures was conducted with backscattered electron (BSE) imagery and energy dispersive X-ray spectrometry (EDS) using a JEOL JXA-8530F Field Emission Electron Probe Microanalyzer (FE-EPMA) in the Earth and Planetary Materials Analysis Laboratory, at the University of Western Ontario.

Quantitative chemical composition data using wavelength dispersive spectrometry (WDS) were also collected with the FE-EPMA in the Earth and Planetary Materials Analysis Laboratory. The beam was operated with an accelerating voltage of 15 kV, probe current of 20 nA, and a beam diameter of 1 μm . Mineral standards used for calibration were as follows: Quartz (in house) for Si; Corundum (Harvard #126097) for Al; Basaltic Glass (Smithsonian USNM 113498/1 VG-A99 - Juan de Fuca Ridge) for Na, Fe, Ti, and Ca; Hornblende (Smithsonian USNM 143965 - Kakanui, New Zealand) for Mg and K.

All shock levels were estimated using microscopic and macroscopic observations, and correlated with the shock stage scheme developed for quartzofeldspathic crystalline rocks based on data from French and Koeberl (2010) and Stöffler and Grieve (2007).

6.4 Observations

A near complete suite of impactites is preserved at the Mistastin Lake impact structure, including shocked basement rocks, monomict impact breccias, polymict lithic impact breccias, and impact melt rocks. The ejecta deposits, uplifted rim and central uplift are partially preserved. In this section, we highlight observations from areas within the collapsed rim of the Mistastin Lake impact structure, including Discovery Hill, South Creek, Côté Creek, Piccadilly Creek, Steep Creek, and the northeast rim region where expansive exposures exist (Figures 6-2, 6-3). Combined, they describe a radial transect outwards from the central uplift across the apparent crater rim. New sites of interest including Piccadilly Creek and contact relationships along South Creek, Côté Creek, and Discovery Hill are reported here for the first time. Complimentary studies by Singleton et al., (2014, 2012, 2011), focus on the central uplift region.

Impactites are unevenly distributed around the lake and Horseshoe Island, primarily within the inner, lower zone. Apart from a large butte called Discovery Hill, impactite units are best exposed along the lake shoreline and steep banks of creeks, and barren hill tops within the rim region (Figure 6-3). The vertical sections along radially trending creeks, with respect to the impact structure, allow for local unit thicknesses and contact relationships to be observed.

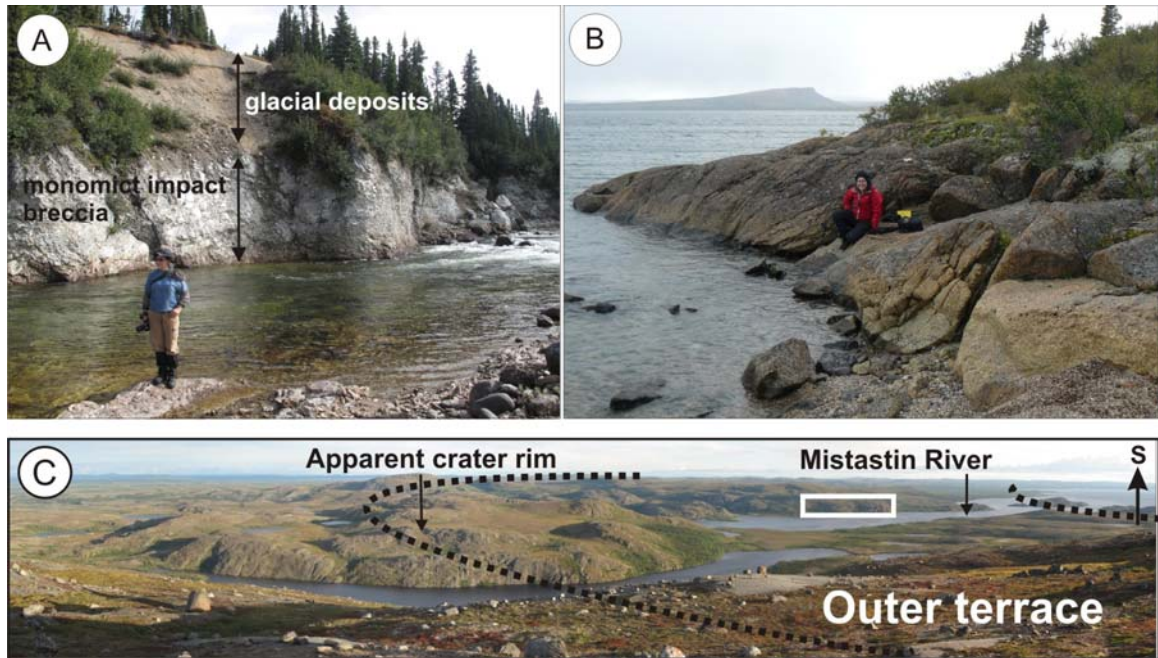


Figure 6-3: Typical rock exposures in Mistastin Lake region. (A) Glacial deposits lying on top of monomict anorthosite breccias along South Creek. Photo shows typical example of vertical exposures along creek banks. (B) Example of flat exposures along the Mistastin Lake shoreline. Outcrop of quartz monzonite along the SW shoreline of Mistastin Lake. (C) Northeast rim region of the Mistastin impact structure, which is dominated by massive granodiorite. Boundaries of rim region outlined in black, dashed line. Box indicates area shown in Figure 6-5C.

6.4.1 Massive and fractured target rocks

The majority of exposed outcrops of the Mistastin Lake region are massive igneous rocks representing the original target rock. The three main target rock lithologies of the Mistastin Lake impact structure include granodiorite, pyroxene and hornblende bearing quartz monzonite (also referred to as mangerite in previous Mistastin literature), and anorthosite, all components of the Mistastin batholiths, described in detail in Currie (1971), Emslie et al. (1980), and Marion et al. (Forthcoming). The quartz monzonite and granodiorite units underlie most of the Mistastin Lake region (Figure 6-2). Several masses of anorthosite are exposed in the region, the largest of which (approximately 60 km²; Emslie et al., 1980) lies southeast of the lake (Figure 6-1).

6.4.1.1 General description

Quartz monzonite and granodiorite massive, target rocks are both coarse grained with an average grain size of 3–4 cm (Figure 6-4a, b). Their matrix tends to weather more easily than the quartzofeldspathic phenocrysts, resulting in knobby surfaces of protruding potassium feldspar augen (Figures 6-4c). Typically, the quartz monzonite outcrops are rustier in colour, due to the higher iron contents, 10 wt. % total Fe_2O_3 , compared to about 2 to 5 wt. % in the granodiorite (Currie, 1971; Marion et al., Forthcoming). The granodiorite unit consists of 20–25 vol% potassium feldspar, 30 vol% plagioclase, 20 vol% quartz, 5–15 vol% hornblende, 5% biotite with abundant accessory minerals apatite and zircon, whereas the quartz monzonite has less quartz and a large amount (50%) of the pyroxene has been altered to hornblende (Currie, 1971; Marion et al., Forthcoming).

Anorthosite rock exposures range in appearance from massive outcrops comprising coarse-grained (1–10 cm), vitreous plagioclase crystals to outcrops dominated by fine grained (mm-sized) feldspar grains, weathering to a buff white colour (Figure 6-4e). The mineral modal abundances within the anorthositic target rocks on average are ~90–95% andesine to labradorite to (An_{32} to An_{55}), ~2–10% clinopyroxene crystals (mm to cm scale), less than 2% quartz, and ~1% Fe-Ti oxides (Currie, 1971b; Taylor and Dence, 1969). The most common alteration product is sericite. Locally, calcite is present up to 3% modal abundance.

6.4.1.2 Distribution in crater structure and shock features

The degree of shock metamorphism preserved within autochthonous targets rocks ranges from low to moderate and correlates with distance from the crater centre (i.e., site of impact). Outcrops of fractured, massive target rocks on Horseshoe Island, near the centre of Mistastin Lake, exhibit fracturing on a macroscopic and microscopic scale and locally planar deformation features in quartz, indicative of shock stages 0 to Ia (Stöffler and Grieve, 2007), which equates to ~5 GPa to 35 GPa (Figure 6-4e). Microscopically, fractures range from irregular fractures within individual crystals to intense fracturing along cleavage planes (Figure 6-4f).

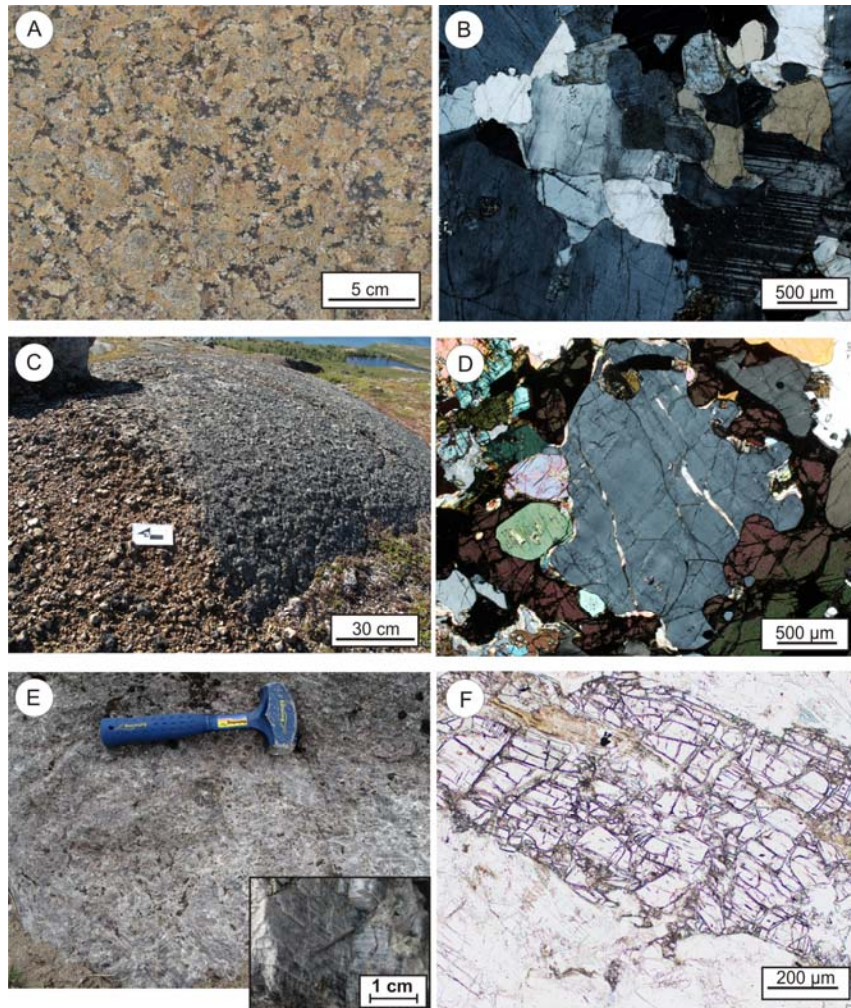


Figure 6-4: Massive target rocks of the Mistastin Lake impact structure. (A) Coarse grained granodiorite. Primary igneous texture is preserved. (B) Thin section microphotograph of granodiorite (cross-polarized light). Primary igneous texture is preserved. Minor fracturing of feldspar crystals. (C) Knobby, weathered surface of quartz monzonite. Can be difficult to distinguish from monomict impact breccias of the same rock type. (D) Thin section microphotograph of massive quartz monzonite, SW shoreline, Mistastin Lake (plane-polarized light), dominated by feldspar and amphibole relatively little affected by impact event. (E) Coarse-grained (1-10 cm) fractured, massive anorthosite, Horseshoe Island. Inset: Fracturing along cleavage planes of feldspar. (F) Thin section microphotograph of massive anorthosite, Horseshoe Island (plane-polarized light) showing fractured nature of feldspar crystal.

Along the southern and western shorelines, and immediately inland from the lakeshore, the target rocks are only minimally affected by the impact event. Fracturing within crystals and on an outcrop scale are the only shock effects observed (shock stage 0). Locally, along the southwest shoreline, some fractures are in-filled by lithic breccias (5–30 cm wide) (Figure 6-5a, b). These dykes contain ~ 25–35% fragments that are sub-angular to sub-round, mm to cm-size, and are the same composition and shock level as the host rock. The matrix particles are less than 0.5 mm in size. Generally, these fractures are radially trending (with respect to the crater centre).

Beyond the shoreline, the majority of exposed outcrops surrounding Mistastin Lake are unfractured igneous rocks (even on a microscopic scale), representing the original target rock that was relatively unaffected by the impact event. The raised, ring of hills surrounding the Mistastin impact structure are dominated by quartz monzonite and granodiorite that have retained their original coarse grained igneous textures and characteristic massive appearance (Figure 6-4a-d).

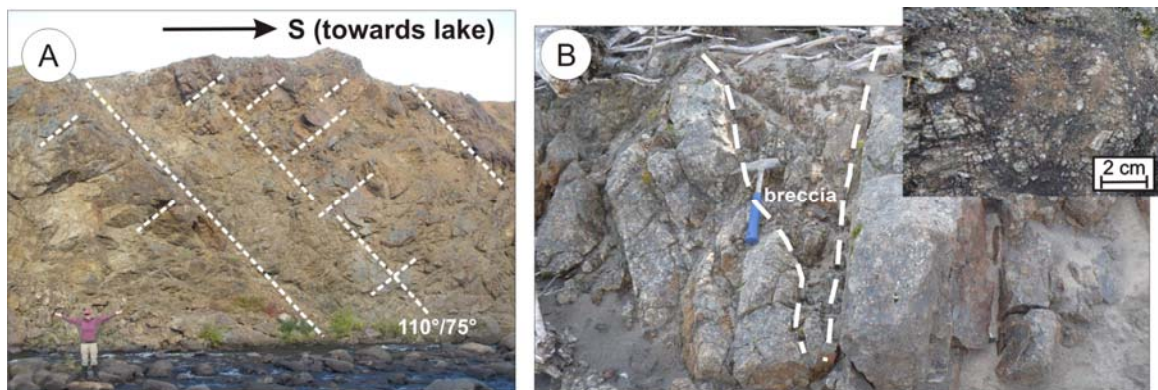


Figure 6-5: Macroscopic fracturing in massive target rocks of the Mistastin Lake impact structure. (A) Massive quartz monzonite exposed along Coté Creek. Note: Perpendicular fracture sets. The more continuous set dips towards the crater centre. (B) Thin breccia-filled fracture parallel to cm-m spaced joint set within quartz monzonite target rock along SW shoreline. Fracture and joint set trend radially from crater centre. Inset: Detail of fragmental, breccia dyke. Note angular to sub-round, mm-cm fragments within fine (<0.5 mm), lithic matrix.

Irregular fractures and m-scale fracture sets are observed throughout the inner and outer zones of the impact structure within fractured target rocks and monomict breccias (Figures 6-5a; see Chapter 5). Some of the radially trending fractures, in respect to the centre of the impact structure, are marked by the presence of breccias, composed of angular to subangular clasts of the same rock type as the adjacent walls (Figure 6-5b).

6.4.2 Monomict impact breccia

6.4.2.1 General description

Monomict breccias of anorthosite and quartz monzonite, where found adjacent to their intact bedrock equivalents, have sharp, cm-scale, to gradational contacts over 1–5 m. Breccia clasts are typically angular to sub-rounded, range from cm to m scale, and make up 70–90% of the rock (Figure 6-6). Upon close inspection, monomict breccias are completely fragmented, including the supporting matrix comprising angular grains <5 mm (Figures 6-6b, d), or zones of pristine crystals are separated by seams of brecciated material. In isolated outcrops, the quartz monzonite variety can be difficult to differentiate from its weathered, massive counterpart (see Figure 6-4c), due to similar mineralogy and weathering patterns. It has a similar knobby texture, however, monomict breccia clasts can be larger than individual augen of the massive quartz monzonite (Figure 6-6b). The surrounding fragmental matrix is fine grained (mm size) and rusty in colour.



Figure 6-6: Textures of monomict breccias of Mistastin Lake impact structure. (A) Quartz monzonite monomict impact breccias from Côté Creek, ~6.5 km from crater center. (B) Detail of Fig. 6A, showing fragmental nature of matrix and brecciated clasts that are larger than individual feldspar augen. (C) Monomict anorthosite impact breccia along South Creek, ~7.5 km from crater center. (D) Thin section microphotograph of monomict anorthosite impact breccia (cross polarized light) showing fragmental nature of crystals and supporting matrix. Fractures along cleavage planes in feldspar crystals form shards.

6.4.2.2 Distribution in crater structure and shock features

Locally, brecciated target rocks were observed within the inner zone of the Mistastin Lake impact structure, from 6 to 8 km from the crater centre. Monomict anorthositic impact breccias are best observed along South Creek. Approximately 7.5 km from the crater centre, vertical cliffs, 10–20 m high and approximately 450 m long, reveal a “sheet” of chalky white monomict anorthosite breccias overlying fractured anorthosite target rock (Figure 6-7). A consistent cm-m scale fracture set dipping ~40° to the

northeast, with a strike line roughly radial from the crater centre is observed throughout these monomict anorthosite impact breccias (Figure 6-7b). They also have a blocky habit defined by a second, later fracture set with meter scale spacing (Figure 6-7b), whereas the fractured anorthosite target rocks appear more fissile, with fracture spacing sub-m scale.

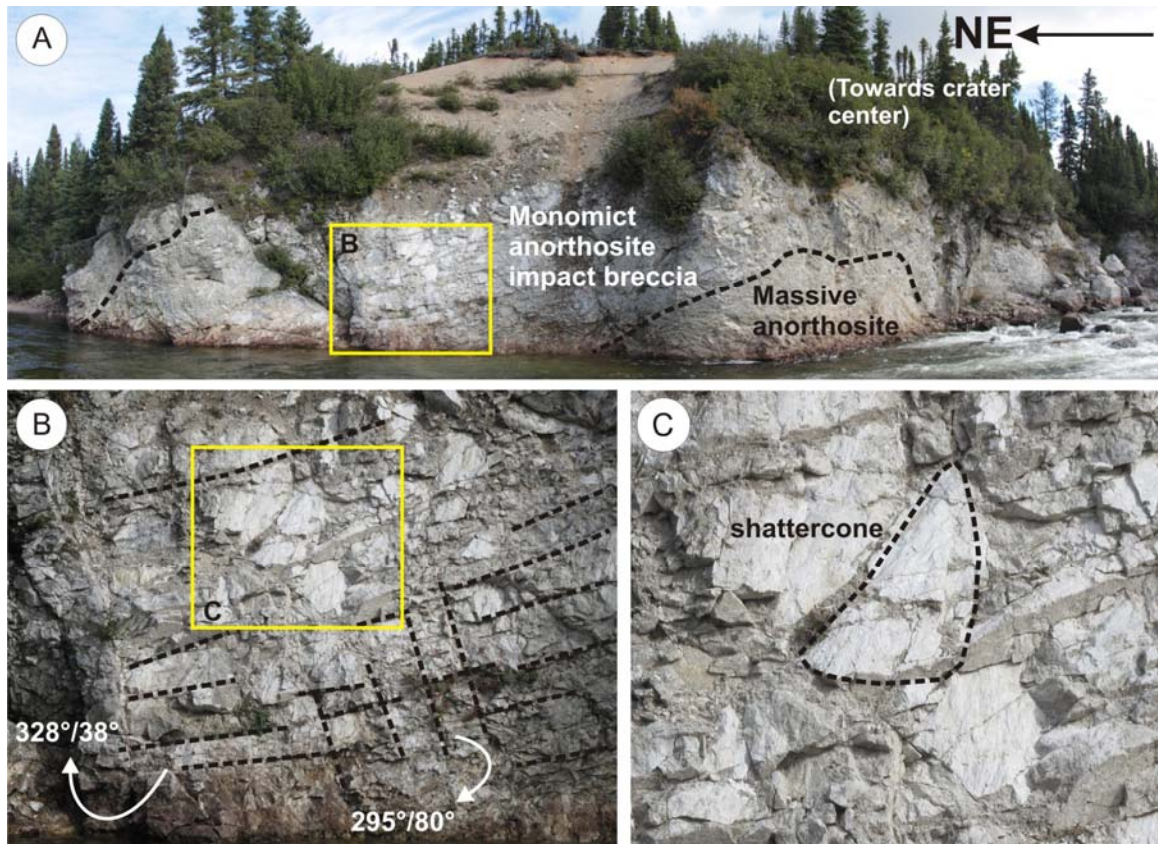


Figure 6-7: Monomict anorthosite breccias, South Creek, Mistastin Lake impact structure. (A) South Creek cliff face, ~15 m high reveals a cross-section of monomict impact breccias that overlies fractured anorthosite target rock. Metre-scale fracture set dipping ~ 40° to the northeast, with a strike line roughly radial from the crater centre is observed throughout these monomict anorthosite impact breccias. (B) Blocky habit of monomict anorthosite breccias defined by a perpendicular fracture set. Location of photo indicated by box in A. (C) Shattercone block within anorthosite monomict impact breccias along South Creek. Location indicated by box in B.

Microscopic shock features in the monomict breccias are primarily irregular fractures and zones of brecciation (Figure 6-6d). Planar fractures in feldspar grains were the feature of highest shock level observed in monomict impact breccias. Fractures typically developed along cleavage planes in feldspar grains resulting in shards (Figure 6-6d). Locally, feldspar grains were rimmed with sericite alteration. Monomict anorthosite breccias with similar microscopic shock features were also observed along Piccadilly Creek, approximately 6 km from the centre of the impact structure.

Macroscopic shock features in the monomict anorthosite breccias unit included shattercones, identified by distinctive striations defining cone shapes observed within large fragments of the monomict anorthosite (Figure 6-7c). Overall, this unit is characterized by Stage 0 shock features, indicative of pressures < 7 GPa.

6.4.3 Polymict lithic impact breccias (melt-free to -poor)

6.4.3.1 General description

Polymict lithic impact breccias consist of different types of angular to subrounded rock and mineral fragments in a groundmass of fine-grained material that does not include identifiable mineral and lithic clasts. These breccias are poorly sorted and the fragment sizes generally range from <1 mm to tens of metres, with an average fragment size of approximately 3–5 cm. Lithic fragments of anorthosite and feldspar mineral clasts are the dominant clast type (~80–90%), with minor amounts of quartz monzonite, granodiorite, pyroxene, and biotite grains (Figures 6-8a, b). Impact glass or its weathered equivalent is rare, amounting up to only up to 2% in atypical instances.

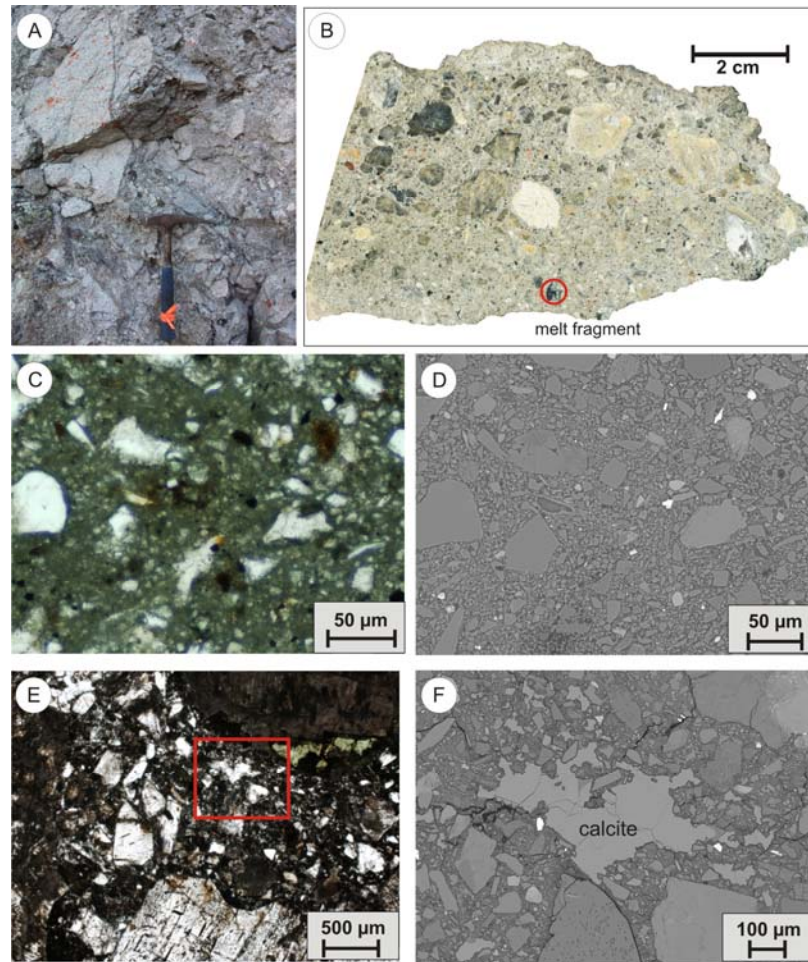


Figure 6-8: Melt-free to -poor, polymict impact breccias of the Mistastin Lake impact structure. (A) Poorly sorted nature of angular to subrounded rock fragments ranging up to m-scale in size. (B) Fragmental nature of fine-grained components of melt-poor, polymict impact breccias. Rare melt fragment indicated by red circle.

Coté Creek. (C) Thin section microphotograph of melt-poor, polymict impact breccias (plane polarized light) showing fragments supported by a dark grey matrix. Sample from Coté Creek. (D) Back-scattered electron image showing same area as

(C). Dark grey groundmass is likely amorphous clay. (E) Thin section microphotograph of melt-poor, polymict impact breccias (plane polarized light) showing predominantly black matrix that also includes irregular bodies of calcite (inside box). Sample from South Creek. (F) Back-scattered electron image of area outlined by box in Figure 6-8E, showing detailed image of irregular bodies of groundmass-forming calcite with embayed outlines.

This impactite type is characterized by a matrix that weathers to a light green, light brown, or light grey colour. The matrix or groundmass of the polymict impact breccias is defined as the fine-grained material surrounding fragments of shocked and unshocked target material (Osinski et al., 2004). It does not include any identifiable mineral and lithic clasts greater than 5-20 μm . Petrographically, the groundmass appears dark grey/brown to black in plane polarized light (Figures 6-8c, e) and can account for up 40–60% of the rock. Backscattered electron images and WDS analyses suggest that this material is amorphous clay; however its exact nature remains unclear (Figure 6-8 and Table 6-1). This material is hydrous as indicated by total weight % values of ~70–90%. Locally, calcite was observed as a secondary phase forming irregular bodies (Figures 6-8e, f).

Table 6-1: Individual analysis of groundmass-forming clays from Mistastin polymict impact breccias from Côté Creek.

Sample #	MM10-05A-2			MM10-34C-1						MM10-45	
Site	Côté Creek			Côté Creek						South Creek	
Analyses #	9	11	13	32	33	34	35	36	37	45	48
SiO ₂	42.97	51.07	44.42	44.17	46.72	49.96	48.67	44.63	48.98	43.43	39.41
MgO	0.42	0.33	0.41	1.39	1.74	1.76	1.81	2.04	1.91	1.50	3.13
Al ₂ O ₃	25.67	29.25	27.58	12.83	15.10	16.06	16.09	13.70	14.99	22.57	19.72
Na ₂ O	0.28	1.09	0.09	0.46	0.48	0.20	0.33	0.41	0.53	0.21	0.12
FeO	4.31	2.88	4.41	5.37	4.94	5.62	6.04	5.24	5.27	1.10	2.37
K ₂ O	0.46	0.25	0.34	0.33	0.34	0.30	0.37	0.35	0.39	0.13	0.09
TiO ₂	0.07	0.06	0.04	0.04	0.08	0.08	0.08	0.07	0.08	0.04	0.06
CaO	1.80	3.79	0.97	3.87	3.54	2.88	3.20	3.31	3.59	5.61	4.76
Total	75.97	88.72	78.27	68.46	72.93	76.86	76.57	69.75	75.73	74.57	69.66

6.4.3.2 Distribution in crater structure and shock features

The melt-free to -poor, polymict lithic breccias are observed at all of the major field sites visited within the inner zone of the Mistastin Lake impact structure (Figure 6-2 for names and locations) and stratigraphically overlie fractured and monomict brecciated target rocks. Below, we describe this impactite type from several key locations.

Coté and Piccadilly Creeks

The most extensive outcrops of melt-free to -poor, polymict impact breccia are exposed along creek banks within the first 1 km of Coté Creek (starting at the lake shoreline and moving inland) (Figure 6-9) and 2 km along Piccadilly Creek. Previously interpreted as monomict anorthositic breccias (Marion, 2009), these steep cliffs range in height from 3 m to ~30 m, and appear unconsolidated due to erosion processes (Figure 6-9b). The buff white colouring of the cliff faces is due to high concentration of poorly sorted, randomly orientated, anorthosite fragments; the polymict nature of the impact breccias can only be discerned upon closer inspection (Figure 6-9b).

Subrounded to angular fragments make up 30–40% of the unit. The majority of these fragments are sub-cm in size and ~90% of them are anorthositic. Some of the anorthosite fragments are only mildly fractured (very low shock), retaining their labradorite sheen; while others are more highly shocked (containing maskelynite) with a dull, buff white, chalky appearance. Locally, large anorthositic blocks, 5–10 m in diameter, were noted (Figure 6-9b). Other fragment lithologies include granitic material up to 50 cm in size, smaller quartz monzonite clasts with a maximum size of ~10 cm, and rounded pink potassic feldspar grains. Rarely, cm-scale fragments of glass or its weathered equivalent were observed (<1%) (Figure 6-8b), however, most of these Coté Creek polymict impact breccias are free of glass fragments.

Along Piccadilly Creek, the first 1 km inland from the lake shore is dominated by fractured quartz monzonite target rock, and at ~ 1 km, a distinct ~130 m long cliff, 8–10 m high exposure of polymict lithic breccias dominated by anorthositic fragments overlain by impact melt rock is exposed (Figure 6-9c), similar to sites along Coté Creek.

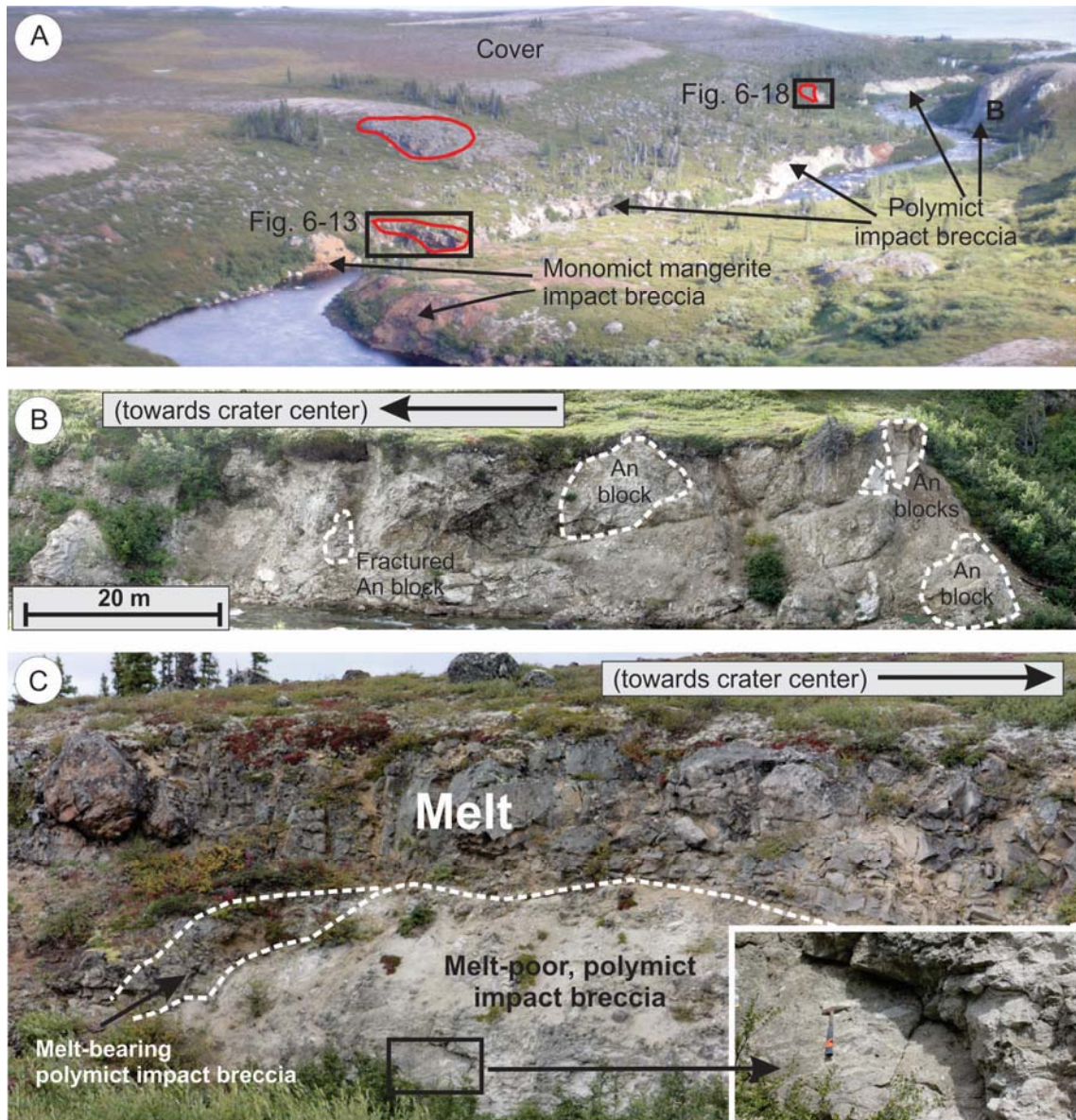


Figure 6-9: Melt-free to -poor polymict impact breccias along Côté and Piccadilly Creeks. (A) Aerial view of Côté Creek showing distribution of impactites, looking east. Outcrops of impact melt rock outlined in red. Letter B indicate location of following image. (B) Near mouth of Côté Creek, buff white cliffs, ~80 m long and ~20 m tall comprise melt-poor, polymict breccias dominated by anorthositic fragments (“An block”) (location marked as B in Fig. 6-9A). (C) 10 m high cliff face along Piccadilly Creek, ~6 km from crater centre showing melt overlying melt-poor polymict breccias. Inset: Detail of fragmental nature of unit.

South Creek

Other notable outcrops of melt-free to –poor polymict breccia were found along South Creek and the south shoreline. Along a steep face on the east side of South Creek (Figure 6-10a), a layer of polymict breccia overlies fractured anorthosite target rock. This layer tapers downwards, along a 5 m extension fracture that has sharp boundaries and separates fractured anorthosite and monomict, anorthosite breccia units (Figures 6-8e, 6-10). This unit contains large angular, anorthosite blocks (0.5–1m) with an average fragment size of 2–4 cm. Flat outcrops of light grey, polymict breccias along the southern shoreline of Mistastin lake are similar to those observed along Coté Creek (Figures 6-10c, d).

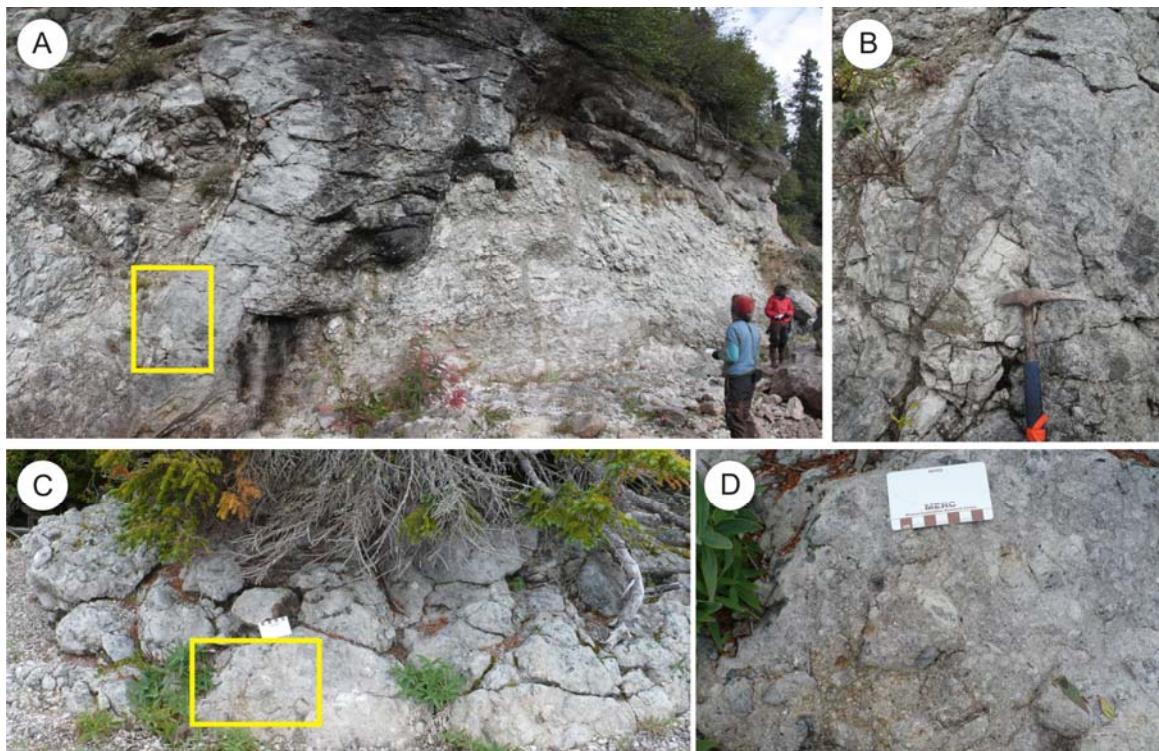


Figure 6-10: South shore and South creek melt-poor, polymict lithic breccias. (A) Layer of polymict breccia overlying fractured anorthosite target rock, South Creek. (B) Detail of box outlined in A, showing anorthosite clast in breccia. (C) Flat outcrops of melt-poor polymict lithic breccias along the southern shoreline. (D) Detail of box outlined in C, showing cm size anorthosite fragments.

Discovery Hill

Along the south side where the melt unit thins out, a contact with underlying polymict breccia is exposed over a ~100 m extent (Figure 6-11). The boundary is relatively sharp with little mixing between the two units. The breccia contains ~ 40%, mm-cm size, subrounded to angular, granodiorite fragments in a dark gray, fine-grained matrix (Figure 6-11d). Locally, large m-scale blocks of granodiorite were observed. No glass fragments were observed within the breccia.

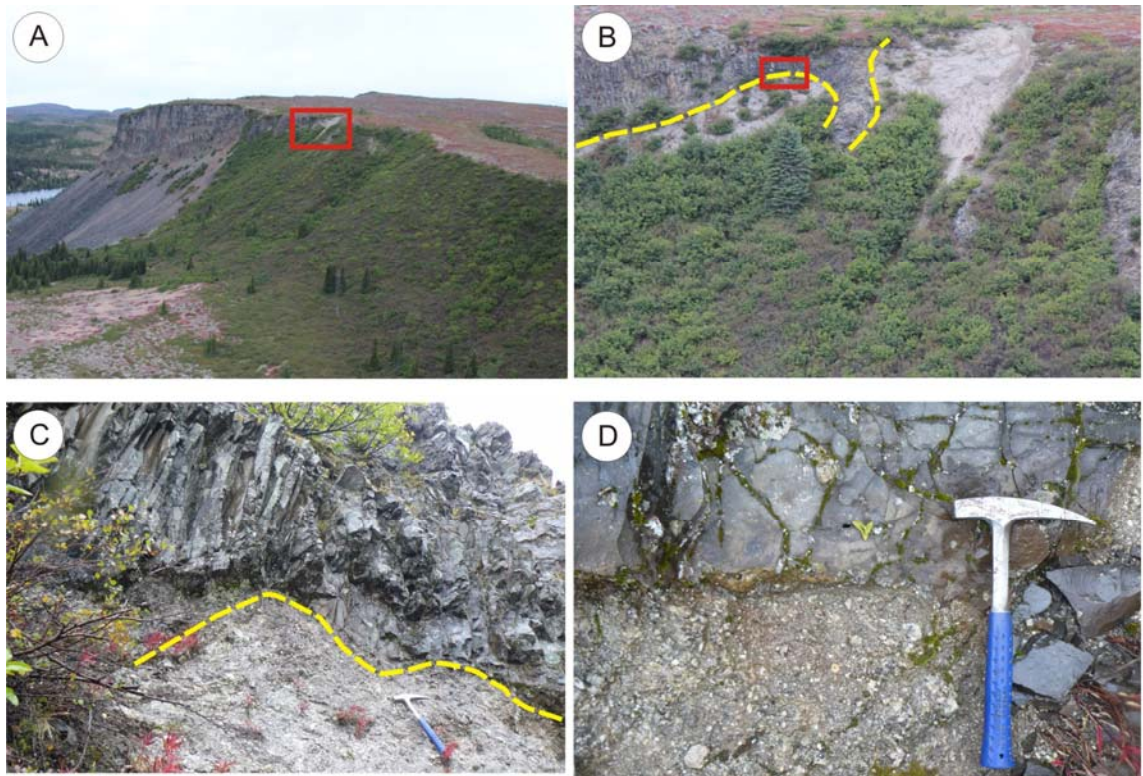


Figure 6-11: Discovery Hill (A) Aerial view of south side of Discovery Hill showing 80 m thick unit of impact melt rock with vertical cooling fractures. (B) Detailed view of box in A. (C) Detailed view of contact in B. Melt-poor, polymict lithic impact breccias underlying melt, Discovery Hill. Melt unit has cm-m spaced, vertical cooling fractures. (D) Detail of contact between impact melt rock overlying melt-poor polymict lithic impact breccia.

Shock Features

Rock and mineral fragments within melt-poor polymict lithic impact breccias exhibit a range of shock metamorphic effects (Figure 6-12), including (from low to high shock level features), irregular fracturing, planar fractures in feldspar and quartz, planar deformation features in quartz, ballen silica, and diaplectic feldspar glass (maskelynite). Typically a minor amount (<2%) of cm-size, impact glass fragments were also observed within breccias dominated by fragments of target rock. Overall, this unit is characterized by fragments with Stage 0 – V shock features, which experienced pressures up to 60 GPa.

Within the South Creek melt-free to -poor polymict impact breccias, zeolite polymorphs of feldspar characterized by anomalous mosaicism made of fan-shaped patches with different undulose extinction patterns were observed. The mosaicism pattern is confined by the original shape of the feldspar grain. Veins of zeolite material were also noted. Locally, patches and thin rims of zeolites were found to be associated with maskelynite and may be an alteration product of this phase (Figures 6-12e, f). Pickersgill et al. (2015), identified the zeolite in South Creek samples as levyne – Ca using micro-X-ray diffraction (μ XRD) and electron probe microanalysis (EPMA).

Zeolite laths with a composition close to chabazite-Ca ($\text{Ca}_{0.5}\text{Na,K}_4[\text{Al}_4\text{Si}_8\text{O}_{24}]\cdot 12\text{H}_2\text{O}$) were observed within Côté Creek polymict impact breccias (Table 6-2). These minerals display open-space filling textures (e.g., veins) and cross-cut the more homogenous clay groundmass. Both levyne-Ca and chabazite-Ca are typically known to occur naturally in cavities of basaltic rocks (Deer et al. 2004), and Chabazite-Ca has been observed in numerous impact structures (e.g., Popigai, Kara, Puchezh-Katunki; Naumov, 2002).

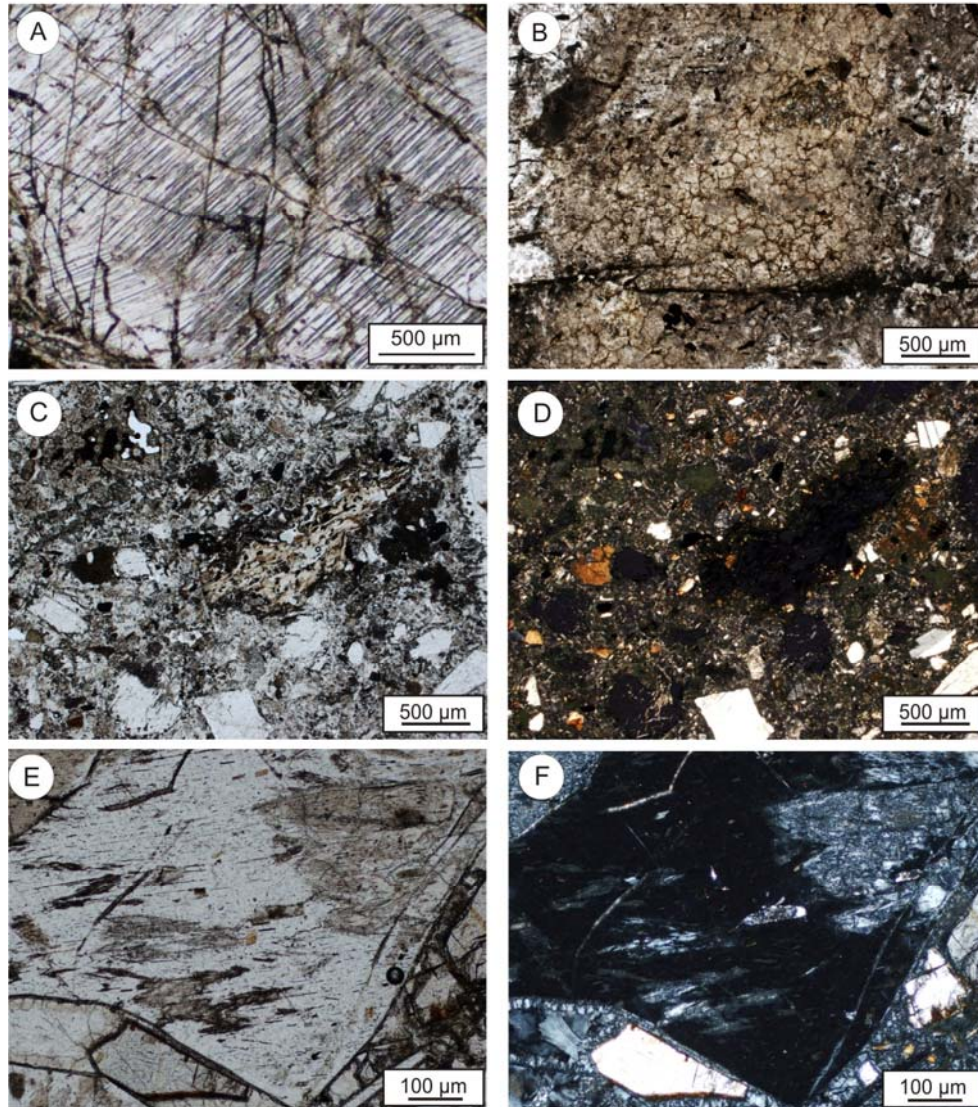


Figure 6-12: Thin section microphotographs showing range of metamorphic shock effects in polymict impact breccia fragments. (A) Planar deformation features observed in quartz from a melt-poor, polymict impact breccia, locality (plane-polarized light). (B) Toasted, ballen quartz observed in melt-poor, polymict impact breccias, South Creek (plane-polarized light). (C) Fragmental nature of melt-poor, polymict impact breccias, showing rare melt fragment and maskelynite, Coté Creek (plane-polarized light). (D) Same area as (C), cross-polarized light. Maskelynite and melt fragments are isotropic. (E) Maskelynite grain (clear) with patches of zeolite alteration and thin zeolite rim, South Creek (plane-polarized light). (F) Same area as (E), cross-polarized light. Maskelynite grain is isotropic (completely dark).

Table 6-2: Average composition of zeolites from Mistastin Lake polymict impact breccias from Côté Creek.

Sample #	MM10-05A-2			
Analysis #	1	2	5	6
SiO ₂	50.87	51.63	54.75	45.98
MgO	0.19	0.33	0.23	0.44
Al ₂ O ₃	22.48	20.51	21.54	20.53
Na ₂ O	0.06	0.33	0.30	0.60
FeO	0.54	0.66	0.34	9.55
K ₂ O	0.43	0.59	0.82	0.41
TiO ₂	BD	0.06	0.01	0.09
CaO	8.71	7.78	8.23	1.10
Total	83.26	81.88	86.23	78.69

6.4.4 Impact melt-bearing polymict lithic impact breccias

6.4.4.1 General description

The melt-bearing polymict impact breccias are similar in fragment and groundmass content to the melt-free to -poor polymict impact breccias previously described, with the exception that they can also have a brown matrix and contain up to 40% impact melt fragments. We use the term “melt” here, but the fragments range from glassy to completely crystallized, devitrified and/or altered. The melt fragments range from mm-cm in size with aspect ratios ranging from 1:1 to 10:1 for elongated, sinuous fragments. Melt mantles are also present around target rock fragments.

6.4.4.2 Distribution in crater structure and shock features

Impact melt-bearing polymict lithic impact breccias were found in different stratigraphic settings within the collapsed rim region: 1) as a zone between melt rocks overlying melt-poor polymict breccias, 2) as a dyke within massive target rock, and 3) as a lens within a thick unit of impact melt rocks. They exhibit the same range of shock features as the melt-free to -poor polymict impact breccias.

Coté and Piccadilly Creeks

Along Coté Creek (Figure 6-13) and Piccadilly Creek, (Figure 6-9c), approximately 5 to 6.5 km from the crater centre, units of melt-bearing polymict impact breccia with light grey, fine-grained, lithic matrix and melt fragments were observed between melt-poor polymict impact breccia and overlying melt rocks (Figures 6-13, 6-14). A unit of impact melt rock along Coté Creek, defines a U-shaped contact between impact melt rock and polymict breccia, approximately 25 m across at its widest part. The sides of the U-shape, dip sub-vertically and are characterized by a sharp contact between the impact melt rock and polymict breccias.

Along the base of the U-shape contact, the amount of impact melt fragments increases as proximity to the overlying impact melt rock contact increases (Figure 6-13). The boundary between the polymict breccia with impact melt fragments and the clast-rich impact melt is transitional over 1–3 m. Within this transitional zone, the two units are intermingled with sinuous and amoeboid shaped lens and stringers of each unit (Figure 6-13); it can be difficult to define the matrix material in this transition zone.

The impact glass melt fragments within the melt-poor breccias through the transition to melt-rich breccias have different shapes and textures. Within the underlying polymict breccia (which only has <2% of glass fragments), the impact glass fragments range in appearance. Some have sharp boundaries in which the internal flow fabric has clearly been truncated (Figure 6-14a). Others have more irregular boundaries (Figure 6-14b). Looking closely at the impact melt fragment-bearing breccia with over 10% melt rock fragments, many lithic fragments are mantled by melt (Figure 6-14c). Many of the glassy fragments contain small rock and mineral fragments that are aligned with the long axis of the fragment (Figure 6-14d). In addition, ropey textures within impact melt rock were observed within the transition zone, where impact melt content is up to 50%. In this transition zone, impact melt-rich zones are characterized by crystallites of plagioclase (Figure 6-14e).

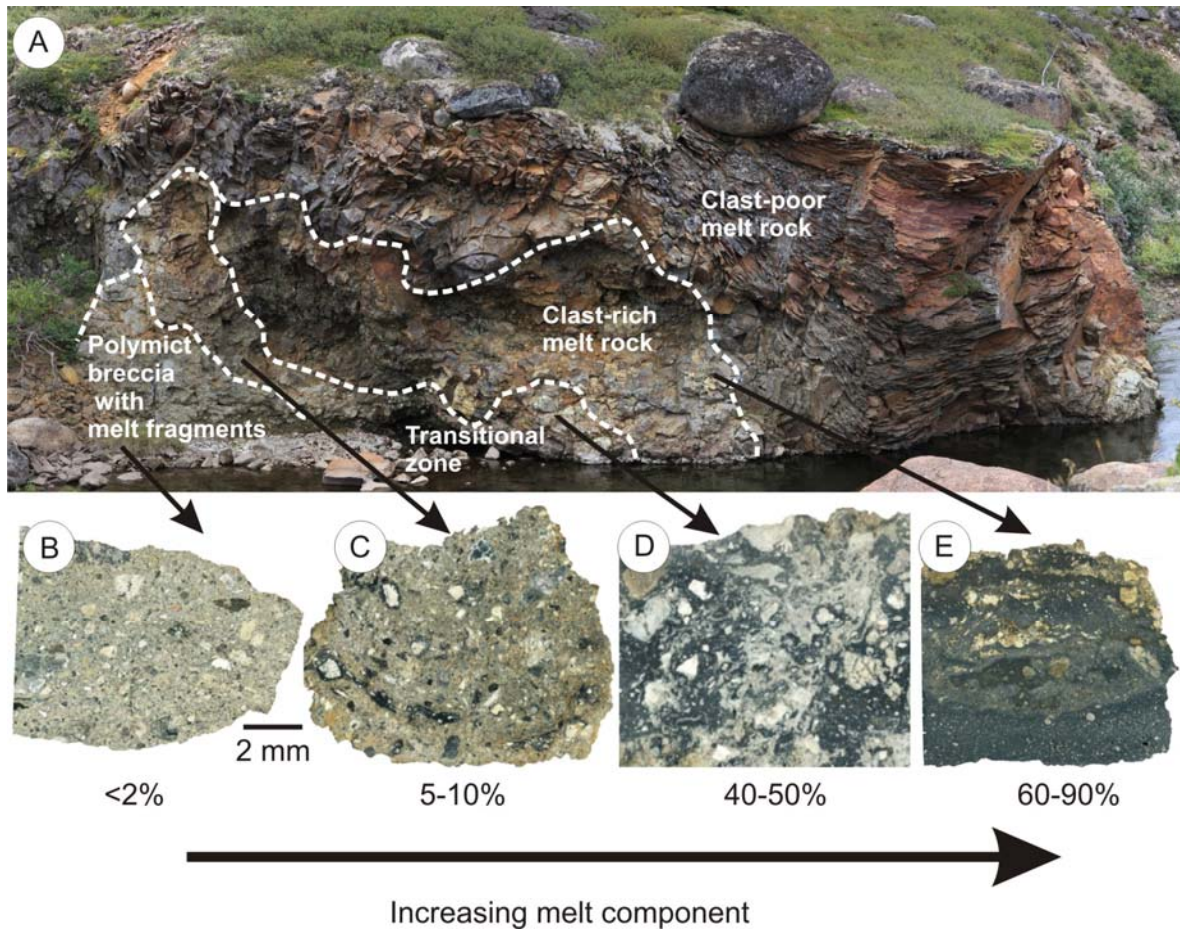


Figure 6-13: (A) Coté Creek site of U-shaped contact between impact melt rock and polymict breccia. Along the base of the U-shape contact, the amount of impact melt fragments increases as proximity to the overlying melt rock contact increases, as indicated in (B) through (E).

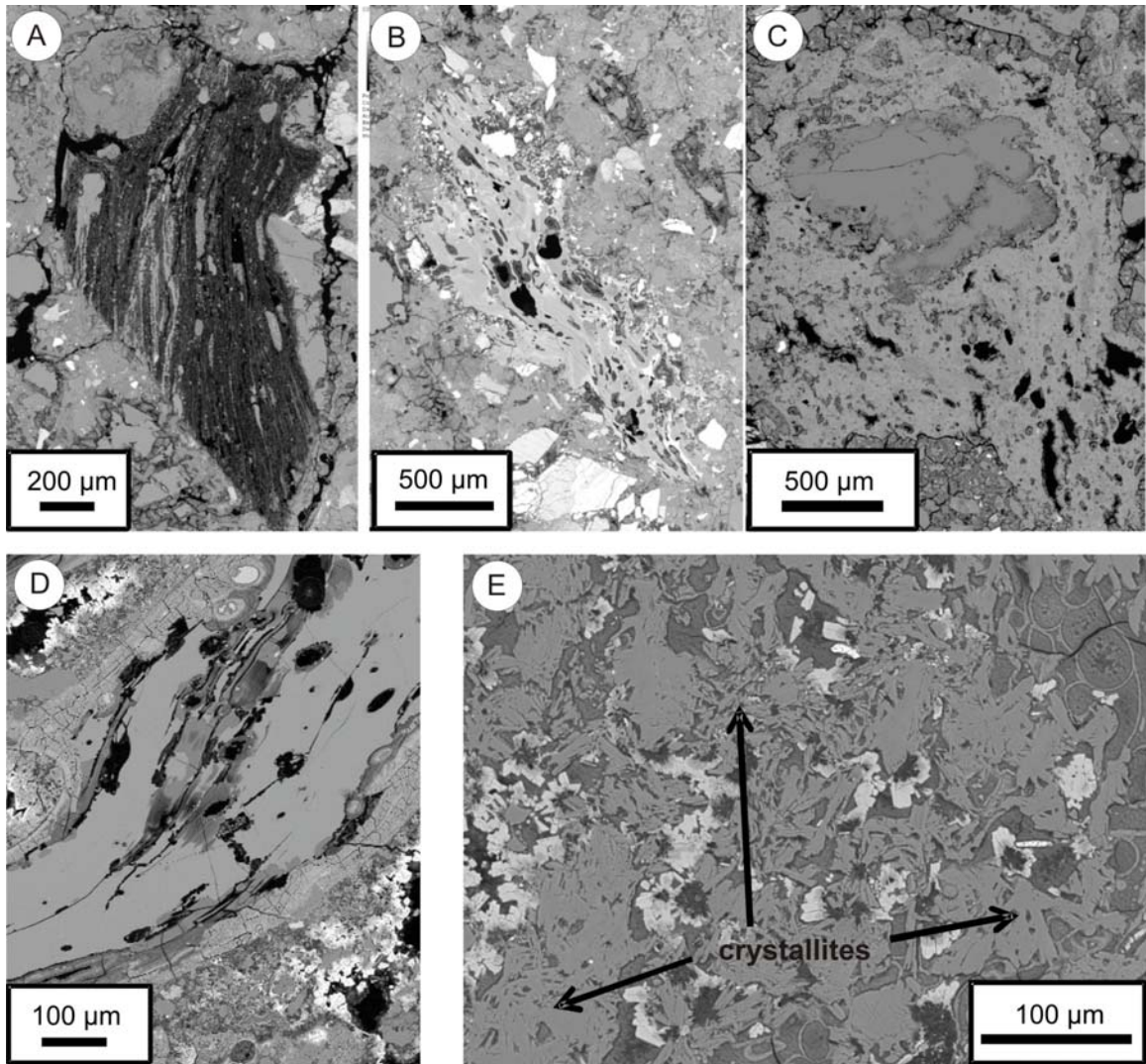


Figure 6-14: Backscattered electron (BSE) images of impact melt fragments within transitional zone between polymict breccias and overlying impact melt rock along Coté Creek as seen in Figure 6-13. (A) Detail of impact melt fragment in polymict breccia with <2% impact melt rock fragment (Figure 6-13b). Note: sharp boundary that truncates internal flow fabric. (B) Irregular boundary of impact melt fragment in same unit as A. (C) Detail of lithic fragment mantled by impact melt in polymict breccia with over 10% melt rock fragments. (D) Glassy fragment containing small rock and mineral fragments that are aligned with elongated side. Same unit as C. (E) Crystallites within impactite unit composed of 50% impact melt and 50% lithic material, as seen in Figure 6-13d.

Steep Creek

Steep Creek is dominated by exposures of massive quartz monzonite and quartz monzonite monomict breccia. Locally, fractures dipping steeply towards the lake are tens of m apart. A unique feature was observed along an expansive cliff face ~1 km upstream from the mouth of the creek: a steeply dipping dyke (strike 100°, dip 80°) comprising polymict lithic breccia with ~30% impact glass fragments (Marion et al., Forthcoming; Pickersgill et al., 2012). The exposed length of the dyke is approximately 18 m; it tapers downwards to the south and the northern thicker end is obscured by vegetation (Figure 6-15a, b). The boundary of the dyke within the host quartz monzonite unit is sharp and is characterized by a rusty, fine-grained, 5–10 cm thick zone (Figure 6-15c).

Overall the unit is composed of ~70% fractured rock and mineral fragments that are >20 µm, within a groundmass of mostly fragmental material, too small to discern by optical microscope and <3% amorphous cement. Plagioclase is the dominant clast type (~40%) and most of these grains over 0.5 mm are now diaplectic glass (maskelynite). Other clast types include quartz (~10%) with PDFs and PFs; pyroxene and biotite grains (<5%).

The impact melt fragments account for ~30% of the unit. They are glassy and vary from discrete, randomly oriented, elongate, sinuous pieces (Figure 6-15d) to amorphous zones within the breccia. The melt rock fragment edges range from irregular (Figure 6-15e) to sharp, wherein, internal fabrics are cut-off by the sharp edges (Figure 6-15f), and may exhibit both characteristics within a single fragment (Figure 6-15g). Locally, mineral and lithic clasts are mantled by impact glass (Figures 6-15h).

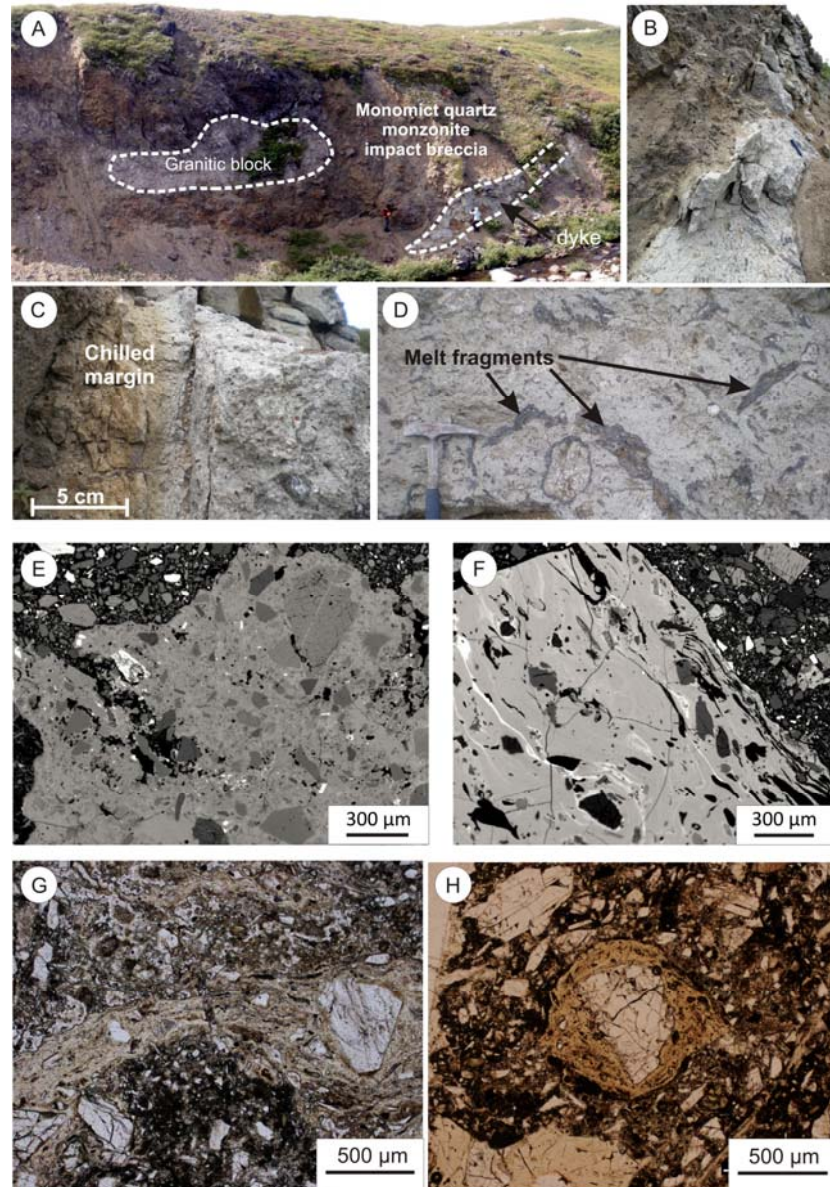


Figure 6-15: Steep Creek outcrop (A) Steeply dipping dyke (strike 100°, dip 80°) comprising polymict lithic breccia with 10-40% melt fragments. Exposed length ~18 m. (B) Detail of dyke looking up from bottom of exposure. (C) Chilled boundary of dyke is sharp and is characterized by a rusty, fine grained, 5-10 cm thick zone. (D) Randomly oriented, elongate, sinuous impact melt fragments. (E) Backscattered electron (BSE) image of irregular boundary of impact melt fragment. (F) BSE image of sharp edge of impact melt fragment (at top of image) that truncates internal fabric. (G) Elongated, sinuous impact melt fragment. Note sharp break in middle of melt fragment. (H) Feldspar fragment mantled by impact glass.

Discovery Hill

A 1 m x 6 m lens of rusty, polymict lithic impact breccia containing melt fragments was found within the middle of the 80 m thick Discovery Hill melt rock unit (Figure 6-16). The contact between the two units varied, from straight and sharp to anastomosing with thin melt fingers intruding into the breccia unit (Figures 6-16c, d). This polymict impact breccia is comprised of ~30% subround to angular, cm-mm scale, rock and minerals fragments and ~5% melt fragments. Maskelynite was not observed. Low shock features such as fractures were observed in plagioclase and quartz grains. Impact melt fragments were observed as sinuous, altered, glass fragments and mantling lithic clasts (Figure 6-16d), and were more concentrated near the boundary with surrounding melt rocks. Crystallites in the impact melt unit were present within 5 cm of boundary with the melt-bearing polymict lithic impact breccias (Figure 6-16d).

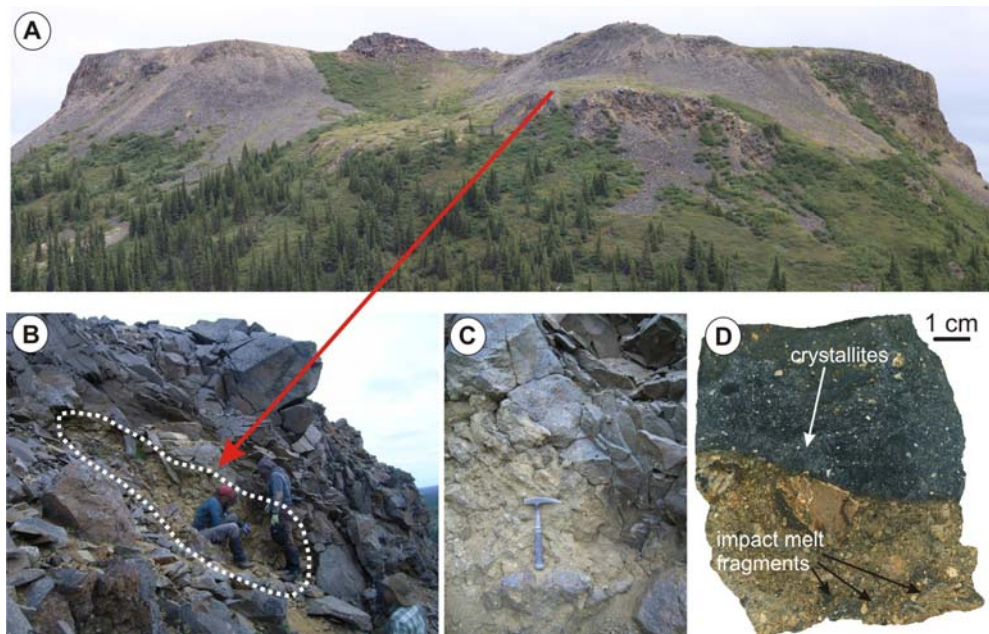


Figure 6-16: (A) Location of melt-bearing polymict impact breccias lens within 80 m thick Discovery Hill unit of impact melt. (B) Extent of 1 m x 6 m lens of rusty, polymict lithic impact breccia containing melt fragments. (C) Sharp to anastomosing contact between melt-bearing polymict impact breccia lens and impact melt. (D) Polished slab showing the sharp contact and crystallites within the impact melt unit up to 5 cm from boundary with polymict impact breccias lens.

6.4.5 Melt Rocks

6.4.5.1 General Description

All of the exposed melt rocks within the Mistastin impact structure are aphanitic to glassy matrix and range from clast-rich, to clast-poor, to clast-free. Coarser matrix grains are associated with thicker, clast-poor melt units whereas finer grains are associated with the thin melt units and clast-rich areas (Marion et al., Forthcoming). The highest concentration of clasts within melt rocks is near boundaries with underlying monomict and polymict breccias. Near this boundary, the clasts are mostly lithic fragments. Farther from this basal contact, the melt is clast-poor and the clasts are predominantly weakly shocked plagioclase and quartz, with lesser amounts of hypersthene, Fe-Ti oxides, apatite, and zircon (Marion et al., Forthcoming). Few areas in the melt are completely clast free, even the thickest units (80 m) contain minor μm -scale clasts. The melt rocks also contain differing sizes and amount of vesicles. Marion et al. (Forthcoming) used vesicularity as a criterion to estimate the amount of erosion that took place throughout the crater structure. The impact melt geochemistry has been well characterized by Grieve (1975), Marchand and Crocket (1977), Marion and Sylvester (2010), with an overall initial impact melt composition a mixture of 73% anorthosite, ~7% quartz monzonite, and ~20% granodiorite.

6.4.5.2 Distribution in Crater Structure

The distribution of impact melt rocks around the western two thirds of Mistastin Lake was mapped by Currie (1971) and Grieve (1975). Marion et al. (Forthcoming) describes the main outcroppings of melt, which vary in thickness from 10s of cm along the shoreline up to ~80 m at the Discovery Hill site. Melt rocks were observed within the inner zone, within a 2 km perimeter from the south and west shoreline (Figure 6-2). The following sections describe the contact relationships between the melt and adjacent units.

Shoreline

Along the south shore, outcrops of melt rock, ranging in thickness from 10s of centimetres to a few metres, overlie massive, fractured target rocks and polymict impact breccia dominated by anorthosite fragments (Figure 6-17a). Locally, distinct centimetre thick dykes of melt rocks in massive and fractured target rocks were observed (Figure 6-17b).

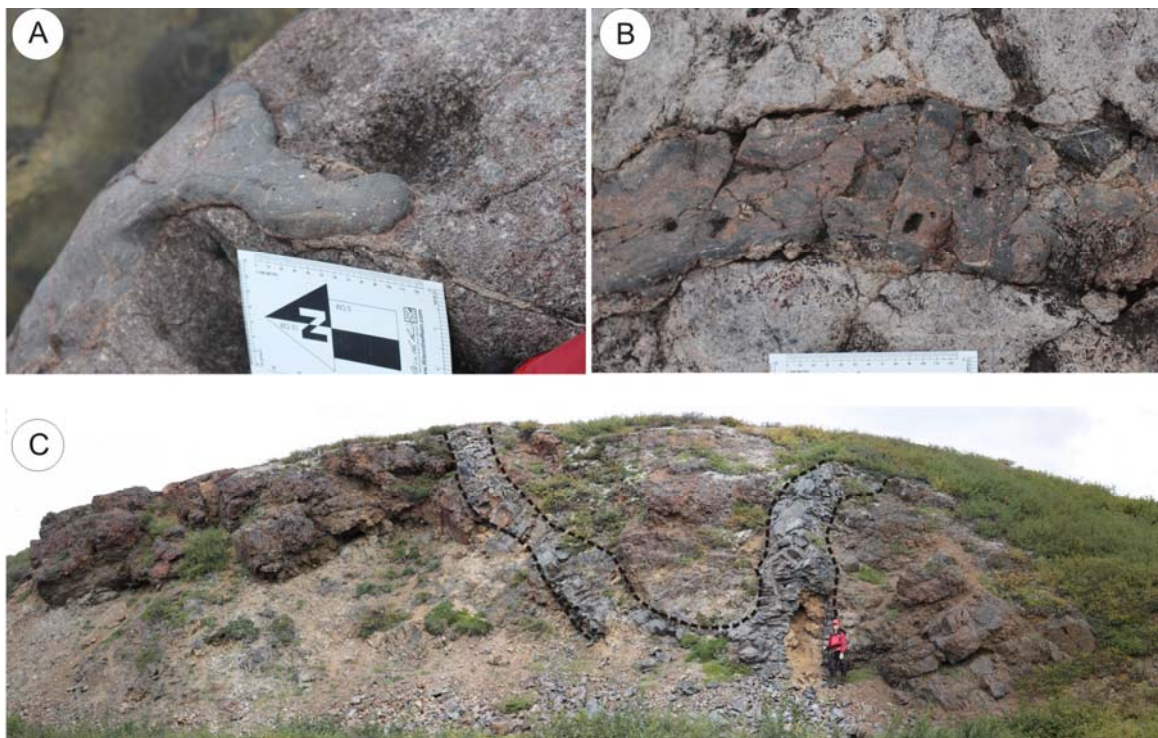


Figure 6-17: Impact melt rocks. (A) Locally, a thin, veneer of melt rock, overlying massive, fractured anorthosite target rocks, along S shoreline of Mistastin lake. (B) Example of the numerous impact melt rock dykes found within massive anorthosite target rock along S shoreline of Mistastin lake. (C) Piccadilly creek melt dyke, dipping 40° towards NNE (into the hill side). The surrounding rocks are quartz monzonite.

Piccadilly and Côté Creeks

Roughly 1.75 km inland along Piccadilly Creek from the shoreline, a dyke of melt rock in fractured quartz monzonite target rock was observed (Figure 6-17c). The contact is sharp and locally, small (cm size) fragments of the host quartz monzonite rock was found along the dyke edge, otherwise the melt was clast-poor.

Thicker units of melt rock (up to ~8 m) were observed in two outcrops along Côté Creek spaced ~350 m apart (Figure 6-9 shows location of outcrops in Figures 6-13 and 6-18). These melt units overlie polymict breccias, and grade upwards from glassy, clast-rich melt rocks at the base (Figures 6-13, 6-18a) to crystalline melt rocks with fewer clasts with increasing distance from the underlying breccias (Figure 6-18b). Curvilinear, cooling cracks in the clast-poor melt rock are roughly parallel to the contact with underlying breccias (Figures 6-13a, 6-18a). The transition zone between these two units is characterized by pockets of clast-rich melt rock, ropey textures of melt rock, and zones of polymict lithic breccia that contain melt fragments (Figure 6-18d). Within the basal, clast-rich portion of the melt rock, flow banding is locally observed around clasts (Figure 6-18c). Tapered flow patterns indicate a westerly sense of flow direction, away from the crater centre. A third massive outcrop, ~40 m², of melt rock was observed west of Côté Creek (see Figure 6-9a).

Discovery Hill

The most expansive unit of melt rock forms the highest portion of Discovery Hill which has been described in detail previously by Grieve (1975) and Marion et al.

(Forthcoming). This hill forms a distinct topographic high, in the form of a ramp shape dipping towards the lake (Figure 6-11a). Its form has been attributed to glacial erosion (Grieve, 1975). The high end of Discovery Hill is situated ~ 2 km radially inland (west) from the Mistastin shore at an elevation of 120 m above lake level. The top part of the ramp is primarily covered in vegetation and unconsolidated material, however the north, west, and south sides reveal exceptional exposures of impact melt rock (Figure 6-11a).

The exposed melt unit is wedge-shaped and is thickest on the west end. The basal contact of the melt package is mostly obscured as the lower portion of the cliff faces is covered

by unconsolidated talus slopes or vegetation. However, along the south side a sharp contact with melt-poor, polymict breccia was observed (Figure 6-11). The melt unit appears to taper in thickness to the east. Two tiers of columnar joints are developed along the south side exposed melt rock unit. Large m-sized (~6 x 8 m) quartz monzonite clasts are found within the melt unit on the north and west sides of the butte and atop the hill. The vertical joints curve around these quartz monzonite boulders.

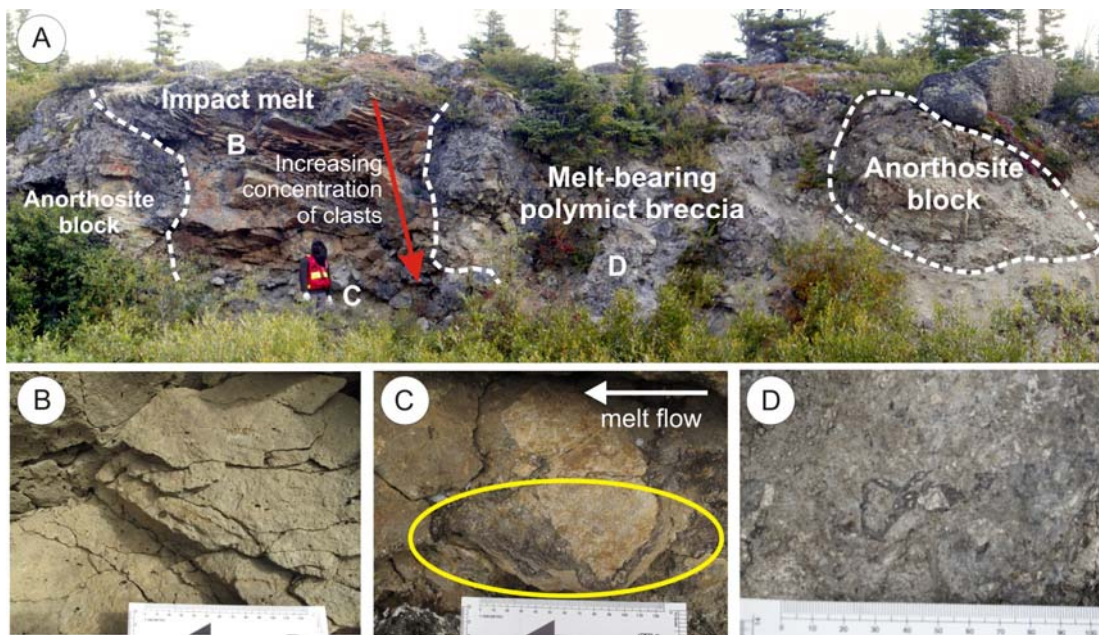


Figure 6-18: (A) Exceptional outcrop along steep bank of Coté Creek showing contact of melt-bearing polymict impact breccias underlying impact melt rocks. Note: Cooling cracks in overlying impact melt unit. Letters indicate locations of following photos. (B) Detail of clast-poor, impact melt rock. (C) Flow banding around a clast within basal portion of melt unit, indicates flow in westerly direction (away from the centre of the impact structure). (D) Melt-bearing polymict impact breccias.

6.4.6 Summary of Mistastin Lake impactites

The Mistastin Lake impact structure provides a rare opportunity to study a near complete suite of impactites exposed at surface. Vertical sections along Discovery Hill, South Creek, Côté Creek, Piccadilly Creek, Steep Creek, and the NE rim region reveal contact relationships and unit thicknesses, allowing a complete stratigraphy to be described (see Figure 6-2 for distribution of units). Table 6-3 provides a summary of this stratigraphy with descriptions of each impactite unit.

6.5 Discussion

6.5.1 Impactite stratigraphy

Impactites are grouped according to the extent to which they have been moved from their original pre-impact location by the impact. They are subdivided into three categories: 1) autochthonous (formed in place), 2) parautochthonous (moved but appear to be in place), and 3) allochthonous (formed elsewhere and clearly moved to their current location) (Grieve and Therriault, 2013). Many terrestrial impact structures have been eroded to such a degree that only the underlying autochthonous target rocks are preserved or the crater structure has been infilled by later sedimentary units and thus impactites can only be accessed through drilling. In both cases, it is difficult to have a clear understanding of the spatial occurrence of impactities with respect to the crater structure. The Mistastin Lake impact structure offers a unique opportunity to study a complete suite of impactites in which their geological context (i.e., contact relationships) can be observed in the field.

Key exposures of impactites at Mistastin describe a radial transect outwards from the central uplift across the apparent crater rim. Figure 19 shows a sectional view across the Mistastin Lake impact structure.

Table 6-3: Description of Mistastin Lake impactites units in stratigraphic order from bottom to top.

Impactite	Crater Location*	Nature of matrix	Clasts	Shock level**	Secondary minerals
Massive and fractured target rocks	Inner zone Outer zone Central uplift	Crystalline	N/A	<i>Shock level: 0</i> Macro- and microscopic fracturing. Central uplift: locally PDFs in quartz.	sericite, calcite
Monomict breccia	Inner zone	Angular fragments <5 mm; locally zones of pristine crystals separated by seams of brecciated material.	Angular to sub-rounded, range from cm to m scale, and make up 70-90% of the rock.	<i>Shock level: 0</i> Macro- and microscopic fracturing, shattercones	sericite, calcite, Ca-zeolite
Polymict lithic breccias (melt fragment poor)	Inner zone	Up to 40-60 % of rock. Dark grey/brown to black in plane polarized light. Fine-grained mineral and lithic clasts < 20 µm. Amorphous clay.	30-40% of rock poorly sorted; subrounded to angular fragments <1 mm up to tens of metres, average size 3-5 cm within fine grained matrix. 80-90 % Anorthosite fragments and feldspar mineral clasts. < 5% quartz monzonite and granodiorite clasts. <3% pyroxene, biotite, accessory minerals Other fragment lithologies include granitic material up to 50 cm in size quartz monzonite clasts up to ~10 cm. Rare cm-scale melt rock fragments (<1%)	<i>Clasts: Shock level: 0 - IV</i> Fractured anorthosite clasts that retained labradorite sheen; PDFs in quartz clasts; maskelynite; rare melt fragments.	Calcite Ca-zeolite
Polymict lithic breccias (with melt fragments)	Inner zone:	Same as above.	Similar to above, except up to 40% impact melt rock fragments, and less target rock/mineral fragments. Impact melt fragments: mm-cm in size, aspect ratios 1:1 to 10:1 for elongated, sinuous fragments. Melt mantles around target rock fragments.	<i>Clasts: Shock level: 0 - IV</i> Fractured anorthosite clasts that retained labradorite sheen; PDFs in quartz clasts; maskelynite; up to 40% melt fragments.	Calcite Ca-zeolite
Melt rocks	Inner zone Modified transient cavity	Vesicular, aphanitic to glassy matrix and range from clast-rich, to clast-poor, to clast-free. Coarser matrix grains associated with thicker, clast-poor melt units, finer matrix associated with thin melt units and clast-rich areas.	Highest concentration of clasts near boundaries with underlying monomict and polymict breccias. Farther from this basal contact, the melt is clast-poor and the clasts are predominantly weakly shocked plagioclase and quartz, with lesser amounts of hypersthene, Fe-Ti oxides, apatite, and zircon.	<i>Shock Level: IV</i> Rock glasses and crystallized melt rocks (quenched from whole melt rocks).	Calcite vugs

*See Figure 6-2 for distribution of impactites. For a list of sample collection coordinates see Appendix D.

**Shock level based on schemes developed for quartzofeldspathic crystalline rocks by French, 1998 and Stöffler and Grieve, 2007.

A general stratigraphy, from bottom to top includes (cf., Grieve, 1975; Marion et al., Forthcoming; Osinski et al., 2008):

- A) Unshocked target rocks;
- B) Autochthonous/parautochthonous shocked and fractured target rocks;
- C) Parautochthonous monomict lithic breccias;
- D) Allochthonous polymict lithic breccias (melt-poor and melt-bearing);
- E) Allochthonous impact melt rocks (grading from clast-rich to clast-poor from bottom to top).

Similar successions have been described at other impact structures including: Manicouagan, which also has a crystalline target (Currie, 1972; Murtaugh, 1976), Haughton, which has a sedimentary target (Osinski et al., 2005), and Ries which has a mixed target of sedimentary units overlying crystalline target rocks (Hörz, 1982).

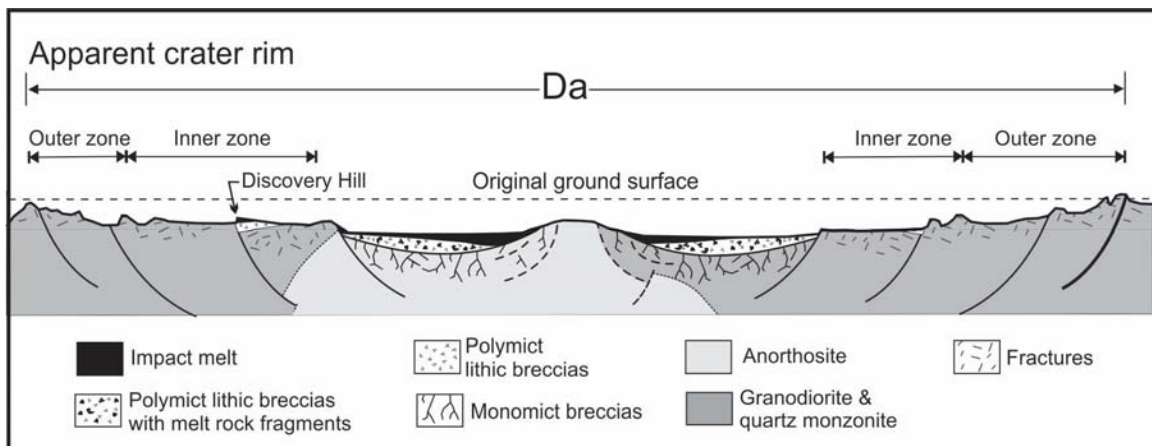


Figure 6-19: Schematic cross-section of the Mistastin Lake impact structure, idealized transect from southwest to northeast across the crater. Present-day surface after erosion and glaciation; Da = diameter of apparent crater rim. Curved, listric faults represented in cross-sections are not continuous laterally. Zones are bound by raised hills and short faults.

Unshocked target rocks underlie all impactite units. Although the original crystalline stratigraphy of the batholith is unknown, the high concentration (~90%) of anorthosite fragments within allochthonous breccias and as the main component of impact melt, suggests that the anorthosite body was at least the width and depth of the transient cavity, an intermediate form in the development of the final crater formed immediately after impact from which shocked material was ejected.

Autochthonous, fractured target rocks are found in the collapsed rim region of the Mistastin impact crater and make up the raised ring of hills that define the apparent crater rim. They would have experienced shock pressures < 2 GPa, too low to produce distinctive shock-deformation effects, but high enough to exceed the yield strengths of near-surface crustal rocks, forming faults and fractures (French, 1998). The degree of brittle deformation decreases beyond the apparent crater rim, as evident from a decreasing concentration of lineaments, interpreted as fractures, in the northwest region surrounding the impact structure (Chapter 5), similar to findings from the El'gygytgyn structure in Siberia (Gurov et al., 2007).

Parautochthonous monomict breccias are found within the structural uplift and within the inner zone of the Mistastin impact structure. The material of the structural uplift experienced greater shock metamorphic effects including PDFs in quartz (Pickersgill et al., 2015). Parautochthonous monomict breccias within the inner zone, most notably along South Creek, were too distant from the point of impact to experience shock metamorphic effects (Table 6-3). Their low shock level and the presence of overlying allochthonous polymict impact breccias (see section 6.5.2) suggests that these monomict impact breccias were originally outside the transient cavity and were faulted down during cavity modification.

Allochthonous polymict impact breccias and impact melt rocks were found within the inner zone of the Mistastin impact structure and are discussed in detail in the following section. Outcrop-scale, radially trending dykes (with respect to the crater centre) along the Mistastin shoreline and within the inner zone (Figures 6-5b, 6-15a, and 6-17c), are interpreted to have developed within radial fractures that formed early in the in the crater-

forming process during the outward growth of the transient cavity. These dykes were formed by intruding allochthonous material, such as breccias and melt and locally by culmination along the fracture planes resulting in monomict breccias (e.g., Figure 6-5b).

6.5.2 Impact ejecta

Impact ejecta is defined here as any target material, regardless of its physical state, that is transported beyond the rim of the transient cavity (Osinski et al., 2011), including impact melt or impact breccias. The Mistastin Lake impact structure provides unequivocal evidence of impact melt ejecta that flowed over ballistically emplaced, polymict lithic impact breccias within the collapsed rim region.

6.5.2.1 Ballistic ejecta

During the excavation of the transient crater, material from concentric zones of different shock levels is mobilized and ejected ballistically out of the transient cavity forming an airborne “ejecta curtain”; a sheet-like concentration of ejecta that moves outwards in a truncated cone geometry (Oberbeck, 1975). This ejected material contains material from a range of different shock levels regardless of the velocity of ejection (Melosh, 1989). Even the lowest velocity ejecta may contain a significant amount of highly shocked impactites (Melosh, 1989). As ballistic material lands, secondary cratering, a process referred to as ballistic sedimentation (Oberbeck, 1975) occurs, and a continuous ejecta blanket forms. During outward crater growth, rocks around the periphery of the bowl-shaped transient crater collapse downward and inward to form a series of blocks and/or terraces along the outer margin of the crater structure (French, 1998). Products of the ballistic ejecta blanket can therefore be expected within the modified, collapsed rim region of a complex crater where they were deposited prior to crater collapse, interior to the final crater rim (Dressler and Reimold, 2001; Osinski et al., 2011; Stöffler et al., 2002). In fact, in fresh craters, the ejecta blanket is thickest at the crater rim region, beyond which deposits are thin and patchy (Melosh, 1989; Osinski et al., 2011). Perhaps the most well-documented occurrence of an complex crater ejecta blanket deposit resulting from ballistic sedimentation on Earth, is the Bunte Breccia of the Ries impact

structure (e.g., Hörz et al., 1983) a poorly sorted, massive, polymict lithic breccia unit of generally low shock level (Hörz, 1982).

Polymict lithic impact breccias were observed within the inner zone of the Mistastin Lake impact structure, along radial streams to the south and west of Mistastin Lake, including South Creek, Côté Creek, and Piccadilly Creek, and underlying the thick unit of impact melt rock at Discovery Hill. Moving radially away from the centre of the Mistastin impact structure, the first 1 km of Côté Creek is dominated by polymict breccias, previously interpreted as monomict anorthosite breccia (Currie, 1971; Grieve, 1975; Marion et al., *Forthcoming*), and lie stratigraphically above nearby fractured quartz monzonite target rocks. This reinterpretation is significant as this unit was previously interpreted either as crater floor, where monomict breccia is common, or collapsed crater rim wall (e.g., Grieve, 1975).

The unsorted, sub-round to rounded nature and the range of metamorphic effects in the target rock fragments of the polymict impact breccias (e.g., irregular fractures, planar fractures, planar deformation features, diaplectic glass, and impact melt fragments) support a ballistic ejecta origin of this unit. Locally, blocks tens of metres in size were initially interpreted as in place target rock largely due to their size. Typically, the extent of their size is obscured by unconsolidated material. After examining the 4 km extent of Côté Creek leading into the lake, none of the anorthosite blocks are interpreted to be in place and their location is attributed to movement resulting from the impact event. These blocks are associated with polymict breccia, suggesting that they are also allochthonous in nature. Locally, one such block contains fractures filled with polymict breccia with brown matrix. The breccia dyke does not cross-cut into the adjacent grey, polymict breccia suggesting that it formed within the anorthosite block before it was transported. The block may have originated from the crater floor, been intruded by the breccia dyke during the early stage of the impact event, and then transported during the excavation stage. These properties are equivalent to the well-studied Bunte Breccia at the Ries impact structure (Hörz, 1982), which is acknowledged as ballistic ejecta.

6.5.2.2 Non-ballistic ejecta: Impact melt-rich material

The main body of impact melt is generated by the time the original transient cavity reaches its maximum size during the excavation stage of crater formation, before central uplift formation in complex craters and rim collapse begins in the modification stage (Melosh, 1989; Osinski et al., 2011). Field observations of terrestrial craters and numerical models suggest that central uplifts partially collapse to varying degrees and may originally overshoot the original target surface and then collapse (Collins et al., 2002). This movement can impart an additional outward momentum to the melt within the transient cavity, resulting in flow toward and over the collapsing crater rim and onto the proximal ballistic ejecta blanket, forming a second thinner and potentially discontinuous layer of non-ballistic ejecta (Osinski et al., 2011). Oblique impacts and local topography of the target region also influence the final resting place of melt deposits beyond the transient cavity.

Later melt ejecta phases, deposited as ‘melt ponds’, have been observed on top of ballistic ejecta blanket deposits in lunar images (Hawke and Head, 1977; Howard and Wilshire, 1975). Recent studies using images from the Lunar Reconnaissance Orbiter Camera (LROC) have revealed flow features within terrace rim melt deposits (e.g., Ashley et al., 2012; Öhman and Kring, 2012). Terrestrial observations of impact melt ejecta overlying ballistically emplaced impact breccia ejecta are rare. The Ries impact structure in Germany, offers some of the best preserved and exposed ejecta deposits within the rim region of a complex impact structure on Earth, with a distinctive two-layer ejecta configuration (Hörz, 1982). As noted above, it is generally accepted that the lower unit, termed Bunte Breccia – a poorly sorted, massive, polymict lithic breccia – formed by ballistic sedimentation (Hörz et al., 1983). The formation mechanism of the upper unit of ‘suevites’, including unsorted to poorly sorted breccias that contain impact melt fragments, has several interpretations. Early workers suggested it was deposited sub-aerially as an ejecta plume (Engelhardt, 1990; Engelhardt and Graup, 1984); however, this explanation is not supported by more recent numerical models (Artemieva et al., 2013), petrographical studies (Bringemeier, 1994), and detailed field and microanalytical investigations (Osinski et al., 2004), which suggest they were emplaced as surface

flow(s), either comparable to pyroclastic flows or as ground-hugging volatile- and melt-rich flows.

Isolated outcrops of impact melt rocks overlying polymict breccia within the inner zone of the Mistastin impact structure, along Côté Creek, Piccadilly Creek, and Discovery Hill, are not interpreted as being continuous with the original melt sheet that would have developed within the original transient cavity as concluded by previous studies (Grieve, 1975; Marion et al., Forthcoming). Melt rock deposits along and adjacent to Côté Creek are interpreted as remnants of an isolated melt unit that was at least 200m x 1000 m in extent before erosion (Figure 6-9a). Field and BSE observations indicate that the melt rocks were molten at the time of, and after, deposition. Evidence of this includes chilled, ropey textures within the melt unit at the boundary with the underlying polymict breccias and crystalline groundmass phases displaying quench textures, both indicating rapid crystallization from a melt.

Steep creek banks along Côté Creek, allow a three dimensional view of the unit. Locally, a curved trough of impact melt rocks with vertically dipping sides define a flow channel (Figure 6-13). The melt rocks overlie polymict breccia characterized by unsorted, cm size fragments of anorthosite and plagioclase of mixed shock level from low to high (up to 35 GPa) with less than 2% of melt fragments. At the base of the trough, a transitional zone in which the melt unit had mixed with the underlying polymict breccia is indicative of rapid melt flow. The amount of melt fragments increases as proximity to the overlying melt rock contact increases (Figure 6-13). Within the transitional zone, melt-bearing impact breccia with over 10% melt fragments, contain many lithic fragments that are mantled by melt (Figure 6-14c) and many of the glassy fragments have irregular boundaries and contain small rock and mineral fragments that are aligned with the elongated side of the fragment (Figure 6-14d). These observations indicate that these melt fragments were still hot and viscous during mixing with the breccias unit and then cooled rapidly. Chilled features (e.g., ropey textures, crystallites) close to the boundary, also suggest that the underlying breccia unit was much cooler than the flowing melt.

Discovery Hill, an 80 m thick unit of melt rock, lies within the collapsed rim region of the Mistastin impact structure, situated above the current lake level. Its wedge shape is the result of glaciation. Locally, a sharp contact with underlying melt-poor, polymict breccia was observed (Figure 6-11). Due to the location within the collapsed rim region and polymict nature of the breccia, this unit of polymict impact breccia is interpreted to have been emplaced ballistically. The lack of mixing between the overlying melt and the breccia, indicates that the melt pooled on top of the breccia or moved slowly overtrop without disrupting the unconsolidated polymict breccia. These contact relationships are identical to the suevite – Bunte Breccia contact at the Ries impact structure. These observations suggest that the Discovery Hill melt unit was emplaced as a melt pond, where melt pooled within a topographic low on a slump block within the collapsed crater rim region. In addition, cooling fractures around large m-sized (~6 x 8 m) quartz monzonite clasts within the melt unit and thin, chilled melt veinlets within the quartz monzonite pieces support melt cooling in place over ejecta blocks.

Overall, the contact relationships of melt units within the Mistastin Lake collapsed rim region with underlying units and distribution suggest that the melt originally flowed along channels or pooled forming melt ponds, subsequent to the deposition of ballistic ejecta. These units are interpreted to be analogous to impact melt ponds and channels that overlie the blocky continuous ejecta blankets as seen on the Moon (Hawke and Head, 1977; Howard and Wilshire, 1975; Osinski et al., 2011).

6.5.3 ‘Suevite’ formation mechanism(s)

The study of impact melt-bearing polymict lithic breccias, also termed ‘suevite’ is an area of active research. The first use of the term ‘suevite’ was to describe polymict impact breccias containing clasts of impact melt glass in a clastic matrix (Pohl et al., 1977) from the Ries impact structure in Germany, and some Ries studies have suggested a common formational mechanism for this type of rock as ‘fallout’ from an ejecta plume (Engelhardt, 1997) or as a ground surge after ballistic ejection (Newsom et al., 1990, 1986). The definition was modified to include the fact that the matrix can contain glass particles and that the matrix is better described as ‘particulate’ rather than ‘clastic’ (Stöffler and Grieve, 2007). The current literature record and the use of the term ‘suevite’

are inconsistent and somewhat confusing, therefore, the descriptive term melt-bearing polymict lithic impact breccias has been used instead throughout our study.

Melt-bearing polymict impact breccias have been reported within crater structures beneath (e.g., Manicougan impact structure: Dressler, 1990; Murtaugh, 1976) and above the impact melt sheet (e.g., Brent crater: Grieve, 1978; Sudbury impact structure: Grieve and Stöffler, 1991), within the modified rim region, and beyond the crater rim at different stratigraphic levels (Ries impact structure: Engelhardt, 1990). Many samples have only been accessed through drill holes and thus their spatial distribution with respect to the crater structure can be uncertain. In addition, it has been noted that melt-free lithic impact breccias and melt-bearing impact breccias can grade into each other (Ferrière et al., 2007; Grieve, 1978; Masaitis, 1999). Given the range of distribution within the impact crater structure it is difficult to believe that all melt-bearing polymict lithic impact breccias have the same genesis.

Field and petrographic observations of Mistastin Lake melt-bearing impact breccia units support three distinct formational mechanisms from a single impact event, based on contact relationships with adjacent impactites and melt-fragment morphology and concentration:

1. Impact melt-bearing polymict impact breccias within the inner zone formed at the interface where hot impact melt flowed over cooler, ballistically emplaced melt-poor to -free polymict impact breccias. This appears to be the most common mechanism at Mistastin (e.g., Figures 6-13 and 6-18).
2. The presence of dykes of impact melt-bearing polymict impact breccia suggests a mechanism whereby a hot lithic flow moved laterally along the ground and then intruded as a fracture fill into target rocks. Melt glass coatings on lithic clasts likely occurred as the clasts were rotated during transportation in the presence of melt. Some melt fragments have sharp boundaries in which the internal flow fabric has clearly been truncated, while others have more irregular boundaries, which suggest that the fragments were still viscous when deposited as part of the breccia unit (Figure 6-15).

3. Discrete lens of melt-bearing polymict impact breccia within the middle of an 80 m thick impact melt rock unit situated on an inner zone, suggests that this lens may have originated from the transient crater base and been incorporated into the melt rock that forms the pond during the emplacement process (i.e., this lens could essentially represent a rip-up clast incorporated during transport) (Figure 6-16).

Determination of the genesis of each unit was only possible through detailed field mapping of the contact relationships, and thus interpretation of 'suevite' formation mechanisms of other impact structures based solely on petrographical data is cautioned.

6.5.4 Hydrothermal alteration

A zone of high-temperature and high-permeability rocks is created near the surface, as a result of impact events. The temperature, pressure, and permeability of this zone in mid-sized craters can allow hot-water circulation for several thousand years or more (Naumov, 2005). Post-impact hydrothermal deposits can form throughout the impact structure (Osinski et al., 2005), including: (1) interior of central uplifts; (2) regions of intense and complex faulting within the outer margin of central uplifts; (3) at the base and edge of the modified transient crater - fill impact melt rocks and breccias; (4) in the faulted crater rim region in the form of pipe structures that may represent fossil hydrothermal springs and fumaroles; and (5) within post - impact sedimentary fill deposits. The dominant hydrothermal assemblage includes clay minerals, various zeolites, calcite, and pyrite, indicative of hydrothermal alteration at low temperatures (<300–350 °C). Post-impact zeolites can exhibit a well-defined spatial distribution, wherein Ca-zeolites are mainly found within monomict and polymict breccias and high-silica and alkali zeolites are found in impact melt rocks (Naumov, 2005).

Within the Mistastin Lake impact structure, secondary minerals attributed to hydrothermal alteration are present in all impactites (Table 6-3), and are of highest concentration in anorthosite monomict and polymict lithic breccias. The clay-rich groundmass of the impact breccias of the inner zone likely formed by the interaction of surficial aqueous fluids with shocked minerals and impact glass fragments within the

heated rocks. Platy Ca-zeolite minerals (Table 6-2 and Pickersgill et al., 2015) have replaced most feldspars (up to ~70 vol %) in South Creek polymict breccias and locally found within all impact breccias. This material is hydrous as indicated by total weight % values of ~70-90%, which may be attributed to post-impact hydrothermal fluids and/or from the crystalline basement rocks which could account for ~3% H₂O (Marion and Sylvester, 2010). The Mistastin zeolites display open-space filling textures (e.g., veins) and cross-cut the more homogenous clay groundmass, suggesting that they formed from the circulation of hydrothermal fluids along fractures in the already lithified breccias. These zeolites preferentially replace feldspar grains, and may specifically be the alteration product of maskelynite. Perhaps analagous to the Manicouagan impact structure, zeolites in the collapsed rim region may be associated with low temperature (< 270°C) hot springs driven by residual heat from peripheral melt (Spray et al., 2010).

The Mistastin impact structure offers a wealth of material, within a defined geological context of a crater structure, for future work focusing on characterizing impact-generated hydrothermal fluids in crystalline target rocks. Specifically, detailed studies of the chemical alteration of impactite materials, secondary minerals, and fluid inclusions hosted in hydrothermal mineral phases and in shock-generated deformation features, including stable isotope studies, would help constrain the composition, temperature, and sources of post-impact fluids.

6.6 Summary: A new emplacement model for Mistastin Lake impactites

The Mistastin Lake impact structure is an example of a complex crater that is well exposed in three dimensions and only moderately eroded. As such, it is an excellent location to examine impact crater structure and emplacement of impactites.

A multi-stage model for the origin and emplacement of impact melt rocks and the formation of impact ejecta is proposed for the Mistastin Lake impact structure based on a synthesis of the field and petrographic observations presented herein. This model, as described by Osinski et al. (2011), involves the generation of a continuous ejecta blanket during the excavation stage of cratering, via the conventional ballistic sedimentation and

radial flow model as originally proposed by Oberbeck (1975), followed by the emplacement of more melt-rich, ground-hugging flows during the terminal stages of crater excavation and the modification stage of crater formation. The discovery of impact breccias and impact melt ejecta deposits at Mistastin are particularly important. While they lie within the rim of the original crater, they lie outside the initial transient crater and are, therefore, by definition ejecta. Ejecta deposits are only preserved at one other Canadian impact crater – the Houghton impact structure, Devon Island (Osinski et al., 2005).

Ballistic ejecta from the Mistastin Lake impact structure was emplaced very soon after impact. For comparison, ballistic ejecta was emplaced within ~5 min, based on calculations for the Ries impact structure which is of similar size (Hörz, 1982). Overlying melt rocks observed within the inner zone, along Côté Creek, Piccadilly Creek, and Discovery Hill, were emplaced at a later time during the modification stage of crater formation. Thus, there was a substantial temporal hiatus and, therefore, a change in emplacement mechanism between the deposition of the polymict breccias and the impact melt rocks in the collapsed rim region of the Mistastin Lake impact structure.

The movement of melt throughout the modification process also facilitated the formation of melt-bearing, lithic impact breccias (i.e., suevite) at different stratigraphic levels. This study documents clear evidence of differing formational mechanisms from a single impact event.

6.7 References

- Ashley, J.W., Robinson, M.S., Hawke, B.R., Van Der Bogert, C.H., Hiesinger, H., Sato, H., Speyerer, E.J., Enns, a. C., Wagner, R. V., Young, K.E., Burns, K.N., 2012. Geology of the King crater region: New insights into impact melt dynamics on the Moon. *J. Geophys. Res. E Planets* 117, 1–13. doi:10.1029/2011JE003990
- Artemieva, N.A., Wünnemann, K., Krien, F., Reimold, W.U., Stöffler, D., 2013. Ries crater and suevite revisited—Observations and modeling Part II: Modeling. *Meteorit. Planet. Sci.* 48, 590–627. doi:10.1111/maps.12085

- Bringemeier, D., 1994. Petrofabric examination of the main suevite of the Otting Quarry, Nördlinger Ries, Germany. *Meteoritics* 417–422.
- Collins, G.S., Melosh, H.J., Morgan, J. V, Warner, M.R., 2002. Hydrocode Simulations of Chicxulub Crater Collapse and Peak-Ring Formation. *Icarus* 157, 24–33.
doi:10.1006/icar.2002.6822
- Currie, K.L., 1971a. Geology of the resurgent cryptoexplosion crater at Mistastin Lake, Labrador: Geological Survey of Canada, Bulletin 207. Dept. of Energy, Mines and Resources, Ottawa, Canada.
- Currie, K.L., 1971b. The composition of anomalous plagioclase glass and coexisting plagioclase from Mistastin Lake, Labrador, Canada. *Mineral. Mag.* 38, 511–517.
- Currie, K.L., 1972. Geology and petrology of the Manicouagan resurgent caldera, Quebec, *Geol. Surv. Can. Bull.*
- Dressler, B., 1990. Shock metamorphic features and their zoning and orientation in the Precambrian rocks of the Manicouagan Structure, Quebec, Canada. *Tectonophysics* 171, 229–245. doi:http://dx.doi.org/10.1016/0040-1951(90)90101-D
- Dressler, B.O., Reimold, W.U., 2001. Terrestrial impact melt rocks and glasses. *Earth-Science Rev.* 56, 205–284. doi:10.1016/S0012-8252(01)00064-2
- Dumont, R., Jones, A., 2012. Aeromagnetic Survey Mistastin Batholith, NTS 13M/14, Quebec and Newfoundland and Labrador, Geological Survey of Canada, Open File 7159, scale 1:50 000.
- Emslie, R.F., Cousens, B., Hamblin, C., Bielecki, J., 1980. The Mistastin Batholith, Labrador-quebec : An Elsonian Composite Rapakivi Suite. doi:10.4095/124073
- Engelhardt, von W., 1990. Distribution, petrography and shock metamorphism of the ejecta of the Ries crater in Germany—a review. *Tectonophysics* 171, 259–273.
doi:http://dx.doi.org/10.1016/0040-1951(90)90104-G

- Engelhardt, von W., 1997. Suevite breccia of the Ries impact crater, Germany: Petrography, chemistry and shock metamorphism of crystalline rock clasts. *Meteorit. Planet. Sci.* 32, 545–554. doi:10.1111/j.1945-5100.1997.tb01299.x
- Engelhardt, W. V., Graup, G., 1984. Suevite of the Ries crater, Germany: Source rocks and implications for cratering mechanics. *Geol. Rundschau* 73, 447–481.
- Ferrière, L., Koeberl, C., Reimold, W.U., 2007. Drill core LB-08A, Bosumtwi impact structure, Ghana: Petrographic and shock metamorphic studies of material from the central uplift. *Meteorit. Planet. Sci.* 42, 611–633. doi:10.1111/j.1945-5100.2007.tb01064.x
- French, B.M., 1998. *Traces of Catastrophe: A handbook of shock-metamorphic effects in terrestrial meteorite impact structures*, LPI Contribution No. 954. Lunar and Planetary Institute, Houston.
- French, B.M., Koeberl, C., 2010. The convincing identification of terrestrial meteorite impact structures: What works, what doesn't, and why. *Earth-Science Rev.* 98, 123–170.
- Grieve, R.A.F., 1975. Petrology and chemistry of the impact melt at Mistastin Lake crater, Labrador. *Geol. Soc. Am. Bull.* 86, 1617–1629.
- Grieve, R.A.F., 1978. The melt rocks at Brent crater, Ontario, Canada, in: *Lunar Planetary Conference IXX*. pp. 2579–2608.
- Grieve, R.A.F., 2006. Mistastin, in: *Impact Structures in Canada*. Geological Association of Canada, pp. 115–120.
- Grieve, R.A.F., Cintala, M.J., 1992. An analysis of differential impact melt-crater scaling and implications for the terrestrial impact record. *Meteoritics* 27, 526–538.
- Grieve, R.A.F., Stöffler, D., 1991. The Sudbury structure: controversial or misunderstood? *J. Geophys. Res.* 96, 22753–22764.

Grieve, R.A.F., Therriault, A.M., 2013. Impactites: their characteristics and spatial distribution, in: Osinski, G.R., Pierazzo, E. (Eds.), *Impact Cratering: Processes and Products*. Wiley-Blackwell, Hoboken, NJ, pp. 90–105.

Gurov, E.P., Koeberl, C., Yamnichenko, A., 2007. El'gygytgyn impact crater, Russia: Structure, tectonics, and morphology. *Meteorit. Planet. Sci.* 42, 307–319.
doi:10.1111/j.1945-5100.2007.tb00235.x

Hawke, B.R., Head, J.W., 1977. Impact melt on lunar crater rims, in: Roddy, D.J., Pepin, R.O., Merrill, R.B. (Eds.), *Impact and Explosion Cratering*. Pergamon Press, New York, pp. 815–841.

Hervé, G., Gilder, S.A., Marion, C.L., Osinski, G.R., Pohl, J., Petersen, N., Sylvester, P.J., 2015. Paleomagnetic and rock magnetic study of the Mistastin Lake impact structure (Labrador, Canada): Implications for geomagnetic perturbation and shock effects. *Earth Planet. Sci. Lett.* 417, 151–163. doi:10.1016/j.epsl.2015.02.011

Hörz, F., 1982. Ejecta of the Ries Crater, Germany, in: Silver, L.T., Schultz, P.H. (Eds.), *Geological Implications of Impacts of Larger Asteroids and Comets on the Earth*. Geological Society of America, Boulder, pp. 39–55.

Hörz, F., Ostertag, R., Rainey, D.A., 1983. Bunte Breccia of the Ries - Continuous deposits of large impact craters. *Rev. Geophys. Sp. Phys.* 21, 1667–1725.

Howard, K.A., Wilshire, H.G., 1975. Flows of impact melt at lunar craters. *J. Res. U.S. Geol. Surv.* 237–251.

Klassen, R.A., Thompson, F.J., 1990. Open File 2170: Glacial history, drift composition, and till geochemistry, Labrador.

Mader, M.M., Osinski, G.R., Tornabene, L.L., 2013. Structural geology of the Mistastin Lake Impact Structure, Labrador, Canada, in: *44th Lunar and Planetary Science Conference*.

- Mak, E.K., York, D., Grieve, R.A.F., Dence, M.R., 1976. The age of the Mistastin Lake crater, Labrador, Canada. *Earth Planet. Sci. Lett.* 31, 345–357.
- Marchand, M., Crocket, J.H., 1977. Sr isotopes and trace element geochemistry of the impact melt and target rocks at the Mistastin Lake crater, Labrador. *Geochim. Cosmochim. Acta* 41, 1487–1495.
- Marion, C.L., 2009. Geology, distribution and geochemistry of impact melt at the Mistastin Lake impact crater, Labrador. ProQuest, UMI Dissertations Publishing.
- Marion, C.L., Sylvester, P.J., 2010. Composition and heterogeneity of anorthositic impact melt at Mistastin Lake crater, Labrador. *Planet. Space Sci.* 58, 552–573.
doi:10.1016/j.pss.2009.09.018
- Marion, C.L., Sylvester, P.J., Leitch, A.M., Forthcoming. Vesicularity and distribution of impact melt at Mistastin Lake crater, Labrador, Canada. *Meteorit. Planet. Sci.*
- Masaitis, V.L., 1999. Impact structures of northeastern Eurasia: The territories of Russia and adjacent countries. *Meteorit. Planet. Sci.* 34, 691–711. doi:10.1111/j.1945-5100.1999.tb01381.x
- McCormick, K.A., Taylor, G.J., Keil, K., Spudis, P.D., Grieve, R.A.F., Ryder, G., 1989. Sources of clasts in terrestrial impact melts: Clues to the origin of LKFM, in: *Proceedings of the 19th Lunar and Planetary Science Conference*. Lunar and Planetary Institute, pp. 691–696.
- Melosh, H.J., 1989. *Impact cratering: A geologic process*. Oxford University Press, New York.
- Murtaugh, J.G., 1976. Manicouagan impact structure. Pen-File Report DPV-432.
- Naumov, M.V., 2002. Impact- generated hydrothermal systems: data from Popigai, Kara, and Puchezh - Katunki impact structures, in: Plado, J., Pesonen, L.J. (Eds.), *Impacts in Precambrian Shields*. Springer - Verlag, Berlin, pp. 71–117.

- Naumov, M. V, 2005. Principal features of impact-generated hydrothermal circulation systems: mineralogical and geochemical evidence. *Geofluids* 5, 165–184. doi:10.1111/j.1468-8123.2005.00092.x
- Neish, C.D., Madden, J., Carter, L.M., Hawke, B.R., Giguere, T., Bray, V.J., Osinski, G.R., Cahill, J.T.S., 2014. Global distribution of lunar impact melt flows. *Icarus* 239, 105–117.
- Newsom, H.E., Graup, G., Iseri, D.A., Geissman, J.W., Keil, K., 1990. The formation of the Ries Crater, West Germany; Evidence of atmospheric interactions during a larger cratering event. *Geol. Soc. Am. Spec. Pap.* 247, 195–206. doi:10.1130/SPE247-p195
- Newsom, H.E., Graup, G., Sowards, T., Keil, K., 1986. Fluidization and hydrothermal alteration of the suevite deposit in the Ries Crater, West Germany, and implications for Mars. *cal Res. B Solid Earth Planets* 91, 239 – 251.
- Oberbeck, V.R., 1975. The role of ballistic erosion and sedimentation in lunar stratigraphy. *Rev. Geophys. Sp. Phys.* 13, 337–362.
- Öhman, T., Kring, D. a., 2012. Photogeologic analysis of impact melt-rich lithologies in Kepler crater that could be sampled by future missions. *J. Geophys. Res. E Planets* 117, 1–21. doi:10.1029/2011JE003918
- Osinski, G.R., 2004. Impact melt rocks from the Ries structure, Germany: an origin as impact melt flows? *Earth Planet. Sci. Lett.* 226, 529–543. doi:10.1016/j.epsl.2004.08.012
- Osinski, G.R., Grieve, R.A.F., Collins, G.S., Marion, C., Sylvester, P., 2008. The effect of target lithology on the products of impact melting. *Meteorit. Planet. Sci.* 43, 1939–1954.
- Osinski, G.R., Grieve, R.A.F., Spray, J.G., 2004. The nature of the groundmass of surficial suevite from the Ries impact structure, Germany, and constraints on its origin. *Meteorit. Planet. Sci.* 39, 1655–1683. doi:10.1111/j.1945-5100.2004.tb00065.x

Osinski, G.R., Spray, J.G., Lee, P., 2005. Impactites of the Haughton impact structure, Devon Island, Canadian High Arctic. *Meteorit. Planet. Sci.* 40, 1789–1812.

Osinski, G.R., Tornabene, L.L., Grieve, R.A.F., 2011. Impact ejecta emplacement on terrestrial planets. *Earth Planet. Sci. Lett.* 310, 167–181. doi:10.1016/j.epsl.2011.08.012

Phinney, W.C., Simonds, C.H., 1977. Dynamical implications of the petrology and distribution of impact melt rocks, in: Roddy, D.J., Pepin, R.O., Merrill, R.B. (Eds.), *Impact and Explosion Cratering*. Pergamon Press, New York, pp. 771–790.

Pickersgill, A.E., Osinski, G.R., Flemming, R.L., 2015. Shock effects in plagioclase feldspar from the Mistastin Lake impact structure, Canada. *Meteorit. Planet. Sci.* 50, 1546–1561. doi:10.1111/maps.12495

Pickersgill, A.E., Osinski, G.R., Mader, M.M., 2012. A formational model for an impact melt-bearing breccia dyke at the Mistastin Lake impact structure, Labrador, Canada, in: 43rd Lunar and Planetary Science Conference, Abstract 2473. Woodlands, TX.

Pohl, J., Stöffler, D., Gall, H., Ernstson, K., 1977. The Ries impact crater, in: Roddy, D.J., Pepin, R.O., Merrill, R.B. (Eds.), *Impact and Explosion Cratering*. Pergamon Press, New York, pp. 343–404.

Singleton, A.C., Osinski, G.R., Grieve, R.A.F., Shaver, C., 2011. Characterization of impact melt-bearing impactite dykes from the central uplift of the Mistastin Lake impact structure, Labrador. Abstract 2250, in: 42nd Lunar and Planetary Science Conference. The Woodlands, Texas.

Singleton, A.C., Osinski, G.R., Grieve, R.A.F., Shaver, C., 2012. Characterization of glasses in impact breccia dykes at the Mistastin Lake impact structure, Labrador, in: 43rd Lunar and Planetary Science Conference. The Woodlands, Texas.

Singleton, A.C., Ward, M.J., Woll, A.R., Osinski, G.R., 2014. Characterization of impact glass clasts from the Mistastin impact structure using synchrotron radiation spectroscopy. Abstract 5404, in: 77th Annual Meteoritical Society Meeting. Casablanca, Morocco, p. 5404.

- Spray, J.G., Thompson, L.M., Biren, M.B., O'Connell-Cooper, C., 2010. The Manicouagan impact structure as a terrestrial analogue site for lunar and martian planetary science. *Planet. Space Sci.* 58, 538–551. doi:10.1016/j.pss.2009.09.010
- Stöffler, D., Artemieva, N.A., Pierazzo, E., 2002. Modeling the Ries-Steinheim impact event and the formation of the moldavite strewn field. *Meteorit. Planet. Sci.* 37, 1893–1907. doi:10.1111/j.1945-5100.2002.tb01171.x
- Stöffler, D., Grieve, R.A.F., 2007. 11. Impactites. Recommendations by the IUGS Subcommission on the Systematics of Metamorphic Rocks, in: Fettes, E., Desmons, J. (Eds.), *Metamorphic Rocks : A Classification and Glossary of Terms : Recommendations of the International Union of Geological Sciences Subcommission on the Systematics of Metamorphic Rocks*. Cambridge University Press, pp. 82–92.
- Taylor, F.C., Dence, M.R., 1969. A probable meteorite origin for Mistastin Lake, Labrador. *Can. J. Earth Sci.* 6, 39–45.
- Young, K.E., Mercer, C.M., Soest, M.C. Van, Hodges, K. V, Wartho, J.-A., Biren, M.B., 2014. An examination of noble gas geochronology and thermochronology in the context of dating impact events, in: 45th Lunar and Planetary Science Conference, Abstract #2670. Woodlands, TX, pp. 4–5. doi:10.1002/jgre.20118.

Chapter 7

7 Discussion of the suitability of the Mistastin Lake impact structure as a lunar analogue site

On the Moon – one of the highest priority targets for the Canadian and international space communities – impact cratering is considered the most important geological process (Hiesinger and Head, 2006; National Research Council, 2007). This is manifest in the immense number of impact craters on the lunar surface, from the small to the large, with the South–Pole Aitken (SPA) basin at ~2500 km in diameter being one of the largest impact craters in the solar system.

Unlike Earth, the Moon preserves a rock record dating back to the first few hundred million years of solar system formation. It holds the answers to major questions, such as whether a Late Heavy Bombardment (LHB) affected the terrestrial planets, which has implications for understanding the habitability of the early Earth. In this respect, key sites of scientific and exploration interest for early return missions to the Moon lie in the South Pole-Aitken basin region that is dominated by anorthositic rocks and impact craters.

Although impact craters are the dominant geological landform on the Moon, relationships between specific lunar craters and their impactites (i.e., rocks affected by an impact event) are typically poorly constrained. In order to maximize scientific return from future lunar missions, it is useful to study terrestrial impact craters to better understand impact processes and products – this could help determine best locations for lunar sample collection to address specific science objectives. Lunar studies will require the investigation of regolith and bedrock and thus methods that help locate surface and subsurface lithological units and ways to sample these components will be critical. In particular, impactites, including melt rocks and breccias, are key components to test the lunar cataclysm hypothesis. In addition, testing geological technologies and operational strategies at impact structures on Earth will allow refinement of system designs and mission concepts, helping us prepare for lunar exploration.

7.1 Choosing the Mistastin Lake impact structure as a lunar analogue site

The site selection process for planetary exploration missions is a long and detailed process. As a case study, the selection of the landing sites for the Mars Exploration Rovers (MER) involved broad participation of the science community via four open workshops, and narrowed an initial list of potential sites to four finalists based on a series of science and engineering requirements (Golombek et al., 2003). The engineering constraints included (1) latitude for maximum solar power; (2) elevation; (3) low horizontal winds, shear, and turbulence in the last few km; (4) low 10-m-scale slopes to reduce airbag spin-up and bounce, (5) moderate rock abundance to reduce abrasion or strokeout of the airbags, and (6) a radar-reflective, load-bearing, and trafficable surface safe for landing and roving that is not dominated by fine-grained dust (Golombek et al., 2003). Many of these requirements relate to evaluating hazards associated with landing. In terms of science, the requirement is that the landing site must be capable of addressing the science objectives of the mission, which in the case of MER was “to determine the aqueous, climatic, and geologic history of sites on Mars, where conditions may have been favorable to the preservation of evidence of possible prebiotic or biotic processes” (Golombek et al., 2003).

Science objectives for the ILSR lunar analogue missions were based on results from the Sixth Canadian Space Exploration Workshop (CSEW6) hosted by the Canadian Space Agency (CSEW6 Steering Committee, 2009), and included: understanding impact chronology, shock processes, impact ejecta and potential mineral resources, at a lunar analogue site (Marion et al., 2012). At the time of site selection, for this lunar analogue work, 177 confirmed impact sites were known on Earth (Earth Impact Database, 2009 <http://www.passc.net/EarthImpactDatabase>) – they formed the initial list of potential sites for the ILSR analogue missions. Based on the MER site selection process – which holds for all other recent missions, such as Mars Science Laboratory (MSL) – the site selection process can be split into 4 main stages, all of which are applicable for the ILSR analogue missions:

1. Global site survey – This stage involves compiling a list of all potential landing sites that broadly fit the engineering and science requirements (e.g., during the MER site selection process, 185 potential sites were identified based on accessible terrain or engineering constraints and then an invitation was made to the science community to identify additional sites; Golombek et al., 2003).
2. Down selection– This list of sites is then discussed and prioritized according to the engineering and science requirements. Several sites are then chosen for further study and discussion.
3. Regional site selection – Eventually, one (or two in the case of the twin MER missions) landing site is selected. This site will be the highest priority science site as well as meeting the engineering requirements.
4. Local targeting – Within this broad region, further study is required to choose the specific landing site.

For lunar analogue missions, the requirements are obviously slightly different. For example, on the Moon, latitude is important for power constraints - this requirement is not applicable for an analogue mission. However, the fidelity of an analogue activity is critical (Snook and Mendell, 2004). Fidelity aims to relate various factors in an analogue activity, from the geological terrain (i.e., is the geology of the site a close geological analogue for the planetary body in question), and the environment (temperature, limited vegetation coverage, degree of isolation), to the logistics and corresponding mission operations infrastructure.

In order to achieve a high-fidelity analogue mission that met the ILSR science objectives to further the understanding of impact chronology, shock processes, impact ejecta and potential resources, at a lunar analogue site, five requirements that would take into account the science fidelity, logistics, and terrain requirements from a technology perspective for the impact site were defined. In order of decreasing importance, these requirements and their rationales were:

1. Exposure – The impact site and its lithologies should not be buried (by soil or sediments), heavily vegetated, or submerged by water. If a crater is buried, completely vegetated, or submerged, then it is not possible to conduct any surface operations.
2. Accessibility – The impact site should not be in a country with an official Department of Foreign Affairs Travel Warning, or in a country where logistics are either very difficult and/or expensive and/or hazardous; this includes sites with severe permitting restrictions. If a crater is not accessible, then it is not sensible or safe to consider it for an analogue mission.
3. Preservation and availability of science targets – The impact site should be relatively well preserved, such that impact melt rocks and other important impact materials and features of scientific value are observable in the field. Some or all of the following impact features are required: (a) impact melt-bearing breccias or impact melt rocks; (b) shocked rocks and minerals; (c) impact ejecta; (d) resources (ground ice and/or ore minerals). If virtually all the impact materials have been eroded then there is little scientific value in visiting a site and the analogue mission will not achieve its science goals.
4. Terrain – There are several attributes by which a site may be judged in terms of applicability to planetary rover guidance, navigation, and control testing (a) lack of vegetation; (b) size; (c) topography; (d) rock distribution; (e) lighting. If the terrain is such that the mission objectives cannot be met then this disqualifies a site as a potential candidate.
5. Lunar-like geology – The geology of the Moon on a regional scale is relatively simple, being dominated by two main crystalline rock types: the feldspathic highlands and the basaltic maria. In order to be a good geological analogue for the Moon, the site should contain crystalline rock types common on the Moon. Sedimentary rocks are not present on the Moon, therefore, craters developed entirely in such rocks are considered low fidelity for this particular requirement. However, sites with a mixed crystalline–sedimentary target are useful in order to

estimate the depth of origin of impact ejecta using the stratigraphy of the sedimentary layers.

Through the above selection process, four sites met requirements 1–3. These were (in alphabetical order): Manicouagan (Quebec), Mistastin Lake (Labrador), Ries (Germany), Sudbury (Ontario). Only the Mistastin Lake impact structure met all 5 requirements and was identified as being the highest priority science lunar analogue site (see Table 7-1).

Overall, the Mistastin Lake impact structure, northern Labrador, Canada (55°53'N; 63°18'W), offers a unique opportunity to study preserved impactites of similar lunar mineralogy and outcrop characteristics, and to understand the origin and emplacement of lunar impact ejecta. It is comparable to many of the moderate-sized complex impact craters on the Moon (150–200 km in diameter) when scaled for gravity differences. Grieve (1974) was the first to compare Mistastin Lake impact melt rocks with Apollo samples of melt rocks from anorthositic lunar highlands, and suggested that they formed in similar manners (i.e., from melting of the target rock due to impact). The preservation of an almost complete suite of impact lithologies at Mistastin Lake, including ejecta deposits, facilitates the construction of a near intact section through an intermediate, complex crater. Anorthosite is a major target rock type at Mistastin and is present throughout the crater in various stratigraphic settings.

Table 7-1: Requirements for selection of the Mistastin impact structure, Labrador as a lunar analogue site.

Site Selection Requirements			Data Requirements		Data Source
Requirement	Mistastin Qualities	Data type	Keydata properties	<i>In situ</i> / aerial/ satellite	Relationship to lunar mission data
(1) Lunar-like Geology	The 3 main target rocks are crystalline; the principal type is anorthosite, similar to the lunar highlands. Rock texture and consolidation is variable.				
(2) Preservation	Mistastin Lake impact structure is young (~36 Myr old) and possesses multiple preserved crater-fill units including breccias and impact melt rocks. Mistastin Lake impact structure, represents an intermediate-size, complex crater. There have not been any significant metamorphism or deformation events since the impact event ~36 Ma (Chapter 6).	Known from previously published literature and confirmed by <i>in situ</i> field studies. Impactites have been identified by, e.g., (Grieve, 1975; Marion et al., Forthcoming).	<i>In situ</i> mapping: on a metre scale.	<i>In situ</i> , aerial photographs.	Impact melt rocks visible in existing Clementine data and in Lunar Reconnaissance Orbiter imagery.
(a) Presence of impact melt-bearing breccias or melt rocks	Presence of impact melt bearing rocks previously documented (Grieve, 1975; Marion et al., Forthcoming).	Known from previous <i>in situ</i> field studies.	<i>In situ</i> mapping: cm to m scale Lidar scanner: up to mm resolution.	Data previously collected by field geologist.	Future rover/lander-mounted microscope or spectrometer; future lunar manned mission.
(b) Presence of shocked rocks and minerals	Shocked minerals have been identified at Mistastin up to 35 GPa given the presence of diaplectic glass (Grieve, 1975)	Petrographic microscope work and spectrometry. Not currently known to be detectable from orbit.	Level of shock metamorphism, presence of shock features.	Data to be collected <i>in situ</i> and in laboratory on returned samples.	Future rover/lander-mounted microscope or spectrometer.
(c) Presence of impact ejecta	Impact ejecta identified during a reconnaissance visit in 2009.	N/A	N/A		Impact ejecta easily discernable in existing Clementine data.

(d) Presence of ground ice	The extent of ground ice in the Mistastin area is not extensively known but permafrost is assumed to be discontinuous.	Canadian Permafrost maps.	Depth of ground ice and level of continuity.	N/A	Lunar Prospector and Clementine showed possible ice on the lunar south pole. Confirmed by the recent LCROSS impact.
(3) Exposure of science targets:	<p>The site is well exposed as it lies in a dominantly tundra environment. A central portion is under a lake, but the central uplift is exposed.</p> <p>Original crater has been differentially eroded by glacial and fluvial processes (Grieve and Cintala, 1992; Marion et al., Forthcoming; Phinney and Simonds, 1977), however, a subdued rim and distinct central uplift are still observed (Grieve, 1975).</p> <p>Inner portion of the Mistastin Lake impact structure is covered by the Mistastin Lake and the surrounding area is locally covered by soil/glacial deposits and vegetation.</p> <p>Two islands, Horseshoe and Bullseye Islands, roughly within the centre of the lake, represent the remains of a central uplift structure.</p> <p>Topography directly surrounding the lake is slightly elevated in blocky steps extending up to 5 km away from the shoreline.</p>	Known by <i>in situ</i> field work, evident from air photos and satellite imagery.	Air photos: scale 1:4000 and 1:7000; Landsat and Radarsat 2 data from 15–120 m and 8–100 m resolution, respectively.	<i>In situ</i> , aerial and satellite.	Not a factor on the Moon where all targets will be exposed.
(4) Terrain					
(a) Terrain: Lack of vegetation	Higher altitudes have very little vegetation including the rim region and central uplift. The lake edge has variable vegetation.	Previous field studies, topo maps, air photos and Landsat images show the areas which lack vegetation.	Topographic map scales are 1:50,000 Landsat Resolution of 15 – 120 m Air photos: scale 1:4000 and 1:7000.	Aerial and satellite images.	Not a factor on the Moon where there is no vegetation.

(b) Terrain: Size	Mistastin Lake impact structure is estimated to be ~26 km in diameter (Chapter 5). There are 200-500m ² rover-friendly areas.	Topographic maps and Landsat images show the extent of the crater.	Topo maps at 1:50,000 scale Landsat is from 15 – 120 m resolution.	Satellite.	LROC imagery and Clementine imagery clearly show sizable craters in the Moon.
(c) Terrain: Topography	There is much topographic variability at Mistastin: from large plateaus to river deltas to steep cliffs to rolling hills.	Previous <i>in situ</i> fieldwork and topographic maps (radar)	Topographic maps 1:50,000 scale	Aerial/ Satellite	Topography of the Moon was obtained using laser altimetry and stereo image analysis most recently by Clementine.
(d) Terrain: Rock distribution	The 3 main target rocks are crystalline; the principal type is anorthosite, similar to the lunar highlands. Rock texture and consolidation is variable.	<i>In situ</i> field studies.	N/A	<i>In situ</i>	SPA Basin consists dominantly of anorthosite materials with varying particle sizes and distribution (e.g., fine regolith to impact breccias to impact melt).
(e) Terrain: Lighting	Mistastin Lake is has approximately 15 hours of daylight a day during the summer.	N/A	N/A	N/A	Studies can be conducted in either dark or light as can be said for different areas of SPA Basin.
(5) Accessible	<p>The site has been previously visited and is known to be accessible.</p> <p><i>Twin Otter access.</i> 3 landing strips exist around the crater.</p> <p><i>Accommodations:</i> There is no infrastructure at the field site. All supplies needed for a remote field camp, including tents, cooking supplies, food, etc. are brought to the site.</p> <p><i>Power</i> at the Mistastin field site will be supplied using generators and solar panels.</p>	Previous fieldwork	N/A	N/A	N/A

7.2 Application of the Mistastin Lake lunar analogue site to lunar exploration

7.2.1 Comparative planetology

Observations of the lunar surface provide a topographic understanding of impact crater structures, which has facilitated the formation of crater classification schemes (e.g., Schultz, 1976). Currently, terrestrial impact craters provide the only means with which to ground truth such observations, particularly with respect to the third dimension (i.e., subsurface characteristics and contacts between units, which are not evident in lunar images or sampling). One of the principal characteristics of lunar complex impact craters is the formation of terraced rims and emplacement of ejecta deposits within this zone. Recent high resolution images of complex lunar craters (e.g., NASA Lunar Reconnaissance Orbiter, JAXA Kaguya orbiter) have started to reveal the complexity of impactite diversity within terraced rims and potential modes of emplacement (e.g., King crater: Ashley et al., 2012; Kepler crater: Öhman and Kring, 2012). Images of Tycho crater (Figure 7-1) on the Moon reveal melt ponds within the terraced rim region, similar to the interpretation of the Discovery Hill impact melt unit in the Mistastin Lake impact structure.

The Mistastin Lake impact structure provides a terrestrial comparison to study impact melt deposits within the collapsed rim region of a complex crater. For example, Ashley et al. (2012) suggested that melt making up the Al-Tusi impact melt pond just beyond the lunar King crater rim arrived in different stages based on viscid forms and flow features observed within Lunar Reconnaissance Orbiter Narrow Angle Camera (NAC) images. They interpreted the late stage melt to be more viscous. Evidence from the Discovery Hill impact melt deposit, interpreted as an impact melt pond (Chapter 6), suggests that this melt moved more slowly than elsewhere in the crater, as the contact with underlying impact breccia is sharp. By combining both lunar and terrestrial observations, a deeper understanding of impactite emplacement and impact processes is possible.

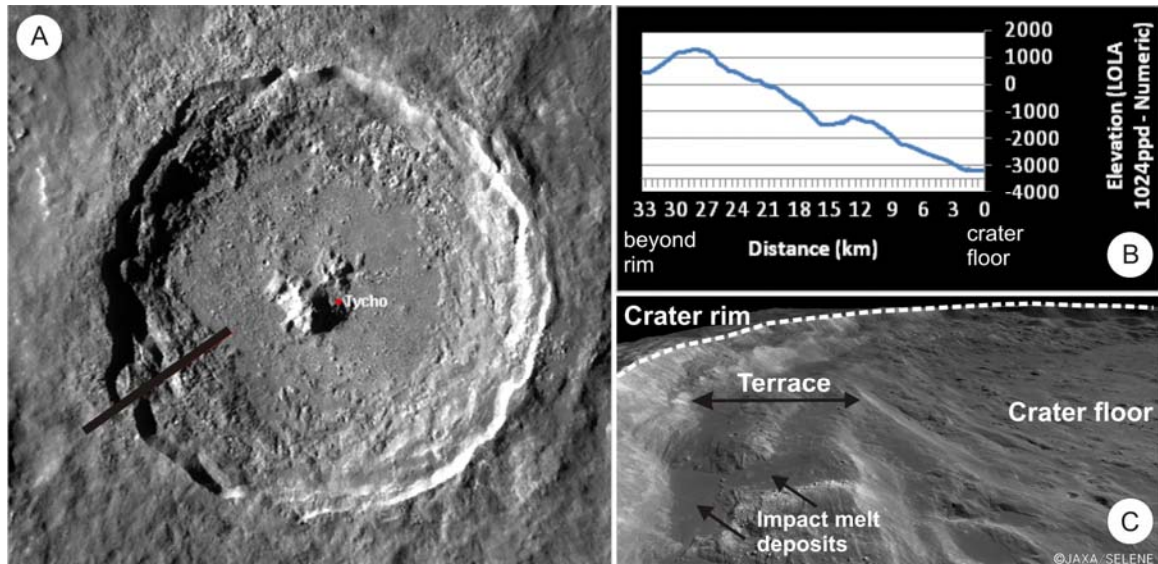


Figure 7-1: (A) Tycho crater, 86 km in diameter, 43.31°S 11.36°W. Image credit: Lunar Reconnaissance Orbiter, NASA. Black line indicates location of profile line used in B. (B) Profile showing stepped topography of Tycho crater rim region. (C) Melt ponds on terraced rim of Tycho Crater imaged by KAGUYA's Terrain Camera, JAXA.

7.2.2 Lunar sample selection

New lunar samples are a high priority for the international scientific community. In order to help determine optimal sampling locations and maximize scientific return for future lunar missions, it is useful to study terrestrial impact craters to better understand impact processes and products. Lunar studies will require the investigation of regolith and bedrock. Impactites, including melt rocks and breccias, will be key components to help answer fundamental questions of planetary evolution (e.g., lunar cataclysm hypothesis).

Future lunar missions will aim to directly determine the age of key impact craters (e.g., South Pole Aiken Basin) in order to elucidate the cratering history of the Moon and by extension the inner solar system. Samples will likely need to be returned to Earth to take advantage of sophisticated laboratory instrumentation and techniques for geochronological studies. Choosing appropriate samples for such work will be a critical

element of future mission design. Impact-melt lithologies will likely be the first choice in any dating effort (Stöffler, 2006), as they will provide crystallization ages of impact melting events.

Studying the Mistastin Lake impact structure as a lunar analogue can help unravel this history as it can be considered an end member; impact products were derived from a single impact event versus lunar impact products that have likely experienced multiple events. The daunting task of dating lunar rocks becomes increasingly obvious when studying the diversity and complexity of impact products produced from a single impact event.

Geochronological and exploration strategies can be vetted at a site such as Mistastin, before being applied to the more complex task of unraveling lunar sample histories. Executional tasks, such as geostatistical sampling and grid-style geophysical surveys, were shown to be well suited for autonomous or teleoperated robotic operations (Chapter 2). Adaptive-exploratory approaches, such as reconnaissance and contact mapping, require an understanding of regional geological context and are best carried out by teleoperation of a rover with input from a Mission Control science team, or preferably, by a geologist astronaut with ‘boots on the ground’ that can make decisions more quickly and cover more ground than can a rover in the same amount of time.

In addition, analytical techniques, including *in situ* instruments (e.g., portable XRF, Raman) can be tested on appropriate lunar analogue samples and their precision and accuracy can then be compared to laboratory based counterparts. All of this work could help establish scientific requirements for where and what samples to collect in order to address lunar science questions. Ultimately this feedback could carry forward into systems engineering design processes, such that hardware designed will be adequate to meet the task without being over designed. For example, if a rover or astronaut can collect impact melt rock from proximal impact ejecta without having to go to the bottom of a crater this could result in a simpler, less expensive, and potentially less risky mission design.

7.3 Future work

7.3.1 Analogue mission evaluation

Analogue missions that integrate scientific, technological, and operational activities are still in their infancy, with missions across the globe all happening within the past 5-15 years. In regards to evaluation design, when metrics and anecdotal feedback methods are employed, their development process and data analysis are not described in the literature. This makes it difficult to test the validity and reliability of these methods. For example, without this transparency (e.g., who collected data, when was data collected, who analysed data and how was it analysed) it is uncertain if the data collection process itself is affecting the quality of data collected.

I suggest future analogue studies partner with Social Scientists to develop a Mixed Methods evaluation approach; specifically an Exploratory Sequential Design that will be used to optimize ‘instruments’ (i.e., measurement tools; Creswell, 2003). Evaluation measures used in previous analogue missions (e.g., DRATS, PLRP, etc.) should be reviewed and classified using a program logic model framework. The outputs (typically metrics collected) should be linked to intended and achieved outcomes, and their effectiveness should be assessed.

Building off of these results, the findings could be used to develop measures that could be administered to a larger sample (i.e., other analogue missions). These measures could materialize as an open-ended survey instrument that combines components of both quantitative and qualitative methodologies, i.e., mixed-methods surveys (Creswell, 2003). For example, in regards to understanding and evaluating how enabling technologies and different exploration strategies affect practices for geological field work on the lunar surface, the developed instrument could measure geologists’ outcomes against criterion-referenced learning outcomes, such as ability to conduct scientific measurements and observations, formulate interpretations, and to present findings based on gathered evidence and newly constructed knowledge.

It could take into account, how various elements affect the evaluation of geological knowledge gained, for example: scientific fidelity of analogue site, expertise of the

geologist-astronaut, constraints of conducting planetary field work (dependence on technology for survival and to conduct geological field work), and effectiveness of enabling technology for conducting geological field work on planetary surface. I recommend using guiding principles for survey design (e.g., Siragusa and Dixon, 2006) to create rigorous and trustworthy surveys.

7.3.2 Mistastin Lake impact structure

The Mistastin Lake impact structure is one of the best preserved complex impact structures on Earth and offers a wealth of impactite material that are correlated to parts of a defined impact structure. It is a tremendous resource for understanding hypervelocity impact cratering processes and formation of impact products. This project provides a basis from which future studies could build upon. Specifically, future work could include:

- Characterization of impact-generated hydrothermal fluids that affected the Mistastin Lake target rocks. Specifically, detailed studies of the chemical alteration of impactite materials, secondary minerals, and fluid inclusions hosted in hydrothermal mineral phases and in shock-generated deformation features, including stable isotope studies, would help constrain the composition, temperature, and sources of post-impact fluids in crystalline target rocks.
- Compare and contrast textural and chemical analyses of impact melt clasts from melt-bearing, polymict impact breccia units. Field evidence shows that there were at least three different formation processes for this type of impactite (Chapter 6) – are there specific textural or chemical features that reflect this and could be used in other impact craters in which the formation mechanism is not clear from field relationships?
- Detailed geophysical and drilling surveys beneath Mistastin lake. These studies would help determine the underlying stratigraphy within the disrupted transient cavity and would help assess the original volume of impact melt generated by the impact event.

7.4 References

- Ashley, J.W., Robinson, M.S., Hawke, B.R., Van Der Bogert, C.H., Hiesinger, H., Sato, H., Speyerer, E.J., Enns, a. C., Wagner, R. V., Young, K.E., Burns, K.N., 2012. Geology of the King crater region: New insights into impact melt dynamics on the Moon. *J. Geophys. Res. E Planets* 117, 1–13. doi:10.1029/2011JE003990
- Carlson, A.E., LeGrande, A.N., Oppo, D.W., Came, R.E., Schmidt, G. a., Anslow, F.S., Licciardi, J.M., Obbink, E. a., 2008. Rapid early Holocene deglaciation of the Laurentide ice sheet. *Nat. Geosci.* 1, 620–624. doi:10.1038/ngeo285
- Creswell, J.W., 2003. *Research Design: Qualitative, Quantitative, and Mixed Method Approaches*, 2nd ed. SAGE Publications, Thousand Oaks, California.
- CSEW6 Steering Committee, 2009. Canadian Scientific Priorities for the Global Exploration Strategy, in: 6th Canadian Space Exploration Workshop Dec 1–3 2008. St. Hubert, Qc.
- Golombek, M.P., Grant, J.A., Parker, T.J., Kass, D.M., Crisp, J.A., Squyres, S.W., Haldemann, A.F.C., Adler, M., Lee, W.J., Bridges, N.T., Arvidson, R.E., Carr, M.H., Kirk, R.L., Knocke, P.C., Roncoli, R.B., Weitz, C.M., Schofield, J.T., Zurek, R.W., Christensen, P.R., Fergason, R.L., Anderson, F.S., Rice, J.W., 2003. Selection of the Mars Exploration Rover landing sites. *J. Geophys. Res. Planets* 108, n/a–n/a. doi:10.1029/2003JE002074
- Grieve, R.A.F., 1974. Lunar impact melts and terrestrial analogs: Their characteristics, formation and implications for lunar crustal evolution, in: Gose, W.A. (Ed.), *Proceedings of the Fifth Lunar Science Conference*, Vol. 1. Pergamon Press, New York, pp. 261–274.
- Grieve, R.A.F., 1975. Petrology and chemistry of the impact melt at Mistastin Lake crater, Labrador. *Geol. Soc. Am. Bull.* 86, 1617–1629.

Grieve, R.A.F., Cintala, M.J., 1992. An analysis of differential impact melt-crater scaling and implications for the terrestrial impact record. *Meteoritics* 27, 526–538.

Klassen, R.A., Thompson, F.J., 1990. Open File 2170: Glacial history, drift composition, and till geochemistry, Labrador.

Marion, C.L., Osinski, G.R., Abou-Aly, S., Antonenko, I., Barfoot, T., Barry, N., Bassi, A., Battler, M., Beauchamp, M., Bondy, M., Blain, S., Capitan, R.D., Cloutis, E.A., Cupelli, L., Chanou, A., Clayton, J., Daly, M., Dong, H., Ferrière, L., Flemming, R., Flynn, L., Francis, R., Furgale, P., Gammel, J., Garbino, A., Ghafoor, N., Grieve, R.A.F., Hodges, K., Hussein, M., Jasiobedzki, P., Jolliff, B.L., Kerrigan, M.C., Lambert, A., Leung, K., Mader, M., McCullough, E., McManus, C., Moores, J., Ng, H.K., Otto, C., Ozaruk, A., Pickersgill, A. E. Pontefract, A., Preston, L.J., Redman, D., Sapers, H., Shankar, B., Shaver, C., Singleton, A., Souders, K., Stenning, B., Stooke, P., Sylvester, P., Tripp, J., Tornabene, L.L., Unrau, T., Veillette, D., Young, K., Zanetti, M., 2012. A Series of robotic and human analogue missions in support of lunar sample return, abstract #2333, in: 43rd Lunar and Planetary Science Conference. The Woodlands, Texas.

Marion, C.L., Sylvester, P.J., Leitch, A.M., Forthcoming. Vesicularity and distribution of impact melt at Mistastin Lake crater, Labrador, Canada. *Meteorit. Planet. Sci.*

Öhman, T., Kring, D. a., 2012. Photogeologic analysis of impact melt-rich lithologies in Kepler crater that could be sampled by future missions. *J. Geophys. Res. E Planets* 117, 1–21. doi:10.1029/2011JE003918

Phinney, W.C., Simonds, C.H., 1977. Dynamical implications of the petrology and distribution of impact melt rocks, in: Roddy, D.J., Pepin, R.O., Merrill, R.B. (Eds.), *Impact and Explosion Cratering*. Pergamon Press, New York, pp. 771–790.

Schultz, P.H., 1976. Floor-fractured lunar craters. *Moon* 15, 241–273.

Siragusa, L., Dixon, K.C., 2006. A research methodology : the development of survey instruments for research into online learning in higher education . *Issues Educ. Res.*

Snook, K.J., Mendell, W.W., 2004. The need for analogue missions in scientific human and robotic planetary missions, in: XXXV Lunar and Planetary Science Conference, Abstract #2130. League City, Texas.

Stöffler, D., 2006. Cratering History and Lunar Chronology. *Rev. Mineral. Geochemistry* 60, 519–596. doi:10.2138/rmg.2006.60.05

Appendix A: Evaluation Plan for ILSR analogue program

An evaluation plan was developed for the ILSR analogue program using a program logic model, which links traverse planning and execution, geological data collection and interpretation, and data management with necessary qualitative observations to be made (Table 4-2). A template was made for documentarians and team leads within the Mission Control team and notes were recorded for all team meetings. These written documents were used as data to inform rigorous lessons learned that could be supported from multiple perspectives.

Instructions to team members filling out reports:

The key to capturing lessons learned regarding traverse planning and execution, geological data collection and interpretation, and data management is to document CONTEXT, which can be multi-faceted. Key points to keep in mind are:

- Written notes are our primary data. Please veer on the side of writing too much rather than too little. Also, you don't need to be concerned with grammar or spelling mistakes. Content is the key.
- Written feedback/comments are critical to provide context and understanding of any quantitative data collected.

Flight Director Daily Report Form

Role:

Name:

Date:

Week and Day of Analogue Mission:

Traverse Name:

Note: Report can be in bullet point form if preferred.

Results

- Summarize results of Tactical process for each day.

Description of Process

- Record and describe any difficulties with Tactical process.
- Record what factors helped Tactical process (e.g., number of team members involved, etc.).
- Suggestions for Improvements (Lessons Learned)

Additional Comments:

GIS Lead Daily Report Form

Name:

Date:

Week and Day of Analogue Mission:

Traverse Name:

Note: Report can be in bullet point form if preferred.

Timelines

- Record time to assimilate data from each traverse.

Results

- Summarize results of GIS process for each day.
- How were different data sets integrated? What role(s) facilitated this?

Description of Process/Lessons Learned

- Record and describe any difficulties with GIS/integration process.
- Record what factors helped/hindered process
- Suggestions for Improvements (Lessons Learned)

Planning Manager Daily Report Form

Role:

Name:

Date:

Week and Day of Analogue Mission:

Traverse Name:

Note: Report can be in bullet point form if preferred.

Results

- Summarize results of Planning process for each day.

Description of Process

- Record and describe any difficulties with Planning process.
- Record what factors helped Planning process (e.g., number of team members involved, etc.).
- Suggestions for Improvements (Lessons Learned)

Additional Comments:

Science Interpretation Lead Daily Report Form

Role:

Name:

Date:

Week and Day of Analogue Mission:

Traverse Name:

Note: Report can be in bullet point form if preferred.

Timelines

- Record timeline to interpret data (as a team) from each traverse.

Results

- Summarize results of interpretation process for each day.

Description of Process

- Record and describe any difficulties with interpretation process.
- Record what factors helped interpretation process (e.g., number of team members involved, etc.). What hindered process?
- Suggestions for Improvements(Lessons Learned)

Science Manager Daily Report Form

Role:

Name:

Date:

Week and Day of Analogue Mission:

Traverse Name:

Note: Report can be in bullet point form if preferred.

Results

- Summarize results of Planning process for each day.

Description of Process

- Record and describe any difficulties with Science process.
- Record what factors helped Science process (e.g., number of team members involved, etc.).
- Suggestions for Improvements (Lessons Learned)

Additional Comments:

Mission Control Science Documentarian

Pre EVA

- Update Mission Control binder and WIKI with any updated Traverse Plans

During EVA

- Essentially recording daily timeline and procedures of Tactical Process in Mission Control.
- Listen to astronaut and CAPCOM dialogue.
- Record notes on laptop.

***Header for each day's report** (can write in notebook at start of day):*

- Date: e.g., Aug. 29, Week 1, Day 1
- Traverse Name:
- Documentarian Name:

***Record throughout day** (In order of priority):*

- *Documentarian* make note of the decision-making process of astronaut and Mission Control Science Team during site selection and detailed outcrop mapping. How much input is provided by each team? Does this change depending on Objectives of traverse? (Note: Documentarian must be familiar with Science Objectives of the mission, see Mission Binder or WIKI).
- Essentially recording the Science Interpretation and Decision Making Process
 - Records Time
 - Meeting Name/Topic of Discussion,
 - Who participated,
 - Main points of Discussion,
 - Decisions Made/Action items,
 - How decision made (consensus, etc.)

Mission Control Tactical Documentarian

Header for each day's Report(can write in notebook at start of day):

- Date: e.g., Aug. 29, Week 1, Day 1
- Traverse Name:
- Tactical Documentarian Name:

During EVA

- Mark locations of Astronauts on GIS map
- Records daily timeline and procedures of Tactical Process in Mission Control.
- Listen to astronaut and CAPCOM dialogue.
- Record notes on laptop.

Record throughout day(In order of priority):

- *Documentarian* record time and duration of each communication between the astronauts and CAPCOM and reason for exchange (e.g., clarification of voice description, request for data, scientific discussion regarding working hypothesis, weather update, etc).
- Essentially recording Tactical Decision Making Process
 - Decisions Made/Action items,
 - How decision made (Flight Director, etc.)

List of Daily Meetings

Leadership council

The ‘Council’ meets to discuss the day before the full team arrives. This may include a link-up with the field team. As during FD2.

Opening briefing

Review the mission status and the day’s plan. Need only be about 15 minutes with the full group

Astronaut link-up

Discuss the EVA plan, its science goals, and mission status with the astronauts.

EVA Debrief and Strategic discussion

As the astronauts finish their EVA and undertake stand-down activities, the Mission Control team is free to reflect on the results of the EVA and the mission status, and to consider the implications for the next day.

Astronaut linkup and science discussion

Mission Control connects with the astronauts again, to follow up on their status, see how they felt the EVA went, and bookend the EVA. This is followed by the main science discussion, where the astronauts describe what they’ve seen, and discuss it with the Science team. It’s a chance to survey the observations and thoughts of the astronauts, and to compare these with the hypotheses of the Science team, as well as for the astronauts to ask any questions with regards to things they’ve seen.

Following the science discussion with the astronauts, Mission Control presents the next day’s traverse plan to the astronauts – it’s an overview only, with the detailed plan to be

uploaded in text form afterward for the astronauts to review in the evening. This is the time, however, for the astronauts to get their initial buy-in to the plan.

Closing Briefing and Strategic discussion

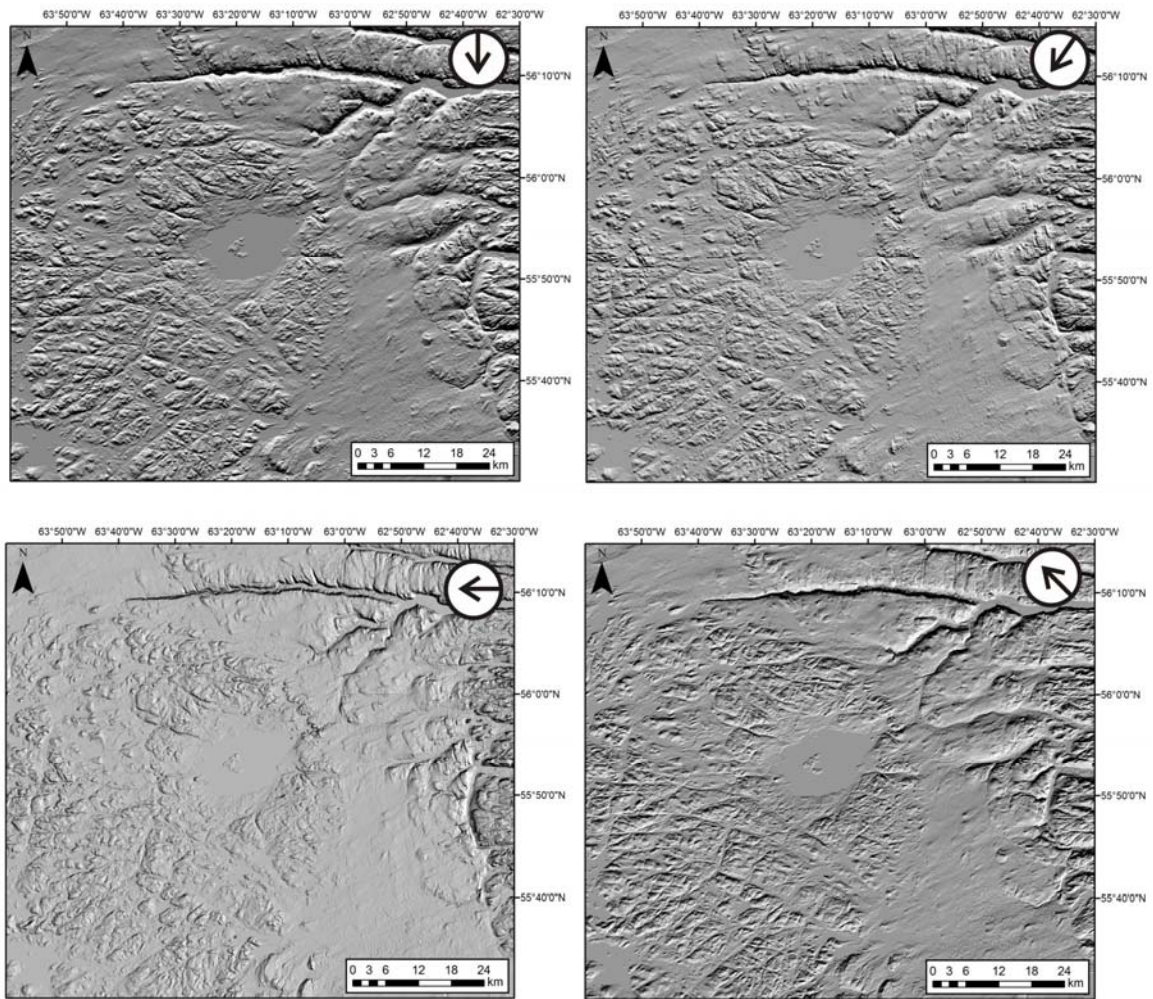
A brief closing briefing in Mission Control reviews the day's activities and the outlook for the next day. Mission Control makes any necessary changes to the plan stemming from the discussion with the astronauts, uploads it in the appropriate form for the astronauts to review overnight and use during the EVA, and dismisses.

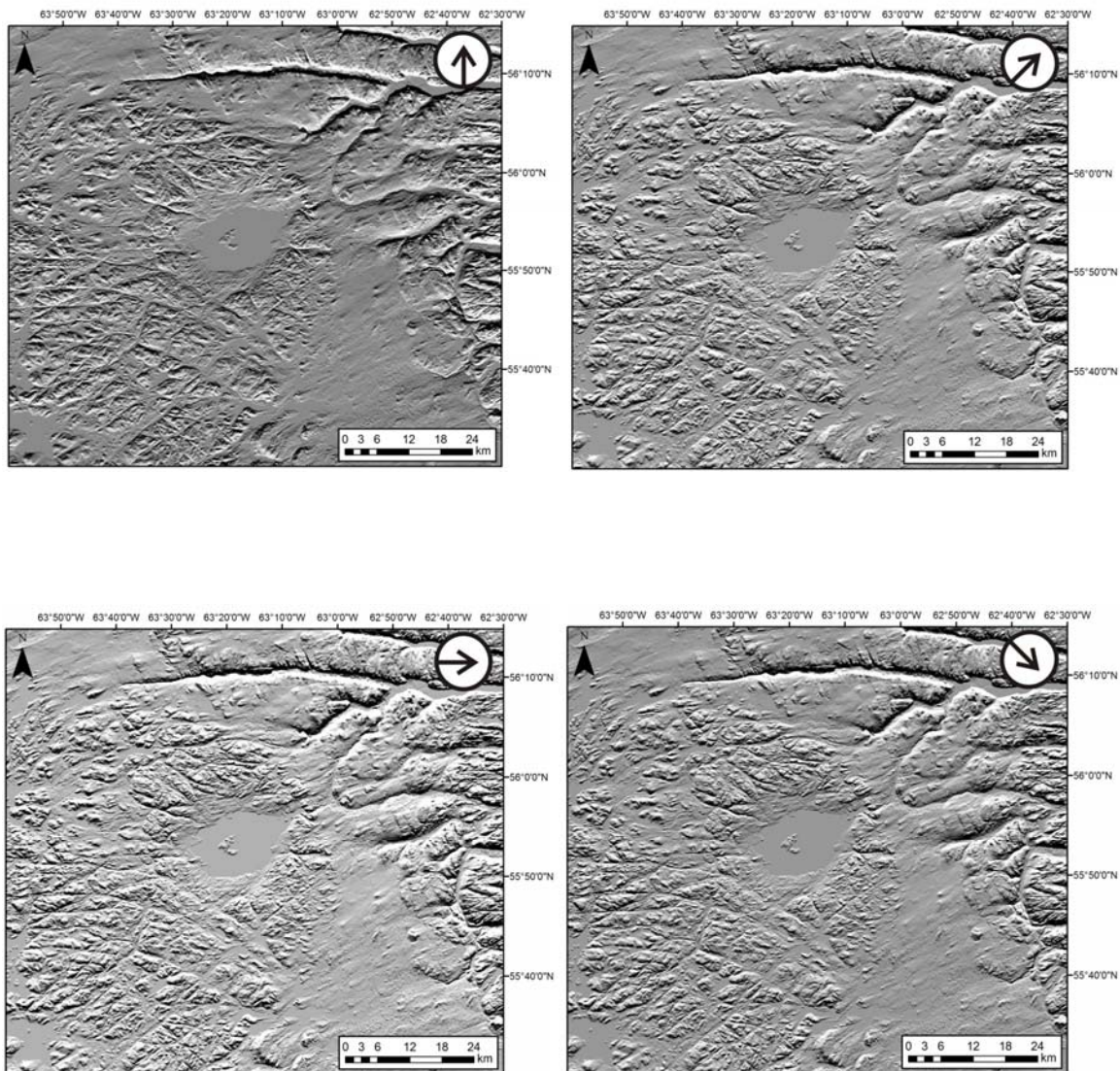
Leadership council

The leadership 'Council' meets once more at the end of the day.

Appendix B: Sun shaded relief images

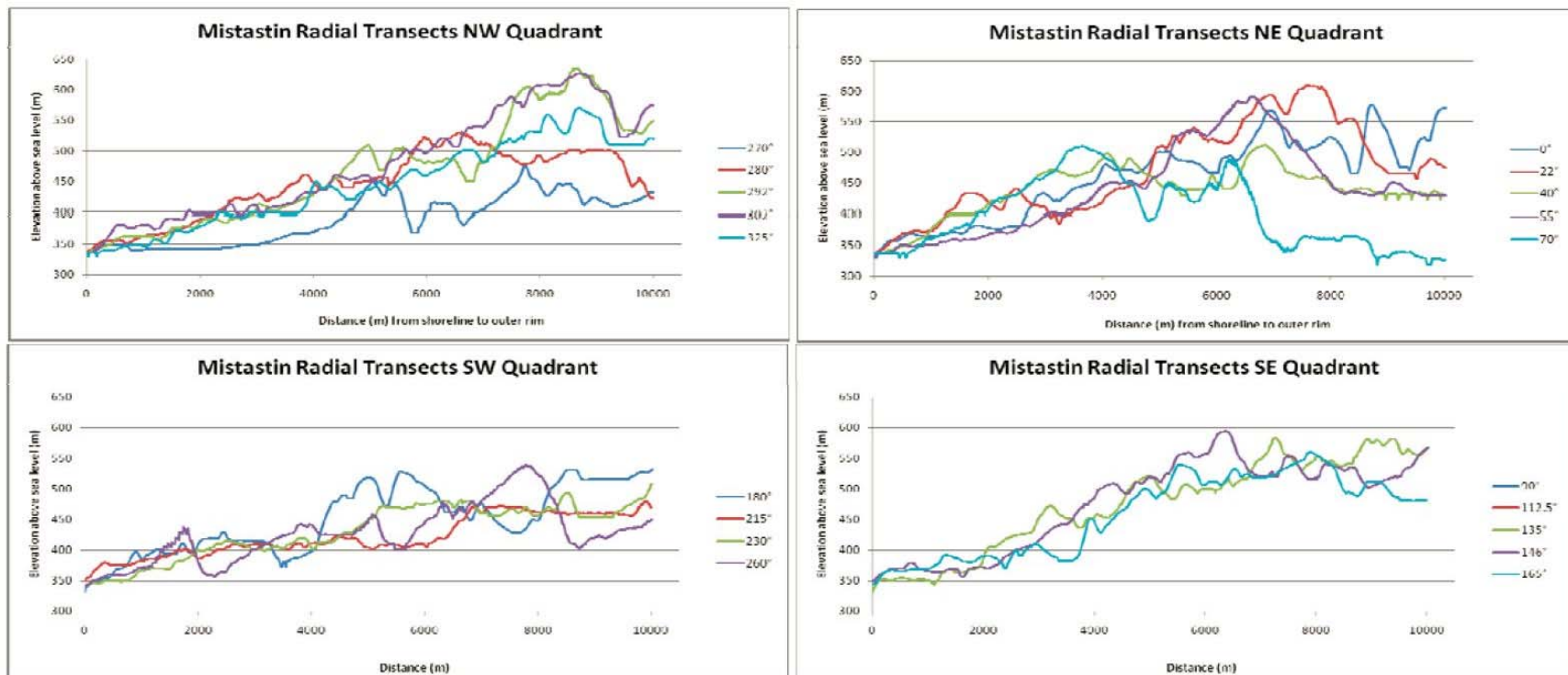
Shaded relief images from different sun angles generated using the ENVI software program. Eight different shaded relief images were generated with a sun angle of 30° above the horizon, each from a different azimuth direction at 45° intervals. White circles with arrows denote azimuth of sun.





Appendix C: Radial profiles

Twenty radial profiles across the impact structure were created in ENVI using the mosaic DEM as the reference image. The profile lines were spaced 22.5° apart, starting from the lakeshore across the highest topographical high and further outward to the distance of ~ 42 km from the impact structure centre. A distance of up to 10 km, that includes the inner and outer zones of the Mistastin Lake impact structure, is shown in radial profiles below.



Appendix D: List of samples collected from Mistastin Lake impact structure

Locality Number	Rock Type Melt = impact melt rock; PB = polymict breccia; MB = monomict breccia; AN = anorthosite; GRDT = granodiorite; QM = quartz monzonite	Field Site (Location within crater structure)	Location (UTM Zone 20)	
			Easting	Northing
MM11-009a	PB	Coté Creek (Inner Zone)	475622	6196766
MM11-009b	PB	Coté Creek (Inner Zone)	475622	6196766
MM11-009c	AN (block in PB)	Coté Creek (Inner Zone)	475622	6196766
MM11-010a	PB	Coté Creek (Inner Zone)	475464	6197101
MM11-010b	AN (block in PB)	Coté Creek (Inner Zone)	475464	6197101
MM11-0011a	PB	Coté Creek (Inner Zone)	475459	6197083
MM11-0011b	AN (block in PB)	Coté Creek (Inner Zone)	475459	6197083
MM11-0012a	AN (block in PB)	Coté Creek (Inner Zone)	475428	6197000
MM11-0012b	PB	Coté Creek (Inner Zone)	475428	6197000
MM11-0012c	PB (Pink Vein)	Coté Creek (Inner Zone)	475428	6197000
MM11-0020	MELT	Coté Creek (Inner Zone)	475332	6197385
MM11-0021a	Melt (clast rich)	Coté Creek (Inner Zone)	475332	6197385
MM11-0021b	GRDT (clast)	Coté Creek (Inner Zone)	475332	6197385
MM11-0022a	Melt	Coté Creek (Inner Zone)	475464	6197101
MM11-0022b	GRDT (clast)	Coté Creek (Inner Zone)	475464	6197101
MM11-0022c	PB	Coté Creek (Inner Zone)	475464	6197101
MM10-003a	PB (melt bearing)	Coté Creek (Inner Zone)	475332	6197385
MM10-003b	Melt (clast rich)	Coté Creek (Inner Zone)	475332	6197385
MM10-004	Melt (clast rich)	Coté Creek (Inner Zone)	475332	6197385
MM10-005a	PB (melt bearing)	Coté Creek (Inner Zone)	475332	6197385

Locality Number	Rock Type Melt = impact melt rock; PB = polymict breccia; MB = monomict breccia; AN = anorthosite; GRDT = granodiorite; QM = quartz monzonite	Field Site (Location within crater structure)	Location (UTM Zone 20)	
			Easting	Northing
MM10-005b	PB (melt bearing)	Coté Creek (Inner Zone)	475332	6197385
MM10-005c	Melt (clast rich)	Coté Creek (Inner Zone)	475332	6197385
MM10-005d	Melt	Coté Creek (Inner Zone)	475332	6197385
MM10-006	Melt	Coté Creek (Inner Zone)	475332	6197385
MM10-006a	PB (melt bearing)	Coté Creek (Inner Zone)	475332	6197385
MM10-006b, c, d	Melt (ropey texture)	Coté Creek (Inner Zone)	475332	6197385
MM10-007	PB (melt bearing)	Coté Creek (Inner Zone)	475320	6197324
MM10-007a	Melt (clast rich)	Coté Creek (Inner Zone)	475320	6197324
MM10-008	PB (melt bearing)	Coté Creek (Inner Zone)	475332	6197385
MM10-009a	PB (melt bearing)	Coté Creek (Inner Zone)	475332	6197385
MM10-009b	Melt (clast rich)	Coté Creek (Inner Zone)	475332	6197385
MM10-010	Melt (clast rich)	Coté Creek (Inner Zone)	475332	6197385
MM10-011	MB (anorthosite)	Coté Creek (Inner Zone)	475464	6197101
MM10-012	PB	Coté Creek (Inner Zone)	475464	6197101
MM10-013	An (clast in PB)	Coté Creek (Inner Zone)	475464	6197101
MM10-014	Melt (clast rich)	Coté Creek (Inner Zone)	475464	6197101
MM10-015	Melt (clast poor)	Coté Creek (Inner Zone)	475464	6197101
MM10-016	An (clast in PB)	Coté Creek (Inner Zone)	475450	6197112
MM10-017	MB (quartz monzonite)	Coté Creek (Inner Zone)	474955	6197571
MM10-017a	QM (clast in breccia)	Coté Creek (Inner Zone)	474955	6197571
MM10-017b	MB (quartz monzonite)	Coté Creek (Inner Zone)	474955	6197571
MM10-034a	AN (clast in PB)	Coté Creek (Inner Zone)	490098	6199261

Locality Number	Rock Type Melt = impact melt rock; PB = polymict breccia; MB = monomict breccia; AN = anorthosite; GRDT = granodiorite; QM = quartz monzonite	Field Site (Location within crater structure)	Location (UTM Zone 20)	
			Easting	Northing
MM10-034b	PB matrix	Coté Creek (Inner Zone)	490098	6199261
MM10-034c	PB	Coté Creek (Inner Zone)	490098	6199261
MM10-035	MB (anorthosite)	Coté Creek (Inner Zone)	475354	6197103
MM09-035a	AN	Coté Creek (Inner Zone)	475446	6197111
MM09-035b	Melt	Coté Creek (Inner Zone)	475446	6197111
MM09-035c	Melt	Coté Creek (Inner Zone)	475446	6197111
MM09-035d	AN	Coté Creek (Inner Zone)	475459	6197107
MM09-035e	AN	Coté Creek (Inner Zone)	475465	6197098
MM09-036	PB	Coté Creek (Inner Zone)	475319	6197377
MM09-005		Coté Creek (Inner Zone)	475436	6197106
MM09-006	PB (melt bearing)	Coté Creek (Inner Zone)	475311	6197342
MM10-018	GRDT/QM	Piccadilly Creek (Inner Zone)	475741	6197979
MM10-019	AN (block in PB)	Piccadilly Creek (Inner Zone)	475624	6198198
MM10-020	PB (melt bearing)	Piccadilly Creek (Inner Zone)	475624	6198198
MM10-021	Melt	Piccadilly Creek (Inner Zone)	475641	6198195
MM10-022	Melt	Piccadilly Creek (Inner Zone)	475641	6198195
MM10-023	PB (melt bearing)	Piccadilly Creek (Inner Zone)	475641	6198195
MM10-024	PB (melt bearing)	Piccadilly Creek (Inner Zone)	475641	6198195
MM10-025	AN (clast in MB)	Piccadilly Creek (Inner Zone)	475641	6198195
MM10-026	Suevite. Melt in contact with suevite	Piccadilly Creek (Inner Zone)	475641	6198195
MM10-027a	PB (melt bearing)	Piccadilly Creek (Inner Zone)	475641	6198195

Locality Number	Rock Type Melt = impact melt rock; PB = polymict breccia; MB = monomict breccia; AN = anorthosite; GRDT = granodiorite; QM = quartz monzonite	Field Site (Location within crater structure)	Location (UTM Zone 20)	
			Easting	Northing
MM10-028	An (block in PB)	Piccadilly Creek (Inner Zone)	475641	6198195
MM10-029a	MB (anorthosite)	Piccadilly Creek (Inner Zone)	475641	6198195
MM10-029b	PB	Piccadilly Creek (Inner Zone)	475641	6198195
MM10-030	MB (anorthosite)	Piccadilly Creek (Inner Zone)	475641	6198195
MM10-031	MB (quartz monzonite)	Piccadilly Creek (Inner Zone)	475362	6198406
MM10-032	Melt/MB (quartz monzonite) contact	Piccadilly Creek (Inner Zone)	475362	6198406
MM09-43	Melt/PB (melt bearing) contact	Piccadilly Creek (Inner Zone)	475624	6198198
MM11-0013	Melt	Discovery Hill (Inner Zone)	473488	6190565
MM11-0014a	Melt	Discovery Hill (Inner Zone)	473359	6190812
MM11-0014b	GRDT (block)	Discovery Hill (Inner Zone)	473359	6190812
MM11-0015a	Melt	Discovery Hill (Inner Zone)	472999	6190387
MM11-0015b	PB	Discovery Hill (Inner Zone)	472999	6190387
MM11-0015c	GRDT	Discovery Hill (Inner Zone)	472999	6190387
MM11-0016	GRDT	Discovery Hill (Inner Zone)	472759	6190372
MM10-001A	PB (melt bearing)	Discovery Hill (Inner Zone)	472834	6190592
MM10-001B	PB (melt bearing)	Discovery Hill (Inner Zone)	472834	6190592
MM10-001C	PB (melt bearing)	Discovery Hill (Inner Zone)	472834	6190592
MM10-001D	Melt/PB (melting bearing) contact	Discovery Hill (Inner Zone)	472834	6190592
MM10-001E	PB (melt bearing)	Discovery Hill (Inner Zone)	472834	6190592
MM10-037	PB	South Creek (Inner Zone)	485756	6188461

Locality Number	Rock Type Melt = impact melt rock; PB = polymict breccia; MB = monomict breccia; AN = anorthosite; GRDT = granodiorite; QM = quartz monzonite	Field Site (Location within crater structure)	Location (UTM Zone 20)	
			Easting	Northing
MM10-038	MB (anorthosite)	South Creek (Inner Zone)	485768	6188417
MM10-039	An clast	South Creek (Inner Zone)	485760	6188448
MM10-040	MB (anorthosite)	South Creek (Inner Zone)	485786	6188429
MM10-041	PB	South Creek (Inner Zone)	485786	6188429
MM10-042	Red veining in contact btw Polymict breccia and Monomict An	South Creek (Inner Zone)	485786	6188429
MM10-043	MB (anorthosite)	South Creek (Inner Zone)	485786	6188429
MM10-044	MB (anorthosite - Pink staining)	South Creek (Inner Zone)	485805	6188395
MM10-045	PB	South Creek (Inner Zone)	485805	6188395
MM10-046	PB	South Creek (Inner Zone)	485781	6188464
MM11-004a	An	South Shore (Inner Zone)	483980	6188118
MM11-004b	An	South Shore (Inner Zone)	483980	6188118
MM11-005	An	South Shore (Inner Zone)	483899	6188140
MM11-006	MB (Anorthosite)	South Shore (Inner Zone)	483807	6188156
MM11-007a	Melt	South Shore (Inner Zone)	483534	6188186
MM11-007b	MB (Anorthosite)	South Shore (Inner Zone)	483534	6188186
MM11-007c	MB (Anorthosite)	South Shore (Inner Zone)	483534	6188186
MM11-008	AN	South Shore (Inner Zone)	483779	6188193
MM10-002	Melt	South Shore (Inner Zone)	475332	6197385
MM10-036	PB (melt bearing)	Steep Creek (Inner Zone)	482151	6200562
MM09-031	MB (quartz monzonite)	Steep Creek (Inner Zone)	482151	6200562

Locality Number	Rock Type Melt = impact melt rock; PB = polymict breccia; MB = monomict breccia; AN = anorthosite; GRDT = granodiorite; QM = quartz monzonite	Field Site (Location within crater structure)	Location (UTM Zone 20)	
			Easting	Northing
MM09-033	PB (melt bearing)	Steep Creek (Inner Zone)	482151	6200562
MM11-0017a	GRDT	SW shoreline (Inner Zone)	473229	6191718
MM11-0017b	PB	SW shoreline (Inner Zone)	473229	6191718
MM11-0018	QM	SW shoreline (Inner Zone)	473307	6191764
MM11-0019	QM	SW shoreline (Inner Zone)	473998	6191177
MM10-032a	GRDT ?	Mistastin River (Highest ring of hills)	490359	6198140
MM10-032b	QM?	Mistastin River (Highest ring of hills)	490359	6198140
MM10-033	GRDT	Mistastin River (Highest ring of hills)	492469	6199019
MM10-047	QM	Mistastin River (Highest ring of hills)	493976	6200649
MM10-048	QM or GRDT	Mistastin River (Highest ring of hills)	494116	6200682

Curriculum Vitae

Name:	Marianne Mader
Post-secondary Education and Degrees:	<p>University of New Brunswick Fredericton, New Brunswick, Canada 1995-2000 B.Sc.</p> <p>Memorial University St. John's, Newfoundland, Canada 2001-2005 M.Sc.</p> <p>International Space University Strasbourg, France 2006-2007 M.Sc.</p> <p>University of Western Ontario London, Ontario, Canada 2009-present PhD</p>
Honours and Awards:	<p>PhD Fellowship, NSERC CREATE "Technologies and Techniques for Earth and Space Exploration" 2012-2014</p> <p>US Antarctic Service Medal 2013</p> <p>AGU Fall Meeting Student Travel Grant Award 2011</p> <p>Lunar Planetary Institute Early Career Development Award 2011</p> <p>Northern Scientific Training Program (NSTP) Award 2010</p> <p>Western Graduate Incentive Scholarship 2009</p> <p>Western Graduate Scholarship (Science) 2009</p> <p>NSERC Postgraduate Scholarship (PGS-D) 2009-2010</p>

European Space Agency, ISU Scholarship
2006-2007

Selected for Department of Foreign Affairs and International Trade
(DFAIT) Canada international placement, Bangkok, Thailand
2005-2006

Dr. Alfred K. Snelgrove Graduate Scholarship in Earth Sciences,
Memorial University
2002-2003

NSERC Postgraduate Scholarship (PGS-M)
2002-2003

Memorial University Postgraduate Research Grant
2001-2002

Geological Assoc. of Canada/ Mineralogical Assoc. of Canada
Scholarship
1999-2000

Canadian Mineral Industry Education Foundation Undergraduate
Scholarship
1998-2000

Selected Participant: Student Industry Field Trip, Canadian Society
of Petroleum Geologists, Canada
1999

N. Myles Brown Undergraduate Scholarship
1997-1998

Related Work Experience

Managing Director, Centres for Earth & Space/Fossils & Evolution
Royal Ontario Museum
2015-present

Co-Founder and Board Member
STEAMLabs non-profit organization
2011-present

Teaching Assistant – Outreach and Education
Centre for Planetary Science & Exploration
University of Western Ontario
2009-2013

	Research Affiliate, Space Science Canadian Space Agency St. Hubert, Qc 2008-2009
Leadership roles in planetary analogue activities:	Science Team Member, Meteorite Hunter, Antarctic Search for Meteorites, Case Western Reserve University Antarctica 2012-2013
	Mission Program Evaluator and Mission Control Logistics Coordinator, UWO Human Follow-On Analogue Mission, Mistastin Lake Impact structure, Labrador 2011
	Mission Program Evaluator, UWO Robotic Sample Return Analogue Mission, Sudbury Impact structure, ON 2011
	Backroom Science Team Member, Mars Analogue Research: Signatures of Life in Freshwater Environments, Pavilion Lake Research Project, Kelly Lake, BC 2011
	Field Scientist, MDA Mars Sample Return Technical Deployment, SP Crater, Arizona 2010
	Field Operations Team Lead, UWO Robotic Precursor Lunar Analogue Mission, Mistastin Lake Impact Structure, Labrador 2010
	Consultant for Mars Analog Path (MAP) Team Project, International Space University, Strasbourg, France 2010
	Researcher and Field Support, Canadian Space Agency Planetary Analogue Research, Axel Heiberg Island, Nunavut 2008
	Field Support, Canadian Space Agency Planetary Analogue Research, Haughton-Mars Project, Devon Island 2007

Publications:

Refereed papers:

Moores J., Francis R., Mader M. M., Osinski G. R., Barfoot T., Barry, N., Basic G., Battler M., Beauchamp, M., Blain, S., Bondy, M., Capitan R. D, Chanou A., Clayton J., Cloutis E., Daly M., Dickinson, C., Dong H., Flemming R., Furgale P., Gammel J., Gharfoor N., Hussein, M., Grieve R., Henrys H., Jaziobedski P., Lambert A., Leung K., Marion, C., McCullough, E., McManus C., Neish C. D, Ng H. H., Ozaruk, A., Pickersgill, A., Preston L. J, Redman D., Sapers, H., Shankar B., Singleton A., Souders K., Stenning B., Stooke P., Sylvester P., Tornabene L. (in press). A Mission Control Architecture for Lunar Sample Return as Field Tested in an Analogue Deployment to the Sudbury Impact Structure. *Journal of Advances in Space Research*, Special Issue: Lunar Exploration.

Antonenko, I., Osinski, G.R., Battler, M., Beauchamp, M., Cupelli, L., Chanou, A., Francis, R., Mader, M.M., Marion, C., McCullough, E., Pickersgill, A.E., Preston, L.J., Shankar, B., Unrau, T., Veillette, D. (2013) Issues of Geologically-Focused Situational Awareness in Robotic Planetary Missions: Lessons from an Analogue Mission at Mistastin Lake Impact Structure, Labrador, Canada. *Journal of Advances in Space Research*, Special Issue: Lunar Exploration.

Non-refereed papers/reports:

Mader, M.M., Love, S., Osinski, G.R. (2014) Geological exploration of other planets: Insights from terrestrial desert, sea, and polar field campaigns. Conference paper for the International Astronautical Congress IAC-14.B6.3.5, Toronto, Canada.

Mader, M.M., Osinski, G.R. (2014) Optimizing scientific return for robotic-human lunar exploration: Case study Impacts Lunar Sample Return (ILSR) analogue mission program. Conference paper for the International Astronautical Congress IAC-14.A5.3-B3.6.9, Toronto, Canada.

Mader, M.M., Eppler, D., Osinski, G.R., Brown, J., Ghafoor, N. (2012) Unifying science-driven and resource exploitation strategies for lunar missions: Applying lessons learned from terrestrial geological exploration and Canadian analogue missions, Conference paper for the International Astronautical Congress IAC-12-A3-2C.5, Naples, Italy.

Mader, M.M., Osinski, G.R., Shankar, B., Tornabene, L., Pickersgill A.E., Marion, C.L., Barfoot, T., (2012) Baseline scientific requirements for a lunar robotic precursor mission: Lessons learned from analogue missions at the Mistastin (Kamestastin) lake impact structure, Canada, Conference paper for the International Astronautical Congress. IAC-12-A5.3-B3.6.3, Naples, Italy.

Battler, M.M., Mader, M.M., Preston, L.J., Moores, J., Osinski, G.R., Cormier, D., McCullough, E., Tornabene, L.T., Pontefract, A. (2012) Evaluation of communication protocols between mission control and astronauts during a series of science driven simulated lunar missions. Conference paper for the International Astronautical Congress IAC-12-B3.7.8, Naples, Italy.

Stenning, B., Osinski, G. R., Barfoot, T.D., Basic, G., Beauchamp, M., Daly, M., Francis, R., Furgale, P., Gammell, J., Ghafoor, N., Jasiobedzki, P., Lambert, A., Leung, K., Mader, M., Marion, C., McCullough, E., McManus, C., Moores, J., Preston, L.J. (2012) Planetary surface exploration using a network of reusable paths. Conference paper for International Symposium on Artificial Intelligence, Robotics and Automation in Space (iSAIRAS), Turin, Italy

Mader, M. (2007) Mineralogical investigation of Canadian Mars analogue sites: Focus on the use of a portable Raman spectrometer, Government of Canada publication: Canadian Space Agency, 60 p.

Abd El Hamed, N., Alabart Lopez, X., Bentz, N., Chim, R., Cornwall, M., Eren, A., Fortunato, A., Kutil, M., Mader, M., Moon, S., Nam, C., Ogunade, I., Porcaro, N., Raisinghani, H., Richardson, J., Schmuck, S., Seenii, A., Valderrama, G., Wierus, M., and Zambrano-Marin, L. (2007) Space Tools supporting Archeological Research and Tasks, International Space University publication, 150 p.

Mader, M. (2005) From Genesis to Juxtaposition: The evolution of the Ivisârtoq Greenstone Belt, SW Greenland, M.Sc. Thesis, Memorial University of Newfoundland, 200 p.

Mader, M. and Crowley, J. (2001) Investigation of gold occurrences, SW Greenland, Greenland Geological Survey, 52 p.

Conference Presentations and Abstracts:

Oral: (*denotes presenter)

Mader, M.M., Osinski, G.R.* (2015) Impactites of the Mistastin Lake impact structure, Canada: Insights into impact ejecta emplacement. Bridging the Gap III: Impact cratering in nature, experiments, and modeling conference, Freiburg, Germany.

Mader, M. M.*, Osinski, G.R., (2013) Impact melt-bearing breccias of the Mistastin Lake impact structure: A unique planetary analogue for ground-truthing proximal ejecta emplacement. American Geophysical Union (AGU) Fall Meeting, San Francisco, CA.

Mader M. M., Marion C. L., Osinski G. R.*, Pickersgill A. E., Singleton A. C., Tornabene L. L. (2013) A Systematic Multi-Year Field Campaign at the Mistastin Lake Impact Structure, Labrador, Canada [#3113], Meteorite Impacts and Planetary Evolution V, Sudbury, Canada

Mader. M. M.*, Osinski, G.R., Tornabene, L., (2013) Structural geology of the Mistastin Lake impact structure, Labrador, Canada. 44th Lunar and Planetary Science Conference, Houston, TX.

Mader, M. M.*, Antonenko, I., Osinski, G., Battler, M., Beauchamp, M., Cupelli, L., Chanou, A., Francis, R., Marion, C., McCullough, E., Preston, L., Shankar, B., Unrau, T., Veillette, D. (2011) Optimizing lunar sample return: Lessons learned from a robotic precursor lunar analogue mission at the Mistastin Lake impact structure, Labrador,

Canada. The Importance of Solar System Sample Return Missions to the Future of Planetary Science Workshop, Houston, TX.

Mader, M. M., Antonenko, I., Osinski, G.R.*, Marion C., Beauchamp M., Battler, M., Cupelli, L. Chanou, A. Francis, R., McCullough, E., Pickersgill, A., Preston, L. , Shankar, B., Unrau, T., Veillette, D. (2011) Integrated planetary operations at the Mistastin Lake Lunar Analogue Site, Labrador, Canada: Recommendations for future lunar missions. Geological Association of Canada–Mineralogical Association of Canada Conference, Ottawa, ON

Mader, M.M.*, Thomson, L. (2010) Exploring other worlds by exploring our own. Science Teacher's Association of Ontario (STAO) conference, Toronto, ON, Canada.

Mader, M.M.*, Osinski, G., Marion, C., and Sylvester, P. (2010) Mistastin Lake Crater, Labrador as a lunar analogue site. GeoCanada conference, Calgary, AB, Canada.

Osinski G. R., Mader M.M.*, Thomson L., Marion C. (2010). Exploring other world's by exploring our own: Bringing Earth and planetary science to the public. Geological Association of Canada–Mineralogical Association of Canada Annual Meeting. Calgary, Canada, May 2010 (poster).

Mader, M.M.* (2010) Terrestrial analogue activities. International Space University symposium, Strasbourg, France.

Mader, M.M. * (2008) Using analogue missions to develop lunar exploration strategies. Lunar Explorer's Society session, Lunar Exploration Analysis Group (LEAG) conference, Cape Canaveral, Florida, USA.

Mader, M.M.*, Lacelle, D. (2008) Mineralogical investigation at Canadian Analogue Research Sites (CARN) using a portable Raman spectrometer. Atlantic Geoscience Society Colloquium, Dartmouth, NS, Canada.

Bentz, N.*, Eren, A.*, Fortunato, A.*, Mader, M.*, Raisinghani, H.*, Wierus, M*. (2007) Space Tools supporting Archaeological Research and Tasks. International Space University live webcast.

Mader, M.M.*, Sylvester, P.J., Myers, J.S. (2005) Juxtaposed oceanic and continental basalts in the mid-Archean Ivisârtoq greenstone belt, Godthåbsfjord region, southwest Greenland. Geological Association of Canada–Mineralogical Association of Canada Conference, Halifax, NS.

Other contributions to oral presentations:

Antonenko I.*, Mader, M.M., Osinski G.R., Battler M., Beauchamp M., Cupelli L., Chanou A., Francis R., Marion C., McCullough E., Pickersgill A., Preston L., Shankar B., Unrau T. and Veillette D. (2011) Geo-focused situational awareness in robotic planetary missions: Lessons from an analogue mission at Mistastin Lake impact structure, Labrador, Canada (abstract #372). Geological Association of Canada–Mineralogical Association of Canada Conference, Ottawa, ON.

Gilbert, A.M.*, Osinski, G.R., Harrison, T.N., Mader, M.M., Huhn, A., Shankar, B., and Tornabene, L.L. (2013) Mission Planning Using the Google Earth Platform. Astronomy Society of the Pacific conference, San Jose, California

Osinski, G.R.*, Henry, H., Mader, M.M., Thomson, L., Gilbert, A., Papadimos, A., and Brown, P. (2011) Using planetary sciences to raise general science interest. Geological Association of Canada–Mineralogical Association of Canada Conference, Ottawa, ON.

Pickersgill, A. E.*, Osinski, G. R., and Mader, M. M. (2011) Characterization of shock in the impact melt-bearing breccias of the Mistastin Lake impact structure, Labrador (abstract #487). Geological Association of Canada–Mineralogical Association of Canada Conference, Ottawa, ON.

Sylvester, P.J.*, Mader, M.M., and Myers, J.S. (2006) Ultramafic alkaline magmas (meymechites) from the mid-Archean Ivisartoq greenstone belt, Southwest Greenland. Goldschmidt Conference, S5-07.

Poster: (*denotes presenter):

Mader M. M.* , McCullough E., Beauchamp M., Clayton J., Marion C. L., Moores J., Pickersgill A. E., Preston L. J., Shankar B., Osinski G. R., and ILSR team (2012) Science data management during real-time geological lunar analogue missions to the Sudbury and Mistastin Lake impact structures: Recommendations for future ground data systems (abstract #1842). 43rd Lunar and Planetary Science Conference. Houston, Texas, March 2012.

Mader, M.M.*, and Osinski, G. (2011) Insight into lunar impact cratering processes based on field mapping of the Mistastin Lake Impact Structure, Labrador. American Geophysical Union (AGU) Fall Meeting, San Francisco, CA.

Mader, M.M*, Osinski, G., Antonenko, I., Barfoot, T., Battler, M., Beauchamp, M., Chanou, A., Cloutis, E., Daly, M., Capitan, R-D., Francis, R., Ghafoor, N., Grieve, R. A. F., Hodges, K., Jolliff, B. L., Kerrigan, M., McCullough, E., Moores, J., Otto, C., Pickersgill, A., Pontefact, A., Preston, L., Redman, D., Sapers, H., Shankar, B., Singleton, A., Sylvester, P., Tornabene, L. L., Unrau, T., Young, K., and Zanetti, M. (2011) Use of a robotic precursor mission for follow-on human exploration: Case study lunar analogue mission at the Mistastin Lake impact structure (abstract #2033). Lunar Exploration Analysis Group (LEAG) Conference, Houston, TX.

Mader, M.M*, Osinski, G., and Marion, C. (2011) Impact ejecta at the Mistastin Lake impact structure, Labrador, Canada (abstract #2505). 42nd Lunar and Planetary Science Conference, Houston, TX.

Mader, M.M.* , Osinski, G., Marion, C., Dammeier, R., Shankar, B., and Sylvester, P. (2010) Mistastin impact structure: A geological analogue for lunar highland craters. Nördlingen 2010: The Ries crater, the Moon, and the future of human space exploration workshop, Nördlingen, Germany.

Mader, M.M.* , and Osinski, G. (2009) Terrestrial geological field methods and their potential applications to lunar exploration strategies. NASA Lunar Science Forum, NASA Lunar Science Institute, NASA Ames, Moffet Field, California, USA .

Mader, M.M.* (2005) The Ivisârtoq Greenstone Belt, SW Greenland. Advances in Earth Sciences Research Conference: Planetary Geology & the Early Earth, Ottawa, ON, Canada.

Other contributions to poster presentations:

Abou-Aly, S.*, Osinski G. R., Mader M.M., and KRASH Team. (2012) Significance of Science-Tactical Liaison Role in Mission Control for the Krash Lunar Analogue Sample Return Mission (abstract #2310). 43rd Lunar and Planetary Science Conference. Houston, Texas, March 2012.

Blain S.*, Mader M.M., Tornabene L.L., Osinski G.R., and ILSR team. (2012) Significance of mission control Science Documentarian in the KRASH lunar analogue mission (abstract #2079). 43rd Lunar and Planetary Science Conference. Houston, Texas, March 2012.

Chanou A.*, Tornabene L.L., Osinski G. R., Zanetti M., Pickersgill A. E., Shankar B., Marion C., Mader M. M., Souders K. A., Sylvester P., Jolliff B. L., Shaver C., and the KRASH science and operations teams (2012) Impact Melt-Pond Scenario Tested During the KRASH 2011 Analogue Mission at Kamestastin Impact Structure (abstract #2580). 43rd Lunar and Planetary Science Conference. Houston, Texas, March 2012.

Gilbert A.*, Osinski G.R., August T., Mader M.M., McCullough E., Pontefract A., Shankar B., and Singleton A. (2012) The continued growth of the education and outreach program at the Centre for Planetary Science and Exploration (abstract #1626). 43rd Lunar and Planetary Science Conference. Houston, Texas, March 2012.

Marion C.L.*, Osinski G.R., Abou-Aly S., Antonenko I., Barfoot T., Barry N., Bassi A., Battler M., Beauchamp M., Bondy M., Blain S., Capitan R., Cloutis E., Cupelli L., Chanou A., Clayton J., Daly M., Dong H., Ferrière L., Flemming R., Flynn L., Francis R., Furgale P., Gammell J., Garbino A., Ghafoor N., Grieve R. A. F., Hodges K., Hussein M., Jasiobedzki P., Jolliff B. L., Kerrigan M. C., Lambert A., Leung K., Mader

M. M., McCullough E., McManus C., Moores J., Ng H.K., Otto C., Ozaruk A., Pickersgill A. E., Pontefract A., Preston L. J., Redman D., Sapers H., Shankar B., Shaver C., Singleton A., Souders K., Stenning B., Stooke P., Sylvester P., Tripp J., Tornabene L. L., Unrau T., Veillette D., Young K., Zanetti M. (2012) A Series of robotic and human analogue missions in support of lunar sample return (abstract #2333). 43rd Lunar and Planetary Science Conference. Houston, Texas, March 2012.

McCullough, E.*, Pickersgill A.E., Francis R., Bassi A., Shankar B., Mader M.M., Beauchamp M., Osinski G.R., and the KRASH science and operations teams. (2012). Scientific Application of Visual Systems Instrumentation used during Lunar Sample Return Analogue Missions (abstract #2687). 43rd Lunar and Planetary Science Conference. Houston, Texas, March 2012.

Moores J. E.*, Francis R., Osinski G.R., Mader M.M., McCullough E., Preston L. J., Tornabene L. L. and KRASH Operations and Science Team. (2012) Surface operations for mission control during analogue human lunar deployments to Mistastin and Barringer impact structures (abstract #1136). 43rd Lunar and Planetary Science Conference. Houston, Texas, March 2012.

Osinski G.R., Barfoot T., Chanou A., Daly M.G., Francis R., Hodges K.V., Jolliff B.L., Mader M.M., McCullough E.M., Moores J.E., Pickersgill A.E., Pontefract A., Preston L., Shankar B., Singleton A., Sylvester P.J., Tornabene L.L., Young K.E. (2013) Preparing to return to the Moon: Lessons from science-driven analogue missions to the Mistastin Lake impact structure, Canada, a unique lunar analogue site. American Geophysical Union (AGU) Fall Meeting, San Francisco, CA.

Pickersgill A.E.*, Osinski G.R., Beauchamp M., Marion C., Mader M.M., Francis R., McCullough E., Shankar B., Barfoot T., Bondy M., Chanou A., Daly M., Dong H., Furgale P., Gammell J., Ghafoor N., Hussein M., Jasiobedzki P., Lambert A., Leung K., McManus C., Ng H.K., Pontefract A., Stenning B., Tornabene L. L., Tripp J., and the ILSR Team. (2012) Scientific Instrumentation for a Lunar Sample Return Analogue Mission (abstract #2657). 43rd Lunar and Planetary Science Conference. Houston, Texas, March 2012.

Pickersgill A. E.*, Osinski G.R., and Mader M.M. (2012) A Formational Model for an Impact Melt-Bearing Breccia Dyke at the Mistastin Lake Impact Structure, Labrador, Canada (abstract #2473). 43rd Lunar and Planetary Science Conference. Houston, Texas, March 2012.

Shankar B.*, Osinski G.R., Abou-Aly S., Beauchamp M., Blain S., Chanou A., Clayton J., Francis R., Kerrigan M., Mader M.M., Marion C., McCullough E., Moores J. E., Pickersgill A. E., Pontefract A., Preston L. J., and Tornabene L. L. (2012) Lunar Analogue Mission: Overview of the site selection and traverse planning process for a human sortie mission at the Mistastin Lake Impact Structure, Labrador, Canada (abstract #1143). 43rd Lunar and Planetary Science Conference. Houston, Texas, March 2012.

Tornabene L.L.*, Osinski G.R., Mader M.M., Chanou A., Francis R., Joliff B.L., Marion C., McCullough E., Pickersgill A., Sapers H., Souders K., Sylvester P., Young K., Zanetti M., and the KRASH team. (2012) Utility of remote sensing, robotic precursor data & a focused science objective for a follow-on human exploration lunar analogue mission at the Mistastin Lake (Kamestastin) impact structure (abstract #2390). 43rd Lunar and Planetary Science Conference. Houston, Texas, March 2012.

Antonenko I.*, Mader M.M., Osinski G.R., Battler M., Beauchamp M., Cupelli L., Chanou A., Francis R., Marion C., McCullough E., Pickersgill A., Preston L., Shankar B., Unrau T., and Veillette D. (2011) Issues of Geo-Focused Situational Awareness in Robotic Planetary Missions: Lessons from an Analogue Mission at Mistastin Lake Impact Structure, Labrador, Canada (abstract #2576). 42nd Lunar and Planetary Science Conference. Houston, Texas, March 2011.

Beauchamp M.*, Osinski G. R., Unrau T., Marion C., Mader M., Antonenko I., and Barfoot T. (2011) Ground Penetrating Radar (GPR) Investigations of the Mistastin Lake Impact Structure: A Case for GPR on the Moon (abstract #2147). 42nd Lunar and Planetary Science Conference. Houston, Texas, March 2011.

Marion C. L.*, Osinski G. R., Antonenko I., Barfoot T., Battler M., Beauchamp M., Cloutis E., Cupelli L., Chanou A., Daly M., Ferrière L., Flemming R., Francis R.,

Ghafoor N., Grieve R.A. F., Hodges K., Hussain M., Jolliff B. L., Mader M. M., McCullough E., Otto C., Preston L., Redman D., Shankar B., Singleton A., Stooke P., Sylvester P.J., Tornabene L. L., Unrau T., and Veillette D. (2011) A lunar analogue mission: sample return to the south pole-Aitken basin (abstract # 2515). 42nd Lunar and Planetary Science Conference. Houston, Texas, March 2011.

Shankar B.*, Antonenko I., Osinski G. R., Mader M. M., Preston L., Battler M., Beauchamp M., Chanou A., Cupelli L., Francis R., Marion C., McCullough E., Pickersgill A., Unrau T., and Veillette D. (2011) Lunar analogue mission: Overview of the site selection process at Mistastin Lake impact Structure, Labrador, Canada (abstract # 2594). 42nd Lunar and Planetary Science Conference. Houston, Texas, March 08 2011.

Pickersgill A. E.*, Osinski G. R., and Mader M. M. (2011) Shock effects and clast morphology in the impact melt-bearing breccias of the Mistastin Lake impact structure (abstract #126). Year of the Solar System Undergraduate Planetary Science Research Conference at the 42nd Lunar and Planetary Science Conference. Houston, Texas, March 2011.